Neurotrophin receptor p75 extracellular domain as a novel urinary biomarker in Motor Neuron Disease

Stephanie Shepheard
B.MedSc., B.Sc (Hons)

A thesis submitted for the degree of
Doctor of Philosophy
April 2015

Centre for Neuroscience & Department of Human Physiology
School of Medicine
Faculty of Medicine, Nursing & Health Sciences
Flinders University
Adelaide, South Australia

Declaration

I certify that this thesis does not contain without acknowledgement any material previously submitted for a degree or diploma in any university; and that to the best of my knowledge or belief it does not contain any material previously published or written by another person except where due reference is made in the text.

Stephanie Shepheard

Abstract

Motor neuron disease (MND) is a relentlessly progressive neurodegenerative disease, which is typically fatal within 3 years. Objective biomarkers indicative of underlying pathology are crucial for developing treatments, as no effective treatments exist, and the subjective ALS functional rating scale (ALSFRS-r) is the only validated disease progression measure.

The common neurotrophin receptor p75 (p75NTR) binds all neurotrophins and is not normally expressed by motor neurons after birth. However, p75NTR is re-expressed in motor neurons of the $SOD1^{G93A}$ MND mouse model, and motor neurons and Schwann cells of people with MND. Crucially, the p75NTR extracellular domain ($p75NTR^{ECD}$) is cleaved from injured motor neurons and detected in rat urine after sciatic nerve injury.

The aim of this study was to test $p75NTR^{ECD}$ in urine as an objective biomarker of MND. The $SOD1^{G93A}$ MND mouse model was used to investigate urinary $p75NTR^{ECD}$ levels in pre-clinical MND, and people with MND were recruited for urinary $p75NTR^{ECD}$ investigation in the clinic.

The study first addressed the feasibility of urinary $p75NTR^{ECD}$ as a biomarker by using novel detection methods of Immunoprecipitation/Western blot and Immunoprecipitation/Mass Spectrometry. Using Immunoprecipitation/Western blot, urinary $p75NTR^{ECD}$ was detected in $SOD1^{G93A}$ mice throughout life, but was not detected in healthy control mice until the equivalent of end stage disease. Similarly, urinary $p75NTR^{ECD}$ was detected in people with MND, but not healthy individuals via Immunoprecipitation/Western Blot. Urinary $p75NTR^{ECD}$ was detected in people with MND using Immunoprecipitation followed by Orbitrap or Triple-TOF Mass Spectrometry, confirming the presence of peptides from only the extracellular domain of p75NTR.

A novel indirect sandwich ELISA was then developed to quantify urinary $p75NTR^{ECD}$ levels in $SOD1^{G93A}$ mice, people with sporadic MND, and their respective controls. Urinary $p75NTR^{ECD}$ was significantly higher in $SOD1^{G93A}$ mice than healthy age-matched controls prior to disease onset, and throughout disease progression to end stage disease. Additionally, urinary $p75NTR^{ECD}$ changed

in one of two treatments. Riluzole, the only FDA approved MND treatment, had no effect on urinary p75NTR^{ECD} levels or survival and behavioural measurements, whereas treatment with a potential therapy called c29 resulted in significantly decreased urinary p75NTR^{ECD} and a significant behavioural improvement. This is the first description of urinary p75NTR^{ECD} in SOD1^{G93A} mice, showing promise as a biomarker of disease progression and treatment effectiveness.

In people with MND, urinary p75NTR^{ECD} was significantly higher than healthy individuals and people with Multiple Sclerosis. In addition, MND urinary p75NTR^{ECD} trended higher than Parkinson's disease. As determined by testing pre-symptomatic people carrying *SOD1* mutations, urinary p75NTR^{ECD} was significantly increased from, but not prior, to symptom onset. In addition, urinary p75NTR^{ECD} increased with disease progression, and correlated to the ALSFRS-r scale, time from symptom onset, and diagnosis. This is the first time urinary p75NTR^{ECD} has been quantified in clinical MND, showing promise as a prognostic and disease progression biomarker.

The results of this study support the hypothesis that urinary p75NTR^{ECD} is a biomarker of MND in SOD1^{G93A} MND model mice and people with MND, and establishes a solid foundation for using urinary p75NTR^{ECD} as a biomarker in pre-clinical MND models, clinical trials, and the clinic.

Acknowledgements

First, my heartfelt thanks to all the volunteers in this study, particularly those with MND, who graciously provided samples with the knowledge that they themselves would not benefit.

A massive thank you to my primary supervisor Dr. Mary-Louise Rogers, for her endless constructive input and support over the 5½ years I spent with the Neurotrophic Laboratory.

Thank you to my co-supervisor Dr. Tim Chataway for his Mass Spectrometry expertise, and playing the role of devil's advocate during presentation preparation. Thank you to Dr. David Schultz, Senior Clinical Neurologist, whose rapport with his patients and the nurses, and continued support of our research, was crucial for the recruitment of people with MND to our study, and the hassle free collection of biological samples.

Also a big thank you to our collaborators, Associate Professor Lizzie Coulson and team at the University of Queensland, Queensland Brain Institute, and Dr. Michael Benatar and Joanne Wuu from the Miller School of Medicine, University of Miami.

I'd also like to thank fellow PhD student Kevin Smith who provided endless support, and intellectual, and not-so-intellectual, discussions. Also thank you to Brad Rumbelow, Nusha Chegeni, Alex Coella, and the staff of the School of Medicine Animal Facility.

I'd also like to thank my funding sponsors. First, Australian Rotary Health (ARH) and the York family, who awarded me the Neville & Jean York PhD Scholarship for MND, co-funded by Flinders University. I would also like to thank ex-ARH Director, Dr. Richard Wilson, for his continued support and encouragement to present my research to Rotary clubs around Adelaide.

A big thank you the Centre for Neuroscience, Department of Human Physiology, Flinders Medical Centre Foundation, and MND Victoria for conference, research, travel grants, and prizes.

On a personal note, I would like to thank my parents Ruth and Barry, for their unwavering and unconditional support and instilling in me the belief that anything is possible if you put your mind to it. Also a big thank you to my extended family, especially my grandma Lorna, Aunty Alison, Uncle Peter, and Aunty Lorri.

The number of other people who have supported me is a thesis in itself. However, a special mention is required for Hayden, who has proven to be a ridiculously patient and understanding housemate for the last three years. A special thank you to ex-housemates Lauren, Danny, and Nathan, and a shout out to Terri, Hayley, Ellen, Kat, Helen, Karlee, Juszie, Stuart, and Matt.

Publications arising from this research

Shepheard SR, Chataway T, Schultz DW, Rush RA & Rogers ML 2014, 'The Extracellular Domain of Neurotrophin Receptor p75 as a Candidate Biomarker for Amyotrophic Lateral Sclerosis', *PLoS One*, **9**(1): e87398.

Shepheard SR, Chataway T, Schultz D, Rush RA, Rogers M-L 2013, 'Urinary Extracellular Domain of Neurotrophin Receptor p75 measurements as a novel biomarker for Motor Neuron Disease', *Amyotrophic Lateral Sclerosis and Frontotemporal Degeneration*, **14**(S2):116

Shepheard, S, Chataway T, Schultz D, Moey A, Rush RA, Rogers M-L, 2012, 'Body Fluid Biomarkers for Motor Neuron Disease', *Amyotrophic Lateral Sclerosis*, **13**(S1):58

Shepheard, S, Chataway, T, Rush RA, Rogers M-L 2011, 'Biomarker for Motor Neuron Disease', *Amyotrophic Lateral Sclerosis*, **12**(S1):96

Patent arising from this research

Rush RA; Rogers M-L; Shepheard SR; Chataway T. Biomarker for motor neuron disease (MND). PCT patent number PCT/AU2012/000076. August 27, 2013.

Table of Contents

List of Figures

List of Tables

Abbreviations

A875 - human melanoma cell line, p75NTR-positive
ACN - acetonitrile
ALSFRS-r - Amyotrophic Lateral Sclerosis Functional Rating Scale –revised
ALSTDI - Amyotrophic Lateral Sclerosis Therapy Development Institute
AUC - area under curve
B6 - healthy control mice, breed - C57BL/6J
BMI - body mass index
BSA - bovine serum albumin
BSR - baby hamster kidney fibroblast cell lysates, p75NTR-negative
c29 - 29 amino acid peptide from the neurotrophin receptor p75 juxtamembrane 'Chopper' domain, potential MND treatment
C9ORF72 - chromosome 9 open reading frame 72 (*gene*/protein)
CNS - central nervous system
CSF - cerebrospinal fluid
DNA - deoxyribose nucleic acid
DTI - diffusion tensor imaging
DTT - dithiothreitol
EAAT2 - excitatory amino acid transporter-2 (astrocytic glutamate transporter)
ECL - enzymatic chemiluminesence substrate
EIM - electrical impedence myography
ELISA - enzyme linked immunosorbent assay
EMG - Electromyography
FDA - American Food and Drug Administration
FTD - frontotemporal dementia
FUS - Fused in sarcoma (*gene*)
FUS/TLS - Fused in sarcoma /Translocated in Sarcoma (protein coded by *FUS*)
FVC - forced vital capacity
GluC - protease glutamyl endopeptidase
HI - healthy individuals
HRP - horseradish peroxidase
IP - Immunoprecipitation
IP-Orbitrap MS - Immunoprecipitation/Orbitrap Mass Spectrometry
iPSC - induced pluripotent stem cell
miRNA - microRNA
MND - Motor Neuron Disease
mRNA - messenger RNA
MS - Multiple Sclerosis
MUNE - motor unit number estimation
NfL - neurofilament light chain
NGF - nerve growth factor
NSC-34 - mouse neuroblastoma x motor neuron-enriched spinal cord motor neuron-like cell line, p75NTR-positive
Orbitrap-MS - Orbitrap Mass Spectrometry
p75NTR - Neurotrophin receptor p75
$p75NTR^{ECD}$ - neurotrophin receptor p75 extracellular domain
$p75NTR^{FL}$ - Full-length neurotrophin receptor p75
$p75NTR^{ICD}$ - neurotrophin receptor p75 intracellular domain
PBS - phosphate buffered saline

PLS - primary lateral sclerosis
PMA - progressive muscular atrophy
pNfH - phosphorylated neurofilament heavy chain
PNS - peripheral nervous system
Pre-fMND - people carrying MND-linked genetic mutations yet to show symptoms of disease
RIP - regulated intramembrane proteolysis
RNA - Ribonucleic acid
ROC - Receiver Operating Characteristic
ROS - reactive oxygen species
r-p75NTR-Fc - recombinant neurotrophin receptor p75 -Fc fusion protein
r-p75NTR^{ECD}-Fc - recombinant neurotrophin receptor p75 extracellular domain -Fc fusion protein
RT - room temperature
S/N - signal to noise ratio
SDS - sodium dodecyl sulphate
SDS-PAGE - sodium dodecyl sulphate polyacrylamide gel electrophoresis
SOD1 - copper/zinc superoxide dismutase 1 (*gene*/protein)
SOD1^{G93A} - glycine to alanine substitution, position 93, on the superoxide dismutase gene
TACE - tumor necrosis factor α convertase
TARDBP - transactive response DNA binding protein (*gene*)
TBS - Tris buffered saline
TBST - Tris buffered saline, Tween-20
TCA - trichloroacetic acid
TDP-43 - Transactive response DNA binding protein 43 (protein coded by *TARDBP*)
TMB - 3,3′,5,5′-tetramethylbenzidine
Trypsin Gold - serine protease
UPS - ubiquitin proteasome system
VEGF - Vascular endothelial growth factor
WB - Western blot
WT - wild type

Chapter 1. Introduction

1.1. Motor Neuron Disease

1.1.1. A neurodegenerative disease

Motor neuron disease (MND) was first described in 1869 by French neurologist and physician Jean-Martin Charcot (Charcot & Joffory 1869). MND affects upper and lower motor neurons, and is the third most common neurodegenerative disease of the Western world (Hirtz *et al.* 2007). Relentlessly progressive and nearly always fatal, MND presents with heterogeneous symptoms of muscle weakness, atrophy, and paralysis; a result of the selective and progressive loss of upper motor neurons originating in the motor cortex, and lower motor neurons located in the brain stem and ventral horn of the spinal cord (Stifani 2014). Most often, people with MND succumb to disease due to respiratory muscle failure (see Vande Velde *et al.* 2011a for review).

No diagnostic tests or validated biomarkers exist for MND. Disease diagnosis is established using clinical tests which rule out other potential neurodegenerative causes (de Carvalho *et al.* 2008a), while disease progression is measured by subjective functional rating scales (Kaufmann *et al.* 2005). Despite recent advances (**Figure 1.1**), the time between symptom onset and diagnosis is one year (Mitchell *et al.* 2010a, Cellura *et al.* 2012, Nzwalo *et al.* 2014); this delay is worrying as clinical symptoms of MND appear after significant damage has already occurred (Saxena & Caroni 2011, Eisen *et al.* 2014). That is, after axons retract, muscles are denervated, and compensatory mechanisms of re-sprouting and collateral re-innervation fail (see Robberecht & Philips 2013 for review). As a result, later stages of disease progression are often rapid following diagnosis, and the therapeutic window is small. As there is no cure or effective treatment for MND, the average life expectancy following diagnosis is just 3 years (see Robberecht & Philips 2013 for review).

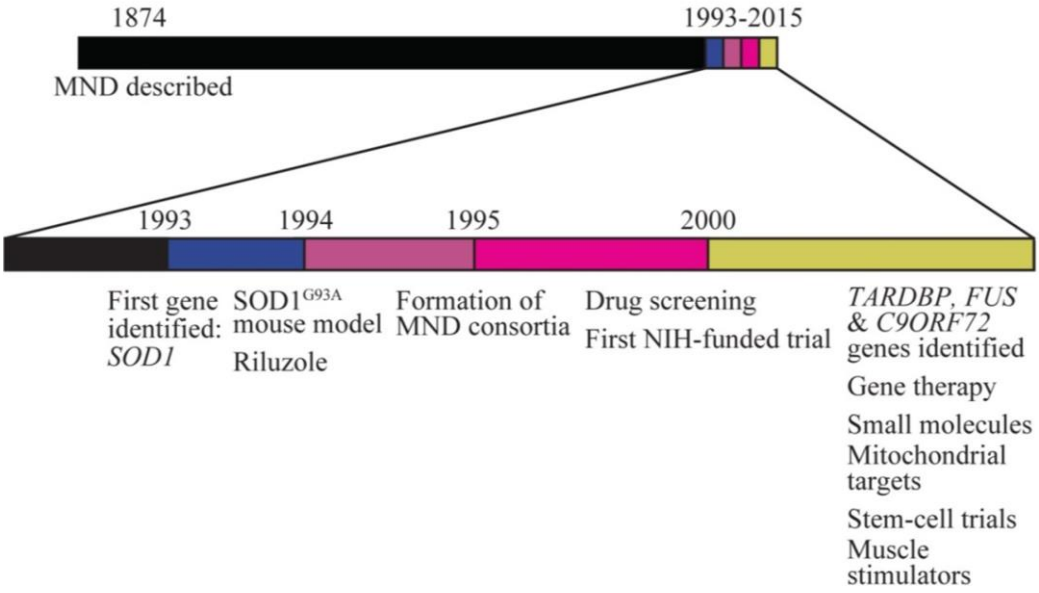

Figure 1.1: Major breakthroughs in MND

Although MND was first described in 1874, major breakthroughs in MND research have only occurred in the last 20 years. The identification of causal genes, and further understanding of the underlying disease processes, paves the way for potential treatment development (adapted from Zinman & Cudkowicz 2011).

1.1.2. Epidemiology

Worldwide, MND has a prevalence of 4.48 per 100,000 (Inter Quartile Range 3.03-6.70) and an incidence of 1.9 per 100,000 (Inter Quartile Range 1.37-2.40) (see Chiò *et al.* 2013b for review). In Australia, 1,900 people have MND, and each day, at least two people die and a further two people are diagnosed (MND Australia 2014). Although MND may be considered rare, with a lifetime risk between 1 in 400 and 1 in 700 (Johnston *et al.* 2006), the personal, societal, and economic burden is significant; the annual cost of disease per individual is estimated at 36,200 Euros (AUD$ ~52 000, 2014; López-Bastida *et al.* 2009, Schepelmann *et al.* 2010). Incidence rates increase suddenly around 40 years of age and peak between 60 and 79 years of age to 10-15 per 100,000 (Logroscino *et al.* 2010 see Chio et al. 2013b for review). Epidemiological studies suggest an increased incidence of MND over time (Pritchard *et al.* 2013), this may be a sign of the world's aging population which equates to a larger number of older citizens (Chiò *et al.* 1995, Cima *et al.* 2009, see Chiò *et al.* 2013b for review), but could also, or instead, be due to epigenetic effects (Pritchard *et al.* 2013) such as prolonged exposure to environmental toxins.

1.1.3. Heterogeneity

A definitive diagnosis of MND requires the presence of both upper and lower motor neuron symptoms, evidence of spread of disease, and ruling out of other diseases using clinical tests such as neuroimaging and electrophysiology (de Carvalho *et al.* 2008a). However, MND is a heterogeneous disease in many aspects; there is an ever-growing plethora of linked genetic factors (Abel 2015), and sites of initial clinical presentation, disease progression rates (see Rowland & Shneider 2001 for review), and involvement of cognitive and behavioural impairments, vary widely. Heterogeneity is even seen in the survival times and age of disease onset within one family, where the same genetic mutation is present in all members with MND (Régal *et al.* 2006).

Additionally, although the average life expectancy following diagnosis is just 3 years, approximately 5% of patients will survive more than 10 years (see Turner *et*

al. 2013a for review), many of which present with pure upper motor neuron or pure lower motor neuron symptoms (Chiò *et al.* 2011). Because of such variation, MND is hard to distinguish from other neurodegenerative diseases affecting motor neurons (see Rowland & Shneider 2001 for review) such as adult-onset spinal muscular atrophy (SMA) (see Turner & Talbot 2013 for review).

Heterogeneity is also evident in the genetic involvement and clinical symptoms of MND. Familial MND is characterised by the presence of a genetically determined inheritance and a large number of genetic mutations in different genes have been implicated. Conversely, sporadic MND has no known genetically inherited links, and accounts for 90% of MND cases, while only 10% are of the familial form (see Turner *et al.* 2013a for review). Although MND is considered heterogeneous, the clinical characteristics of familial and sporadic MND are clinically indistinguishable (see Bruijn *et al.* 2004 for review), and variations in disease onset site, age of onset, rates of progression, and involvement of extra motor features such as frontotemporal lobar degeneration, which can present as dementia (frontotemporal dementia; FTD), are found irrespective of genetic involvement.

Although MND involves both upper and lower motor neuron symptoms, it starts as a focal process involving variable regions, and then spreads throughout the motor system (Ravits & La Spada 2009). Other motor neuron diseases exist with variable mixes of upper motor neuron and lower motor neuron signs. These include progressive muscular atrophy (PMA), with further subtypes of flail arm and flail leg so labelled by initial onset site, in which only lower motor neurons are affected; and primary lateral sclerosis (PLS) in which only upper motor neurons are affected (see Wijesekera & Leigh 2009 for review). Some people with PMA and PLS progress to MND with upper and lower motor neuron involvement, and it is debated as to whether PMA and PLS are separate diseases to MND, or exist on a continuum (Tartaglia *et al.* 2007, Kim *et al.* 2009).

Approximately 75% of people with MND present with initial weakness in limbs (limb onset), while the remaining 25% display muscle weakness first in the tongue and other speech and swallowing muscles (bulbar onset) (see Wijesekera & Leigh 2009 for review). Additionally, population based studies calculate that 5% of people with MND present with frontotemporal dementia (FTD) and a further 15-

50% experience frontotemporal lobar degeneration, resulting in cognitive impairment (Tsermentseli *et al.* 2012).

1.1.4. Environmental and lifestyle risks

The majority of MND cases have no known genetic involvement (see Turner *et al.* 2013a for review) and, particularly before the discovery of genetic mutations, a wide variety of environmental and lifestyle factors have been studied in an attempt to link a common exposure to MND.

On the island of Guam in the Western Pacific, the unusually high instance of MND was linked to the ingestion of a neurotoxin, beta-N-methylamino-1-alanine (BMAA), in the normal diet of the indigenous inhabitants (Spencer *et al.* 1986). BMAA has since been reported to incorporate into proteins in place of the amino acid L-serine and cause protein misfolding and aggregation (Dunlop *et al.* 2013). High incidences of MND have also been found in other Western Pacific areas including Mariana Island, the Kii Peninsula of Japan, and western New Guinea.

Other studies have been more hard pressed to find a link between environmental/ lifestyle factors and MND. Ahmed and Wicklund suggest this may be because low incidence and prevalence rates of MND make large studies difficult to perform, and so studies looking at environmental/lifestyle risk factors and MND are often small, retrospective case studies with a high potential for bias and low statistical power (see Ahmed & Wicklund 2011 for review). Despite this difficulty, many cohorts of people with an increased incidence of MND have been investigated.

A 2005 study found that Italian soccer players have a higher risk of developing MND than the general population (Belli & Vanacore 2005). Suggestions as to the cause include high fitness levels, increased use of dietary supplements and/or steroids (Belli & Vanacore 2005), and head trauma (Piazza *et al.* 2004). Additional studies into fitness levels and physical activity, and a link to MND, have been inconclusive. A large European study recently found that physical activity is not a risk factor for MND (Pupillo *et al.* 2014), whereas others have reported an increased risk of MND with higher levels of leisure time physical activity, and suggest that a genetic profile or lifestyle promoting physical fitness increases the

risk of MND (Huisman *et al.* 2013), such as having a lower body mass index (BMI) (O'Reilly *et al.* 2013, Reich-Slotky *et al.* 2013).

Another population with high fitness levels, that of war veterans, in particular, first Gulf War veterans (Haley 2003, Horner *et al.* 2003), have been associated with an increased risk of MND (Weisskopf *et al.* 2005). However, a later study reported no significant differences between MND incidence in Gulf War veterans and veterans who served during the Gulf War but were not deployed (Barth *et al.* 2009). These findings suggest that an increased incidence of MND in veterans, independent of the branch, years, and place of service, could be related to factors that are increased in military service in general (Weisskopf *et al.* 2005) such as intense physical activity, viral infections, traumatic injury, exposure to cyanotoxins (Cox *et al.* 2009), insecticides, and heavy metals such as aerosolised lead.

The link between increased heavy metal exposure and motor system damage has been studied extensively, with metals such as lead, selenium, aluminium, cadmium, manganese, and mercury all known to cause adverse motor symptoms. However, links between heavy metals and MND are less concrete. One recent study found that men exposed to heavy metals were more likely to develop sporadic MND (Pamphlett 2012), but other studies have been less conclusive (see Callaghan *et al.* 2011, Vinceti *et al.* 2012 for reviews).

In Italy in the 1970s and 1980s, a change in water supply resulted in population exposure to high levels of the heavy metal selenium in the drinking water. The main source of selenium intake in humans is through the diet, and drinking water containing greater than 1µg/L of an inorganic form of selenium, selenate, increased the risk of MND in this population (Vinceti *et al.* 1996, Vinceti *et al.* 2010). In other places, environmental exposure to selenium has been found to induce (Yang *et al.* 1983) or have no effect (Lemire *et al.* 2012), on motor disorders. Laboratory studies show that selenium can penetrate the blood-brain barrier and cause damage to motor neurons, mitochondria, and other CNS components (Glaser *et al.* 2010). In line with this finding, increased selenium is found in the spinal cord (Mitchell *et al.* 1991, Ince *et al.* 1994), and increased selenate is found in the CSF (Vinceti *et al.* 2013), of people with MND. However, no differences are seen in the periphery, in the blood or toenails, between people with MND and healthy individuals (Vinceti *et al.* 1997, Bergomi *et al.* 2002).

No conclusive evidence links MND with other environmental and lifestyle risks widely studied. Farming, which includes exposure to chemicals, animals and their diseases, and requires a high physical load, has been studied, as males exposed to herbicides or pesticides are more likely to develop MND (Malek *et al.* 2012, Pamphlett 2012), but other studies report no such link (Weisskopf *et al.* 2009). Solvent exposure has also been implicated (Pamphlett 2012), but when significance was reached results were weak and the reported confidence intervals were large (see Ahmed & Wicklund 2011 for review).

Similarly, a recent study showed no link between smoking and MND in a large cohort of participants (Pamphlett & Ward 2012), adding to the debate fuelled by previous evidence to the contrary, which suggests that cigarette smoking may be a risk factor for women but not men (Weisskopf *et al.* 2004) or a risk factor for both genders (Nelson *et al.* 2000b). Additional risks may be present in the diet; glutamate and fat intake have been reported as positive risk factors, and a decreased risk of MND has been linked with dietary fibre (Nelson *et al.* 2000a), polyunsaturated fatty acids, and vitamin E (Veldink *et al.* 2007).

Despite these contradictory results, the links between MND and BMAA, selenium, and pesticides have the most supporting evidence and warrant further investigation. Additionally, there are two accepted risks for MND, that of gender, and age. The incidence and prevalence of MND is higher in men (Alonso *et al.* 2009), which is more pronounced in sporadic MND. However, gender appears to play no role in survival (see McCombe & Henderson 2010 for review). As for age risk, MND incidence peaks between 60 and 79 years of age (see Chiò *et al.* 2013b for review) irrespective of gender.

Following the discovery of MND-linked genetic mutations, some apparent geographic clusters of sporadic MND have been linked by a common genetic defect from a common ancestor, e.g., those with GGGGCC hexanucleotide repeat expansions in chromosome 9 open reading frame 72 (*C9ORF72*) (Majounie *et al.* 2012b, Smith *et al.* 2013). Such genetic studies, which have provided clearer answers to questions surrounding MND, have now taken precedence over attempts to link potential environmental or lifestyle factors to MND pathogenesis (see Mitchell 2000 for review).

1.1.5. Genetics

MND linked gene mutations are a relatively recent discovery, and familial MND has been attributed to mutations in many different genes, only a few of which account for large numbers of MND cases. Expanded GGGGCC hexanucleotide repeats in the non-coding region of *C9ORF72* were first reported in 2011 and are linked to the highest proportion (40%) of familial MND cases (DeJesus-Hernandez *et al.* 2011, Renton *et al.* 2011). The second most common gene mutations (20%) are found in the copper/zinc superoxide dismutase 1 (*SOD1*) gene (Rosen *et al.* 1993), the first gene linked to MND in 1993. Other rare mutations leading to MND occur in genes such as transactive response DNA binding protein (*TARDBP*) and fused in sarcoma (*FUS*).

It is estimated that only 10% of MND cases are familial and that ~70% of these cases can be explained by known genetic mutations (see Turner *et al.* 2013b for review, **Figure 1.2**). However, the percentage of familial MND and sporadic MND cases may differ to what is recorded. The number of familial MND cases may be higher, as those reported with sporadic disease could be from a family where inadequate recording of family history, manifestation of MND as different subtypes, or incomplete disease penetrance, exist (see Andersen & Al-Chalabi 2011 for review). Alternatively, familial MND numbers may be lower, as 50-75% of reported familial cases only have one other family member with MND (Conte *et al.* 2012), which, statistically, could be due to chance alone.

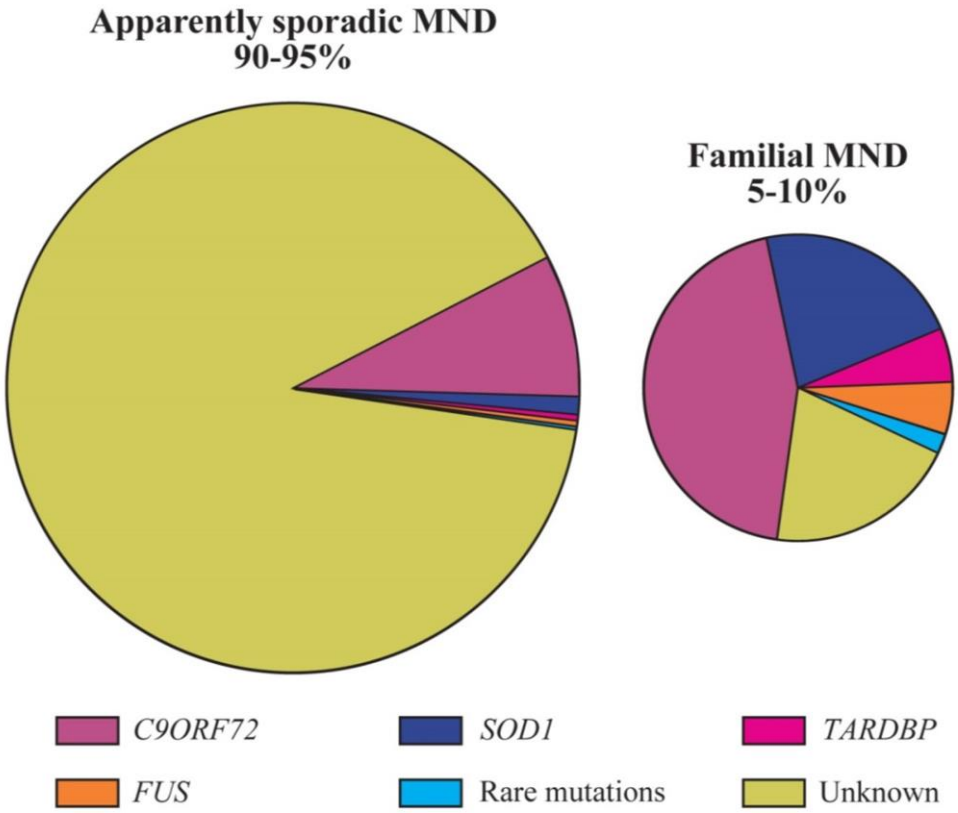

Figure 1.2: The current genetic landscape of MND

Only 5-10% of MND cases report a positive family history of MND or frontotemporal dementia (FTD) and are termed familial MND. At least two-thirds of these cases can be linked to one of four major causal genes, the largest group being those with expansions of the hexanucleotide repeat sequence GGGGCC in *C9ORF72*. These expansions, and mutations of the other genes identified in familial MND, are also detectable in a small but significant proportion of the 90-95% of cases of apparently sporadic MND which report no family history (adapted from Turner *et al.* 2013b).

1.1.5.1. Chromosome 9 open reading frame 72 hexanucleotide repeat (C9ORF72)

In late 2011, expansions of the GGGGCC hexanucleotide repeat in chromosome 9 open reading frame 72 (*C9ORF72*) were identified, and have since been determined as the most frequent cause of familial MND (Chiò *et al.* 2012) (**Figure 1.2**). *C9ORF72* repeats have been linked to approximately 90% of Finnish people with familial MND (Renton *et al.* 2011), 40% of familial MND worldwide (Majounie *et al.* 2012b), and 7% of sporadic MND in people of European descent (see Renton *et al.* 2014 for review).

C9ORF72 mutations have also been linked to frontotemporal dementia (FTD), and may account for 50-70% of MND-FTD cases (Smith *et al.* 2013) and 25% of pure FTD cases (Majounie *et al.* 2012b). A genetic link between MND and dementia was first alluded to in 1991, before the discovery of *SOD1* mutations, when MND and FTD were found in multiple generations of a Swedish family (Gunnarsson *et al.* 1991), but it was not mapped precisely until 2011 (DeJesus-Hernandez *et al.* 2011, Renton *et al.* 2011). The general population has a maximum of 23 copies of the hexanucleotide repeat (range 2-23), whereas people with MND or FTD are estimated to carry 700-1,600 repeats (DeJesus-Hernandez *et al.* 2011) with no significant differences in repeat frequency between MND and FTD (Renton *et al.* 2011). This finding provides evidence that MND and FTD are manifestations of the same disease spectrum. Interestingly, *C9ORF72* expansions have also been linked to Alzheimer's disease (Majounie *et al.* 2012a), and Parkinsonism in some studies (Lesage *et al.* 2013, Nuytemans *et al.* 2013), but not others (Ticozzi *et al.* 2014).

The disease mechanism of *C9ORF72*-linked MND is unknown but there are three theories. First, a decreased expression of *C9ORF72* variants has been found in the frontal cortex, motor cortex, cerebellum, cervical spinal cord and induced pluripotent stem cell lines (iPSCs) of people with *C9ORF72*-MND (Belzil *et al.* 2013, Donnelly *et al.* 2013), though these results have not always been replicated (DeJesus-Hernandez *et al.* 2011, Stewart *et al.* 2012). Second, abnormal GGGGCC repeat-containing RNAs accumulate in the nuclei of cells in the frontal cortex and spinal cord (DeJesus-Hernandez *et al.* 2011) and could cause neurotoxicity through disruption of transcription, or the splicing/processing of mRNAs through the sequestration of RNA-binding proteins and formation of RNA foci, as seen in other

disorders such as spinocerebellar ataxia (White *et al.* 2010). Third, GGGGCC repeat transcripts undergo repeat-associated non-ATG translation (RAN translation). This translation occurs in the absence of an initiating codon and results in the production of polyGA, polyGP and polyGR peptides, which have been detected as insoluble material in brain homogenates and in neuronal inclusions in the CNS of people with *C9ORF72*-linked FTD/MND (Ash *et al.* 2013, Mori *et al.* 2013). Recently, studies have focused on the cellular function of the *C9ORF72* protein, with homology searches suggesting that the C9ORF72 protein may regulate membrane traffic with Rab-GTPase (Levine *et al.* 2013).

People presenting with *C9ORF72*–linked MND have a disease phenotype with younger ages of onset but this varies widely with approximately 50% of mutation carriers developing disease around 55 years of age, and virtually all developing disease by 80 years of age (Majounie *et al.* 2012b). Additionally, *C9ORF72*-linked MND shows shortened survival times (20 versus 26 months), increased rates of cognitive and behavioural impairment, and a strong family history of neurodegenerative disease in comparison to people with MND without this mutation (Byrne *et al.* 2012). *C9ORF72*-linked MND cases also have a different neuropathological 'signature' to other MND cases; TDP-43 inclusions are present, but in different regions (Bede *et al.* 2013).

1.1.5.2. Copper/zinc superoxide dismutase 1 (SOD1)

Mutations in the copper/zinc superoxide dismutase 1 gene (*SOD1*), located on chromosome 21, were the first linked to MND in 1993, when 11 missense mutations were found (Rosen *et al.* 1993). SOD1 mutations account for 12-23% of familial MND and 2-3% of apparently sporadic MND (see Andersen 2006 for review), equating to 1-2% of all MND cases. At present, over 170 different *SOD1* mutations have been identified in people with familial MND (Abel 2015), the majority of which are point mutations of highly conserved amino acids leading to autosomal-dominant inherited disease (see Cleveland & Rothstein 2001 for review). As *SOD1* mutations were the first identified in MND, the normal function and consequences of mutant SOD1 expression on MND pathogenesis is widely studied.

SOD1 is a ubiquitously expressed enzymatic protein that converts toxic superoxide, an inadvertent by-product of inefficient oxidative phosphorylation from the

mitochondria, to water and hydrogen peroxide. The 153 amino acid SOD1 protein, together with a catalytic copper ion and a stabilising zinc ion, form one subunit, and, through non-covalent binding, two subunits form the functional SOD1 homodimer (Fridovich 1986). It was first thought that MND pathology was induced by a loss of SOD1 enzyme function caused by mutations, but studies have since determined that *SOD1* mutations result in a toxic gain of function that is independent of the level of SOD1 enzyme activity. For example, mice which express mutant human SOD1 with full enzyme activity develop disease pathology similar to MND (Gurney *et al.* 1994), and mice with enzymatic inactive mutant SOD1, achieved by knocking out the gene encoding the SOD1 copper chaperone (Subramaniam *et al.* 2002), also develop motor neuron degeneration.

SOD1-linked MND typically presents with asymmetrical onset, normally in the lower limbs, has predominately lower motor neuron features, and extra-motor features have been recorded in some cases (see Andersen & Al-Chalabi 2011 for review). Age of onset and survival times have been linked to specific SOD1 mutations. For example, two high-penetrance SOD1 mutations (G37R and L38V) are linked with a significantly lower mean age of onset of 40 and 41.5 years (Cudkowicz *et al.* 1997). People with $SOD1^{C6G}$ and $SOD1^{C6F}$ mutations survive just a few months after diagnosis, whereas the $SOD1^{L144F}$ mutation can confer survival for decades. Additionally, some SOD1 mutations (A4V, G41S, G93A, R115G) confer short survival times independent of the site of onset, whereas others (G41D, H46R, homozygous D90A) are associated with lower limb onset, very slow ascending weakness and extended survival (Cudkowicz *et al.* 1997, Andersen *et al.* 2003). Other mutations show a wide range of survival times even within families, such as the $SOD1^{G37R}$ mutation, with survival ranging from 2-36 years (Cudkowicz *et al.* 1997).

Interestingly, recent studies have also implicated wild type (WT) SOD1 mediated toxicity in sporadic MND. It is reported that WT SOD1 can fold into abnormal conformations and reproduce some of the cytotoxicity seen with mutated SOD1 in familial MND. Additionally, misfolded WT SOD1 may propagate intracellular pathology in a prion-like manner, causing toxic misfolding in otherwise normal SOD1 proteins (Münch & Betolotti 2011, Grad & Cashman 2013).

1.1.5.3. Fused in sarcoma /Translocated in Sarcoma (FUS/TLS)

Mutations of the RNA processing gene *FUS*, account for approximately 4% of familial MND, are present in less than 1% of sporadic MND cases (see Mackenzie *et al.* 2010 for review), and were first implicated in MND in 2009 (Kwiatkowski *et al.* 2009). *FUS* mutations have been linked to frontotemporal lobar degeneration with many people with *FUS*-linked MND showing, often sub-clinical, frontal dysfunction; approximately 15% of these people later develop FTD (Tsermentseli *et al.* 2012). WT FUS/TLS is a 526 amino acid protein encoded by the *FUS* gene on chromosome 16. It is a ubiquitously expressed, predominantly nuclear protein involved in DNA repair, transcription regulation, RNA splicing and export to the cytoplasm, and mRNA transport (Kwiatkowski *et al.* 2009). As of 2009, 15 mutations had been reported, this number has since increased to 79 (Abel 2015).

FUS/TLS is an RNA binding protein that shuttles between the nucleus and cytoplasm. FUS/TLS binds to more than 5,500 genes and its depletion alters the splicing of nearly 1,000 mRNAs (Lagier-Tourenne *et al.* 2012). Most FUS/TLS mutations disrupt the interaction between FUS/TLS and transportin, which it uses as a carrier for transport; this causes mislocalisation of FUS/TLS to stress granules in the cytoplasm, which may then form inclusions. However, disease mechanisms relating to FUS/TLS are currently unknown, and FUS/TLS specific neurotoxicity could be due to a toxic gain of function, loss of function by depletion of FUS/TLS, or combination of both.

FUS-linked MND cases present with MND, but co-current frontotemporal lobar degeneration (Ticozzi *et al.* 2009), and frontotemporal lobar degeneration (Van Langenhove *et al.* 2010) or FTD (Blair *et al.* 2010) without MND has also been recorded. The age of onset in *FUS*-linked MND is slightly lower than that of people with *SOD1*-linked MND, bulbar onset cases appear more commonly in people with FUS/TLS mutations and, in general, people with *FUS*-linked MND have shorter survival times than SOD1 and TDP-43 cases, although wide variability exists (see Millecamps *et al.* 2010 for review).

1.1.5.4. Transactive response DNA binding protein 43 (TDP-43)

Along with *FUS* mutations, mutations in RNA-binding protein transactive response DNA binding protein 43 (TDP-43), implicate the mechanisms of RNA metabolism as possible underlying causes of MND pathogenesis.

TDP-43 is a ubiquitously expressed, predominately nuclear, 414 amino acid protein encoded by *TARDBP* on chromosome 1. TDP-43 mutations were first discovered in people with MND in 2008 (Gitcho *et al.* 2008, Kabashi *et al.* 2008, Sreedharan *et al.* 2008) after the discovery of TDP-43 in neuronal inclusions in people with MND or frontotemporal dementia (FTD) without tau inclusions (Arai *et al.* 2006, Neumann *et al.* 2006). By early 2015, 52 mutations had been identified (Abel 2015) which are responsible for ~1-5% of familial MND (Chiò *et al.* 2012) and are found in 1.5% of sporadic MND (see Mackenzie *et al.* 2010 for review). Unlike in the SOD1 protein, TDP-43 mutations appear to occur mostly in one area, the highly conserved C-terminal domain, which is involved in the interaction between TDP-43 and other proteins. This suggests that normal protein-protein interactions with TDP-43 may be impaired (see Lagier-Tourenne & Cleveland 2009 for review).

TDP-43 binds DNA and RNA and is involved in transcription, RNA splicing, and RNA transport between the nucleus and cytoplasm (Buratti & Baralle 2008). The role of TDP-43 in messenger RNA (mRNA) splicing is wide ranging; it targets more than 6,000 mRNAs, with the abundance of more than 600 mRNAs, the splicing of 965 mRNAs (Polymenidou *et al.* 2011), and the stability of many non-coding RNAs and microRNAs (Buratti & Baralle 2010) affected when TDP-43 is knocked down. Normally, TDP-43 shuttles between the nucleus and cytoplasm and associates with silenced RNA, moving it from granules to a target site, where the RNA translation is resumed.

In response to stress, TDP-43 accumulates in cytoplasmic stress granules but returns to the nucleus once stress, and the stress granules, disappear (see Robberecht & Philips 2013 for review). This normal response to stress is thought to be exacerbated in MND, where normal nuclear TDP-43 is lost and cytoplasmic accumulation of TDP-43 is found in lower motor neurons, neurons of the neocortex and the hippocampus, and supporting glia (Kwiatkowski *et al.* 2009). It is suggested that mutated TDP-43 is unable to move back to the nucleus, which

results in nuclear RNA processing impairment (Kwiatkowski *et al.* 2009). Additionally, TDP-43 regulates its expression by binding to its own 3' untranslated region, and induces degradation of its own mRNA (Ayala *et al.* 2011). Therefore, sequestration of TDP-43 in cytoplasmic inclusions increases overall TDP-43 expression and a pro-aggregation environment (see Robberecht & Philips 2013 for review). In addition, a newly discovered cytoplasmic role of TDP-43 has been implicated in MND. Alami & colleagues (2014) found that TDP-43 forms cytoplasmic, neurofilament light mRNA-containing granules that undergo bidirectional, mictrotubule-dependent transport, and facilitate the delivery of mRNA to distal parts of the neuron. Studies in *Drosophila*, mice primary neurons, and induced pluripotent stem cell (iPSC)-derived human motor neurons show impaired transport of these granules in neurons with TDP-43 mutations (Alami *et al.* 2014, Jovičić & Gitler 2014).

TARDBP-linked MND cases can present as MND alone, or MND with frontotemporal lobar degeneration (Sreedharan *et al.* 2008, Chiò *et al.* 2010) and/or extrapyramidal signs (Borghero *et al.* 2011). Parkinson's disease (Rayaprolu *et al.* 2013) has also been linked to TDP-43 mutations. Although clinical data is limited, it appears that people with *TARDBP*-linked MND have a slighter later age of onset than those with *SOD1*-linked MND, and bulbar onset seems to be more common (Millecamps *et al.* 2010).

The similarities in mutated FUS/TLS and TDP-43 suggest that these proteins may have a link in the pathology of MND, but this is under debate. Neumann and colleagues (Neumann *et al.* 2009) found that although TDP-43 and FUS/TLS act similarly in MND, cells with FUS/TLS-positive inclusions retained some of the normal nuclear and cytoplasmic FUS/TLS, which is in contrast to the reduction of TDP-43 in the nucleus. Differences in FUS/TLS and TDP-43 pathology were also seen by Vance and colleagues (Vance *et al.* 2009) who found that FUS/TLS-linked MND cases did not have TDP-43-containing inclusions. However, evidence also suggests that the two genes are linked in MND, with the finding of FUS/TLS-containing inclusions in TDP-43-linked MND and the co-localisation of FUS/TLS and TDP-43 in non SOD1-linked MND (Deng *et al.* 2010). Additionally, *FUS* overexpression is able to rescue a *TADRDBP* knock-down phenotype in a Zebra fish model of MND, but the reverse is unsuccessful, suggesting that *TARDBP* and

FUS share a common pathway, with *FUS* downstream of *TARDBP* (Kabashi *et al.* 2011).

In addition to *C9ORF72*, *SOD1*, *FUS*, and *TARDBP*, other rare MND-linked gene mutations exist including *VAPB*, *OPTN*, *UBQLN2*, and *GRN*, as outlined in **Table 1.1**.

Table 1.1: MND linked genes

(adapted from Andersen & Al-Chalabi 2011, Ferraiuolo *et al.* 2011b, Otomo *et al.* 2012, Robberecht & Philips 2013, Abel 2015)

Gene	Locus	Protein	Responsible for	Clinical features in non-pure MND patients	Original paper
C9ORF72 (ALS-FTD1)*****	9p21.2	Unknown	~40-50% fMND; sMND	FTLD; MND-FTLD; Parkinsonism; psychosis	(DeJesus-Hernandez *et al.* 2011, Renton *et al.* 2011)
SOD1 (ALS1)*****	21q22.11	SOD1	~20% fMND	MND-FTLD; PMA	(Rosen *et al.* 1993)
FUS (ALS6)*****	16p11.2	Fused in Sacroma/ Translocated in Sarcoma	~2-5% fMND; sMND	Myxoid liposcarsoma; low grade fibromyoxid sarcoma; MND-FTLD; FTLD	(Kwiatkowski *et al.* 2009, Vance *et al.* 2009)
TARDBP (ALS10)*****	1p36.22	TDP-43	~2-5% MND	MND-FTD, FLTD; Lewy body disease; PD-dementia complex of Guam; Alzheimer's disease *etc.*	(Gitcho *et al.* 2008, Kabashi *et al.* 2008, Rutherford *et al.* 2008, Sreedharan *et al.* 2008)
ALS2 (ALS2)	2q33.1	ALS2/alsin	<1% fMND; jMND	PLSJ; IAHSP	(Hadano *et al.* 2001, Yang *et al.* 2001)
ANG (ALS9)	14q11.1	Angiogenin	< 1% fMND	MND-FTLD; PD; MND-PD	(Greenway *et al.* 2006)
ATXN2 (ALS13)	12q23-q24.1	Ataxin-2	<1% fMND	PMA; SCA2; PSP; neuroblastoma tumours	(Elden *et al.* 2010)
OPTN (ALS12)	10p13	Optineurin	<1% fMND	MND-FTLD; Normal-tension glaucoma; adult-onset primary open angle glaucoma	(Maruyama *et al.* 2010)
PFN1 (ALS18)	17p13.3	Profilin 1	<1% fMND	Deletion: Miller-Dieker syndrome	(Wu *et al.* 2012)

SETX (ALS4)	9q34.13	Probable helicase senataxin	<1% jMND[α]	AOA2; cerebellar ataxia, motor neuropathy	(Chen *et al.* 2004)
UBQLN2 (ALS15)	Xp11.21	Ubiquilin 2	<1% fMND; jMND	MND-FTLD	(Deng *et al.* 2011)
VAPB (ALS8)	20q13.3	VAMP-associated protein B/C	<1% fMND	PLS; PMA; SMA4	(Nishimura *et al.* 2004)
VCP (ALS14)	9p13.3	Valosin-containing protein	<1% fMND	MND-FTLD; FTLD; IBMPFD	(Johnson *et al.* 2010)
CHCHD10 (ALS-FTD2)	22q11.23	Coiled-coil-helix-coiled-coil-helix domain containing 10	MND-FTD	FTD	(Bannwarth *et al.* 2014, Chaussenot *et al.* 2014)
CHMP2B (ALS17(ALS-FTD3))	3p12.1	Charged multivescular body protein 2B	MND	MND-FTLD; FTLD	(Parkinson *et al.* 2006, Cox *et al.* 2010)
DAO	12q24	D-amino acid oxidase	<1% fMND	Schizophrenia	(Mitchell *et al.* 2010b)
DCTN1	2p13	Dynactin subunit 1	MND	-	(Puls *et al.* 2003, Münch *et al.* 2004)
ERBB4 (ALS19)	2q33.3-q34	ErbB4	MND	-	(Takahashi *et al.* 2013)
FIG4 (ALS11)	6q21	Polyphosphoinositide phosphatase	MND	PLS; CMT4J	(Chow *et al.* 2009)
GRN	17q21	Progranulin	<1% fMND	MND-FTLD; FTLD; Dementia with Lewy bodies; CBS	(Benussi *et al.* 2009)

HNRNPA1 (ALS20)	12q13.q	Heterogeneous nuclear ribonucleoprotein A1	MND	Multisystem proteinopathy	(Kim *et al.* 2013)
MATR3 (ALS21)	5q31	Matrin 3	fMND	Distal myopathy 2	(Johnson *et al.* 2014)
NEFH	22q12.2	Neurofilament heavy chain	MND	-	(Figlewicz *et al.* 1994, Skvortsova *et al.* 2004)
PRPH	12q12	Peripherin	sMND	Diabetes type 1?	(Gros-Louis *et al.* 2004, Leung *et al.* 2004)
SPG11 (ALS5)	15q21.1	Spatacsin	jMND	HSP4	(Orlacchio *et al.* 2010, Daoud *et al.* 2012)
SQSTM1	5q35	Sequestosome	MND	MND-FTLD; FTLD	(Fecto *et al.* 2011)
TAF15	17q11.1-q11.2	TATA-binding protein-associated factor 2N	MND	-	(Couthouis *et al.* 2011, Ticozzi *et al.* 2011)
TUBA4A	2q35	Tubulin, alpha 4a	fMND	MND-FTLD	(Smith *et al.* 2014)

ALS3 position 18q21 (Hand *et al.* 2002), ALS7 position 20p13 (Sapp *et al.* 2003) - unknown genes ᵅPhenotype more similar to Silver syndrome than MND. AOA2- Ataxia oculomotor apraxia 2; CBS – Corticobasal syndrome; CMT4J – Charcot Marie Tooth disease 4; fMND – familial MND; FTD – frontotemporal dementia; FTLD – frontotemporal lobar degeneration; HSA4 - Hereditary spastic paraplegia 4; IAHSP – infantile ascending hereditary spastic paralysis; IBMPFD - Inclusion Body Myopathy with Paget's disease of bone and/or Frontotemporal Dementia; jMND – Juvenile MND; PD – Parkinson's Disease; PLS – primary lateral sclerosis; PLSJ – primary lateral sclerosis, juvenile; PMA – progressive muscular atrophy; PSP - Progressive supranuclear palsy; SCA2- Spino-Cerebellar Ataxia-type 2; SMA4 – spinal muscular atrophy 4; sMND – sporadic MND; *****Most common genetic mutations

In addition to gene mutations that are thought to cause MND, over 100 other gene mutations have been proposed to increase MND risk (Abel 2015) but have not been defined in large populations of people. Deletions of one such gene, *SMN1*, are the cause of the fatal, juvenile-onset spinal muscular atrophy (SMA), and an abnormal number of copies of this gene (i.e. 1 or 3) are a genetic risk factor for sporadic MND (Corcia *et al.* 2002, Corcia *et al.* 2006, Blauw *et al.* 2012).

How gene mutations that appear to implicate quite different mechanisms in MND pathology result in selective killing of motor neurons and phenotypically similar disease is hard to determine. However, regardless of whether a person is determined to have MND of familial or sporadic origin, certain characteristics are observed as to which cell populations are first affected by disease progression and what mechanisms appear to contribute to neurodegeneration.

1.1.6. Cell selectivity and underlying pathogenesis

1.1.6.1. Cell selectivity

Many levels of cell selectivity are seen in MND, not only are sensory, autonomic, and cerebellar neurons spared or only affected to a sub-clinical degree, motor neurons are also differentially affected throughout disease pathogenesis.

The term ‘motor neuron’ covers many different subtypes with different molecular, functional, and connectional properties. These subtypes include distinctions based on the muscle fibre that the neurons innervate; α-motor neurons innervate extrafusal (contractile) skeletal muscle and drive contraction, γ-motor neurons innervate intrafusal (proprioceptive) skeletal muscle, and β-motor neurons innervate both muscle types (see Kanning *et al.* 2010 for review). In addition, α-motor neurons are subdivided based on the contractile properties of the motor units they form with muscle fibres; fast-twitch fatigable (FF), fast-twitch fatigue-resistant (FR), and slow-twitch fatigue-resistant (S) (Burke *et al.* 1973). In $SOD1^{G93A}$ MND model mice, different motor neuron subtypes are affected differently by disease progression, with FF α-motor neurons undergoing atrophy earliest (Frey *et al.* 2000) followed by a delayed but rapid and synchronised dying back of FR α-motor neurons and dying back of S α-motor neurons late in disease (Pun *et al.* 2006).

This differential atrophy of motor neurons also occurs in human disease. Electromyography (EMG) patterns are consistent with cycles of de- and re-innervation (de Carvalho *et al.* 2008b), fast twitch motor neurons are affected earliest in sporadic MND cases (Dengler *et al.* 1990), and differential loss of voluntary movement is recorded. For example, most voluntary movement is lost at late stages of MND and there is significant loss of upper motor neurons in the motor cortex and lower motor neurons in the brain stem and spinal cord. However, eye movements, controlled by the cranial motor nuclei of the oculomotor, trochlear and abducens nerves; and voluntary control of the bowel and bladder, innervated by neurons in Onuf's nucleus; are typically retained until terminal stages (Kihira *et al.* 1997, Valdez *et al.* 2012, Brockington *et al.* 2013). People with MND placed on long-term mechanical ventilation show expansion of the typical motor neuron degeneration seen in MND, including loss of basal ganglia neurons (see Swash & Desai 2001 for review) and paralysis of eye movements (Mizutani *et al.* 1992).

Similar patterns of degeneration are seen in other neurodegenerative diseases such as spinal muscular atrophy (Kubota *et al.* 2000) and also in ageing (Kihira *et al.* 1997, Valdez *et al.* 2012), which suggests that the differing susceptibility of motor neurons to degeneration is due to the characteristics of motor neuron subtypes in general, and are not specific to MND (see Kanning *et al.* 2010 for review).

In addition to differences seen in intrinsic motor neuron vulnerability, research from SOD1 mutation studies suggest that the surrounding, non-neuronal environment plays an important role in the susceptibility of motor neurons to degeneration. Clement and colleagues (2003) found that mutant $SOD1^{G37R}$ or $SOD1^{G93A}$ motor neurons, surrounded by normal non-neuronal cells, do not undergo neurodegeneration, whereas normal motor neurons surrounded by mutant non-neuronal cells become damaged. Further studies have confirmed these findings (Pramatarova *et al.* 2001, Lino *et al.* 2002), and these findings suggest that a combination of intrinsic factors and the extracellular environment determine the susceptibility of different motor neuron populations to neurodegeneration. Mostly due to animal model studies, the internal mechanisms underlying motor neuron degeneration during MND are well documented, with numerous intertwined mechanisms being implicated in both familial and sporadic MND.

1.1.6.2. Non–cell autonomy

Multiple studies present evidence that motor neurons are affected by surrounding cells during MND disease pathogenesis (Yamanaka *et al.* 2008a, see Ilieva *et al.* 2009 for review). These findings are not surprising, as motor neurons do not exist and function in isolation and often rely on the supporting cell environment. Indeed, a complex interaction between all cell types in the central nervous system (CNS) plays an important role in disease pathogenesis. Although the initiation and progression events and interaction between disease mechanisms are unknown, investigations using mice models with conditional depletion or expression of mutant SOD1 support the concept that non-neuronal cells contribute to both the onset and progression of MND. For example, when selectively expressed in motor neurons, microglia, astrocytes, or Schwann cells alone, mutant SOD1 does not cause motor neuron degeneration; unlike MND model animals that express mutant SOD1 ubiquitously (Gong *et al.* 2000, Pramatarova *et al.* 2001, Beers *et al.* 2006, Dobrowolny *et al.* 2008, Jaarsma *et al.* 2008, Turner *et al.* 2010). However, loss of mutant $SOD1^{G37R}$ or mutant $SOD1^{G85R}$ from microglia delayed disease progression and increased survival (Boillée *et al.* 2006, Wang *et al.* 2009), and deleting mutant SOD1 from astrocytes also extended survival by slowing disease progression (Yamanaka *et al.* 2008b). These mouse studies show that mutant SOD1 in the surrounding glial cells strongly influences the degeneration of motor neurons. In addition, replacing the myeloid lineage of mutant SOD1 mice with wild type (WT) microglia/macrophages slowed disease progression (Beers *et al.* 2006). This suggests MND develops in multiple cellular compartments that ultimately lead to neuromuscular failure. The contribution that cell types such as astrocytes, microglia, T-cells, oligodendrocytes, and Schwann cells have on MND pathology will now be discussed.

Astrocytes

Astrocytes, the most numerous non-neuronal cell type in the central nervous system (CNS), perform a variety of functions including defense of the CNS, control of the blood brain barrier and blood flow, maintenance of low extracellular levels of glutamate, and maintenance and nourishment of CNS neurons (see Blackburn *et al.* 2009, Lasiene & Yamanaka 2011, Valori *et al.* 2013 for reviews). In MND, astrocytes have been implicated in pathogenesis in two interconnected aspects. The

first, is the contribution of astrocytes to motor neuron death through the secretion of neurotoxic factors, the second, evidence that astrocytes lose some of their normal motor neuron supportive functions and undergo degeneration themselves, thus leaving motor neurons prone to damage.

One main function of astrocytes is to maintain low extracellular glutamate levels through the modulation of the GluR2 subunit of motor neuron AMPA receptors. In SOD1-linked MND, mutant astrocytes lose this modulating ability, thereby exposing motor neurons to an enhanced level of calcium influx, resulting in excitotoxicity and death. Mutant SOD1 motor neurons surrounded by WT astrocytes do not succumb to excitotoxicity, providing evidence that mutant SOD1 astrocytes are pathogenic (Van Damme *et al.* 2007).

Additionally, healthy astrocytes release the neurotrophic factors glial cell line-derived neurotrophic factor, brain-derived neurotrophic factor, ciliary neurotrophic factor, and vascular endothelial growth factor, and the metabolic substrate lactate, in support of motor neurons (see Ekestern 2004, Lasiene & Yamanaka 2011 for reviews). Mutant astrocytes show a reduced capacity to release lactate (Ferraiuolo *et al.* 2011a) and a loss of these supportive factors may also indirectly cause motor neuron death.

Microglia & immune responses

Microglia are the resident macrophage cells of the CNS and are the primary mediators of inflammation (see Khandelwal *et al.* 2011 for review). Normally, microglia play a surveillance role, but, in response to damage, microglia change their morphology and clear the debris from damaged cells. However, in cleaning up debris, microglia release toxic substances such as pro-inflammatory cytokines and reactive oxygen species (ROS) (see Lasiene & Yamanaka 2011 for review). As a result, macrophages provide protection and cause toxicity in MND.

The involvement of microglia is described in many acute and chronic neurological diseases. In MND models and people with MND, microglia activation is detected early in disease pathogenesis (Hall *et al.* 1998), particularly in areas of motor neuron loss (Turner *et al.* 2004), and is correlated with disease progression (Turner *et al.* 2004, Brettschneider *et al.* 2012a, Brettschneider *et al.* 2012b). In SOD1-linked MND, microglial activation is triggered by the secretion of aggregated

mutant SOD1 protein (Roberts *et al.* 2013). The removal or reduction of mutant SOD1 from microglia (Boillée *et al.* 2006, Wang *et al.* 2009), and replacement of microglia with WT microglia via bone marrow transplantation (Beers *et al.* 2006) slows disease progression in SOD1 mutant mice. These studies suggest that mutant microglia play an important role in motor neuron death and rate of disease progression, and this may be due to a reduction in their neuroprotective function (Sargsyan *et al.* 2011, Kawamura *et al.* 2012, Liao *et al.* 2012) and a dysregulation of inflammation (Frakes *et al.* 2014). Additionally, a reduction in neuroprotective T-cells has also been found in SOD1 MND model mice at the symptomatic stage (Kawamura *et al.* 2012).

Oligodendrocytes

Oligodendrocytes are the myelinating cells of the CNS, with one cell providing metabolic support and extending its processes around numerous axons. Oligodendrocytes provide support to neurons in the form of the energy metabolite lactate (Lee *et al.* 2012), but, in MND, this metabolic support is lost.

Similar to microglia and astrocyte changes, oligodendrocyte degeneration is seen in the spinal cord of $SOD1^{G93A}$ MND model mice before motor neuron loss at 60 days of age (Philips *et al.* 2013). Interestingly, the overall number of oligodendrocytes remains steady throughout disease due to an increased proliferation and differentiation of oligodendrocyte precursor cells, called $NG2^{+}$ cells, throughout disease progression (Philips *et al.* 2013). However these new oligodendrocyte cells are unable to provide the metabolic support required by neurons due to reduced expression of the monocarboxylate transporter 1 (Lee *et al.* 2012, Philips *et al.* 2013) which is required for lactate transport. Decreased monocarboxylate transporter 1 expression leads to motor neuron death *in vivo* and *in vitro* (Lee *et al.* 2012) and reduced expression is also seen in people with MND (Lee *et al.* 2012). The ability of $NG2^{+}$ cells to myelinate neurons may also be reduced as lactate regulates myelination, and myelin basic protein is also reduced in the newly differentiated oligodendrocytes of $SOD1^{G93A}$ MND model mice (Philips *et al.* 2013). Additionally, mutant SOD1 results in a reduction of monocarboxylate transporter 1 expression in human embryonic kidney cell experiments, and in $SOD1^{G93A}$ MND model mice (Philips *et al.* 2013).

Schwann cells

Schwann cells, the myelinating cells of the peripheral nervous system (PNS), are intimately associated with all peripheral nerve axons and are essential for their long-term preservation and survival (Reddy *et al.* 2003). Following neuronal damage, Schwann cells lose their differentiated morphology and up-regulate genes linked to promoting axonal growth, neuronal survival, and macrophage invasion, playing a role in clearing debris and guiding the recovering axon (Arthur-Farraj *et al.* 2012). However, in MND, Schwann cells show signs of distress before symptoms arise (Keller *et al.* 2009) and so their normal neurodegeneration response role may be inhibited.

Studies into the role of Schwann cells in MND show contradictory results. Expression of mutant $SOD1^{G37R}$ protein in Schwann cells is not detrimental to motor neurons and has no effect on disease (Turner *et al.* 2010) but $SOD1^{G37R}$ removal from Schwann cells results in an increase in late stage neurodegeneration (Lobsiger *et al.* 2009). Studies in the $SOD1^{G85R}$ mutant mouse show delays in disease onset and extension of survival following Schwann cell $SOD1^{G85R}$ knock-down (Wang *et al.* 2012), but this increase in survival may be due to the unstable nature of the $SOD1^{G85R}$ model.

1.1.6.3. Underlying pathogenesis

There is no consensus as to the primary toxicity of MND. However, cell and animal-based models, and post-mortem examination of people with MND, have provided information about the interconnected mechanisms involved, including glutamate excitotoxicity; oxidative stress; mitochondrial dysfunction; axonal disorganisation and disrupted transport; and the failure of proteostasis and abnormal protein aggregation (**Figure 1.3**).

Excitotoxicity

Fatal to cells, excitotoxicity is described as the mishandling of the excitatory neurotransmitter glutamate, and the subsequent influx of excessive calcium and an increase in nitric oxide formation (Rothstein *et al.* 1990). In healthy neurons, glutamate is removed from the synaptic cleft by re-uptake transporters, mostly by the astroglial glutamate transporter EAAT2. However in MND, the expression of EAAT2 is down-regulated in damaged CNS areas (Rothstein *et al.* 1995, Howland

et al. 2002) and abnormalities in EAAT2 protein expression is found in up to 80% of brain stem and spinal cord tissue (Rothstein *et al.* 1995). Additionally, glutamate levels are increased in the CSF of some people with MND (Rothstein *et al.* 1990, Spreux-Varoquaux *et al.* 2002).

The downstream effects of excitotoxicity may provide a positive feed-forward loop, which further propagates motor neuron damage. Excess calcium entering the cells quickly becomes a problem as motor neurons do not buffer cytosolic levels of calcium well, compared to other neuronal populations (Palecek *et al.* 1999). In MND this may also be due to decreased levels of calcium binding proteins such as calbindin D28k and parvalbumin (Ince *et al.* 1993). Together, this results in the rapid uptake of calcium by the mitochondria, and increased reactive oxygen species production (Rao *et al.* 2003). These reactive oxygen species (ROS) may then exit the motor neuron and disrupt glutamate transport in surrounding astrocytes (i.e. decrease of EEAT2 expression), leading to additional extracellular glutamate accumulation and further excitotoxicity (Rao *et al.* 2003). Additionally, excitotoxicity may arise due to energy metabolism dysfunction under which normal levels of glutamate become toxic (Turner *et al.* 2013a) or through interneuronal dysfunction resulting in unbalanced glutamate activity (Turner & Kiernan 2012).

Oxidative stress

Oxidative stress is caused by an imbalance between the production and breakdown of reactive oxygen species (ROS) such as superoxide and hydrogen peroxide, and/or an inability of the cell to repair oxidative damage. Oxidation stresses aged, non-replicating neurons by causing structural damage to many cellular components, and post-mortem tissue from people with MND has shown elevated oxidative damage to proteins (Shaw *et al.* 1995), lipids (Shibata *et al.* 2001), DNA (Fitzmaurice *et al.* 1996), and RNA (Chang *et al.* 2008). Additionally, markers of oxidative stress have been found at higher levels in the CSF (Smith *et al.* 1998), serum (Simpson *et al.* 2004), and urine (Mitsumoto *et al.* 2008), of people with MND.

In SOD1-linked MND, the normal role of SOD1 as a free radical scavenger may put it at a risk of oxidative damage, and that this may cause cytotoxic misfolding ‘primed’ by mutations and its aggregation (Rakhit *et al.* 2002). Mutant SOD1 may

also cause oxidative stress in SOD1-linked MND; the presence of mutant SOD1 in microglia can lock Rac1 into an active state in the NADPH oxidase complex, which results in the continued production of toxic ROS (Harraz *et al.* 2008). Oxidative stress is also seen in mouse models of MND, primarily in motor neurons and oligodendrocytes, and is first detected early, in pre-symptomatic stages of disease (Ferraiuolo *et al.* 2011b). The presence of mutant TDP-43 also results in oxidative stress in motor neuron cell lines (Duan *et al.* 2010).

Mitochondrial dysfunction

Mitochondria act as an energy source for cells, buffer intracellular calcium, and regulate apoptosis (see Turner *et al.* 2013a for review). These roles are crucial to the health of all cells, and dysfunction can be devastating. Neurons have a higher density of mitochondria than other cell types, making them particularly vulnerable to abnormalities. Mitochondrial abnormalities are seen in a number of neurodegenerative diseases and were first detected in MND in the form of mitochondrial aggregates in muscles and spinal cord motor neurons (Sasaki & Iwata 1996).

Mutant and misfolded SOD1 species are implicated in many aspects of motor neuron mitochondrial damage. Some SOD1-linked damage is seen pre-symptomatically, including prominent vacuolar degeneration and electron transport chain impairments (Jung *et al.* 2002); SOD1 aggregates on the outer membrane of mitochondria which change mitochondrial morphology (Vande Velde *et al.* 2011b); disruption of axonal transport of mitochondria by mutant SOD1 (De Vos *et al.* 2007, Song *et al.* 2013); and the presence of misfolded WT SOD1 (Bosco *et al.* 2010) which results in a depletion of mitochondria in the axons before neurodegeneration.

Additionally, impaired ATP synthesis and reduced calcium buffering is seen in SOD1 mutant cells (Coussee *et al.* 2011) and mouse model motor neurons (Jaiswal & Keller 2009), and SOD1 accumulation in the mitochondrial intermembrane space impedes protein import, causing cytochrome c release and apoptosis (Igoudjil *et al.* 2011).

Proteostasis failure and abnormal protein aggregation

Autophagy and the ubiquitin proteasome system (UPS) are the two major protein degradation pathways in cells. The UPS degrades unneeded and/or damaged proteins, which are tagged with poly-ubiquitin sequences, by proteolysis, and autophagy is the process by which cellular organelles are degraded.

Intracellular inclusions of misfolded and aggregated proteins in motor neurons and oligodendrocytes are a hallmark of MND (Blokhuis *et al.* 2013). These inclusions are characteristic of many neurodegenerative diseases including Parkinson's disease (alpha-synuclein), Alzheimer's disease (tau and lewy bodies), and Huntington's disease (Huntington protein). However, unlike many other neurodegenerative diseases, inclusions commonly found in people with MND do not fit amyloid characteristics (Kerman *et al.* 2010). For example, MND inclusions typically contain the causal mutated protein in familial MND along with ubiquitin and TDP-43, except for SOD1-linked MND, which contain SOD1 but not TDP-43. Such proteins are also seen in inclusions in people with sporadic MND. Additionally, the existence of prion-like domains in SOD1, TDP-43, and FUS/TLS proteins suggests that cross-seeding may occur, which could explain why multiple proteins are seen in MND inclusions (Blokhuis *et al.* 2013).

It is unknown whether the formation and continued presence of abnormal protein inclusions is a toxic or neuroprotective mechanism. Regardless, their presence suggests a misregulation of the UPS, which can prove fatal to cells, as misfolded proteins, such as SOD1, are cytotoxic. Additional evidence for the failure of the UPS is the discovery of mutations in proteins involved in proteostasis, such as UBQLN2 (Ko *et al.* 2004) which binds ubiquinated proteins and delivers them to the UPS and autophagy machinery, and VCP, which unfolds proteins and dissembles complexes in the endoplasmic reticulum, and during proteasomal protein degradation, and autophagy (Meyer *et al.* 2012).

Axonal disorganisation and disrupted transport

Motor neurons can be 5,000 times the volume of other cell types and their extremely long axons depend on transport for the delivery of essential cell components. Therefore, motor neuron survival is reliant upon correctly functioning intracellular transport systems.

Disrupted axonal transport is seen in MND (Perlson *et al.* 2009). Mutations of the transport proteins dynein (Hafezparast *et al.* 2003) and dynactin (Puls *et al.* 2003, Münch *et al.* 2004), involved in retrograde transport, and kinesin-1 (Reid *et al.* 2002), involved in anterograde transport, have been linked to motor neuron degeneration. Additionally, elevated tumor necrosis factor levels disrupt normal kinesin function via a mechanism involving p38 MAPK (Dewil *et al.* 2007). Further studies suggest that changes in retrograde signalling lead to increased transport of stress or cell death-related proteins as opposed to survival-promoting factors in MND, further contributing to motor neuron degeneration (Perlson *et al.* 2009).

Axonal disorganisation and accumulation of mitochondria and neurofilaments are also seen in MND. The accumulation of neurofilaments has been linked to kinesin-1 failure in a kinesin-1 heavy chain KIF5 postnatal knock-out model (Xia *et al.* 2003), and a decrease in neurofilament light chain has been linked to the presence of mutant SOD1 or TDP-43, where mutant SOD1 or TDP-43 binds to NEFL mRNA, sequesters it into stress granules, and prevents neurofilament light chain translation (Volkening *et al.* 2009).

Molecular research into MND disease mechanisms is a new field of research only made possible by genetic mutation discovery and the generation of MND models. What is now clear is that MND is a non-cell autonomous, multi-system disease in which subtypes of motor neurons are the first to be affected. With many potential environmental and lifestyle factors and varied genetic factors contributing to disease pathogenesis, it should come as no surprise that diagnosing MND is not straightforward.

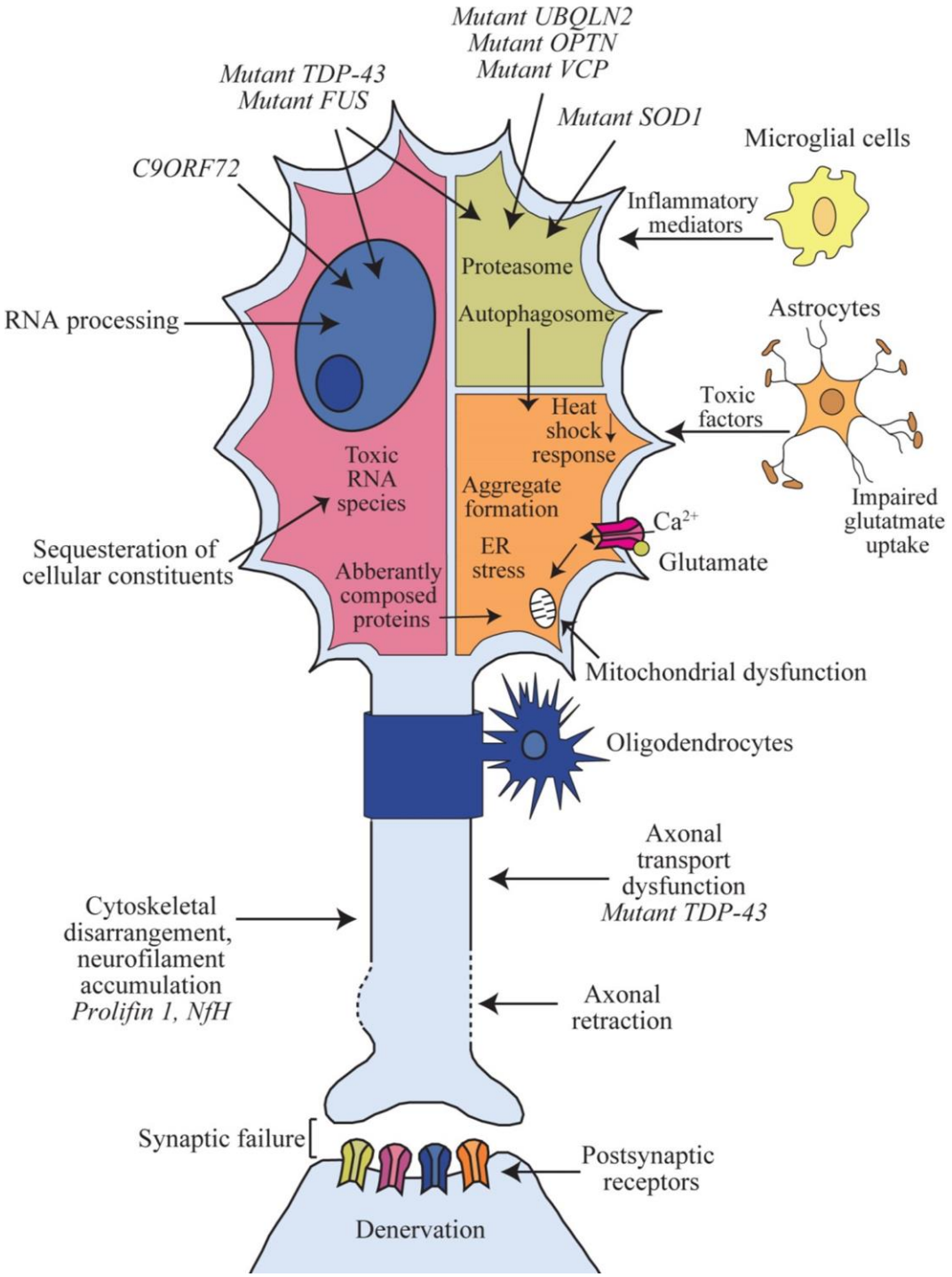

Figure 1.3: Overview of pathogenic mechanisms in MND

Although there is no consensus on the primary toxicity of MND, cell- and animal-based models, and post-mortem examination of people with MND, has elucidated a wide range of interconnected mechanisms altered by disease pathogenesis. These include, disturbance of normal RNA processing, resulting in misassembled proteins and toxic RNA species (■); interference with normal proteasomal or autophagic protein degradation (■); and progressive cellular failure (■) (adapted from Robberecht & Phillips 2013, Turner *et al.* 2013b).

1.2. Diagnosis, progression & treatment

1.2.1. Diagnosis

Early diagnosis of MND is difficult, not only because of its heterogeneous nature, but also because it shows clinical similarity to other neurodegenerative diseases (Brooks *et al.* 2000). Early MND symptoms include walking difficulties, loss of hand dexterity and/or shoulder weakness in limb onset disease, or speech and swallowing problems in bulbar onset disease. The mean delay in time of symptom onset to diagnosis remains at approximately one year (Mitchell *et al.* 2010a, Cellura *et al.* 2012, Nzwalo *et al.* 2014), around a third of the average survival time from symptom onset.

There is no definitive laboratory test to readily and accurately confirm MND in its early stages, and certainty of diagnosis relies on a combination of clinical and electrophysiological criteria that are designed to rule out other potential causes of progressive muscle weakness and paralysis (**Table 1.2**; Rezania & Roos 2013). Clinical guidelines for the diagnosis of MND were first proposed in 1957 (Lambert & Mulder 1957), and in 1990, the El Escorical criteria were established, defining four levels of MND diagnostic certainty (Brooks 1994). These criteria were revised by a second workshop (Brooks *et al.* 2000), and again, following the finding that the criteria were too restrictive for easy recruitment to clinical trials and for MND diagnosis (Traynor *et al.* 2000). Currently, the fourth version of the El Escorial criteria, termed the Awaji criteria, is used for MND diagnosis (**Table 1.3**; de Carvalho *et al.* 2008a).

Reviews of MND diagnostic criteria have found the most recent modifications are in higher agreement with clinical diagnosis of MND than previous revisions, and allow for earlier diagnosis (Chen *et al.* 2010, Douglass *et al.* 2010). For example, the Awaji criteria provide a higher sensitivity of MND diagnosis when measuring fasciculation potentials during the first examination, compared to older criteria, in people with bulbar onset disease (probable/definite MND 82% versus 59%; Noto *et al.* 2012).

It is expected that further modifications to the Awaji criteria will be made as developments produce a more thorough understanding of MND pathogenesis. For

example, under the current criteria, people who present specifically with lower motor neuron damage (progressive muscular atrophy, PMA) are not diagnosed with a form of MND although approximately one-fifth of these people go on to develop upper motor neuron damage within 5 years (Kim *et al.* 2009). Further, there are suggestions that testing for frontal deficits also be added to the diagnostic criteria (Ludolph *et al.* 2012).

Despite these limitations, the current Awaji criteria are the gold standard for MND diagnosis, relying on multiple tests to identify MND from other causes of motor dysfunction. Using these criteria, the diagnosis of MND requires the presence of particular symptoms, along with the absence of evidence that could suggest other possible causes, as outlined in **Table 1.2**. Providing these criteria are met, people are then placed into one of three diagnostic categories; clinically definite, clinically probable, or clinically possible, depending on the certainty of disease diagnosis (**Table 1.3**). Hence, a diagnosis of MND requires the presence of both upper and lower motor neuron symptoms, evidence of spread of disease, and ruling out other diseases using clinical tests such as neuroimaging and electrophysiology.

Theoretically, MND can be differentiated from other conditions as MND mimics are frequently associated with pain, sensory impairment, oculomotor issues, and bowel or bladder problems, all of which are typically absent in MND (**Table 1.4**; de Carvalho *et al.* 2008a). However, in practice, heterogeneous symptoms add to a drawn-out process of elimination and eventual MND diagnosis.

Table 1.2: Requirements for the diagnosis of MND using the Awaji criteria
(adapted from de Carvalho *et al.* 2008a)

Presence of	Absence of
Evidence of lower motor neuron degeneration by clinical, electrophysiological or neuropathological examination	Electrophysiological or pathological evidence of other disease processes that might explain the signs of upper and/or lower motor neuron degeneration, **and**
Evidence of upper motor neuron degeneration by clinical examination, **and**	Neuroimaging evidence of other disease processes that might explain the observed clinical and electrophysiological signs
Progressive spread of symptoms or signs within a region or to other regions; as determined by history, physical examination or electrophysiological tests	

Table 1.3: Diagnostic categories of MND using the Awaji criteria
(adapted from de Carvalho *et al.* 2008a)

MND diagnosis	Defined
Clinically definite	By clinical or electrophysiological evidence by the presence of lower motor neuron *as well as* upper motor neuron signs in the bulbar region and *at least two* spinal regions, or the presence of lower and upper motor neuron signs in *three* spinal regions
Clinically probable	By clinical or electrophysiological evidence of lower and upper motor neuron sings in *at least two regions* with some upper motor neuron signs necessarily rostral (above) the lower motor neuron signs
Clinically possible	When clinical or electrophysiological signs of upper and lower motor neuron dysfunction are found in *only one* region; or upper motor neuron signs are found alone in *two or more* regions; or lower motor neuron signs are found rostral to upper motor neuron signs. Neuroimaging and clinical laboratory studies will have been performed and other diagnoses must have been excluded

Table 1.4: Diseases of motor neurons including those that mimic MND
(adapted from Swash & Desai 2001, Turner & Talbot 2013)

Motor neuron diseases of unknown cause
MND (upper and lower motor neuron damage) with and without frontotemporal dementia
Progressive bulbar palsy
Progressive muscular atrophy (typically lower motor neuron only, pathologic evidence of upper motor neuron involvement)
Primary lateral sclerosis (upper motor neuron damage only)
Juvenile & Guamanian MND
Madras motor neuron disease
Monomelic motor neuron disease
Motor neuron-involvement in multi-system dysfunction
Olivopontocerebellar degenerations, Joseph-Machado disease, Creutzfeldt-Jakob disease, multiple system atrophy, electric and lightning injuries to spinal cord, post irradiation syndromes
MND mimics
Amyotrophy syndromes
Adult onset proximal SMA and Kennedy's syndrome (predominant lower motor neuron, very slow progression with gynaecomastia, and often prominent chin fasiculations)
Postpolio amyotrophy
Physical injury
Radiation myelopathy, post-traumatic syringomyelia
Endocrine diseases
Thyrotoxicosis, hyperparathyroidism
Toxins
Lead, mercury, cyanide (konzo), Oxalyldiaminopropionic acid (lathyrism)
Neuropathies
Multifocal motor neuropathy (weakness greater than wasting, slowly progressive)
CIDP (predominant upper motor neuron, symmetrical, fluctuating, mild sensory features, slowed conduction velocity)
Other - predominant lower motor neuron signs
Neuralgic amyotrophy (severe pain at onset and arrest of progression)
Inclusion body myositis (slowly progressive, predilection for quadriceps and medial forearms especially with serum creatine kinase >1000IU/l)
Other - predominant upper motor neuron signs
Hereditary spastic paraparesis (younger onset, slowly progressive, minimal upper limb involvement, especially with family history)
Primary progressive multiple sclerosis (slowly progressive, often with sensory features, especially where there is possibly MRI evidence of demyelination and positive CSF oligoclonal bands)
Other - mixed motor neuron signs
Cervical myeloradiculopathy (prominent neck pain especially with sphincter involvement, may be pure motor)

CIDP – chronic inflammatory demyelinating polyradiculopathy; SMA – spinal muscular atrophy.

Although a concerted effort is being made to improve the Awaji, and other, clinical testing criteria, there are limitations to depending on clinic-based tests for disease diagnosis. The current delay between onset and diagnosis of one year, using these diagnostic criteria, corresponds to the midpoint of disease duration (Mitchell *et al.* 2010a, Cellura *et al.* 2012, Nzwalo *et al.* 2014), which limits the window of opportunity for possible effective treatments. Aside from the worrying delay to diagnosis, clinic-based tests require rigorous internal controls to maintain reliability and there is a high potential for variability both within individuals with MND, and between clinicians (Gordon *et al.* 2004). The effectiveness of tests is also subject to continued co-operation of participants in performing invasive procedures.

1.2.2. Progression and measures

MND progression is monitored in the clinic by using functional rating scales to measure symptom severity, which are then used to determine when individuals require symptom management such as feeding and/or respiratory assistance. Such functional rating scales include the Amyotrophic Lateral Sclerosis Functional Rating Scale–revised (ALSFRS-r; Kaufmann *et al.* 2005), and forced vital capacity (FVC), a measure of respiratory function (Brinkham *et al.* 1997, Clavelou *et al.* 2013).

The ALSFRS-r, a simple 12 multiple choice questionnaire that measures an individual's capacity to perform every-day activities such as eating and walking (Cedarbaum *et al.* 1999), allows for quick analysis of function, contrary to the difficulties of diagnosis (full ALSFRS-r scale in **Appendix A**). Other disability scales used in MND progression include the historic data based ALS severity scale (Hillel *et al.* 1989) and the Norris (Norris *et al.* 1974) and Appel/Baylor (Appel *et al.* 1987) scales, which are based on clinical test results. The ALSFRS-r is the only disability scale that has been tested for validity and reliability, correlating with general physiological measures of disease progression, such as the global Schwab & England activities of daily living rating scale, and survival estimations in clinical trials (Kaufmann *et al.* 2005, Kaufmann *et al.* 2007, Kollewe *et al.* 2008).

Although the ability to perform everyday tasks is an important measure of progression for people living with MND, it remains that such rating scales are

subjective tests, and are open to bias and misinterpretation. For example the ALSFRS-r presents a more accurate representation of disease status when used as a profile of mean scores from three different domains (bulbar, motor, respiratory) than a global total score (Franchignoni *et al.* 2013), which is used in the clinic.

Forced vital capacity (FVC), a measure of inspiratory muscle strength, is a recommended test for clinical trials and MND management (Brinkham *et al.* 1997) as the majority of MND deaths are due to a decline in respiratory muscles (Vande Velde *et al.* 2011a). FVC as a single measure has been linked to prognosis and disease progression, where a baseline FVC measurement below 75% resulted in a median survival of 2.91 years, compared to 4.08 years for patients with FVC levels above 75% at baseline (Czaplinski *et al.* 2006), but, FVC did not have prognostic relevance in estimating death within 12 months in another study (Wolf *et al.* 2014). FVC testing also faces limitations, in that its accuracy is dependent on the effort and co-operation of individuals being tested, and the training of the administering technical staff (Czaplinski *et al.* 2006).

The above classifications allow for the tracking of disease progression, but currently, no formal disease staging systems are used in the clinic. Two types of staging systems have recently been proposed, one based on the number of regions involved in disease (Roche *et al.* 2012), the other based on the ALSFRS-r (Chiò *et al.* 2013a, Balendra *et al.* 2014). Together with functional rating scales, it is hoped that these staging systems will allow for more accurate tracking of disease progression. However validation of these measurements in large populations is required (Roche *et al.* 2012, Chiò *et al.* 2013a).

1.2.3. Current treatment, management and advances

1.2.3.1. Treatment

At present, therapeutic options are limited; the only FDA approved treatment for MND is the glutamate antagonist Rilutek, marketed as riluzole. A Cochrane meta-analysis of 3 studies, totalling 876 riluzole-treated and 406 placebo-treated people with MND, found that taking riluzole, at 50mg twice a day, improves 1-year survival by about 15% and increases overall life expectancy by just 2-3 months in comparison to placebo-treated individuals (Miller *et al.* 2012). Unfortunately,

riluzole does not repair the already significant damage to the CNS once MND symptoms are apparent, and in the first clinical trial, the beneficial effect of riluzole was not obvious to the people with MND, their families, or their doctors (Bensimon *et al.* 1994). Riluzole is now out of patent (June 18, 2013), and still no other effective treatments have been identified from over 30 clinical trials in MND (Aggarwal & Cudkowicz 2008).

1.2.3.2. Management

As riluzole is unable to cure disease or prolong life expectancy longer than 2-3 months, all remaining MND care is palliative. This includes the provision of walking assists or wheelchairs, off-label standard therapies, assisted ventilation when people with MND are unable to breathe alone, and gastrostomy for nutritional support (see Gordon 2011 for review). Of these palliative care strategies, two potentially prolong survival in people with MND, that of percutaneous endoscopic gastronomy (PEG), which stabilises body weight, and non-invasive ventilation, which is potentially effective in slowing the rate of forced vital capacity (FVC) decline (Miller *et al.* 2009).

Practical management guidelines found that diagnosis and care of people with MND in MND specific, multi-disciplinary clinics results in a longer life expectancy than both care in a generic neurological clinic, and treatment with riluzole (Miller *et al.* 2009). Specialists involved in such MND specific clinics include neurologists, MND nurses, physical, occupational, and respiratory therapists, speech pathologists, dieticians, social workers, pulmonologists, gastroenterologists, and psychiatrists or psychologists (see Gordon 2011 for review).

1.2.3.3. Advances in therapeutics

Although first described by Charcot over 140 years ago (Charcot 1874) most major advances in the understanding of MND have been made in the last 15-20 years (see Zinman & Cudkowicz 2011 for review), and the search for effective treatments has shown significant promise only in the last decade or so.

A plethora of symptomatic drugs are used to treat MND in addition to riluzole, ranging from treatments for fatigue, anxiety, depression, spasticity, cramps, impaired sleep, and constipation (see Gordon 2011 for review), but as yet, there are no effective treatments to halt disease progression.

In 2015, over 15 clinical trials of MND therapies are underway or recruiting to test potential therapeutics (clinicaltrials.gov). Many potential therapeutics have reached phase II clinical trials but have shown disappointing results. For example, lithium showed promising results in a small clinical trial (Fornai *et al.* 2008), but progression to a phase III clinical trial showed it has no effect on disease progression over an 18 month period (UKMND-LiCALS Study Group *et al.* 2013). Another drug, dexpramipexole, touted as one of the most promising drugs since riluzole, showed promise in cell and animal models (Danzeisen *et al.* 2006), and phase I (Bozik *et al.* 2011), and phase II (Cudkowicz *et al.* 2011) trials. However, a phase III study found that dexpramipexole had no benefits over placebo in the rate of ALSFRS-r change from baseline, or time to death (Cudkowicz *et al.* 2013).

Despite these failures, a number of potential therapeutics continue to be tested. These include treatments for mutant genes such antisense *SOD1* (Miller *et al.* 2013) and immunisation using antigenic peptides (Liu *et al.* 2012); treatments for excitotoxicity, targeting molecular chaperones (Arimoclomol; Lanka *et al.* 2009), EAAT2 glutamate receptors (Ceftriaxone; Zhao *et al.* 2014) or sodium channels (Mexiletine; Clinicaltrials.gov: NCT01849770, NCT01811355); treatments targeting axonal outgrowth (Ozanezumab; Meininger *et al.* 2014); muscle contractility (Tirasemtiv; Shefner *et al.* 2013, Hwee *et al.* 2014); or singular cell components such as macrophages (Tocilizumab; Fiala *et al.* 2013, NP001; Miller *et al.* 2014), mitochondria (UDCA; Min *et al.* 2012, Olesoxime; Lenglet *et al.* 2014) astroglia and microglia (Fasudil; Takata *et al.* 2013). Additionally, antioxidants (Edaravone; Ito *et al.* 2008), hypercaloric diets (Wills *et al.* 2014), neurotrophins (VEGF; Clinicaltrials.gov: NCT01384162, NCT01999806, CNTF; Selvaraj *et al.* 2012), and viral and non-viral gene delivery of treatments (Rogers *et al.* 2014) continue to be tested.

Currently, the initial testing of potential new therapies and testing of the underlying mechanisms of disease onset and progression is not possible in people with MND as disease progresses (Turner *et al.* 2013a). In order to study these aspects of disease, many *in vitro* and *in vivo* models of MND have been developed.

1.3. Models

1.3.1. *In vitro* models

Commonly used *in vitro* models of MND include isolated primary motor neurons, whole spinal cord or brain slices, co-culture systems of motor neurons and surrounding glia, and cultured cell lines derived from embryonic spinal cords.

Primary motor neurons, isolated from mouse (Bär 2000) or human (Silani *et al.* 2001) embryonic spinal cords, have been used to map individual neurons. However, rodent-derived isolated primary neurons in these cultures are vulnerable, dependent on trophic factors, and cannot be studied for extended periods of time as, without supporting glia, they die quickly (Bär 2000). In comparison, human-derived motor neurons isolated using this method have been reported to survive for 4 weeks (Silani *et al.* 2001).

Spinal cord slices and co-culture systems of motor neurons and surrounding cells are also used to model MND; these systems better retain the characteristics of *in vivo* motor neurons than cultured motor neurons alone, and provide superior models of whole system disease by incorporating the role of surrounding glia (Tovar-y-Romo *et al.* 2009). Spinal cord or brain slices can be kept alive in culture for months (Bär 2000), and have been used in MND research to test glutamate toxicity on motor neurons (Rothstein *et al.* 1992). A range of co-culture setups exist, from those containing isolated embryonic motor neurons seeded onto glia (Vandenberghe *et al.* 1998), to those including physiologically active mature motor neurons, interneurons, astroglia and peripheral glia (Haastert *et al.* 2005). More recently, a co-culture-based model of the neuromuscular junction has been developed, which cultures motor neuron and glia cell bodies in one microfluidic chamber, and allows for the connection of motor neuron processes and skeletal muscle in a distal chamber (Southam *et al.* 2013).

Motor neuron-enriched cultured cell lines, derived from the spinal cord of embryonic mice or chickens, have been used extensively to model underlying disease pathogenesis. Motor neuron vulnerability to excitotoxicity (Carriedo *et al.* 1996) mediated by calcium (Van Den Bosch *et al.* 2000), and preferential stimulation of reactive oxygen species (ROS) production by glutamate in motor

neurons (Rao *et al.* 2003) were first discovered using these cell lines. One such example is the motor neuron-enriched embryonic mouse spinal cord x immortal neuroblastoma cell line, NSC-34, which is a well-characterised model of MND. NSC-34 cells show properties of motor neurons including generation of action potentials, extension of processes and production, storage, and release of acetylcholine (Cashman *et al.* 1992). Mutant SOD1-expressing NSC-34 cell lines show similar pathogenic mechanisms to human MND, including Golgi apparatus fragmentation (Gomes *et al.* 2008) and mitochondrial dysregulation (Raimondi *et al.* 2006).

Recently, induced pluripotent stem cell-derived motor neurons (iPSCs) made from skin fibroblasts of people with MND have been developed (Dimos *et al.* 2008). TDP-43^{M337V} mutation carrying iPSCs reproduce several aspects of TDP-43-linked MND, such as aggregate formation and reduced cell survival (Bilican *et al.* 2012). This method can also be used to create other cell types from the same donor allowing for the study of cell-specific contributions to MND pathogenesis. However, sample sizes need to be considered using iPSCs cell lines as each line is derived from an individual person.

1.3.2. *In vivo* models

MND *in vivo* models are varied and range from naturally occurring, transgenic or pharmatoxological models including mammals such as mice, rats, and dogs, to simpler models such as fruit flies, zebra fish, worms, and yeast.

1.3.2.1. Naturally occurring models

A number of naturally occurring MND animal models exist, including the *pmn*, *wasted*, and *wobbler* mice strains, and canine degenerative myelopathy.

The *pmn* mouse contains a spontaneous recessive point mutation in the tubulin-specific chaperone E, which leads to progressive motoneuronopathy and death a few weeks after birth (Schmalbruch *et al.* 1991). This model presents with distal axonopathy, but motor neuron cell bodies and proximal axons are relatively spared in contrast to MND (Kennel *et al.* 1996).

The *wasted* mouse phenotype is caused be a DNA deletion preventing expression of the gene encoding the translation elongation factor EG1α2 (Chambers *et al.* 1998). This deletion results in early onset degeneration with vacuolisation in the anterior horn and brainstem motor nuclei (Lutsep & Rodriguez 1989) and lower motor neuron loss, but unlike human MND, upper motor neurons are not affected.

The *wobbler* mouse contains a spontaneous recessive point mutation in vesicular/vacuolar protein sorting 54 (Vps54), resulting in progressive degeneration of upper motor neurons and lower motor neurons, and cellular changes of transport defects, neurofilament aggregation, neuronal hyperexcitability and neuroinflammation, which closely resemble human MND pathogenesis. However, neurodegeneration is not restricted to motor neurons alone with interneurons also decreasing in number (Moser *et al.* 2013).

Another naturally occurring MND model is that of canine degenerative myelopathy, which is caused by the homozygous $SOD1^{E40K}$ mutation. Multiple dog breeds including Pembroke Welsh Corgis and Rhodesian ridgebacks develop this disease, characterised, like human MND, by SOD1 protein aggregation in the spinal cord, progressive loss of motor neurons, and paralysis (Crisp *et al.* 2013, Morgan *et al.* 2013).

Although of use for studying motor neuron degeneration, to date no naturally occurring models show all the signs of human MND pathogenesis. As a result, pharmatoxological and genetic manipulations have also been used in an attempt to better model human disease.

1.3.2.2. Pharmatoxological and transgenic models

Toxins used to induce motor neuron degeneration in animal models include excitotoxins such as β-methylamino-L-alanine (BMAA; de Munck *et al.* 2013), β-oxaylamino-L-alanine (Hugon *et al.* 1988) and kainic acid (Hugon & Vallat 1990, Sun *et al.* 2006), and metal ions such as aluminium (Strong & Garruto 1991). However, none of these models comprise all aspects of MND pathogenesis (Doble & Kennel 2000).

The most commonly used transgenic models of MND are mice and rats carrying mutations in the human *SOD1* gene. To date 13 different SOD1 mouse models have

been developed, all sharing features with human disease including; motor neuron death in the spinal cord and loss of myelinated axons in the ventral roots, accumulation of SOD1 and ubiquitin containing protein aggregations, neurofilament accumulation in degenerating motor neurons, and reactive microglia and astrocytes (see Doble & Kennel 2000 for review). However, these SOD1 rodent models differ in the times of disease onset and progression rates due to differences in mutations, genetic background, gender, and copy number of the *SOD1* gene (**Table 1.5**; Leitner *et al*. 2010). SOD1 mutations have also been used as the basis for MND models in other species including yeast (Bastow *et al.* 2011), worms (Oeda *et al.* 2001), fruit flies (Joyce *et al.* 2011) and zebra fish (Kabashi *et al.* 2011).

Table 1.5: Differences in disease characteristics in mutant SOD1 MND mouse model strains
(adapted from Leitner *et al.* 2010)

Characteristic	**G93A***	**G85R**	**G37R**	**D90A**	**G127X**	**H46R**
Inheritance	Dominant	Dominant	Dominant	Recessive	Dominant	Dominant
Protein aggregation propensity	High	High	Moderate	High	High	Low
Enzyme activity	Active	Inactive	Active	Inactive	Inactive	Inactive
Transgene stability	Stable	Reduced	Reduced	Stable	Unstable	Stable
Disease onset (mo)	Early (3-4)	Late (7.5)	Late (7.5)	Late (12)	Late (8-9)	Moderate (5)
Disease progression (weeks)	Moderate (3)	Fast (2)	Slow (4-6)	Slow (4)	Fast (1-1.5)	Slow (4)
Original publication	(Gurney *et al.* 1994)	(Bruijn *et al.* 1997)	(Wong *et al.* 1995)	(Jonsson *et al.* 2006)	(Jonsson *et al.* 2004)	(Sasaki *et al.* 2007)

*$SOD1^{G93A}$ strain – most well characterised, and only model used in pharmaceutical trials

SOD1 models have helped elucidate many mechanisms of MND pathogenesis such as mitochondrial dysfunction, protein misfolding and aggregation, and non-cell autonomy, and have been central to the understanding of the effects that mutant SOD1 has in MND. However, the differences between SOD1-linked MND and other genetic causes such as *FUS* and *TARDBP* mutations raise questions about the

validity of SOD1 models for all forms of MND. As a result, many other transgenic MND models have been researched. This includes the TDP-43-based models of; mutant carrying mice (Wegorzewska *et al.* 2009, Stallings *et al.* 2010, Swarup *et al.* 2011, Xu *et al.* 2011, Guo *et al.* 2012), rats (Huang *et al.* 2010, Zhou *et al.* 2010), worms (Vaccaro *et al.* 2012), yeast, fruit flies, and zebra fish (see Joyce *et al.* 2011 for review); WT mice (Shan *et al.* 2010, Stallings *et al.* 2010, Wils *et al.* 2010, Xu *et al.* 2010, Igaz *et al.* 2011, Swarup *et al.* 2011, Cannon *et al.* 2012) rats (Zhou *et al.* 2010) and monkeys (Uchida *et al.* 2012) and knock-down and knock-out mice (Kraemer *et al.* 2010).

FUS/TLS models include mutant carrying yeast (Bastow *et al.* 2011), worms (Vaccaro *et al.* 2012), fruit flies (Xia *et al.* 2012), zebra fish (Kabashi *et al.* 2011) and mice (Verbeek *et al.* 2012); human WT carrying mice (Verbeek *et al.* 2012, Mitchell *et al.* 2013) and knock-down zebra fish.

In addition, Alsin knock-down zebra fish and knock-out mice (Gros-Louis *et al.* 2008); over-expressing neurofilament heavy chain (NfH) (Côté *et al.* 1993) or peripherin (Millecamps *et al.* 2006) mice, and NfL^{L394P} point mutation mice (Lee *et al.* 1994b) have been developed, amongst others.

Since the discovery of TDP-43 protein mutations in 2008, 21 mouse and four rat TDP-43 models have been described in the literature (see McGoldrick *et al.* 2013 for review), including overexpression of mutant TDP-43 ($TDP\text{-}43^{A315T}$, $TDP\text{-}43^{M337V}$, $TDP\text{-}43G^{348C}$) or wild type TDP-43. Many of these models have resulted in variable phenotypes, including the $TDP\text{-}43^{A315T}$ mouse model, which can die due to gastrointestinal stasis, prior to the onset of significant neurological symptoms of MND (Guo *et al.* 2012, Esmaeili *et al.* 2013, Hatzpetros *et al.* 2013), unless fed jellified food (Herdewyn *et al.* 2014). Only three of the 25 TDP-43 models produced show the upper motor neuron and lower motor neuron degeneration characteristic of MND. The first such mouse model is the variable $TDP\text{-}43^{A315T}$ (Wegorzewska *et al.* 2009, Guo *et al.* 2012), which overexpresses the human $TDP43^{A315T}$ protein three-fold, and shows a loss of approximately 20% of lower motor neurons, with upper motor neuron degeneration also present. The second and third TDP-43-based mouse models showing upper and lower motor neuron degeneration overexpress WT TDP-43 (Wils *et al.* 2010). Although it is not reported whether axonal degeneration occurs, the fact that WT TDP-43 causes

degeneration highlights the importance of the normal role of TDP-43 (see McGoldrick *et al.* 2013 for review).

Similarly, FUS/TLS based models have had limited success in modelling upper and lower motor neuron degeneration as seen in human MND. Five rat and three mouse transgenic models have been researched with one showing promise; an overexpressing WT FUS/TLS mouse model with lower motor neuron loss of 60%, but no upper motor neuron loss (Mitchell *et al.* 2013). Similar to TDP-43, neurodegeneration caused by overexpression of WT FUS/TLS highlights the crucial role of the WT protein.

To date, no single model has been found to reproduce all the pathological and behavioural changes now recognised in human MND, but mutant SOD1 mouse models are regarded as the best models currently available (see Peviani *et al.* 2010 for review).

1.3.3. SOD1^{G93A} mice – the gold-standard pre-clinical MND model

First developed by Gurney and colleagues, the SOD1^{G93A} transgenic mouse carries multiple copies of a human mutant *SOD1* gene, that codes a protein with a mutation at position 93 where glycine is replaced by alanine (Gurney *et al.* 1994). The insertion of multiple copies of human mutant *SOD1* into mouse chromosome 12, results in the SOD1^{G93A} mouse showing similar disease pathogenesis to human MND, developing adult-onset weakness and atrophy of muscles, leading to paralysis and death (Gurney *et al.* 1994). In addition to similarities in clinical symptoms, the SOD1^{G93A} mouse model reproduces a large number of underlying pathological changes seen in both familial and sporadic human disease, including upper motor neuron and lower motor neuron degeneration, as summarised in **Figure 1.4**.

Two variations of the SOD1^{G93A} mouse model exist, differing by the number of copies of the human mutant *SOD1* gene they carry, which in turn, varies the age of disease onset and rate of disease progression. Expression levels produced by 23-25 copies of mutant *SOD1* produces a more severe phenotype in mice at an earlier age

compared to 8-10 copies, even though they have similar end stage pathologies. The low-copy number strain SOD1^{G93Adl}, results in disease onset at 170-240 days of age, reaching end stage of disease 2-10 weeks after disease onset, depending on genetic background (Alexander *et al.* 2004). SOD1^{G93Adl} mice with a B6 background show a 30% loss of motor units innervating the *extensor digitorum longus* muscle of the hind limb at disease onset of 170 days of age, and have the longest survival of the low-copy genetic backgrounds, reaching end stage of disease at 265 days of age (Acevedo-Arozena *et al.* 2011).

Comparatively, the high-copy number SOD1^{G93A} strain, which is the only model used in pharmaceutical trials, carries 23-25 copies of the mutant *SOD1* gene (Gurney *et al.* 1994). With a mixed C57BL/6J*SJ/LJ background, SOD1^{G93A} mice show behavioural signs of disease onset at 70-90 days of age and reach end stage of disease at ~130 days of age (Heiman-Patterson *et al.* 2005). In comparison, SOD1^{G93A} mice with a pure C57BL/6J (B6) background show behavioural disease signs at ~110 days of age and reach end stage 30-40 days after symptom onset, at 140-160 days of age (Heiman-Patterson *et al.* 2005). Similar to human MND pathogenesis, the underlying loss of motor neurons is present before behavioural symptoms of disease. In SOD1^{G93A} mice, motor neuron loss occurs before motor symptoms occur (Vinsant *et al.* 2013), and by end stage disease, 50% of the total motor neuron pool is lost (Chiu *et al.* 1995, Vinsant *et al.* 2013).

	Birth	10	20	30	40	50	60	70	80	90	100	110	120	130	140/death
	Pre-symptomatic										Onset		Symptomatic → End stage		
Systemic		Delay in righting and forelimb placing				100% muscle strength ↓ maximum running speed	Abnormal running gait 50% loss fast motor units		50% muscle strength	70% loss fast motor units	30% muscle strength 40% loss slow motor units		Hind limb paralysis		
Muscle				Muscle hyper-metabolism		FF neuromuscular junction loss & denervation	Depolarised mitochondria			FR neuromuscular junction loss & denervation	Vacuolised mitochondria			S neuromuscular junction loss & denervation	
Axon			Vacuoles in terminals	Mitochondrial dysfunction at nerve terminals	Mutant SOD1 in dendrites and nerve terminals Impaired retrograde and anterograde transport 100% large ventral root axon survival			Cytoplasmic vacuoles Axonal degeneration Neurofilament accumulation		Mutant SOD1 in cytoplasm 50% large ventral root axon survival		20% large ventral root axon survival	Large mutant SOD1 aggregates		

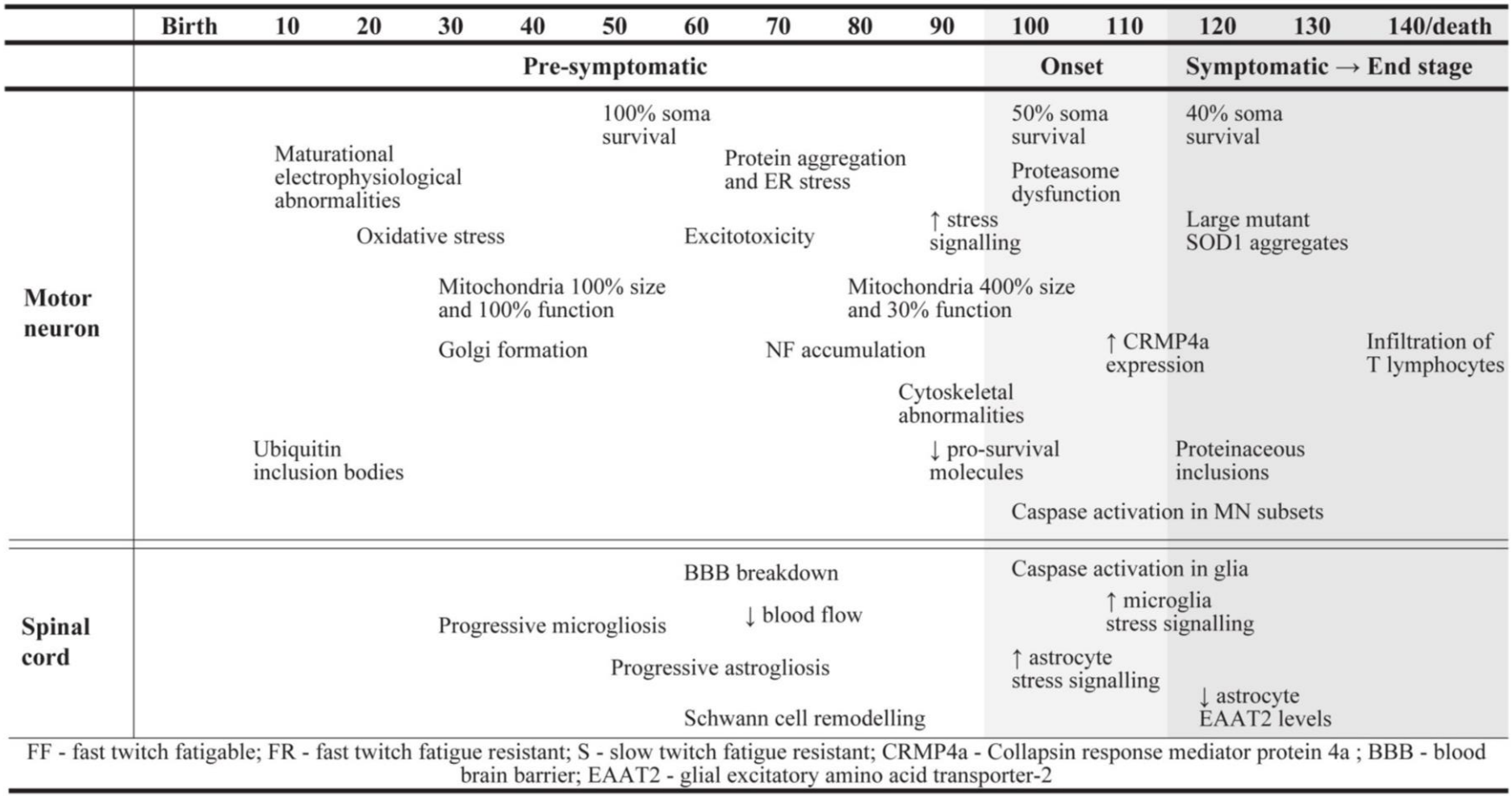

FF - fast twitch fatigable; FR - fast twitch fatigue resistant; S - slow twitch fatigue resistant; CRMP4a - Collapsin response mediator protein 4a ; BBB - blood brain barrier; EAAT2 - glial excitatory amino acid transporter-2

Figure 1.4: Known mechanisms underlying disease pathogenesis in the high-copy number SOD1^{G93A} MND mouse model
(adapted from Kanning *et al.* 2010, Peviani *et al.* 2010)

Choudry & Cudkowicz present guidelines for an ideal animal model of MND, stating that a model must follow the pathogenic process of human disease, exhibit the clinical and pathological signs of human disease, and respond to disease modifying treatments (see Choudry & Cudkowicz 2005 for review). The SOD1^{G93A} mouse model meets the first two criteria, but shows contradictory evidence for the third, where many potential treatments have shown success in the SOD1^{G93A} mouse but have failed to translate to people with MND in phase II/III clinical trials.

A thorough review of this issue found that treatments that were apparently successful in the SOD1^{G93A} mouse (Gurney *et al.* 1996, Gurney *et al.* 1998, Klivenyi *et al.* 1999, Trieu *et al.* 2000, Drachman *et al.* 2002, Van Den Bosch *et al.* 2002, Klivenyi *et al.* 2004, Rothstein *et al.* 2005, Ryu *et al.* 2005, Kiaei *et al.* 2006) did not provide benefits over untreated controls when re-tested under rigorous conditions (Scott *et al.* 2008). This paper resulted in five recommendations for testing potential therapies in the SOD1^{G93A} mouse model; using a minimum of 24 litter-matched, gender-balanced, mice per group, conducting experiments blind to genetic status, tracking non-MND linked deaths, monitoring transgene copy numbers to alleviate interference from low-copy number animals, and using the Cox proportional hazards model for statistical analysis (Scott *et al.* 2008).

No objective biological biomarkers exist in mouse MND models, so current practices for determining disease onset, progression, and the potential benefits of treatments are post-mortem examinations, and survival and behavioural tests (Klivenyi *et al.* 1999, Weydt *et al.* 2003, Miana-Mena *et al.* 2005, Leitner *et al.* 2010). In order to track changes in disease progression over time or to identify the effects of potential treatments, analysis is needed throughout an animal's lifetime. Although useful, the current reliance on subjective behavioural testing is problematic just as the reliance on clinic-based testing is for human disease. These continued problems suggest that an objective biomarker which is able to follow disease progression in disease models is needed for more rapid, successful translation of possible therapeutics to human trials and clinical use.

1.4. Biomarkers

1.4.1. Importance

The American National Institute of Health succinctly defines a biomarker as

> 'a characteristic that can be measured and evaluated as an indicator of normal biological processes, pathological processes, or pharmacological responses to therapeutic intervention' (Atkinson *et al.* 2001).

It is well publicised that the development of biomarkers is a central need in MND (Ludolph *et al.* 2010, Ludolph 2011, Zinman & Cudkowicz 2011, Otto *et al.* 2012, Turner & Benatar 2014), this is due to the multitude of negative results obtained from clinical trials following initial promising results in pre-clinical trials, the lack of effective treatments, and the diagnostic delay.

Objective biomarkers are needed in pre-clinical and clinical MND research, and for use in the clinic (**Figure 1.5**). First, biomarkers are required to make better use of animal models of disease, allowing for objective tracking of disease onset and progression, and measurement of the effectiveness of potential treatments being tested (Ludolph *et al.* 2010). In this regard, biomarkers would minimise animal pain, the number of animals required for testing, and be more specific than current surrogate markers of disease progression and end points such as behavioural tests (Boylan *et al.* 2009). Indeed, re-testing of discarded potential treatments in animal models, using biomarkers, may show that these compounds show promise using a different dose or route of administration.

Second, the length, size, and cost, of clinical trials could be reduced by the use of biomarkers that can distinguish between heterogeneous disease phenotypes, and which have consistent, measureable responses to disease progression and treatment effects (Otto *et al.* 2012, Turner & Benatar 2014). Currently, MND clinical trials are difficult to conduct as the lack of biomarkers means that trials treat MND as a single homogeneous disease and resort to using survival, or subjective clinical outcome measurements such as the Amyotrophic Lateral Sclerosis Functional Rating Scale-revised (ALSFRS-r), as end points. As a result, current clinical trials require large numbers of participants and are of a long duration in order to reliably detect possible therapeutic benefits (see Bowser *et al.* 2006, Gordon & Meininger

2011 for reviews). The American Food and Drug Administration (FDA) (Mani 2004) and European Medicines Agency (Broich 2007) only accept claims of disease modification if a treatment shows a clinical improvement, and a modification to the underlying pathophysiological process of disease. As a result, a disease modifying effect of a potential treatment cannot be claimed based on clinical signs and symptoms alone, but also needs to show changes in a biomarker.

Third, the use of a biomarker in the clinic could be useful in prognosis (Cho *et al.* 2014), particularly to distinguish between patients with a 2-3 year life expectancy, and those who will live another 10 years. Currently, clinicians are only able to treat MND at later stages of the degenerative process; biomarkers would also allow for more personalised, and perhaps earlier, treatment. Disease specific biomarkers would allow for the simple and rapid exclusion of other phenotypically similar diseases, resulting in quicker MND diagnosis (Krüger *et al.* 2013), and people with MND could also be monitored longitudinally to objectively determine disease subtypes (Kurnaz & Seker 2013, Lawicki *et al.* 2013), progression rates (Mascalchi *et al.* 2014) and the on-going effect of treatments. Additionally, at risk family members/population cohorts could undergo screening programs to detect disease before the onset of symptoms and start treatments earlier (Benatar & Wuu 2012). Earlier treatments mean less disability; financial cost (personal and societal); and disease burden.

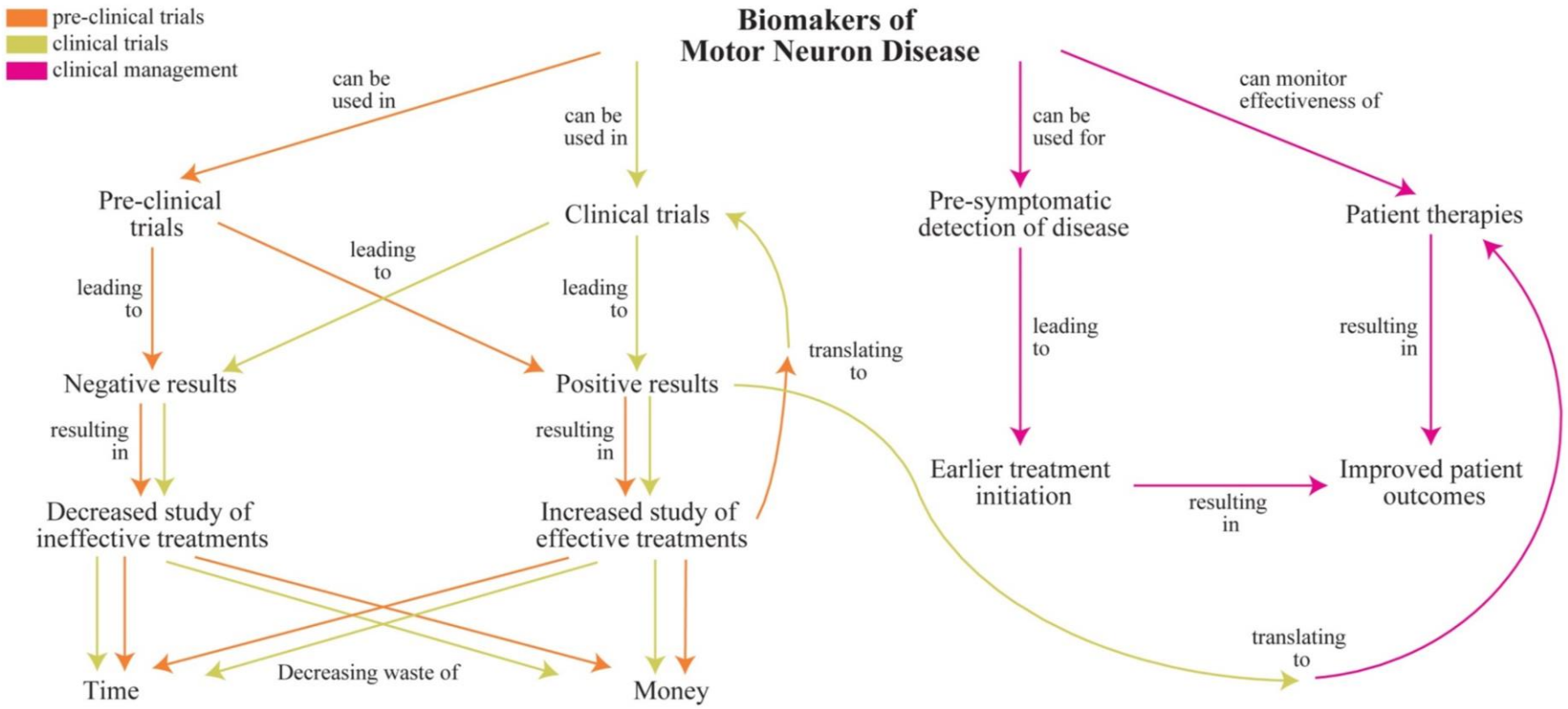

Figure 1.5: Importance of MND biomarkers for the clinic and pre-clinical and clinical trials

The current lack of biomarkers inhibits the successful translation of potential treatments from pre-clinical trials to clinical trials, and also from clinical trials to clinical management of MND. Suitable biomarkers would decrease the time and cost of studies into effective treatments, allowing for more studies into promising treatments, and the translation of these into the clinic. Improved patient outcomes would then be possible using biomarkers for detection of pre-symptomatic disease and earlier initiation of treatments, and monitoring disease progression and the effectiveness of treatments.

1.4.2. Biomarker development considerations

Some of the most important requirements for biomarker discovery are the development of guidelines as to what constitutes a relevant biomarker, and standardised procedures for sample collection, storage, analysis, and quality control (Ludolph 2011, Otto *et al.* 2012, Krüger *et al.* 2013).

It is widely recognised that biomarkers would be useful in pre-clinical models of MND (Ludolph *et al.* 2010, Ludolph 2011). However, the current focus of pre-clinical research is promoting adherence to guidelines of rigorous experimental design in an effort to increase successful translation to the clinic (Scott *et al.* 2008, Ludolph *et al.* 2010, Perrin 2014), as opposed to a focus on biomarker development. As a result, reported potential biomarkers in pre-clinical studies show potential, but often lack sufficiently rigorous experimental design to warrant their use in studies of potential treatments without further testing.

Conversely, biomarker guidelines have been a focus of research for MND clinical trials and the clinic. Otto and colleagues (Otto *et al.* 2012) suggest that the ideal biomarker characteristics for MND fall into eight categories (**Table 1.6**). Given the multifactorial nature of disease pathogenesis in MND, it is unlikely that any one measurement would be able to fulfil all of these criteria. Biomarkers that permit diagnosis at early, even pre-clinical, stages of disease may not be sensitive to disease progression, and would therefore be useful as diagnostic but not prognostic markers. For example, a protein may change in response to disease onset, but then stay at that altered level regardless of disease progression and/or severity. A combination of biomarkers derived from multiple areas may provide greater hope for accurate diagnosis of MND to the exclusion of similar neurodegenerative diseases (Ganesalingam *et al.* 2011, see Turner *et al.* 2013a for review). This is highlighted by the current benchmarks for MND diagnosis, prognosis and monitoring, which use a range of different tests (**Table 1.7**).

Table 1.6: Ideal MND biomarker characteristics for clinical trials and the clinic

(adapted from Otto *et al.* 2012)

1	Sensitive and specific for the heterogeneous syndrome of MND
2	Detectable prior to the onset of significant wasting/weakness
3	Discriminate between clinical phenotypes based on: a. Upper and lower motor neuron involvement e.g., primary muscular atrophy (PMA) and primary lateral sclerosis (PLS) b. Patterns of regional involvement e.g., flail/arm leg, progressive bulbar palsy c. Cognitive involvement i.e., MND versus MND-frontotemporal dementia (FTD) d. Expected survival i.e., 'aggressive' versus 'benign' time course
4	Able to predict regional involvement and the pattern of spread in advance for suitable interventions a. Bulbar dysfunction for early gastronomy (e.g., PEG) b. Respiratory dysfunction for early non-invasive ventilation c. Cognitive impairment
5	Change in a predictable way with disease progression
6	Sensitivity to confidently judge therapeutic response within weeks of challenge
7	Easily accessible and affordable technology
8	Practical to measure in the physically disabled patient

Table 1.7: Types of MND biomarkers and the current benchmarks in clinical trials and the clinic

(adapted from Turner *et al.* 2013a)

Biomarker	**Value**	**Current benchmark**
Diagnostic	Earlier treatment	Neurological history & examination
	Exclusion of MND	Electromyography (Awaji criteria)
Prognostic	Identify patterns of progression	Diagnostic latency
	Stratification in clinical trials	Neurological evaluation (e.g., clinical phenotype)
	Intervention and optimal care	Cox modelling of clinical variables
Monitoring	Identification of ineffective drugs	ALSFRS-r

1.4.3. Potential biomarkers

1.4.3.1. Pre-clinical trials

To date, commonly used biomarkers in the $SOD1^{G93A}$ mouse are those of behavioural tests, including survival, weight changes, neurological scoring based on visual signs of paralysis (Leitner *et al.* 2010), rotarod testing (Jones & Roberts 1968), grip strength and duration, and physiological tests such as Electromyography (EMG; see Weydt *et al.* 2003, Miana-Mena *et al.* 2005 for reviews). Newer pre-clinical MND biomarkers include motor unit number estimation (MUNE; Shefner *et al.* 2006) and electro impedance myography (EIM; Li *et al.* 2012b, Li *et al.* 2013).

As set out in pre-clinical testing guidelines, a minimum of 24 mice per group (Scott *et al.* 2008), or a sufficient number as determined by power analysis (Ludolph *et al.* 2010) is required for pre-clinical testing using the $SOD1^{G93A}$ mouse model. As a result, a limited number of potential biological biomarkers exist in pre-clinical models, as most studies do not reach these requirements. One example is the finding of elevated serum phosphorylated neurofilament heavy chain (pNfH) in a number of different mutant SOD1 expressing mouse models, and a longitudinal increase of serum pNfH in $SOD1^{G93A}$ mice throughout disease progression, in which groups tested consisted of 3-10 mice (Boylan *et al.* 2009). Although promising, larger numbers of mice are required to confirm these results.

1.4.3.2. Clinical trials and the clinic

Genetic mutations linked to MND may be an obvious source of biomarkers but their use is limited as they are only applicable to 5-10% of people with MND (Byrne *et al.* 2011, Chio *et al.* 2012) and even then do not always correlate with disease progression and prognosis (Régal *et al.* 2006). Conversely, potential biomarkers applicable to a wider range of the MND spectrum include neurophysiological, neuroimaging and tissue/fluid biomarkers.

Potential physiological biomarkers include rating scales such as the ALSFRS-r (Cedarbaum *et al.* 1999) and baseline body mass index (BMI; O'Reilly *et al.* 2013, Reich-Slotky *et al.* 2013). Neurophysiological measurements include the neurophysiological index (Cheah *et al.* 2011), motor unit number estimation-based methods (MUNE; Shefner *et al.* 2011), transcranial magnetic stimulation (Floyd *et*

al. 2009, Vucic *et al.* 2011) and electrical impedence myography (EIM; Rutkove *et al.* 2012, Rutkove *et al.* 2014). In addition, numerous advanced brain and spinal cord imaging techniques have been used to look for biomarkers including radionuclide (Kew *et al.* 1993, Turner *et al.* 2005) and magnetic resonance imaging (Carew *et al.* 2011, Verstraete *et al.* 2011, Li *et al.* 2012a).

Body tissues and fluids are also studied for potential MND biomarkers, and advances in proteomics allows for the detection of protein changes at symptom onset and throughout disease progression using these sources. The use of proteins as biomarkers allows for the objective quantification of changes at the molecular level and may provide novel insights into MND pathogenesis.

Over the last 10-15 years, a large number of protein biomarker studies have focused on the cerebrospinal fluid (CSF) and blood. Studies including those measuring changes in inflammatory cytokines (Mitchell *et al.* 2009), chemokines (Kuhle *et al.* 2009), N-acetylaspartate (Simone *et al.* 2011), Nogo-A (Jokic *et al.* 2005, Pradat *et al.* 2007), and proteins in peripheral blood mononuclear cells (Nardo *et al.* 2011) require further testing. In comparison, some well-studied biomarker candidates include the soluble monocyte receptor CD14 (Süssmuth *et al.* 2010), the astrocytic calcium binding protein S100β (Süssmuth *et al.* 2010), tau (Süssmuth *et al.* 2010, Grossman *et al.* 2014), cystatin C (Ranganathan *et al.* 2005, Ranganathan *et al.* 2007, Wilson *et al.* 2010), complement C3 (Goldknopf *et al.* 2006, Ganesalingam *et al.* 2011), neurofilament light chain (NfL) (Zetterberg *et al.* 2007, Tortelli *et al.* 2012, Gaiottino *et al.* 2013), and phosphorylated neurofilament heavy chain (pNfH) (Brettschneider *et al.* 2006, Boylan *et al.* 2009, Ganesalingam *et al.* 2011, Levine *et al.* 2012, Boylan *et al.* 2013).

In one study, tau and the astrocytic proteins CD14 and S100β correlated to levels of upper and lower motor neuron involvement in disease. Higher levels of CSF tau and S100β were seen in people with more upper motor neuron involvement, whereas CSF CD14 was lower in people with lower motor neuron degeneration than it was in people with upper motor neuron degeneration and healthy individuals. In addition, S100β and CD14 levels correlated with survival, showing promise in prognosis (Süssmuth *et al.* 2010). The ratio of phosphorylated tau to total tau has also been studied as a potential biomarker in the CSF (Grossman *et al.* 2014).

Cystatin C, a cysteine protease inhibitor, was first detected as a potential biomarker of MND in the CSF where levels were decreased compared to healthy individuals (Ranganathan *et al.* 2005). Later studies verified this, finding that decreased cystatin C levels in CSF in combination with other proteins (Pasinetti *et al.* 2006, Ranganathan *et al.* 2007) or alone (Wilson *et al.* 2010) showed biomarker potential. Additionally, elevated cystatin C levels are found in the serum of people with MND in comparison to healthy individuals, but are not different to people with other diseases (Wilson *et al.* 2010). Longitudinal CSF cystatin C levels also correlate with progression and baseline CSF levels correlate with prognosis (Wilson *et al.* 2010).

Neurofilament light chain (NfL) was first hypothesised as an MND biomarker in 2007, where it was found to be elevated in the CSF of people with MND, and was lower in SOD1-linked MND than other MND types (Zetterberg *et al.* 2007). These results were confirmed when CSF NfL levels were found to correlate with diagnostic delay, ALSFRS-r decline, and prognosis (Tortelli *et al.* 2012). Serum NfL levels are also increased in people with MND, but this is also the case in people with Alzheimer's disease and Guillan-Barré syndrome (Gaiottino *et al.* 2013).

Using enzyme-linked immunosorbent assays (ELISAs), increased phosphorylated neurofilament heavy chain (pNfH) levels were described as a potential biomarker in the CSF alone (Brettschneider *et al.* 2006), and in comparison to complement C3 levels (Ganesalingam *et al.* 2011), which had been suggested as a biomarker for MND previously (Goldknopf *et al.* 2006). Multiple studies showed a correlation between CSF pNfH levels and prognosis (Brettschneider *et al.* 2006, Levine *et al.* 2012) and pNfH has also been tested in serum as a diagnostic and prognostic biomarker (Boylan *et al.* 2009, Boylan *et al.* 2013).

Despite these early promising results, further work needs to be undertaken to find disease progression markers. In addition, promising prognostic markers found in the CSF such as pNfH and NfL should be validated by testing them in large, cross-institutional cohorts longitudinally and collecting samples with standardised protocols for direct comparisons (Bowser *et al.* 2011, Otto *et al.* 2012, Krüger *et al.* 2013). This need is highlighted by a recent study, which tested a number of potential CSF protein biomarker candidates across different laboratories in Europe,

finding insignificant or contradictory results for all tests except CSF pNfH (Lehnert *et al.* 2014).

Of equal importance to the establishment of guidelines for defining the characteristics of a suitable biomarker, are considerations of biomarker sources. Currently, CSF and serum have been the focus of protein biomarker discovery, but other biofluids should also be studied, including urine.

To date, urinary proteins have not been used extensively as a biomarker source in neurological conditions (Krüger *et al.* 2013), with only two potential urine proteins, collagen, and collagen metabolite glucosylgalactosyl hydroxylysine, investigated in people with MND (Ono *et al.* 1999, Ono *et al.* 2001). However, urinary proteins as a biomarker source have been widely studied in other diseases (Shao *et al.* 2011) including renal disease (Pejcic *et al.* 2010), acute pancreatitis (Comte *et al.* 2006), sleep apnoea (Polotsky & O'Donnell 2007), and cancers (Husi *et al.* 2013). Urine is increasingly becoming recognised as a good source for monitoring physiological processes and diseases, and looking for potential biomarkers (Adachi *et al.* 2006, Thongboonkerd *et al.* 2006, Albalat *et al.* 2011). Urine has advantages over other biomarker sources (**Table 1.8**) in that its collection is simple, painless, and non-invasive (Thongboonkerd *et al.* 2006, Nolen *et al.* 2013) and repeat samples can be taken over time, which makes longitudinal sampling in individual people simple (Otto *et al.* 2012).

The composition of urine also has advantages for biomarker discovery. Urinary protein comes from glomerular filtration of plasma, excretions from epithelial cells in the urinary tract, epithelial cells themselves, and urinary exosomes (see Barratt & Topham 2007 for review). In contrast to CSF and blood, urine does not contain significant cell, lipid, or large protein numbers (see Barratt & Topham 2007, Albalat *et al.* 2011 for reviews), as abundant serum proteins are normally reabsorbed during renal filtration, resulting in a less complex proteome (Ye *et al.* 2006). This simpler proteome lends itself to extensive analysis with multiple groups developing urinary proteome 'fingerprints' of healthy individuals (Adachi *et al.* 2006, Mischak *et al.* 2010, Husi *et al.* 2013, Nolen *et al.* 2013) allowing for comparison to potential biomarkers of disease. Another advantage of urine is its stability. The low molecular mass proteome does not undergo significant changes if urine is stored for up to 3 days at 4°C or 6 hours at room temperature (Schaub *et al.*

2004, Theodorescu *et al.* 2006). This is in stark comparison to serum where clotting during preparation involves enzymatic activity which results in the cleavage of proteins (Teisner *et al.* 1983, Koomen *et al.* 2005, Good *et al.* 2007).

Like any other biomarker source, there are potential drawbacks to using urine. One example is that there is no physiological need for precise homeostatic control of any proteins present. As a result, the variability of the urinary proteome is thought to be much larger than plasma (Nagaraj & Mann 2011). Second, urine varies greatly in volume and protein concentration. However, these issues can be accounted for in analysis, by standardising protein amount or concentration against the total protein present, or using more precise methods of accounting for urine dilution and variability by comparing protein to creatinine, osmolarity (Chadha *et al.* 2001, Richmond *et al.* 2005) or cystatin C (Conti *et al.* 2005, Baxmann *et al.* 2008).

Currently, the potential of protein biomarkers have benefits over those based on clinical tests and imaging techniques. Changes in protein levels in response to disease are objective, unlike clinical tests, which can be biased due to peoples' opinions and ongoing cooperation, and biased by doctors, and technicians performing tests. Additionally, imaging techniques are expensive and require advanced technical skill, whereas changes in protein biomarkers could be determined by simple laboratory tests of CSF, blood or urine. One such promising protein biomarker is the cell membrane receptor, neurotrophin receptor p75.

Table 1.8: Properties of human biological fluids used for biomarker discovery
(adapted from Bowser *et al.* 2011, Turner *et al.* 2013a)

Biofluid	Benefits	Issues
Cerebrospinal fluid (CSF) 0.2-0.5g/L (Ekegren *et al.* 2008)	Close to regions in which cell death occurs	Obtaining samples invasive; repeat samples virtually unattainable
Blood/ serum 60-80 g/L (Ekegren *et al.* 2008)	Easier to access than CSF	High protein complexity and overall concentration; enzymes degrade proteins during clotting; biomarkers may be diluted from systemic biological factors unrelated to MND
Urine < 0.01g total/day (Adachi *et al.* 2006)	Easier to access than both CSF and blood/serum; painless collection; longitudinal sample collection possible; stable proteome	Variability due to lack of homeostatic control; biomarkers may be diluted from systemic biological factors unrelated to MND

1.5. Neurotrophin receptor p75

1.5.1. Structure

A class of proteins called neurotrophins play a crucial role in the development, maintenance, survival, and death of neurons and non-neuronal cells through multiple cell membrane receptors, including the common neurotrophin receptor p75 (p75NTR) (Chao 2003, Hennigan *et al.* 2007, Ibáñez & Simi 2012). p75NTR (tumour necrosis factor receptor superfamily member 16/low-affinity nerve growth factor receptor), first described as 'a transmembrane glycoprotein of approximately 75,000 daltons ($p75^{NGFR}$)' (Yan & Chao 1991) is most well-known for its interactions with all neurotrophins, and its contradictory cellular role, promoting cell survival or inducing apoptosis depending on interactions with ligands, other cell receptors, and the surrounding environment (see Ibáñez & Simi 2012 for review).

Though the actions of p75NTR are varied and numerous, its structure **(Figure 1.6**) is not complex, and the amino acid sequence of human p75NTR was first deduced in 1986 (Johnson *et al.* 1986). The human p75NTR protein (Uniprot ID P08138), at 427 amino acids in length, consists of an extracellular domain ($p75NTR^{ECD}$) with a cleavable 28 amino acid signal peptide and four 40 amino acid, negatively charged, cysteine-rich domain repeats (Johnson *et al.* 1986), two of which have been determined as the binding sites of neurotrophins (He 2004). This is followed by a serine/threonine-rich region, a single transmembrane domain, and a 155 amino acid intracellular domain ($p75NTR^{ICD}$) (Johnson *et al.* 1986). The $p75NTR^{ICD}$ contains an 80 amino acid death domain (Liepinsh *et al.* 1997), and a 29 amino acid juxtamembrane domain, called the 'Chopper' domain, which is N-terminal to the death domain and has been identified as having the ability to induce cell death if it remains membrane bound (Coulson *et al.* 2000). The cysteine-rich domains and the death domain make p75NTR a member of the tumour necrosis factor receptor family. Evolutionary homology exists across species with a 90.21% homology seen between humans and mice. In mice, the p75NTR protein (Uniprot ID Q9Z0W1) is shorter by 10 amino acids, at 417 amino acids in length (Tuffereau *et al.* 1998).

1.5.2. Cellular function

Since its discovery, many functions have been linked to p75NTR (see Dechant & Barde 1997 for review, Skeldal *et al.* 2011). It is most commonly known for its ability to bind all the neurotrophins; nerve growth factor (NGF), brain-derived neurotrophic factor (BDNF), neurotrophin 3 (NT-3) and neurotrophin 4/5 (NT-4/5) with a similar nanomolar affinity (Rodriguez-Tébar *et al.* 1990, Rodriguez-Tébar *et al.* 1992), and was first characterised as being able to facilitate the survival signals mediated by tropomysin-related kinase (Trk) receptors (Wolf *et al.* 1995).

Not only can p75NTR bind all mature neurotrophins (Rabizadeh *et al.* 1993, Frade *et al.* 1996), and the immature form of neurotrophins, called pro-neurotrophins (Lee *et al.* 2001), alone, it also binds ligands in complexes with other receptors. Interactions between p75NTR, Trk receptors (TrkA, TrkB and TrkC) and mature neurotrophins normally result in cell survival and differentiation signalling, increasing the Trk receptors affinity for neurotrophins (Hemsptead *et al.* 1991, Bibel *et al.* 1999). In contrast, interactions between p75NTR, pro-neurotrophins, and the cell receptor sortilin, result in cell death (Nykjaer *et al.* 2004). p75NTR is also a receptor for non-neurotrophin ligands including the amyloid-beta (Aβ) peptide of amyloid precursor protein (Fombonne *et al.* 2009), and the neurotoxic fragment of prion protein (Della-Bianca *et al.* 2001). The multiple ligand and receptor binding partners of p75NTR result in a number of different downstream functions in different cell types at different stages of development (Schor 2005), which makes it hard to determine the downstream effects of p75NTR in a given situation (**Table 1.9**). Additionally, p75NTR can function without ligand binding and the presence of the extracellular domain ($p75NTR^{ECD}$) (Tyurina *et al.* 2005).

In rodent development, p75NTR is highly expressed in areas such as sensory and sympathetic neurons, spinal cord and brainstem motor neurons (Ernfors *et al.* 1989), and neurons of the cerebral cortex, cerebellum, hippocampus, basal forebrain and caudate putamen (Mobley *et al.* 1989, Friedman *et al.* 1991), playing a role in neuronal pruning, cell death (Raoul *et al.* 2000) and survival (Lee *et al.* 1994a, Ferri *et al.* 1997). In rat motor neurons, these high p75NTR expression levels decrease postnatally to 5% of neonatal levels by four weeks of age (DiStefano & Johnson 1988) and p75NTR is not found in healthy adult motor

neurons (Ernfors *et al.* 1989). In the healthy adult mouse spinal cord, p75NTR is not detected in motor neurons, and is only detected in dorsal horn sensory neurons and in a very small cluster of spinal motor neurons near the sacral area, which are thought to be the mouse homologue of Onuf's nucleus (Koliatsos *et al.* 1994, Copray *et al.* 2003). Similar developmental regulation and postnatal expression decrease occurs for human p75NTR (see Ibáñez & Simi 2012 for review). Additionally, it has been proposed that post mitotic cells such as motor neurons, that expressed p75NTR during development, are primed to re-express p75NTR under stress or injury conditions (see Ibáñez & Simi 2012 for review).

p75NTR is one of more than 60 transmembrane receptors that undergoes regulated intramembrane proteolysis (RIP) (Kanning *et al.* 2003), the inhibition of which influences p75NTR signal transduction pathways, such as neuronal survival (Kenchappa *et al.* 2006, Underwood *et al.* 2008). RIP involves the cleavage of the extracellular domain ($p75NTR^{ECD}$) by tumor necrosis factor α-converting enzyme (TACE)/ADAM17, releasing the $p75NTR^{ECD}$ into the extracellular space (Chao 2003, Weskamp *et al.* 2004). The remaining membrane-tethered stub of p75NTR is then cleaved by a presenilin-dependent γ-secretase, releasing the intracellular domain ($p75NTR^{ICD}$) into the cytosol of the cell (Kanning *et al.* 2003) (**Figure 1.6**) where it has been found to localise to the nucleus, and modulate transcription (Parkhurst *et al.* 2010). The rate of p75NTR RIP is reported to not be affected by ligand binding in some studies (Kanning *et al.* 2003, Sykes *et al.* 2012), but other studies have reported that pro-apoptotic ligand binding in sympathetic neurons induces RIP (Kenchappa *et al.* 2006, Kenchappa *et al.* 2010). Signals induced by TrkA (Kanning *et al.* 2003, Sykes *et al.* 2012) and TrkB activation (Kanning *et al.* 2003), and sortilin (Skeldal *et al.* 2012) have also been reported to regulated p75NTR RIP.

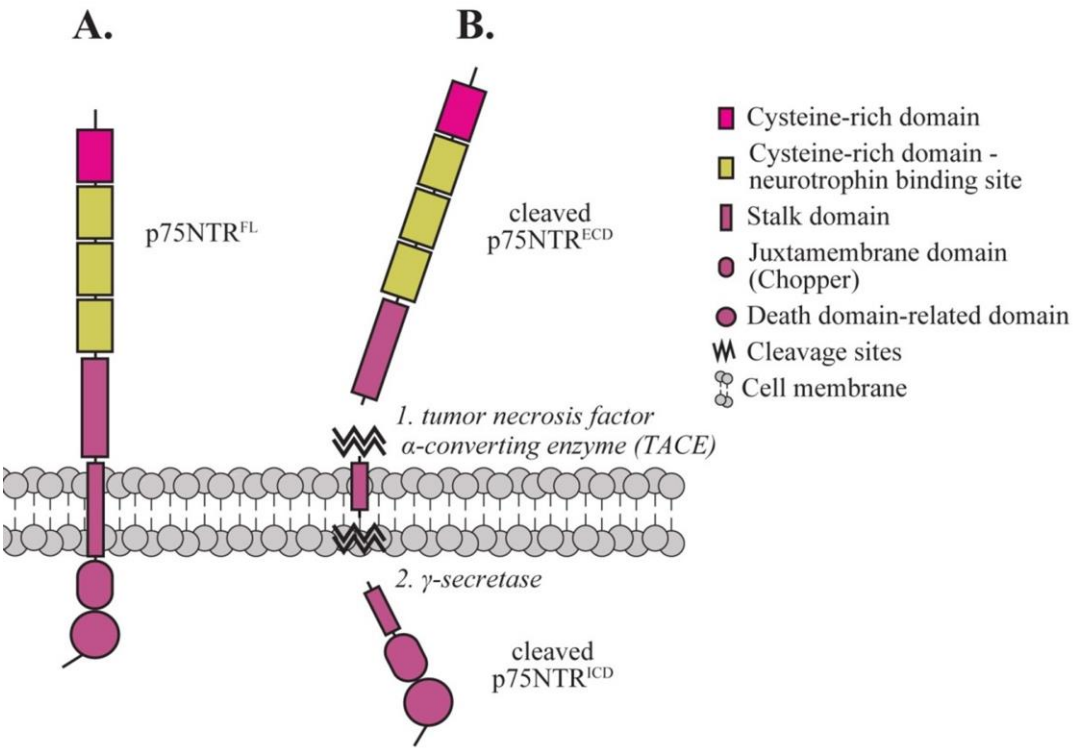

Figure 1.6: Structure and cleavage of neurotrophin receptor p75

A. Full-length neurotrophin receptor p75 ($p75NTR^{FL}$) includes four cysteine-rich domains (▮) in the extracellular domain ($p75NTR^{ECD}$). The cysteine-rich domains are attached to an extracellular 'stalk' (▮) and this, to a single transmembrane domain (▮) which is highly conserved across species. Intracellularly, the p75 receptor consists of a juxtamembrane domain (●; chopper domain) and the carboxy-terminal domain, which contain the globular six-helix 'death domain' (●). The neurotrophin binding site is primarily cysteine-rich domain repeats 2-4 (▮), and the cysteine-rich domains and death domain make p75NTR a member of the tumour necrosis factor receptor family. **B.** p75NTR is one of 60 transmembrane receptors that undergoes regulated intramembrane proteolysis, resulting in the cleavage of the extracellular domain ($p75NTR^{ECD}$) by tumor necrosis factor α-converting enzyme (TACE), and the intracellular domain ($p75NTR^{ICD}$) by ɣ-secretase (adapted from Johnson *et al.* 1986, Liepinsh *et al.* 1997, Coulson *et al.* 2000, Chao 2003, He 2004, Weskamp *et al.* 2004, Kenchappa *et al.* 2010, Skeldal *et al.* 2011).

Table 1.9: Neurotrophin receptor p75 interacts with many cellular proteins resulting in varied downstream outcomes
(adapted from Tuffereau *et al.* 1998, Della-Bianca *et al.* 2001, Nykjaer *et al.* 2004, Schor 2005, Fombonne *et al.* 2009)

Example of p75NTR- interacting proteins	Function
Amyloid-beta (Aβ) peptide of amyloid precursor protein	Cell death
Caveolin-1	Neurotrophic signalling
FAP-1, RIP-2	Survival
NRAGE, necdin	Cell cycle progression
NRIF, NADE	Cell death
Prion protein	Cell death
Rabies viral capsid glycoprotein	Potential viral infection
RhoA GTPase	Neurite extension
SC-1	Cell cycle progression
Sortilin cell receptor	Cell death
TRAF4, TRAF6, DTRAF1	Survival
TrkA, TrkB, TrkC cell receptors	Neurotrophic signalling

1.5.3. Role in injury and disease

Following nervous system injury, multiple signalling pathways that are normally only active during development are re-activated. Numerous studies have reported that p75NTR re-expression is part of one such pathway (Taniuchi *et al.* 1986, Ernfors *et al.* 1989, Brunello *et al.* 1990, Saika *et al.* 1991, Lindner *et al.* 1993, Ferri *et al.* 1997, Kokaia *et al.* 1998, Roux *et al.* 1999, Nassenstein *et al.* 2003, Tsukamoto *et al.* 2003), and it is one of many signalling molecules robustly re-expressed in motor neurons, and other cell types, by injury (see Ibáñez & Simi 2012 for review). The mechanisms that induce p75NTR re-expression during injury and neurodegeneration remain ill defined.

Instances in which p75NTR is re-expressed in motor neurons or Schwann cells of rodents include peripheral (Taniuchi *et al.* 1986, Ernfors *et al.* 1989) and central (Brunello *et al.* 1990) nerve injury, and nerve transection (Saika *et al.* 1991, Ferri *et al.* 1997). Following such injuries, if nerve re-innervation occurs, the expression of p75NTR returns to normal levels (Ernfors *et al.* 1989).

Similarly in humans, p75NTR is re-expressed in motor neurons in response to neurological diseases, deficits, and syndromes, and has been implicated in conditions such as cerebral ischemia (Kokaia *et al.* 1998), seizure (Roux *et al.* 1999), Alzheimer's disease (Lindner *et al.* 1993, Tsukamoto *et al.* 2003) and bronchial asthma (Nassenstein *et al.* 2003).

Of particular interest is the increased expression of p75NTR in spinal cord motor neurons (Seeburger *et al.* 1993, Lowry *et al.* 2001) and denervated Schwann cells in people with MND (Kerkhoff *et al.* 1991). Seeburger and colleagues (1993) detected p75NTR, TrkA, and TrkB mRNA in spinal cord α-motor neurons, and found some surviving motor neurons contained p75NTR mRNA in the cervical, thoracic, and lumbar levels of the spinal cord in people with MND, but not healthy individuals. Comparatively, TrkB mRNA was detected at all levels of the spinal cord in people with MND at higher levels than in healthy individuals and TrkA mRNA was not detected in any spinal cord sections.

Another small cohort study (Lowry *et al.* 2001) identified the expression of p75NTR in cervical (C8) spinal motor neurons in post mortem tissue of people with

MND but not age and gender matched healthy individuals. Kerkhoff and colleagues (Kerkhoff *et al.* 1991) examined the peripheral nerves and ventral roots of people with MND and healthy individuals post-mortem using immunohistochemistry, and found p75NTR expression in the Schwann cells of degenerated nerve fibres in peripheral nerves, ventral roots and to a lesser extent, dorsal roots, in MND but not healthy individuals.

p75NTR up-regulation has also been detected in motor neurons of the low- and high-copy number $SOD1^{G93A}$ mouse model of MND (Lowry *et al.* 2001, Copray *et al.* 2003), which develop motor neuron degeneration and progressive paralysis (Gurney *et al.* 1994). Lowry and colleagues ($SOD1^{G93A}$ high-copy model; 2001) found p75NTR re-expression in motor neurons of the lumbar spinal cord in symptomatic $SOD1^{G93A}$ mice at 112 days of age, but p75NTR was absent in these mice before symptoms at 28 and 56 days of age. Similarly, Copray and colleagues (SOD1G93Adl low-copy model; 2003) detected p75NTR protein and mRNA in motor neurons in the ventral lumbar segment of the spinal cord. While end stage mice were not tested, p75NTR was detected in the motor neurons of symptomatic 210 day old $SOD1^{G93Adl}$ mice but not in younger $SOD1^{G93Adl}$ mice or healthy controls (Copray *et al.* 2003).

In conjunction with re-expression of p75NTR, an up-regulation of tumor necrosis factor α-converting enzyme (TACE) (Hurtado *et al.* 2001), and cleavage of p75NTR by TACE (Srinivasan *et al.* 2007), which results in the release of $p75NTR^{ECD}$ in the extracellular space as part of RIP, has also been reported in response to injury. Fitting with this observation, is the detection of $p75NTR^{ECD}$ in the urinary protein of rats following sciatic nerve injury (DiStefano & Johnson 1988). Additionally, $p75NTR^{ECD}$ is present in amniotic fluid and infant human urine when p75NTR is normally expressed during development. Urine $p75NTR^{ECD}$ levels then decrease to low but detectable levels in adult human urine when p75NTR is normally down-regulated in most cell types, including motor neurons (Zupan *et al.* 1989, DiStefano *et al.* 1991).

p75NTR re-expression following injury can cause further damage through multiple downstream mechanisms including a decrease in synaptic activity, reduction of dendritic complexity and spine density, and induction of axonal degeneration (see Ibáñez & Simi 2012 for review). A reduction of this damage is possible through the

knock-out of p75NTR; survival of motor neurons (Ferri *et al.* 1997) Schwann cells (Syroid *et al.* 2000) and oligodendrocytes (Beattie *et al.* 2002) is improved in p75NTR knock-out mice following injury, in comparison to WT mice.

As in its downstream signalling effects, re-expression of p75NTR in response to adult injury may have dual functions. Ibanez & Simi suggest that p75NTR re-expression is part of a homeostatic program that removes defective neurons, axons and synapses after a small injury. However, in response to injury on a larger scale, such as severe lesions or neurodegenerative disease including MND, p75NTR up-regulation, re-expression and signalling results in a cascade of irreversible damage (see Ibáñez & Simi 2012 for review).

1.6. Concluding remarks

A crucial step in the identification of a biomarker of MND that is sensitive to disease onset, progression, and potential treatments is to find candidates that are indicative of the pathological process underlying MND. An obvious pathological process that occurs in MND is loss of motor neurons and withdrawal of growth factor support. An indicator of this process is the shedding of $p75NTR^{ECD}$ from motor neurons during the apoptotic process and from Schwann cells that fail to connect with retracting and degenerating motor neurons. So, could $p75NTR^{ECD}$ be a marker of motor neuron degeneration and thus a biomarker of MND? One relevant place to start is by examining easy accessible biological fluids, such as urine, for $p75NTR^{ECD}$. The $SOD1^{G93A}$ mouse model, although not perfect, is the only MND model used in pre-clinical research, and using these mice to examine biomarkers still holds promise. However, the gold standard is examining the viability of potential biomarkers in people living with MND. If the effectiveness of therapeutics can be measured by biomarkers, improved approaches for treatment of MND will follow.

1.7. Hypothesis & Aims

It is hypothesised that the presence of the extracellular domain of the neurotrophin receptor p75 ($p75NTR^{ECD}$) in urine is a biomarker for MND.

This study aims to detect and quantify $p75NTR^{ECD}$ levels in urine of the $SOD1^{G93A}$ MND mouse model and people with MND. The following chapters describe the development, optimisation, and use of experimental methods for the detection and quantification of $p75NTR^{ECD}$ in urine to determine the usefulness of urinary $p75NTR^{ECD}$ as a biomarker of MND.

Chapter 2. Materials and Methods

2.1. Standard preparation

2.1.1. Cell culture

Cultured cells were used as positive and negative controls for full-length p75NTR ($p75NTR^{FL}$) and the p75NTR extracellular domain ($p75NTR^{ECD}$) in Immunoprecipitation (IP) and/or Western blot (WB) experiments. A motor neuron enriched embryonic spinal cord x immortal neuroblastoma motor neuron-like cell line (NSC-34; Cashman *et al.* 1992), human-derived p75NTR from A875 melanoma cells (Giard *et al.* 1973) and rat-derived p75NTR from C6 glioma cells (Benda *et al.* 1968) were used as p75NTR-positive controls. Baby hamster kidney fibroblast cell lysate (BSR; Rogers *et al.* 2006) was used as a p75NTR-negative control. All cells were cultured in Dulbecco's modified Eagle's medium containing 1% L-Glutamine and 1% penicillin-streptomycin-glutamine and either 10% fetal bovine serum (FBS) (NSC-34 and A875 cells) or 5% FBS and 10% normal horse serum (C6 cells) (Invitrogen Life Technologies, Mulgrave, Australia).

2.1.2. Total protein quantification

Estimation of total protein in lysates and immunoprecipitated samples was performed with the BioRad *DC* Protein Assay Kit Microplate Assay Protocol as per manufacturer's instructions (BioRad, California, USA, Cat. # 500-0116) using 96 well assay plates (Costar Corning; Invitro Tech, Aust. Cat. # 2595). Assay results were read with a Perkin Elmer Victor X4 Multilabel Plate Reader at 750nm, room temperature (RT). Bovine serum albumin (BSA) (Sigma-Aldrich, Castle Hill, Australia, Cat. # A7906) standards of 1mg/ml, 0.8mg/ml, 0.4mg/ml, 0.2mg/ml, and 0.1mg/ml were used for standard curves and sample protein concentrations were calculated using Microsoft Excel.

Additionally, human urinary protein levels were measured by standard clinical analysis using a Roche/Hitachi Modular analyser (SA Pathology), with a turbidmetric assay.

2.1.3. Lysate preparation

Cells were spun at 400g, washed twice with Phosphate buffered saline (PBS - pH 7.3, 10mM Na_2HPO_4, 1.8mM KH_2PO_4, 2.7mM KCl, 137mM NaCl), containing protease & phosphatase inhibitors (Roche, Basel, Switzerland; PhosSTOP - phosphatase inhibitor Cat. # 04 906 837 001, cOmplete - protease inhibitor Cat. # 11 697 498 001), and then resuspended in Lysis buffer (Tris buffered saline, 1% Triton X-100, pH 7.2) containing protease & phosphatase inhibitors. Cells were then disrupted with a Retsch Tissue Lyser (setting 3.0, 3min, Qiagen; Rogers *et al.* 2010) and then spun with a refrigerated benchtop centrifuge (Sigma-Aldrich, Castle Hill, Australia, Cat. # 1-15K) at 14,000g, 4°C to remove cell debris. Following total protein quantification (see **2.1.2**), supernatant was divided into aliquots and stored at -80°C.

2.1.4. ELISA standards

Mouse recombinant p75NTR-Fc (r-p75NTR-Fc; Biosensis, Adelaide, Australia Cat. # PE-1704-25), and mouse (R&D Systems, Minnesota, USA, Cat. # 1157) and human (R&D Systems, Minnesota, USA, Cat. # 367-NR) r-p75NTR^{ECD}–Fc fusion proteins were used on 96 well assay plates (Costar Corning, Invitro Tech, Australia, Cat. # 2595), in triplicate, to create standard curves for the analysis of mouse- and human-derived samples.

2.2. Antibodies

2.2.1. In-house antibodies

Mouse anti-human p75NTR monoclonal antibodies (MLR1 and MLR2; Rogers *et al.* 2006) were purified from cell-conditioned supernatant produced by culturing hybridoma cell lines. Supernatant was recirculated over Protein G Agarose affinity columns for 3 days, 4ºC using a peristaltic pump as per manufacturer's instructions (Millipore, Massachusetts, USA, Cat. # 16-266). After washing unbound proteins with PBS, bound proteins were eluted using 0.1M Glycine (PBS based, pH 2.7) and eluted proteins were returned to pH 7 using 2M Tris. HiTrap desalting columns (GE, Cat. # 17-1408-01) were then used for buffer exchange to PBS (pH 7.4) and antibodies concentrated using 100kDa cut-off spin columns at 2,300g, 4°C (Millipore, Massachusetts, USA, Cat. # UFC810024). Final antibody concentrations were calculated at 280nm using the extinction coefficient of IgG of 1.37 (1mg/ml, path length 1cm) (Johnstone & Thorpe 1988) using a spectrophotometer (Shimadzu, Japan), and antibodies were stored at 4°C.

2.2.2. Commercial antibodies

Anti-p75NTR^{ECD} antibodies were purchased from R&D Systems and Alomone Labs, or donated (**Table 2.1**). Secondary antibodies conjugated with horseradish peroxidase (HRP) were purchased from Jackson ImmunoResearch Laboratories (Pennsylvania, USA).

Table 2.1: Commercial antibodies used

Specificity	Source
Goat anti-mouse p75NTR^{ECD}	R&D Systems, Cat. # AF1157 /Sigma-Aldrich, Cat. # N5788
Goat anti-human p75NTR^{ECD}	R&D Systems, Cat. # AF367
Mouse anti-human p75NTR (ME20.4)	Kindly supplied by Prof. AH Ross (Ross *et al.* 1984)
Rabbit anti-human p75NTR^{ECD}	Alomone Labs Cat. # ANT007
Bovine anti goat-HRP	Jackson ImmunoResearch Laboratories Cat. # 805 035 180
Donkey anti-mouse-HRP	Jackson ImmunoResearch Laboratories Cat. # 715 035 150
Donkey anti-rabbit-HRP	Jackson ImmunoResearch Laboratories Cat. # 711 035 152

2.3. Gel electrophoresis & Western blot

2.3.1. 1D SDS-PAGE

SDS-PAGE (Laemmli 1970) was performed using an XCell SureLock Mini-Cell system (Life Technologies, California, USA, Cat. # EI0002) with 10 or 12 well NuPAGE Novex 4-12% Bis-Tris Mini Gels (Life Technologies, California, USA, Cat. # NP0321BOX or NP0322BOX). Samples were prepared by heating for 5min, 95°C with Sodium dodecyl sulphate (SDS), Dithiothreitol (DTT), and Bromophenol blue marker. Immunoprecipitated (IP) samples were mixed with Bromophenol blue before being separated by SDS-PAGE, as samples were previously boiled during the IP protocol (see **2.4.2**).

Each gel used for Western blot was run with one lane containing 10µl BioRad Precision Plus Dual-Colour marker (BioRad, California, USA, Cat. # 161-0374). Gels were run in Running Buffer (50mM MOPS, 50mM Tris, 1mM SDS, 3.5mM EDTA) at 200V and 110mA, until the marker and Bromophenol blue were 0.5cm from the bottom of the gel, approximately 1hr.

2.3.2. Western blot

Following SDS-PAGE, samples were transferred from gels to nitrocellulose membranes (Life Technologies, California, USA, 0.45µm pore size, Cat. # LC2001) using the transfer equipment compatible with the Invitrogen XCell *SureLock* Mini-Cell system (Life Technologies, California, USA, Cat. # EI0002) (Renart *et al.* 1979, Towbin *et al.* 1979). Transfers were run at 30V, 200mA, 1hr and 7mins on ice using Transfer Buffer (25mM Bicine, 25mM Bis-tris, 1mM EDTA) with 20% Methanol. Gels were treated with Coomassie Blue (Stain: 0.1% Coomassie dye, 50% methanol, 10% acetic acid; destain: 50% methanol, 10% acetic acid) to confirm that sufficient transfer of samples had occurred.

After transfer, Western blot (WB) membranes were blocked for 2hrs, room temperature (RT), or overnight, 4°C, with Tris buffered Saline Tween-20 (TBST; 20M Tris-base, 150mM Sodium Chloride, 0.1% Tween-20) containing 7% skim milk, and a primary antibody was added at 4°C overnight in TBST containing 1% skim milk. Following 6x15min wash steps with TBST 1% skim milk, secondary

antibody was added for 2hrs RT (1/5000 in TBST 1% skim milk), membranes were washed 6x15min with TBST 1% skim milk and then placed in 1xTBS (20M Tris-base, 150mM Sodium Chloride, pH 7.4) for visualisation. An enzymatic chemiluminesence substrate (GE, Australia, Cat. # RPN2232) was used to visualise protein bands using a Fuji Imager system (LAS 4000, Australia) and recorded using FujiFilm Global MultiGauge® electrophoretic software.

2.3.3. Sypro Ruby total protein stain

Sypro Ruby total protein stain was applied to WB nitrocellulose membranes, before antibody addition, for use as a loading control as per manufacturers' instructions (Invitrogen, Australia, Cat. # S-11791). Stained membranes were imaged using a Fuji Film Imager (LAS4000) using a 605DF40 filter and iris setting of 0.85, and then blocked with TBST containing 7% skim milk for 2hrs, RT, before continuing the WB protocol.

2.4. p75NTR^{ECD} precipitation

2.4.1. Trichloroacetic acid precipitation

Mouse urinary protein samples were precipitated using a method modified from Thongboonkerd (2006). Urinary samples were first spun at 12,000g, 4°C, with 100% Ethanol nine times the volume of the original sample, for optimal purification. One spin at 15,000g with 13% Trichloroacetic acid, and two spins at 15,000g with 100% Acetone at 4°C were then performed. Precipitated samples were resuspended in 2xSDS, using a water bath sonicator when required to aid in dissolving, quantified for total protein (see **2.1.2**) and subject to SDS-PAGE and WB (see **2.3**).

2.4.2. Immunoprecipitation

Mouse and human urinary protein, cell lysates, bovine serum albumin (BSA), and r-p75NTR^{ECD}-Fc fusion protein were immunoprecipitated (Harlow & Lane 1988). Urinary samples were diafiltered using spin columns, spun at 2,500g (Millipore, Massachusetts, USA; Cat. # UFC800324) or 12,000g (Millipore Massachusetts, USA; Cat. # UFC500324) at 4°C. Each sample was concentrated and washed ten times the initial sample volume with 1xPBS, before being resuspended to the original volume.

Samples were pre-cleared with Protein G Agarose beads (Millipore, Massachusetts, USA, Cat. # 16-266) to remove non-specific binding between the sample and beads. However, r-p75NTR-Fc was not pre-cleared with Protein G Agarose beads due to an interaction between human –Fc and Protein G (as per manufacturer's instructions). Samples were mixed with 20µl of Protein G Agarose beads and rotated for 30min at 4°C or 15min, RT. After centrifugation at 1,000g, samples were removed from Protein G Agarose beads, capture antibody was added, and samples rotated overnight at 4°C. Samples were then mixed with 10µl of Protein G Agarose for 1hr, RT.

After centrifugation at 14,000g, supernatant was removed, and Protein G Agarose beads were resuspended in 2xSDS with DTT and heated at 95°C. After centrifugation at 14,000g and Protein G Agarose bead removal, remaining

supernatant was quantified for total protein (see **2.1.2**) and subject to SDS-PAGE (see **2.3.1**) and downstream analyses.

2.5. Mass Spectrometry

2.5.1. Sample preparation

Samples to be analysed by Mass Spectrometry (MS) underwent preparation similar to the IP protocol. Urine was diafiltered with PBS using 100kDa cut-off spin columns (Millipore, Massachusetts, USA; 3ml, Cat. # UFC810024) then, after removal of pre-clearing Protein G Agarose beads (mixed 30min, RT), capture antibody, mouse anti-human p75NTR (MLR2), was added and rotated overnight.

After collection using Protein G Agarose beads (Millipore, Massachusetts, USA, Cat. # 16-266), samples were eluted from Protein G Agarose beads with 17.0µl 0.1M Glycine (rocked, 1hr, RT, pH 2.7) and returned to a pH of 7 with 3.3µl 500mM Sodium hydroxide. Then, samples were reduced with 1.7µl 100mM DTT in 100mM Ammonium bicarbonate (shaken 5min 65°C), and alkylated with 1.7µl 100mM Iodoacetamide in 100mM Ammonium bicarbonate (shaken 30min, 30°C). Reduced/alkylated samples were digested overnight at 37°C using 12.5µg/ml of protease Glutamyl endopeptidase (GluC; New England BioLabs, Massachusetts, USA, Cat. # P8100S) or 12.5µg/ml of Trypsin Gold (Promega, Wisconsin, USA, Cat. # V5280). After incubation with enzymes, tubes were centrifuged for 2min, 2,000g, RT, and supernatant was collected and placed into glass MS vials and stored at 4°C until analysis.

2.5.2. Orbitrap-Mass Spectrometry analysis

10µl of GluC or Trypsin Gold digested samples were analysed using a LTQ Thermo Orbitrap XL linear ion trap Mass Spectrometer (Thermo-Fisher Scientific, Massachusetts, USA), fitted with a nanospray source. Samples were applied to a 300µm i.d. x 5µm Acclaim® C18 PepMap 100 precolumn (Dionex, California, USA, Cat. # 160297), and separated on a 75mm x 150mm C18 5µm 100Å column (Nikkyo Technos, Tokyo, Japan), using a DionexUltimate 3000 HPLC (Dionex, California, USA), with a 55min gradient from 2% Acetonitrile (ACN) to 45% ACN containing 0.1% formic acid at a flow rate of 200nl/min followed by a step to 77% ACN for 9min. The MS was operated in positive ion mode, with one FTMS scan of mass/charge (m/z) 300-2000 at 60,000 resolution in the FTMS analyser, followed

by ITMS or FTMS product ion scans of the 6 most intense ions with dynamic exclusion of 15 seconds, 10ppm low and high mass width relative to reference mass, an exclusion list of 500 proteins, and collision-induced dissociation energy of 35%. Only ions with a charge state of greater than +2 were selected for MS/MS of GluC or Trypsin Gold digested peptides (Wilson *et al.* 2011).

Resultant spectra were searched with Proteome Discoverer Software version 1.2.0.208 (Thermo Scientific) using the Sequest algorithm against the UniProt human (taxonomy 9606) database version May 2013. Search parameters were identical for Trypsin Gold and GluC treated samples, as follows: Trypsin or GluC as the enzyme with up to two missed cleavages; a mass tolerance for peptide identification of the precursor and product ions of 15ppm and 0.8Da respectively; and variable modifications of carbamidomethylation, oxidation of methionines, and phosphorylation of serines, threonines, and tyrosines. Filters included peptides of confidence value above 99%, count only rank one peptides, count peptide only in top-scored proteins, and at least two unique peptides sequenced for each protein.

2.5.3. Triple TOF-Mass Spectrometry analysis

10µl of GluC or Trypsin Gold digested samples were analysed using a SCIEX TripleTOF 5600+ Mass Spectrometer fitted with a nanospray source (SCIEX, Victoria, Australia). Samples were applied to a Polar 3µm precolumn (0.3 x 10 mm, SGE Analytical Science, Victoria, Australia) and eluted onto a spraytip 5µm C18 column (75mm x 150 mm with a bead pore size of 100Å; Nikkyo Technos, Tokyo, Japan), using an Eksigent Ekspert 415 nanoLC (SCIEX, Victoria, Australia). Peptides were eluted using a 35-minute gradient from 5% to 25% ACN containing 0.1% formic acid at a flow rate of 300nl/minute over 35min, followed by a second gradient to 40% ACN over 7min and a further step to 95% acetonitrile for 11 minutes. The MS was operated in positive-ion mode with one MS scan of mass/charge (m/z) 350 to 1,500, followed by collision-induced dissociation fragmentation of +2 to +5 charge state ions that were greater than 250 counts per second for a maximum of 100 candidate ions.

Resultant spectra were searched with Protein Pilot software version 4.5 Beta (SCIEX) using the Paragon algorithm against the UniProt human (taxonomy 9606) database version September 2014. Search parameters were identical for Trypsin Gold and GluC treated samples, as follows: Trypsin or GluC as the enzyme; detected protein threshold of >0.05 (10%); sample type as identification; ID focus on biological modifications; thorough search effort; *Homo Sapiens* species; and variable modification of carbamidomethylation. Filters included; peptides of confidence value above 99%; false discovery rate of below 1%; and competitor error margin of 2.0.

2.6. Enzyme linked immunosorbent assay

2.6.1. Indirect one-site ELISA

96 well assay plates (Costar Corning, Invitro Tech, Australia, Cat. # 2595) were coated with mouse or human r-p75NTR^{ECD}-Fc antigen at 2µg/ml in Coating buffer (25mM Na_2CO_3, 25mM $NaHCO_3$, 0.01% Thimerosal, pH 9.6) and incubated overnight at 4°C, with gently agitation. Plates were then washed with Wash buffer (50mM Tris, 0.5M NaCl, 1mM EDTA, 0.1% Triton-X, pH 7) using a BioRad 1575 Immunowash Microplate washer (BioRad, California, USA, Cat. # 170-7009) for 5x2mins and blocked with Blocking buffer (25mM Na_2CO_3, 25mM $NaHCO_3$, 1% bovine serum albumin (BSA), 0.01% Thimerosal, pH 9.6) for a minimum of 1hr at 37°C with no agitation. Plates were washed again, for 3x2mins before the addition of 0.4µg/ml detecting antibody in Sample buffer (1M NaCl, 100mM Tris, 4mM EDTA, 2% BSA, 0.01% Thimerosal, 0.2% Triton-X, pH 7) for 2hrs, RT, with gentle agitation.

Following another wash of 5x2mins, the secondary antibody was added to wells in Sample buffer for 2.5hrs, RT slowly agitating. Plates were washed for 5x2mins and then 50µl of 3,3',5,5'-tetramethylbenzidine colour substrate kit (TMB, BioRad, California, USA, Cat. # 172-1067) was added to each well. After sufficient colour development, 50µl of 2M Sulphuric acid was added to each well, stopping the reaction. Plates were then read with a PerkinElmer Victor X4 Multilabel Plate Reader (Massachusetts, USA, Cat. # 2030-0040) at 450nm, RT.

2.6.2. Indirect sandwich ELISA

2.6.2.1. Initial protocol

96 well assay plates (Costar Corning, Invitro Tech, Australia, Australia Cat. # 2595) were coated with 2µg/ml capture antibody (mouse anti-human p75NTR MLR1 or MLR2) in Coating buffer (25mM Na_2CO_3, 25mM $NaHCO_3$, 0.01% Thimerosal, pH 9.6) and incubated for 18hrs, 4°C, with gentle agitation. Plates were then washed with Wash Buffer (0.5M NaCl, 1mM EDTA, 0.1% Triton X-100, 50mM Tris, pH 7) using a BioRad 1575 Immunowash Microplate washer (BioRad, California, USA, Cat. # 170-7009) for 5x2mins and blocked with Blocking buffer

(25mM Na_2CO_3, 25mM $NaHCO_3$, 0.01% Thimerosal, 1% BSA, pH 9.6) for a minimum of 1hr, RT with no agitation. Plates were washed again, for 3x2mins before the addition of the required antigen in ELISA Sample buffer (1M NaCl, 4mM EDTA, 2% BSA, 0.01% Thimerosal, 0.2% Triton X-100, 100mM Tris) for 4hrs, RT, with gentle agitation.

Following another wash of 5x2mins, 1µg/ml detecting antibody (goat anti-mouse $p75NTR^{ECD}$ antibody; R&D Systems, Minnesota, USA, Cat. # AF1157 /Sigma-Aldrich, Castle Hill Australia, Cat. # N5788), in ELISA Sample buffer, was added and incubated overnight, 4°C, with gentle agitation. Plates were then washed 5x2mins before the addition of the secondary antibody (bovine anti-goat HRP; Jackson ImmunoResearch, Cat. # 805 035 180) at 0.8µg/ml in ELISA Sample buffer for 2.5hrs, RT, with gentle agitation. Plates were then washed for 5x2mins and 50µl of 3,3',5,5'-tetramethylbenzidine colour substrate kit (BioRad, California, USA, Cat. # 172-1067) was added to each well. After 15min, 50µl of 2M Sulphuric acid was added to each well, stopping the reaction. Plates were read with a Perkin Elmer Victor X4 Multilabel Plate Reader (Perkin Elmer, Massachusetts, USA, Cat. # 2030-0040) at 450 nm, RT.

2.6.2.2. Final protocol

96 well assay plates (Costar Corning, Invitro Tech, Australia Cat. # 2595) were coated with 4µg/ml capture antibody (mouse anti-human p75NTR MLR1) in Coating buffer (25mM Na_2CO_3, 25mM $NaHCO_3$, 0.01% Thimerosal, pH 9.6) and incubated for 18hrs, 4°C, gently agitating. Plates were then washed with Wash buffer (5% 20xPBS, 0.05% Tween-20, pH 7.4) using a BioRad 1575 Immunowash Microplate washer (BioRad, California, USA, Cat. # 170-7009) for 4x2mins and blocked with ELISA Sample buffer (5% 20x PBS, 2% BSA, 0.05% Tween-20, 0.01% Thimerosal, pH 7.3) for a minimum of 1hr, 37°C with no agitation. Following blocking, antigen in ELISA Sample buffer was incubated for 20hrs at RT, with gentle agitation.

Detecting antibody (goat anti-mouse $p75NTR^{ECD}$; R&D Systems, Minnesota, USA, Cat. # AF1157/ Sigma-Aldrich, Australia, Cat. # N5788) at 1µg/ml in ELISA Sample buffer was added and incubated for 1hr, RT, with gentle agitation. Plates were then washed 4x2mins before the addition of the secondary antibody (bovine

anti-goat HRP; Jackson ImmunoResearch, Cat. # 805 035 180) at 0.8µg/ml in ELISA Sample buffer for 1hr, RT with gentle agitation. Plates were then washed for 4x2mins and 50µl of 3,3',5,5'-tetramethylbenzidine colour substrate kit (TMB, BioRad, California, USA, Cat. # 172-1067) was added to each well. After 15min, 50µl of 2M Sulphuric acid was added to each well, stopping the reaction. Plates were read with a Perkin Elmer Victor X4 Multilabel Plate Reader (Perkin Elmer, Massachusetts, USA, Cat. # 2030-0040) at 450nm, RT.

Additionally, a commercially available human p75NTR sandwich ELISA (R&D Systems, Minnesota, USA, Cat. # DY367) was tested against the in-house developed sandwich ELISA, as per manufacturer's instructions, or using the optimum incubation times developed for the in-house ELISA.

2.7. Colony maintenance and tracking of disease in SOD1^{G93A} mice

2.7.1. Colony maintenance

High copy number SOD1^{G93A} MND model mice (Jackson Laboratories strain: B6.Cg-Tg(SOD1*G93A)1Gur/J), with a pure C57BL/6J (B6) background, and a minimum of 23 copies of the mutant human *SOD1* gene which codes for a mutant SOD1^{G93A} protein, were bred within the Flinders University School of Medicine Animal Facility (Animal Welfare Committee Ethics Approval # 795.11, Flinders University Institutional Biosafety Committee OGTR Exemption # 2007-08).

The SOD1^{G93A} colony was maintained by breeding SOD1^{G93A} males with healthy control B6 females; resultant litters were expected to contain 50% human mutant SOD1^{G93A} carrying transgenic mice and 50% B6 healthy control mice (Gurney *et al.* 1994). The DNA profile of each pup was tested by analysing DNA, obtained from ear notches upon weaning, using real-time polymerase chain reaction with appropriate primers (Leitner *et al.* 2010) to test for the presence of the human mutant *SOD1* gene, as per ALS Therapy Development Institute (ALSTDI) guidelines (Leitner *et al.* 2010) by Cerberus Sciences (Adelaide). Additionally, the number of human mutant *SOD1* genes carried by males used for breeding was tested to ensure that breeding mice contained a minimum of 23 copies, as per ALSTDI guidelines (Leitner *et al.* 2010).

2.7.2. Neurological score

A neurological scoring method developed for SOD1 mice (Leitner *et al.* 2010) was used as a primary indicator of disease progression (**Table 2.2**). In accordance with ethics approval, a neurological score of three was used as end stage of disease for Flinders University-based SOD1^{G93A} mice (approx. 145-160 days of age). Neurological scoring was performed at 40, 60, 80, 100, and 120 days of age, then every three days thereafter until a neurological score of two was recorded, at which time, food was placed on bedding. Neurological scores were then measured daily from a neurological score of two, to the progression to a neurological score of three,

upon which soaked food was made available until euthanasia which was performed as soon as possible.

Table 2.2: Neurological scoring methods for SOD1^{G93A} mice
(adapted from Leitner *et al.* 2010)

Score	Explanation
0	Full extension of hind limbs away from lateral midline when mouse is suspended by its tail, and mouse can hold this for 2 seconds, suspended 2-3 times
1	Collapse or partial collapse of leg extension towards lateral midline (weakness) or trembling of hind limbs during tail suspension
2	Toes curl under at least twice during walking of 30 centimetres, or any part of foot is dragging along cage bottom/table*
3	Rigid paralysis or minimal joint movement, foot not being used for forward motion**
4	Mouse cannot right itself within 30 seconds from either side***

*If one hind limb is scored as 2, food pellets are left on bedding
**Upon reaching a neurological score of 3, soaked food is left on bedding until euthanasia
*** In accordance with ethics approval, SOD1^{G93A} mice in our colony were culled before reaching a neurological score of 4.

2.7.3. Weight

Flinders University-based mice (untreated and riluzole-treated) were weighed at 40, 60, 80, 100, and 120 days and then twice weekly until end stage (Neurological score 3; **Table 2.2**). Measuring weight loss and neurological scores together ruled out a loss of health from non-MND related symptoms, and a decrease in weight of 10% from maximum weight was also used as an indicator of disease progression.

University of Queensland-based mice were weighed from the start of experiments at 9 weeks (~60 days) of age, until close to end stage, when they were monitored daily. A decrease in weight of 20% from maximum weight was used as end stage of disease for University of Queensland-based SOD1^{G93A} mice treated with the potential treatment c29 or vehicle control.

2.7.4. Grip duration

Flinders University-based mice were tested on their gripping capacity in both fore limbs and hind limbs by placing mice on a mesh cage and inverting the mesh for the mice to hang upside-down (Miana-Mena *et al.* 2005). This was tested at 40, 60, 80, 100, and 120 days of age, and thereafter once weekly until mice were unable to grip onto the cage lid. Testing was repeated three times each trial with a break of 2mins between, and a cut-off of 90secs to determine grip duration.

2.7.5. Rotarod testing

University of Queensland-based mice were tested for motor function using the rotarod test beginning from 10 weeks (~70 days) of age. Each weekly session consisted of three trials on the elevated accelerating rotarod (Ugo Basile, Italy) beginning at 5rpm/min and accelerating to 20rpm/min over 20secs, for a total duration of 3mins.

2.7.6. MND treatment administration

A cohort of Flinders University-based SOD1^{G93A} and B6 healthy control mice were administered riluzole, or water, by oral gavage, twice weekly, from 30 days of age until end stage of disease (neurological score of 3). Fresh solutions of riluzole (Sanofi-Aventis, Paris, France) were made twice weekly to ensure a constant dose equating to 30 mg/kg per day (Waibel *et al.* 2004).

A cohort of University of Queensland-based SOD1^{G93A} mice were administered c29, a 29 amino acid peptide of p75NTR juxtamembrane 'Chopper' domain, or a vehicle control, by collaborators. Approximately 5mg/kg/day of c29 or vehicle control was administered through a 28-day subcutaneous osmotic minipump (flow rate of 0.11µl/hr; Alzet, California, USA, Cat. # 1004) which was replaced monthly, from 9 weeks (~60 days) of age until end stage of disease (a drop of 20% from maximum weight).

2.8. Urinary sample collection and biochemistry analysis

2.8.1. Mice sample collection

Urinary samples were obtained from Flinders University-based untreated and riluzole-treated SOD1^{G93A} and B6 healthy control mice of 40, 60, 80, 100, and 120 days of age and at end stage of disease (~145-160 days, defined as a neurological score of 3, see **Table 2.2**).

Additionally, a small number of urine samples were collected from p75NTR Exon III knock-out mice (Lee *et al.* 1992) at different ages, for use as p75NTR negative controls. Urinary samples were collected using a metabolic cage, except for end stage samples, which were obtained directly from the bladder upon euthanasia. All samples were immediately placed in tubes on ice before being transferred to long-term storage at -80°C.

Urinary samples were obtained from University of Queensland-based c29-treated and vehicle SOD1^{G93A} mice weekly from ~85 days of age until end stage of disease (~145-160 days, defined as a drop of 20% from maximum weight). Urinary samples were collected using a metabolic cage, except for end stage samples, which were obtained directly from the bladder upon euthanasia. All samples were immediately placed in tubes on ice before being transferred to storage at -80°C. Samples were shipped to Flinders University on dry ice and stored at -80°C until analysis.

2.8.2. Human sample collection

Urine samples were collected from people diagnosed with MND (n=41), people carrying MND-linked *SOD1* mutations without signs of symptoms (pre-fMND; n=24), Parkinson's disease (PD; n=10), Multiple Sclerosis (MS; n=9) and people with no known health problems (healthy individuals, HI; n=23). People with MND were diagnosed as having sporadic MND (n=38) or familial MND (n=3) under the categories of 'clinically definite' or 'clinically probable', using the Awaji criteria (4th revision of the El Escorical criteria) (de Carvalho *et al.* 2008a). People with MND variants under the headings of 'Sporadic MND', and 'Genetically-determined

(familial, hereditary) MND' were included, whereas 'MND-plus syndromes', 'MND with laboratory abnormalities of uncertain significance' and 'MND-mimic syndromes' were excluded. A maximum of five urine samples were collected from each person diagnosed with MND over approximately a one-year period for longitudinal studies, and for longitudinal studies of people with pre-fMND, a maximum of four urine samples over 4 years were collected. Additionally, clinical information pertaining to disease was obtained for all participants.

Study participants were recruited from clinics at the Repatriation Hospital, Daw Park, Adelaide or Flinders Medical Centre, Bedford Park, Adelaide (courtesy of Dr. David Schultz, Dr. Owen Davies, Dr. Margaret Bulling & Dr. Andrew Moey; Southern Adelaide Clinical Human Research Ethics Committee Approval (SACHREC) # 229.11 & 58.12), or through the *pre-fALS* study at the Miller School of Medicine, University of Miami, Miami, Florida (courtesy of Dr. Michael Benatar & Joanne Wuu; University of Miami Human Research Subjects Office Approval # 20101021, SACHREC Approval # 352.13). Samples collected in Adelaide were stored in standard urine pots on ice for no longer than 4 hours before centrifugation in a refrigerated centrifuge (Sigma-Aldrich; Cat. # 6K15) at 2,000g, 4°C, 5min as per Human Kidney and Urine Proteome Project guidelines (Yamamoto 2010), followed by division into aliquots, and storage at -80°C. Samples acquired from the *pre-fALS* study were shipped to Flinders University on dry ice and stored at -80°C until analysis.

2.8.3. Urine biochemistry analysis

Mouse urinary creatinine was measured using a creatinine kit based upon the Jaffe reaction, as per manufacturers' instructions (Enzo Life Sciences, New York, USA, Cat. # ADI-907-030A). Briefly, urine samples were diluted 1:10 with dH_2O, and creatinine was measured at 490nm using a Perkin Elmer Victor X4 Multilabel Plate Reader (Perkin Elmer, Massachusetts, USA, Cat. # 2030-0040) after 30mins.

Human urinary creatinine and urea levels were measured by standard clinical analysis using a Roche/Hitachi Modular analyser (SA Pathology), with enzymatic analysis for creatinine and turbidmetric assay for protein.

2.9. Data analysis

A combination of Microsoft Excel, Graph Pad Prism6 (San Diego, USA) and IBM SPSS Statistics22 (Armonk, USA) were used for statistical analysis of data. Image compilation was performed using a combination of Graph Pad Prism6, Adobe Illustrator, and Adobe Photoshop software.

For ELISAs, standard curves were plotted and used for urinary $p75NTR^{ECD}$ calculations using Microsoft Excel and Prism6. Comparisons of curves were performed using r^2 values of linear regression, and signal to noise (S/N) ratios.

For mouse results, two-way ANOVAs with Bonferroni's post-hoc analyses were performed on data obtained from urinary $p75NTR^{ECD}$ levels, weight measurements, neurological scores, and grip duration testing, to evaluate parameters over time. Rotarod results were analysed using the non-linear (curve fit) function in Prism6. Percentage survival was determined by the creation of a Kaplan-Meier survival curves and Log-rank analyses.

For human data analysis, urinary $p75NTR^{ECD}$ levels, and urinary and clinical characteristics were compared using independent or Welch's t-tests, Pearson's correlations, and one-way ANOVAs, with Bonferroni's post-hoc analysis as required. Urinary $p75NTR^{ECD}$ discriminatory power was determined using Receiver Operating Characteristic (ROC) curve analysis, with the area under the curve (AUC) used as discriminatory accuracy. The relationship between urinary $p75NTR^{ECD}$ levels and ALSFRS-r scores or time was determined using Pearson's correlations.

Chapter 3. Detection of p75NTR^{ECD} in urine of SOD1^{G93A} mice and people with MND

3.1. Introduction

The first aim of this study was to determine if p75NTR^{ECD} is present in the urine of SOD1^{G93A} mice that model MND, and people living with MND, for use as a biomarker of disease. To do this, urine samples were tested using Immunoprecipitation (IP), followed by Western blot (IP/WB) or Mass Spectrometry (IP/MS). The IP/WB method was used to detect p75NTR^{ECD} in samples, and required the optimisation of a pair of antibodies in order to capture p75NTR^{ECD} (IP) and detect p75NTR^{ECD} in protein transferred to nitrocellulose membranes from SDS-PAGE (WB). IP/MS was used to sequence immunoprecipitated p75NTR^{ECD} in samples to confirm the detection of p75NTR^{ECD}.

An Immunoprecipitation (IP) procedure utilises the interaction of antigens and antibodies by precipitating antigens out of solution using their respective antibodies (Harlow & Lane 1988). IP is used widely to investigate the presence, abundance, size, up or down regulation, stability, post-translational modifications and interactions of proteins (Kaboord & Perr 2008). Western blotting (WB) (Renart *et al.* 1979, Towbin *et al.* 1979) also relies on antigen-antibody interactions, and involves the electrophoretic transfer of proteins from SDS-PAGE gels (Laemmli 1970) to membranes, which allows for the subsequent detection and visualisation of specific proteins using antibodies and colourimetric or fluorometric substrates.

An earlier paper (Zupan *et al.* 1989) first showed the presence of p75NTR^{ECD} in human urine and human derived A875 melanoma cells with a radio-immunoprecipitation procedure. Zupan and colleagues used iodinated NGF to label p75NTR, and an anti-rat p75NTR antibody to capture the complex, which was then run on gels and identified by radioactivity. Before the advent of sensitive imaging technologies for WB, radio-immunoprecipitation was a commonly used technique. Now, sensitive chemiluminescent WB is used, which does not require the use of radioactivity. This technique relies on a chemiluminescent signal from a peroxidase labelled secondary antibody applied to the WB, which is imaged on a cooled-CCD camera (Alegria-Schaffer *et al.* 2009).

In order to detect p75NTR^{ECD}, the combination of IP and WB requires two antibodies that detect different epitopes (Harlow & Lane 1988). One antibody is

used as an Immunoprecipitation antibody, capturing p75NTR^{ECD} during IP, while the other antibody is used for p75NTR^{ECD} detection in WB, with both antibodies detecting different epitopes of p75NTR^{ECD}. In addition, the antibody used for p75NTR^{ECD} capture (IP) needed to be made in a different animal species than the anti-p75NTR antibody used for detecting p75NTR in WB. These conditions ensure that the secondary antibody conjugated to horseradish peroxidase (HRP) used in WB, binds only to the detection antibody, and does not cross-react to the anti-p75NTR capture antibody used during IP.

To confirm that p75NTR^{ECD} was present in the urine of people with MND, urine samples were subject to IP followed by Mass Spectrometry (IP/MS). Mass Spectrometry analysis has a wide range of applications as it can provide qualitative and quantitative information about the molecular composition of organic and inorganic samples in gas, liquid, or solid states, from samples the size of atoms to proteins (see Finehout & Lee 2004 for review). For this study, Mass Spectrometry was used to measure the mass of peptide ions fragmented within the machine, to determine the amino acid sequence of peptides by comparing the masses to theoretical values using the Swissprot database (UniProt consortium 2014). Orbitrap- and Triple TOF MS analyses were chosen for their ability to identify specific proteins within complex mixtures of biological origin (Baldwin 2004). Thus, this technique can be used to validate findings made through IP/WB.

The aim of this chapter addresses the first step in analysing p75NTR^{ECD} as a MND biomarker, by determining if p75NTR^{ECD} is present in the urine of SOD1^{G93A} mice and people with MND.

3.2. Development of Immunoprecipitation/ Western blot for p75NTR^{ECD} detection

In order to detect p75NTR^{ECD} from mouse- and human-derived sources, a number of different antibodies were first tested in Western blot (WB; see **2.3**). As shown in **Figure 3.1.A**, the polyclonal goat anti-mouse p75NTR^{ECD} antibody specifically detects bands at the expected molecular weight of full-length p75NTR (p75NTR^{FL}; ~70-75kDa) and the extracellular domain (p75NTR^{ECD}; 50-55kDa) in mouse- (NSC-34 motor neuron-like cell line; **Figure 3.1.A**, **lane 3**) and human-derived (A875 melanoma; **Figure 3.1.A**, **lane 2**) p75NTR-positive cell lysates. However, no bands correlating to p75NTR species were detected in p75NTR-negative cell lysates (BSR fibroblast; **Figure 3.1.A**, **lane 1**).

The polyclonal goat anti-mouse p75NTR^{ECD} antibody was then used in WB to detect p75NTR^{ECD} in mouse urine. First, protein was Trichloroacetic acid (TCA)-precipitated from urine samples taken from SOD1^{G93A} MND model mice (SOD1^{G93A}), which are expected to have increased urinary p75NTR^{ECD} as MND symptoms develop, and C57BL/6J (B6) healthy control mice (see **2.4.1**; Thongboonkerd *et al.* 2006). After protein quantification, 20µg of protein from each sample was subject to WB using 0.4mg/ml goat anti-mouse p75NTR^{ECD} and bovine anti-goat HRP antibody at 1:5,000, for p75NTR^{ECD} detection (**Figure 3.1.B**).

Bands at the expected molecular weight of p75NTR^{FL} and p75NTR^{ECD} were detected in the p75NTR-positive mouse derived cell lysate (NSC-34 motor neuron-like cell line; **Figure 3.1.B**, **lane 11**). Additionally, a band at the molecular weight of p75NTR^{ECD} was seen in the urinary protein from SOD1^{G93A} mice at end stage of disease (**Figure 3.1.B**, **lane 9**). Urinary p75NTR^{ECD} was not detected in samples from SOD1^{G93A} mice at younger ages, or in B6 healthy controls, despite the fact that staining the WB membrane with Sypro Ruby total protein stain as a loading control, before the addition of antibodies, showed loading of urinary protein from every sample (see **2.3.3**; **Figure 3.1.C**).

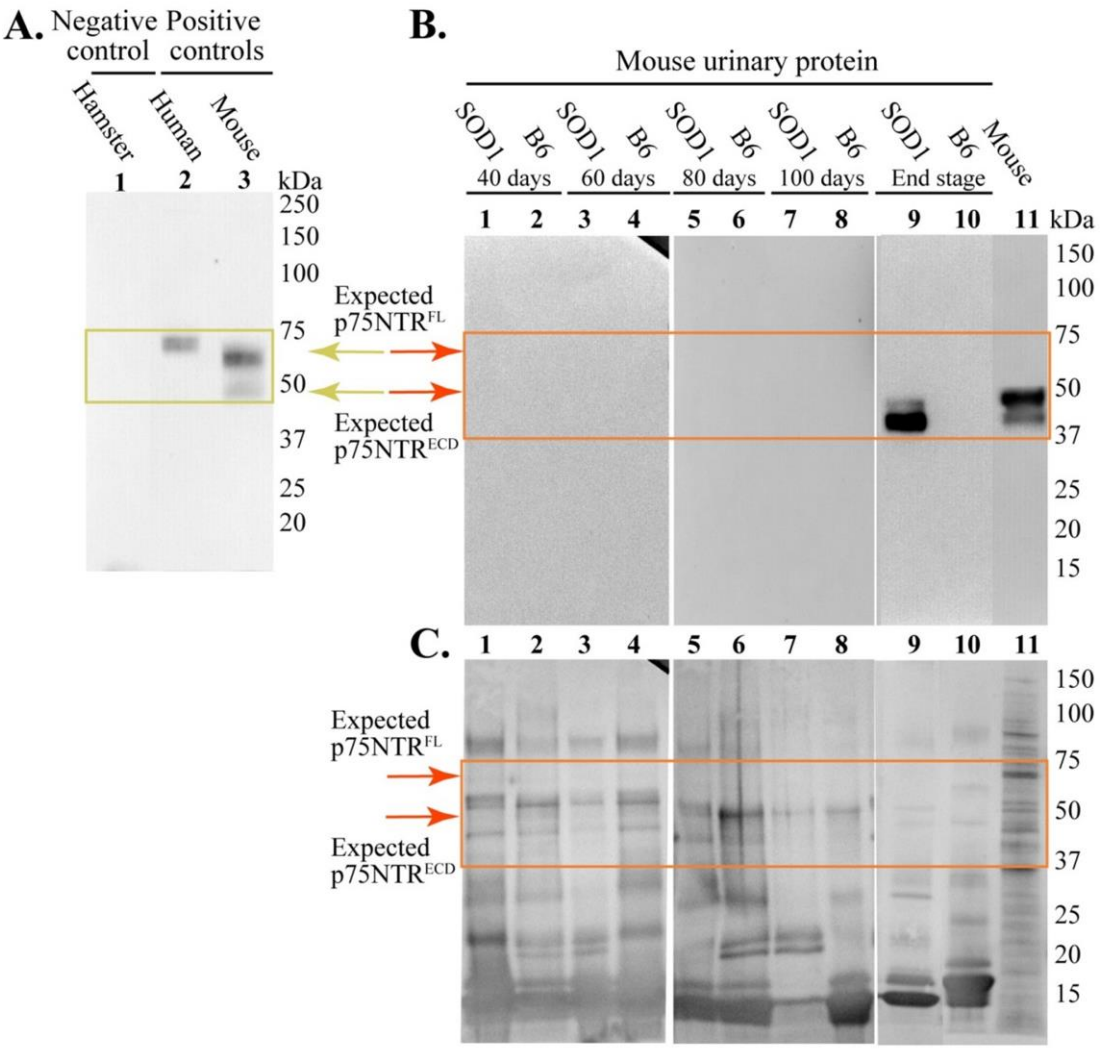

Figure 3.1: Testing of goat anti-mouse p75NTR^{ECD} antibody with cell lysates in Western Blot, and Western blot and Sypro Ruby stain for p75NTR^{ECD} and total protein in trichloroacetic acid-precipitated urine from SOD1^{G93A} and B6 healthy control mice

A. The specificity of goat anti-mouse p75NTR^{ECD} polyclonal antibody was tested using 20µg of mouse- (**lane 3**, NSC-34, motor neuron-like cell line) and human - (**lane 2**, A875 melanoma) derived p75NTR-positive cell lysates and hamster- (BSR) derived p75NT- negative cell lysates (**lane 1**) using Western blot (WB). **B.** 20µg of TCA-precipitated protein from mouse-derived cell lysates, and SOD1^{G93A} and B6 healthy control mice urine at 40 (**lanes 1** and **2**), 60 (**lanes 3** and **4**), 80 (**lanes 5** and **6**), and 100 days of age (**lanes 7** and **8**), and end stage of disease (**lanes 9** and **10**) was separated by SDS-PAGE and subject to WB, using 0.4mg/ml goat anti-mouse p75NTR^{ECD} antibody and bovine anti-goat HRP (1:5,000) for p75NTR^{ECD} detection. **C.** Prior to antibody treatment, the WB membrane (in **B.**) was stained with Sypro Ruby protein stain to visualise total protein loading.

Previous studies have reported that p75NTR is detectable in spinal cord motor neurons of $SOD1^{G93A}$ mice prior to end stage, using immunohistochemistry (Lowry *et al.* 2001). As such, the absence of detectable urinary $p75NTR^{ECD}$ before end stage of disease in $SOD1^{G93A}$ mice suggests that the WB method may not be sensitive enough for $p75NTR^{ECD}$ detection. To address this, a method that was able to enrich $p75NTR^{ECD}$ from samples was sought to further test urine samples from $SOD1^{G93A}$ mice across disease progression. This was achieved by replacing the TCA precipitation method with an antibody-based immunoprecipitation, prior to WB (IP/WB; see **2.4.2**). This step allowed for the enrichment of $p75NTR^{ECD}$, increasing the sensitivity of detection. In addition, the use of two antibodies specific for $p75NTR^{ECD}$, the first antibody selectively capturing $p75NTR^{ECD}$ from solution during IP, and the second antibody selectively detecting a different epitope of $p75NTR^{ECD}$ in WB, increased the specificity of $p75NTR^{ECD}$ detection.

To determine the optimum pair of antibodies for $p75NTR^{ECD}$ enrichment and detection using IP/WB, 500µg of immunoprecipitated protein from cells expressing p75NTR, derived from mice (NSC-34 motor neuron-like cell line), humans (A875 melanoma) and rats (C6 glioma), was used for $p75NTR^{ECD}$ detection (**Figure 3.2**). An optimised antibody pair would be able to detect $p75NTR^{ECD}$ at two different epitopes without cross-reactivity. These antibody pairs were identified by detection of bands at the expected molecular weight of mouse and human $p75NTR^{FL}$ (~70-75kDa) and/or $p75NTR^{ECD}$ (50-55kDa) in cell lysates subject to WB alone (one antibody; **Figure 3.2.A-D**, **lanes 6-8**), which were then enriched in the same lysates subject to IP/WB (two antibodies; **Figure 3.2.A-D**, **lanes 3-5**, **Figure 3.2.E**, **lanes 4-6**, and **Figure 3.2.F**, **lanes 2-4**).

The specificity of the IP/WB procedure was tested using multiple controls. An antibody control with no cell lysate (**Figure 3.2.A-D**, **lane 2**, **Figure 3.2.E**, **lane 3**, and **Figure 3.2.F**, **lane 1**), confirmed that the secondary HRP-conjugated antibodies detected the 25kDa light chain IgG of the primary antibody used for $p75NTR^{ECD}$ capture during IP, but not the heavy chain at 50kDa, which would interfere with $p75NTR^{ECD}$ detection. The specificity of the antibody pair for p75NTR was also tested by replacing recombinant p75NTR protein containing a human-derived –Fc fragment (Fc-part of human IgG1, 230 amino acids; r-p75NTR-Fc) or urine with bovine serum albumin (BSA) that has no known p75NTR. **Figure 3.2.A-E**, **lane 1**,

shows no bands at the molecular weight of p75NTR species in BSA samples, unless spiked with mouse r-p75NTR^{ECD}-Fc (**Figure 3.2.E**, **lane 2**).

The aim of the IP was to enrich p75NTR^{ECD}, allowing for the detection of mouse- and human-derived p75NTR^{ECD} in WB. From the antibodies tested, two antibody pairs that enriched and detected mouse and human p75NTR^{ECD} were identified; the in-house developed monoclonal mouse anti-human p75NTR (MLR1) and polyclonal goat anti-mouse p75NTR^{ECD}, and the in-house developed monoclonal mouse anti-human p75NTR (MLR2) and goat anti-mouse p75NTR^{ECD}, as seen in **Figure 3.2.A** and **C**. Although there was some variability in the IP experimental procedure, as seen by variations in the amount of light chain IgG (25kDa) detected within individual blots, e.g., lower amounts in **Figure 3.2.C** and **D**, **lane 4**, this does not discount the fact that the above mentioned antibody pairs enrich and detect mouse- and human-derived p75NTR.

The other antibody pairs tested did not enrich p75NTR^{ECD} and/or detect both mouse- and human-derived p75NTR^{ECD}. The rabbit anti-human p75NTR^{ECD} and mouse anti-human p75NTR (MLR2) antibodies only enriched and detected human derived p75NTR^{FL} and p75NTR^{ECD} in IP/WB (**Figure 3.2.B**, **lane 4**). Additionally, the combination of rabbit anti-human p75NTR^{ECD} and mouse anti-human p75NTR (MLR1) antibodies did not enrich mouse and human p75NTR^{ECD} in IP/WB (**Figure 3.2.D**, **lanes 4**, **5**) as compared to WB alone (rabbit anti-human p75NTR^{ECD} detection; **Figure 3.2.D**, **lanes 7**, **8**). Using goat anti-mouse p75NTR^{ECD} antibody for p75NTR^{ECD} capture, and mouse anti-human p75NTR (MLR2) antibody (**Figure 3.2.E**, **lanes 4-6**) or mouse anti-human p75NTR (MLR1) antibody (data not shown) for detection, was also unsuccessful in mouse- and human-derived p75NTR^{ECD} enrichment and detection in IP/WB, as the monoclonal mouse anti-human p75NTR (MLR1) and (MLR2) antibodies bind to specific p75NTR conformations and so do not work well under WB conditions (Rogers *et al.* 2006). Finally, the combination of goat anti-mouse p75NTR^{ECD} for p75NTR^{ECD} capture, and rabbit anti-human p75NTR antibody for detection was tested. As shown in **Figure 3.2.F**, this antibody pair did not enrich p75NTR^{ECD} in mouse- and human-derived lysates, as shown by light bands at the molecular weight of p75NTR (**Figure 3.2.F**, **lanes 3**, **4**).

In comparison, the use of 5µg of mouse anti-human p75NTR (MLR2) antibody for p75NTR^{ECD} capture in IP, followed by p75NTR^{ECD} detection using 0.4mg/ml of

goat anti-mouse p75NTR^{ECD}, and bovine anti-goat HRP antibody at 1:5000 (**Figure 3.2.A**) enriched p75NTR^{ECD} and showed minimal non-specific binding. As such, this antibody combination was chosen as the optimal antibody set for IP/WB detection of mouse- and human-derived p75NTR^{ECD}.

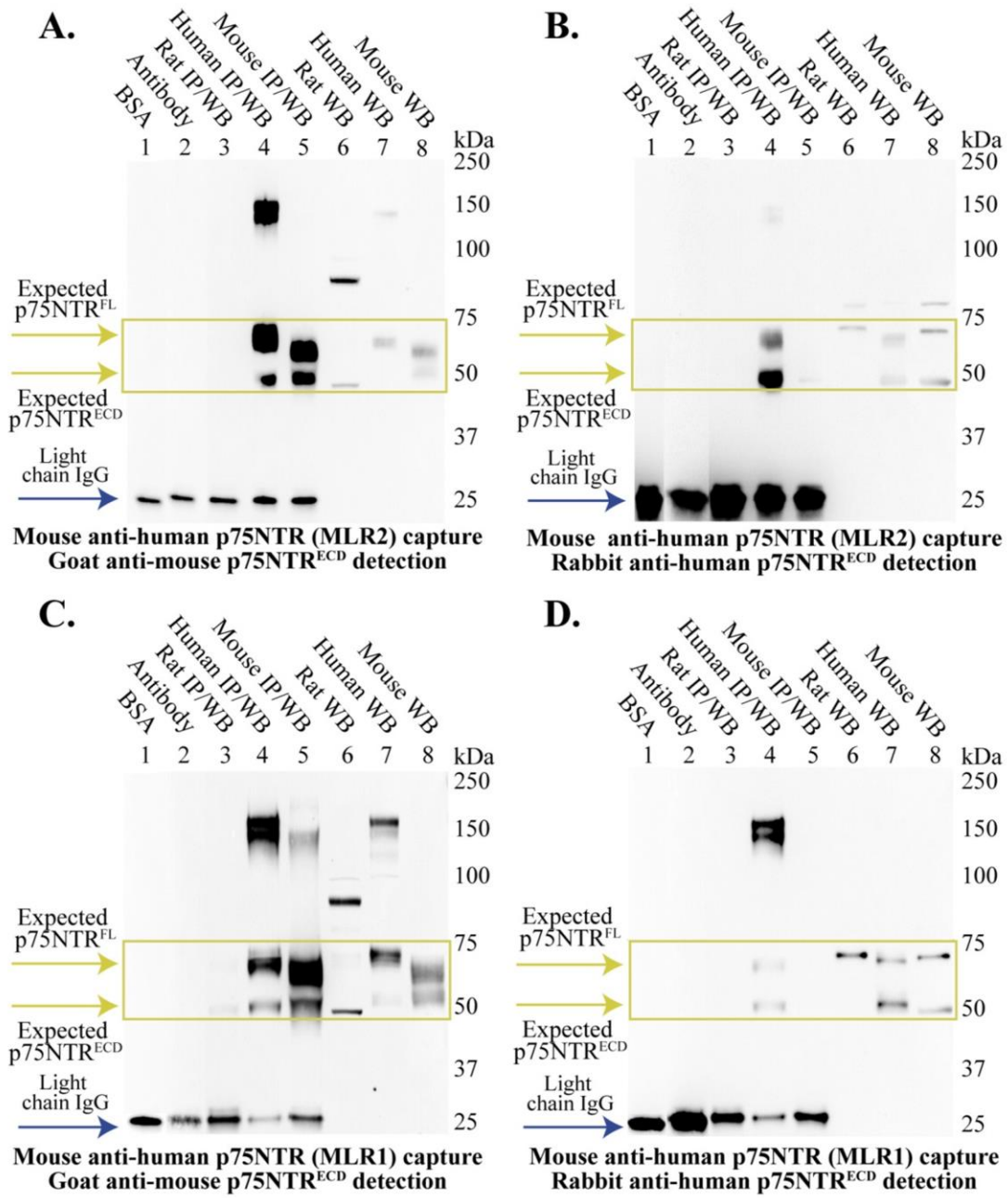

Figure 3.2: Detection of p75NTR using Immunoprecipitation/Western blot of mouse-, human-, and rat-derived cell lysates

500µg of p75NTR-positive mouse- (NSC-34 motor neuron like cell line), human- (A875 melanoma), and rat- (C6 glioma) derived cell lysates were subject to Immunoprecipitation (IP) using 5µg of mouse anti-human p75NTR (MLR2) antibody (**A.** and **B.)** or mouse anti-human p75NTR (MLR1) antibody (**C.** and **D.**) for p75NTR capture. Samples were then subject to SDS-PAGE and Western blot (WB) and detected with 0.4mg/ml goat anti-mouse $p75NTR^{ECD}$ antibody and bovine anti-goat HRP (1:5,000) (**A.** and **C.**) or**.** rabbit anti-human $p75NTR^{ECD}$ antibody at 1:500 and donkey anti-rabbit HRP (1:5,000) (**B.** and **D**). In addition, cell lysates were subject to WB alone, and bovine serum albumin (BSA) and an antibody control with no cell lysate were used as negative controls in IP/WB.

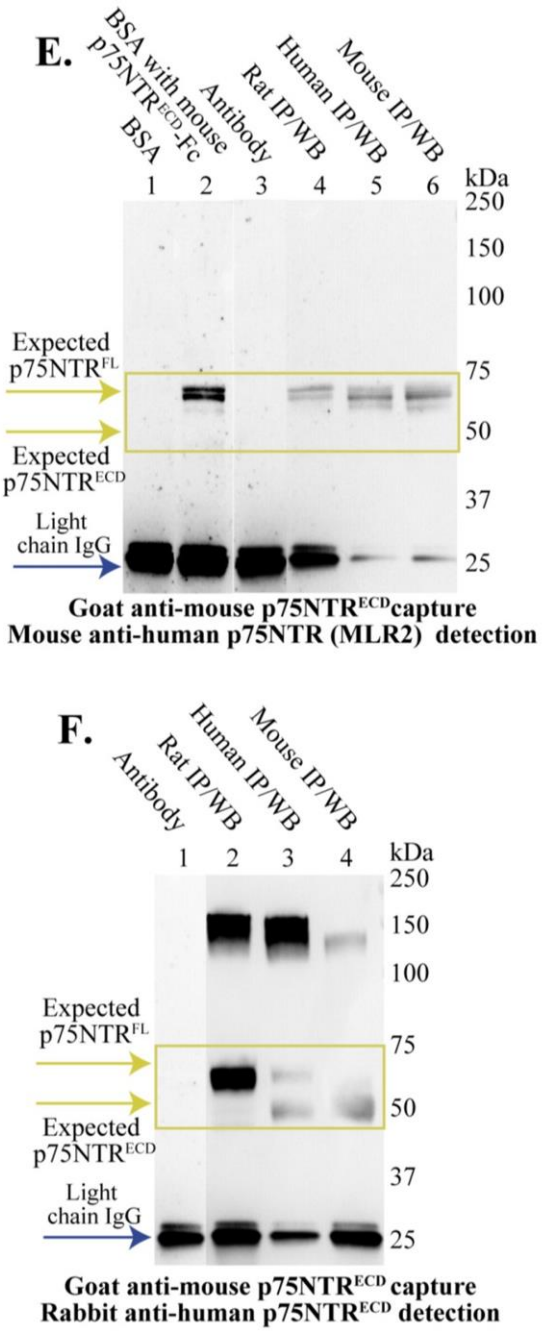

Figure 3.2: Detection of p75NTR using Immunoprecipitation/Western blot of mouse-, human- and rat-derived cell lysates

500µg of p75NTR positive mouse-, human-, and rat-derived cell lysates were subject to Immunoprecipitation (IP) using 5µg of goat anti-mouse $p75NTR^{ECD}$ antibody for p75NTR capture. Samples were then subject to SDS-PAGE and Western blot (WB) and detected with **E.** 0.01mg/ml mouse anti-human p75NTR (MLR1) antibody and donkey anti-mouse HRP (1:5,000) or **F.** rabbit anti-human $p75NTR^{ECD}$ antibody at 1:500 and donkey anti-rabbit HRP (1:5,000) for $p75NTR^{ECD}$ detection. In addition, bovine serum albumin (BSA) and an antibody control with no cell lysate were used as negative controls, and BSA spiked with mouse r-$p75NTR^{ECD}$-Fc was used as a positive control in IP/WB.

3.3. Detection of p75NTR^{ECD} in urine using Immunoprecipitation/Western blot

3.3.1. IP/WB detection of p75NTR^{ECD} in urine of SOD1^{G93A} mice

Following the development of a IP/WB protocol for p75NTR^{ECD} enrichment and detection, urine samples from SOD1^{G93A} mice and B6 healthy control mice at ages 40, 60, 80, and 100 days of age and end stage of disease (145-160 days) were tested for the presence of p75NTR^{ECD} using this method. Briefly, urine samples were diafiltered (see section **2.4.2**) and total protein quantified, with 110µg protein from each sample immunoprecipitated using 5µg of mouse anti-human p75NTR (MLR2) antibody. Samples were then subject to WB using 0.4mg/ml goat anti-mouse p75NTR^{ECD} antibody and bovine anti-goat HRP at 1:5,000.

The bovine anti-goat HRP antibody is cross adsorbed against the 50kDa IgG of many species including mouse and human, but detects the 25kDa light chain IgG. As such, a band at 25kDa was seen in all IP/WB treated samples, indicative of the light chain of the antibody used in the IP step (**Figure 3.3**, **all lanes**).

As seen in **Figure 3.3**, bands at the molecular weight of p75NTR^{ECD} were detectable in urine samples from multiple ages of SOD1^{G93A} mice, and were first detectable in SOD1^{G93A} mice pre-symptomatically at 60 days of age (**Figure 3.3**, **lane 4**). Additionally, p75NTR^{ECD} was detectable in SOD1^{G93A} mice at 80 and 100 days of age, through to end stage of disease (**Figure 3.3**, **lanes 6**, **8**, **10**). Conversely, bands at the expected molecular weight of p75NTR^{ECD} were not seen in the urine of B6 healthy, age-matched control mice (**Figure 3.3**, **lanes 1**, **3**, **5**, **7**) until the equivalent of end stage disease (**Figure 3.3**, **lane 9**; ~145-160 days, n=3 blots).

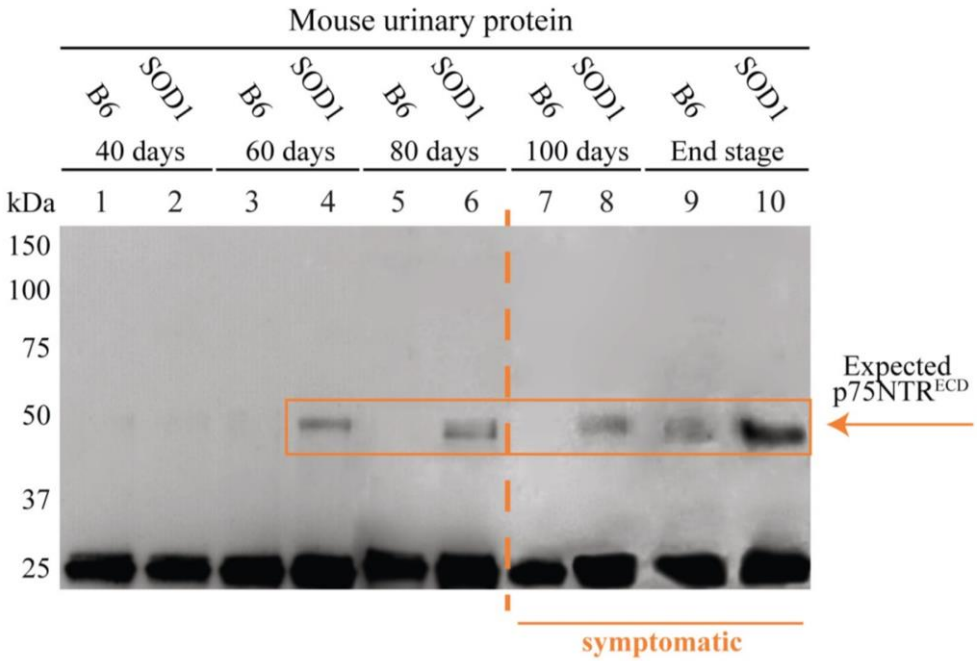

Figure 3.3: Detection of p75NTR^{ECD} in the urine of SOD1^{G93A} and B6 healthy control mice using Immunoprecipitation/Western blot

110µg of urinary protein from SOD1^{G93A} (SOD1) mice and B6 healthy control mice at 40, 60, 80, and 100 days of age, and end stage of disease, was subject to Immunoprecipitation (IP) using 5µg of mouse anti-human p75NTR (MLR2) antibody for p75NTR^{ECD} capture. Samples were then subject to Western blot (WB) using 0.4mg/ml goat anti-mouse p75NTR^{ECD} and bovine anti-goat HRP (1:5,000) antibodies for p75NTR^{ECD} detection. The bovine anti-goat conjugated HRP antibody is cross adsorbed against the 50kDa heavy chain IgG of a wide range of species, but detects the 25kDa light chain of IgG, as seen in all samples run through the IP/WB procedure.

3.3.2. IP/WB detection of p75NTR^{ECD} in urine of people with MND

Urinary protein from people with sporadic MND and healthy individuals was also tested for the presence of p75NTR^{ECD} using IP/WB, with 500µg of urinary protein from each individual subject to IP, and then WB after diafiltration. The same combination of antibodies, mouse anti-human p75NTR (MLR2) for p75NTR^{ECD} capture during IP, and goat anti-mouse p75NTR^{ECD} with bovine anti-goat HRP (**Figure 3.4**) for p75NTR^{ECD} detection in WB, was used.

Human-derived (A875 melanoma) cell lysates were used as p75NTR-positive controls, and bands at the expected molecular weight of p75NTR^{FL} and p75NTR^{ECD} were detected in these lysates when subject to the WB procedure (**Figure 3.4**, **lane 3**). The use of two different antibodies against p75NTR further enriched p75NTR^{FL} and p75NTR^{ECD} detection in these lysates using IP/WB (**Figure 3.4**, **lane 2**). Baby hamster-derived kidney fibroblast cell lysates (**Figure 3.4**, **lane 1**) were used as p75NTR-negative controls, and did not show bands at the molecular weight of p75NTR species.

Importantly, urine from two people with sporadic MND showed bands at the expected molecular weight of p75NTR^{ECD}. The first sample (**Figure 3.4**, **lane 4**) was from a 72-year-old male with three years of bulbar onset MND symptoms (MND05), the second, a 70-year-old female with 4 and a half months of limb onset MND symptoms (**Figure 3.4**, **lane 5**; MND18). In comparison, p75NTR^{ECD} was not detectable in the urine of two healthy individuals (HI; **Figure 3.4**, **lanes 6**, **7**), females of 44 (MND10) and 71 years of age (MND16).

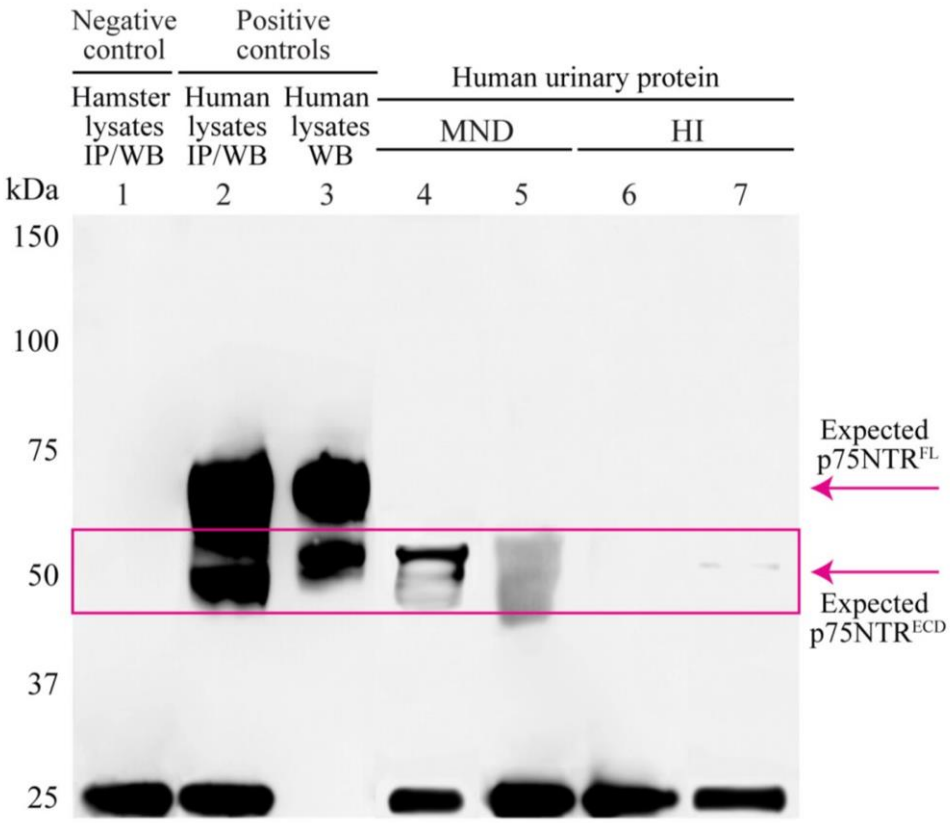

Figure 3.4: Detection of p75NTR^{ECD} in the urine of people with sporadic MND and healthy individuals using Immunoprecipitation/Western blot

500µg of urinary protein from people with sporadic MND and healthy individuals (HI), and 500µg of p75NTR-negative hamster-derived, and p75NTR-positive human-derived cell lysates were subject to Immunoprecipitation (IP) using 5µg of mouse anti-human p75NTR (MLR2) antibody for p75NTR^{ECD} capture. Samples were then subject to Western blot (WB) using 0.4mg/ml goat anti-mouse p75NTR^{ECD} and bovine anti-goat HRP (1:5,000) antibodies for p75NTR^{ECD} detection. The bovine anti-goat conjugated HRP antibody is cross adsorbed against the 50kDa heavy chain IgG of a wide range of species, but detects the 25kDa light chain of IgG, as seen in all samples run through the IP/WB procedure.

3.4. Development of Orbitrap Mass Spectrometry for p75NTR^{ECD} detection

In order to validate the detection of p75NTR^{ECD}, Mass spectrometry was used to identify p75NTR^{ECD} Immunoprecipitated from the urine of people with MND. Orbitrap- (Orbitrap-MS) and Triple TOF-Mass Spectrometry (Triple TOF-MS) were chosen as the validation method as they allowed for specific identification of proteins (Baldwin 2004) detectable in the urinary samples with high resolution and mass accuracy (Perry *et al.* 2008, Zubarev & Makarov 2013) after enzymatic digestion.

First, the method for p75NTR^{ECD} detection with MS needed to be optimised. As the aim was to produce the maximum number of peptides within the detection limits of the Orbitrap-MS for p75NTR^{ECD} sequencing, the hypothetical cleavage sites of the p75NTR^{ECD} peptide using different enzymes was analysed using Swissprot online databases (Swiss Institute of Bioinformatics 2014a, Swiss Institute of Bioinformatics 2014b). Results of this analysis showed that the enzyme Trypsin Gold, which cleaves at the carboxyl side of lysine or arginine except when either is followed by a proline (Keil 1992), and is typically used for MS protein digestion (Baldwin 2004), has a small number of hypothetical cleavage sites for p75NTR^{ECD}. As such, Trypsin Gold digestion of p75NTR^{ECD} would result in a small number of large peptide fragments, which could pose problems for the production of sufficiently small sized peptides for analysis in the Orbitrap-MS. Theoretically, Orbitrap-MS can detect peptides with a mass to charge ratio (m/z) of 300-1000, which translates to a mass range of 600-2,000Da for doubly charged ions, and 900-3,000Da for triply charged ions. However, in practice, it is difficult to effectively fragment peptides over a mass of 2,500Da as the Orbitrap-MS uses a fixed collision energy, which is suitable for smaller ions, but is usually insufficient for very large ions. As a result, the mass range for peptide cleavage in this setup is between 600 and 2,000Da, with peptides between 2000 and 2,500Da in mass also possible to fragment (Perry *et al.* 2008).

Using Swissprot analysis, Trypsin Gold has 12 hypothetical cleavage sites for human-derived p75NTR^{ECD} (**Figure 3.5.A**) resulting in seven fragmentable peptides (**Appendix B**, **Table 1**). In comparison, the use of the enzyme glutamyl

endoproteinase GluC (V8) results in a higher number of hypothetical peptides for human p75NTR^{ECD} within the Orbitrap-MS detection range. GluC preferentially cleaves at glutamic acid (Birktoft & Breddam 1994), and has 24 hypothetical cleavage sites for human-derived p75NTR^{ECD} (**Figure 3.5.A**) resulting in 16 fragmentable peptides (**Appendix B**, **Table 2**).

For mouse-derived p75NTR^{ECD} (**Figure 3.5.B**), Trypsin Gold cleavage results in five potential peptides of the size fragmentable by Orbitrap-MS, and a further two between 2000 and 2,500Da in mass, which may be fragmented (**Appendix B**, **Table 3**). Additionally, GluC has 24 hypothetical cleavage sites for mouse-derived p75NTR^{ECD} (**Figure 3.5.B**), resulting in 13 peptides of the size fragmentable by Orbitrap-MS, with one additional peptide between 2000 and 2,500Da in mass, which may be fragmented (**Appendix B**, **Table 4**).

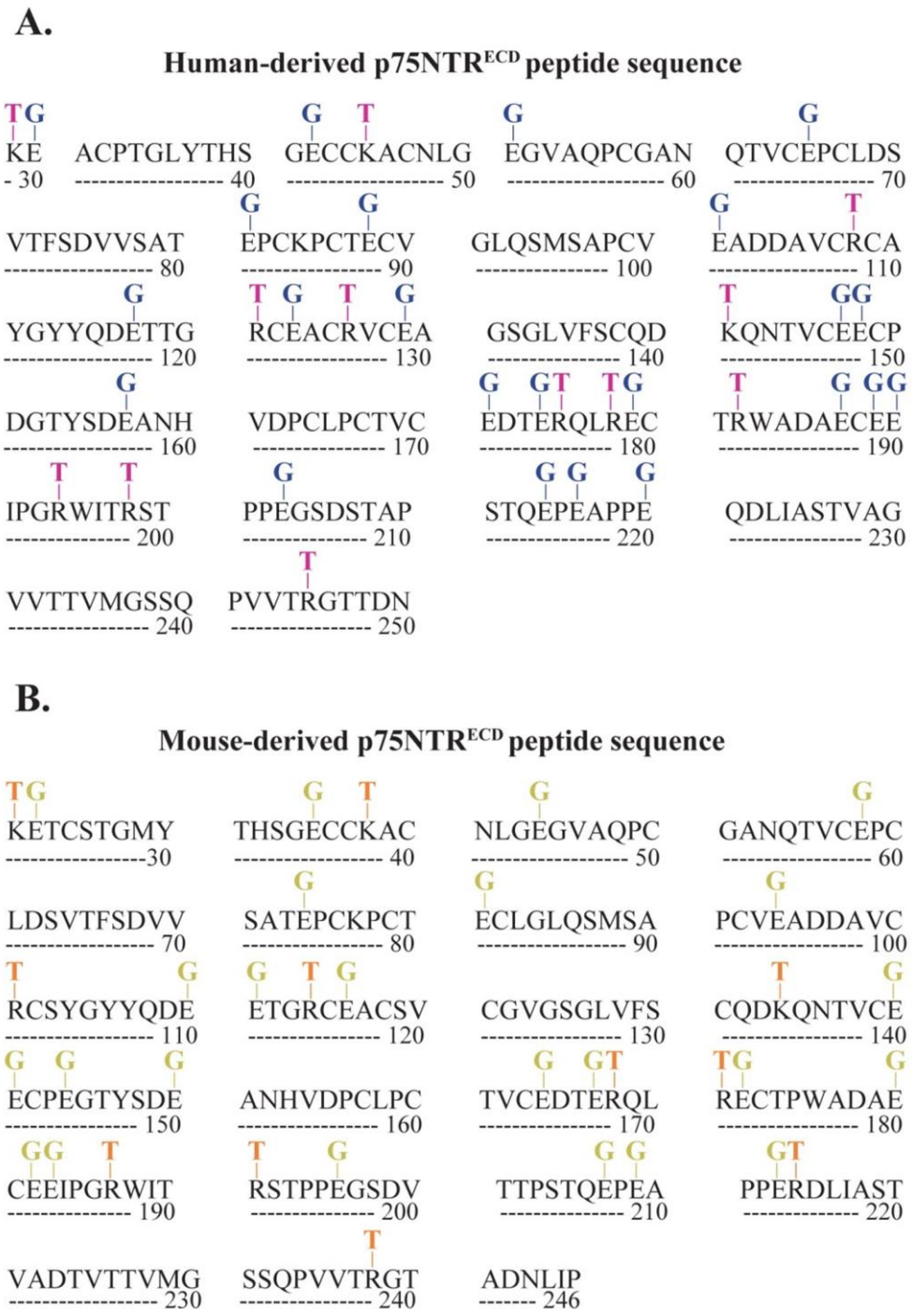

Figure 3.5: Hypothetical enzyme cleavage sites of p75NTR^{ECD} using Trypsin Gold or GluC

A. Trypsin Gold (T) treatment of human p75NTR^{ECD} resulted in 12 hypothetical cleavage sites resulting in peptides within the Orbitrap-MS detection limit that covered approximately of 35.1% of the protein sequence. Using endoproteinase GluC (G), 23 potential cleavage sites with an approximate coverage of 69.8% of the protein sequence was predicted **B.** Twelve hypothetical cleavage sites with a coverage of 55.1% of the protein sequence was found using Trypsin Gold (T) treatment of mouse-derived p75NTR^{ECD}, whereas GluC (G) showed 24 hypothetical cleavage sites and 62.2% coverage (Swissprot).

After predicting the hypothetical cleavage sites of p75NTR^{ECD} using GluC and Trypsin Gold, a sample preparation method was developed involving p75NTR^{ECD} Immunoprecipitation with mouse anti-human p75NTR (MLR1) antibody and in-solution digestion of p75NTR^{ECD}.

In order to ensure that sample proteins were in a single chain form for in-solution enzymatic digestion and subsequent Orbitrap-MS analysis, IP proteins were denatured and alkylated. This procedure used Dithiothreitol (DTT) to break disulphide bonds, and then Iodoacetamide to add alkyl groups to the free sulfhydryl groups on the cysteine residues of the protein samples, ensuring that the disulphide bonds did not reform (Link & LaBaer 2011).

The procedure for in-solution digestion using Trypsin Gold and GluC was first trialled on mouse r-p75NTR-Fc after reducing and alkylating with DTT and Iodoacetamide respectively. **Table 3.1** shows the results of the post-IP/Orbitrap-MS mass spectra analysis using Proteome Discoverer software, which identified p75NTR^{ECD} peptides from mouse derived r-p75NTR-Fc using GluC or Trypsin Gold.

Table 3.1: Identification of p75NTR^{ECD} peptides from mouse r-p75NTR-Fc after diafiltration, IP, denaturisation, alkylisation, digestion with GluC or Trypsin Gold, & analysis using Orbitrap-MS

p75NTR^{ECD} (Q9Z0W1: 22-246)	Peptide sequence	Average mass (Da)	Charge state
GluC digestion			
70-88 (19aa)	SVTFSDVVSATEPCKPCTE	2113.94390	2
158-171 (14aa)	ANHVDPCLPCTVCE	1671.69341	2
Trypsin Gold digestion			
172-187 (16aa)	ECTPWADAECEEIPGR	960.39917	2
172-187 (16aa)	ECTPWADAECEEIPGR	960.39844	2
172-187 (16aa)	ECTPWADAECEEIPGR	640.60144	3

Urinary p75NTR^{ECD} was immunoprecipitated from samples using Protein G Agarose beads, and so protein needed to be eluted from the Protein G Agarose beads used in the IP procedure before Orbitrap-MS analysis. Therefore, a protocol was established to elute the sample proteins from a small volume (30µl) of Protein

G Agarose; this involved elution using 17.0µl of 0.1M Glycine at pH 2.5 and then restoring a neutral pH of 7 with 3.3µl of 0.5M Sodium hydroxide.

Hence, the final protocol for urinary $p75NTR^{ECD}$ detection using IP/Orbitrap-MS involved; urinary sample diafiltration; IP of urinary $p75NTR^{ECD}$ with 5µg of mouse anti-human p75NTR antibody (MLR2); precipitation with Protein G Agarose beads; elution with 0.1M Glycine; neutralisation with 0.5M Sodium hydroxide; reduction with $1/10^{th}$ the sample volume of DTT; and alkylation using $1/10^{th}$ the sample volume of Iodoacetamide. Finally, the sample was subject to GluC or Trypsin Gold digestion, and then Orbitrap-MS.

3.5. Detection of p75NTR^{ECD} in urine of people with MND using IP/Orbitrap-MS

p75NTR^{ECD} was detected in the urine of two people with MND using the optimised IP/Orbitrap-MS protocol (see **2.5.1**), and analysis using Proteome Discoverer software. Peptides of p75NTR^{ECD} were identified in the urine of MND patient MND32/2, a 63-year-old male with 2 years of MND symptoms, with both GluC (3 peptides and Trypsin Gold (2 peptides; **Table 3.2.A**). In line with this result, p75NTR^{ECD} was detected in the urine of MND patient MND26, an 82-year-old male with 2.3 years of MND symptoms, using GluC (11 peptides; **Table 3.2.B**). However, no p75NTR^{ECD} peptides were detected in the urine of this patient with Trypsin Gold.

The p75NTR^{ECD} peptide sequence coverage from the analysis of urinary protein from two people with MND using IP/Orbitrap-MS is presented in **Figure 3.6**. Overall, GluC digestion resulted in the identification of seven unique peptide sequences with coverage of 37.6% of p75NTR^{ECD}, whereas Trypsin Gold digestion resulted in the identification of two unique peptide sequences and sequence coverage of 12.2%.

Table 3.2.A: Identification of p75NTR^{ECD} peptides from urine of MND patient #MND32/2 after diafiltration, IP, denaturisation, alkylisation, digestion using GluC or Trypsin Gold & analysis using Orbitrap-MS

p75NTR^{ECD} (P08138: 29-250)	Peptide sequence	Average mass (Da)	Charge state
GluC digestion			
70-88 (19aa)	SVTFSDVVSATEPCKPCTE	2113.94560	2
158-171 (14aa)	ANHVDPCLPCTVCE	1671.69402	2
158-171 (14aa)	ANHVDPCLPCTVCE	1672.67620	2
130-147 (18aa)	AGSGLVFSCQDKQNTVCE	1999.88848	2
Trypsin Gold digestion			
127-141 (15aa)	VCEAGSGLVFSCQDK	1656.73857	2
183-194 (12aa)	WADAECEEIPGR	1432.61907	2

Table 3.2.B: Identification of p75NTR^{ECD} peptides from urine of MND patient #MND26 after diafiltration, IP, denaturisation, alkylisation, digestion using GluC or Trypsin Gold & analysis using Orbitrap-MS

p75NTR^{ECD} (P08138: 29-250)	Peptide sequence	Average mass (Da)	Charge state
GluC digestion			
102-117 (16aa)	ADDAVCRCAYGYYQDE	1955.75798	2
158-171 (14aa)	ANHVDPCLPCTVCE	1671.69597	2
158-174 (17aa)	ANHVDPCLPCTVCEDTE	2016.81352	2
89-101 (13aa)	CVGLQSMSAPCVE	1437.61955	2
70-89 (19aa)	SVTFSDVVSATEPCKPCTE	2113.94512	2
70-89 (19aa)	SVTFSDVVSATEPCKPCTE	2113.94638	3
70-89 (19aa)	SVTFSDVVSATEPCKPCTE	2113.94756	2
70-89 (19aa)	SVTFSDVVSATEPCKPCTE	2113.94634	2
70-89 (19aa)	SVTFSDVVSATEPCKPCTE	2113.94748	3
70-89 (19aa)	SVTFSDVVSATEPCKPCTE	2113.94267	2
70-89 (19aa)	SVTFSDVVSATEPCKPCTE	2113.94780	2
Trypsin Gold digestion			
No peptides detected			

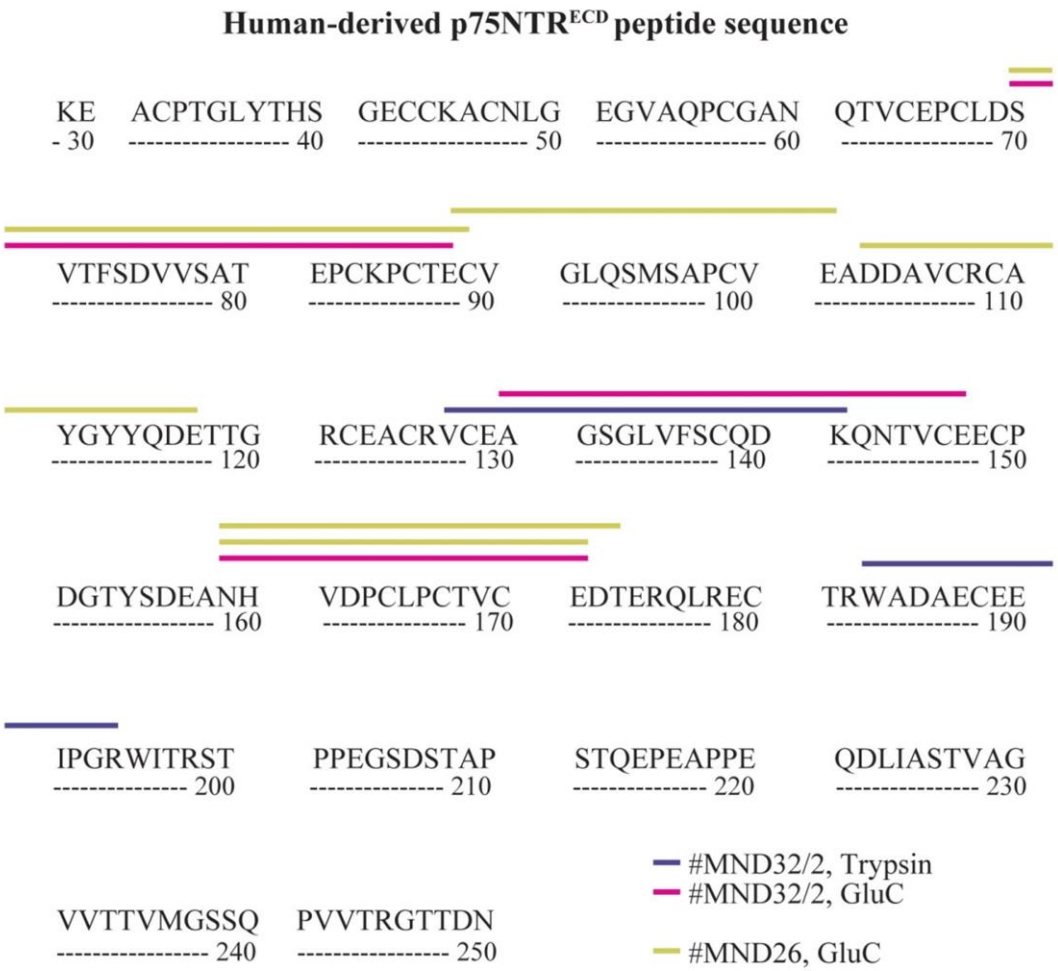

Figure 3.6: Coverage of p75NTR^{ECD} detected in the urine of two people with MND using Trypsin Gold or GluC digestion in Immunoprecipitation/Orbitrap-Mass Spectrometry

Urine samples from two different people with MND were tested for the presence of p75NTR^{ECD}. Samples were diafiltered, then subject to immunoprecipitation (IP), denaturisation, and alkylisation before GluC or Trypsin Gold digestion and Orbitrap-Mass Spectrometry analysis. For urine sample MND32/2, two peptides were identified using Trypsin Gold digestion (—), and four peptides were identified using GluC digestion (—) resulting in p75NTR^{ECD} peptide coverage of 12.2% and 23.1% respectively. GluC digestion of urine samples MND26 resulted in 11 peptides of p75NTR^{ECD}, equating to 28.9% coverage (—). Overall, Trypsin Gold digestion of two urine samples from people with MND resulted in the identification of two unique peptide covering 12.2% of the p75NTR^{ECD} sequence. In comparison, GluC digestion resulted in the identification of seven unique peptides, equating to coverage of 37.6% of p75NTR^{ECD}. For both enzymes, only peptides from the extracellular domain of p75NTR were detected.

3.6. Detection of p75NTR^{ECD} in urine of people with MND using IP/Triple TOF-MS

Using the optimised IP/Orbitrap-MS protocol (see **2.5.1**), p75NTR^{ECD} was also detected in the urine of two people with MND using a Triple TOF Mass Spectrometer and analysis using Protein Pilot software after IP. Peptides of p75NTR^{ECD} were identified in the urine of MND patient MND29/2, a 54-year-old female with 1.7 years of MND symptoms, with both and GluC (3 peptides) and Trypsin Gold (4 peptides; **Table 3.3.A**). p75NTR^{ECD} peptides were also detected in the urine of MND patient MND22/2, an 83-year-old male with 2.2 years of MND symptoms, using GluC (3 peptides) and Trypsin Gold (9 peptides; **Table 3.3.B**, representative spectra **Appendix C**).

The p75NTR^{ECD} peptide sequence coverage from the analysis of urinary protein from two people with MND using IP/Triple TOF-MS is presented in **Figure 3.7**. Overall, GluC digestion resulted in the identification of three unique peptide sequences with coverage of 16.3% of p75NTR^{ECD}, whereas Trypsin Gold digestion resulted in the identification of nine unique peptide sequences and sequence coverage of 47.5%.

Table 3.3.A: Identification of p75NTR^{ECD} peptides from urine of MND patient #MND29/2 after diafiltration, IP, denaturisation, alkylisation, digestion with GluC or Trypsin Gold & analysis using Triple TOF-MS

P75NTR^{ECD} (P08138:29-250)	Peptide sequence	Average mass (Da)	Charge state
GluC digestion			
31-42 (13aa)	ACPTGLYTHSGE	1291.550293	2
43-51 (9aa)	CCKACNLGE	1110.425659	2
158-171 (14aa)	ANHVDPCLPCTVCE	1670.685059	2
Trypsin Gold digestion			
96-108 (13aa)	SAPCVEADDAVCR	1448.602417	2
109-121 (13aa)	CAYGYYQDETTGR	1582.635864	2
127-141 (15aa)	VCEAGSGLVFSCQDK	1655.728394	2
183-194 (12aa)	WADAECEEIPGR	1431.608887	2

Table 3.3.B: Identification of p75NTR^{ECD} peptides from urine of MND patient #MND22/2 after diafiltration, IP, denaturisation, alkylisation, digestion with GluC or Trypsin Gold & analysis using Triple-TOF MS

P75NTR^{ECD} (P08138:29-250)	Peptide sequence	Average mass (Da)	Charge state
GluC digestion			
31-42 (13aa)	ACPTGLYTHSGE	1291.550293	2
43-51 (9aa)	CCKACNLGE	1110.425659	2
158-171 (14aa)	ANHVDPCLPCTVCE	1670.685059	2
Trypsin Gold digestion			
29-45 (17aa)	KEACPTGLYTHSGECCK	1996.844116	4
30-45 (16aa)	EACPTGLYTHSGECCK	1868.749146	3
95-108 (14aa)	MSAPCVEADDAVCR	1579.642944	2
96-108 (13aa)	SAPCVEADDAVCR	1448.602417	2
97-108 (12aa)	APCVEADDAVCR	1361.570435	2
109-121 (13aa)	CAYGYYQDETTGR	1582.635864	2
127-141 (15aa)	VCEAGSGLVFSCQDK	1655.728394	2
142-175 (34aa)	QNTVCEECPDGTYSDEANHVDP CLPCTVCEDTER	4039.554688	4
183-194 (12aa)	WADAECEEIPGR	1431.608887	2

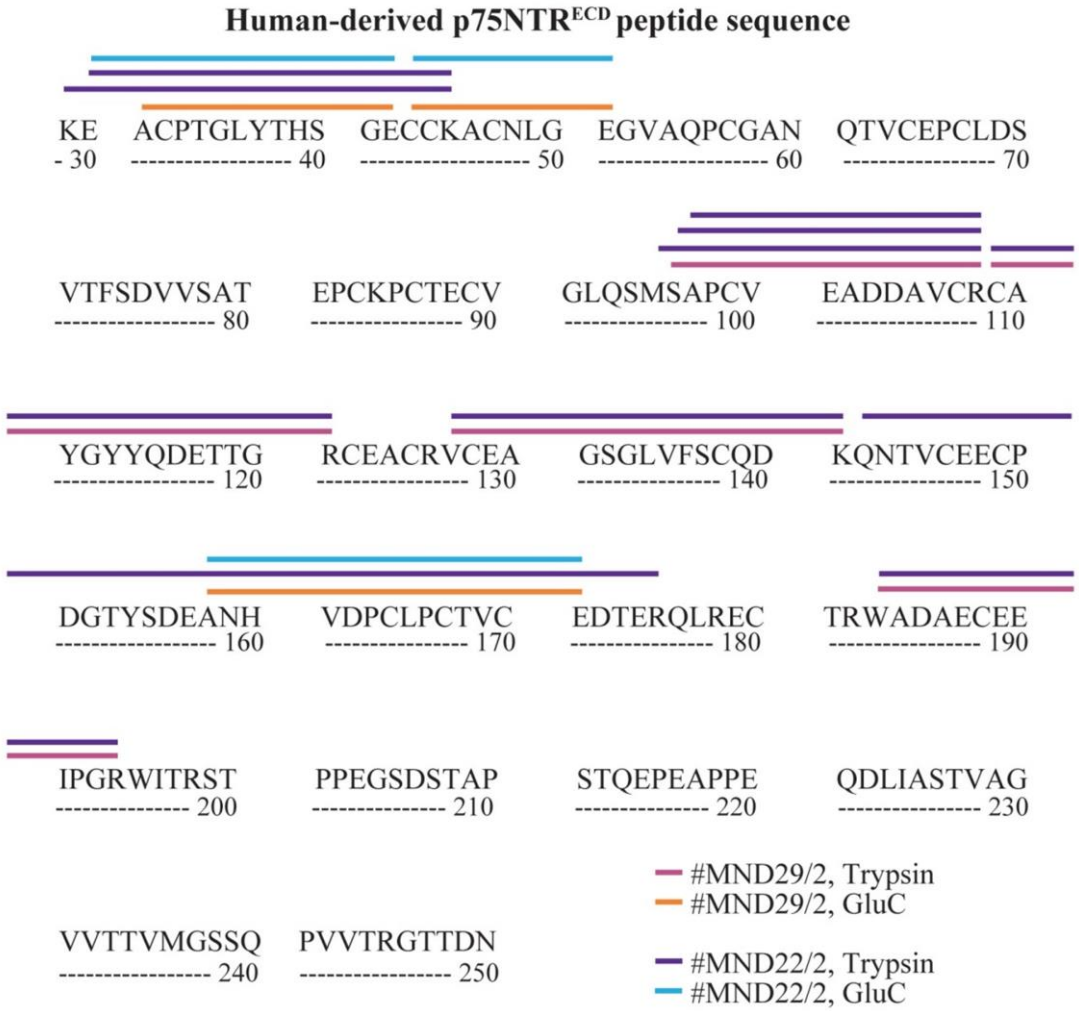

Figure 3.7: Coverage of p75NTR^{ECD} detected in the urine of two people with MND using Trypsin Gold or GluC digestion in Immunoprecipitation/Triple TOF-Mass Spectrometry

Urine samples from three different people with MND were tested for the presence of p75NTR^{ECD}. Samples were diafiltered, then subject to immunoprecipitation (IP), denaturisation, and alkylisation before GluC or Trypsin Gold digestion and Triple TOF-Mass Spectrometry analysis. For urine sample MND29/2, four peptides were identified using Trypsin Gold digestion (—), and three peptides were identified using GluC digestion (—) resulting in p75NTR^{ECD} peptide coverage of 23.9% and 16.3% respectively. Trypsin Gold digestion (—) of urine sample MND22/2 resulted in nine peptides of p75NTR^{ECD}, equating to 47.5% coverage, and GluC digestion (—) resulted in three p75NTR^{ECD} peptides and coverage of 16.3%. Overall, Trypsin Gold digestion of two urine samples from people with MND resulted in the identification of nine unique peptide covering 47.5% of the p75NTR^{ECD} sequence. In comparison, GluC digestion resulted in the identification of three unique peptides, equating to coverage of 16.3% of p75NTR^{ECD}. For both enzymes, only peptides from the extracellular domain of p75NTR were detected.

3.7. Discussion

The aim of this chapter was to determine if p75NTR^{ECD} is present, and detectable, in the urine of SOD1^{G93A} mice and people with MND, to ascertain if urinary p75NTR^{ECD} could be used as a biomarker of MND. In order to test this, a Western blot (WB) method was first used for p75NTR^{ECD} detection. An antibody produced in goats, that could detect mouse- and human-derived p75NTR, including p75NTR^{FL} and p75NTR^{ECD}, was used. Using this method, a band at the expected molecular weight of p75NTR^{ECD} (~50kDa) was detected in end stage SOD1^{G93A} MND model mice. These mice develop overt paralysis and motor symptoms of MND, with behavioural symptoms of disease becoming apparent at ~110 days of age (Heiman-Patterson *et al.* 2005). Previous studies have detected an up-regulation of p75NTR in spinal cord motor neurons of these mice prior to end stage (Lowry *et al.* 2001). As such, it was hypothesised that p75NTR^{ECD} may be detectable in the urine of SOD1^{G93A} mice prior to end stage of disease. In order to test this hypothesis an Immunoprecipitation (IP) procedure was used to enrich p75NTR^{ECD} from urinary samples. The addition of this antibody-based protein precipitation method allowed for enrichment of p75NTR^{ECD}, increasing the sensitivity of p75NTR^{ECD} detection. In addition, the use of two different antibodies against p75NTR^{ECD} in IP/WB increased the specificity of p75NTR^{ECD} detection by binding to two different epitopes of p75NTR^{ECD}.

Two monoclonal antibodies, mouse anti-human p75NTR (MLR1 and MLR2), were tested as p75NTR^{ECD} capture antibodies in the IP/WB procedure. These antibodies were made in p75NTR Exon III knock-out mice, required as p75NTR is preserved across species, and are conformational antibodies which can detect mouse- and human-derived p75NTR^{FL} and p75NTR^{ECD} (Rogers *et al.* 2006). The use of a second anti-p75NTR^{ECD} antibody that binds to a separate epitope of p75NTR^{ECD} during WB allowed for p75NTR^{ECD} detection. A polyclonal goat anti-mouse p75NTR^{ECD} antibody was chosen for p75NTR^{ECD} detection, as its combination with mouse anti-human p75NTR (MLR1) or (MLR2) antibodies resulted in p75NTR^{ECD} detection in IP/WB. The use of mouse anti-human p75NTR (MLR2) and goat anti-mouse p75NTR^{ECD} antibodies allowed for the development of a unique IP/WB procedure able to capture, enrich, and detect mouse and human p75NTR^{FL} and p75NTR^{ECD} with sensitivity and specificity.

The specificity of the IP/WB procedure was shown through the testing of cell lysates positive (mouse, NSC-34 motor neuron-like cell line; human, A875 melanoma; rat, C6 glioma) and negative (hamster, BSR) for $p75NTR^{ECD}$, bovine serum albumin (BSA) with and without mouse r-$p75NTR^{ECD}$, and an antibody control that contained PBS in place of a cell lysate. Using the mouse anti-human p75NTR (MLR2) and goat anti-mouse $p75NTR^{ECD}$ antibody pair, mouse- and human-derived cell lysates positive for $p75NTR^{ECD}$, along with BSA spiked with mouse r-$p75NTR^{ECD}$, showed bands at the molecular weight of $p75NTR^{ECD}$. In comparison, cell lysates produced from rats (C6 glioma) that contain $p75NTR^{ECD}$ which should not be detectable by antibodies made against mice and humans, cell lysates negative for $p75NTR^{ECD}$ (hamster, BSR), and samples of BSA or PBS alone, did not show bands at the molecular weight of $p75NTR^{ECD}$. In addition, a high molecular weight (~150kDa) band was detected in the human-derived A875 cell lysates, this may be a dimer of p75NTR, and has been previously shown (Zupan & Johnson 1991).

Testing of urine from $SOD1^{G93A}$ mice using WB and IP/WB resulted in $p75NTR^{ECD}$ detection in the urine of this MND model for the first time. Importantly, IP/WB detected $p75NTR^{ECD}$ in the urine of $SOD1^{G93A}$ mice pre-symptomatically, from 60 days of age, approximately 50 days before behavioural signs of motor symptoms (Heiman-Patterson *et al.* 2005). Urinary $p75NTR^{ECD}$ was then detected throughout disease progression until end stage in $SOD1^{G93A}$ mice, whereas $p75NTR^{ECD}$ was only detectable at the equivalent of end stage of disease in healthy B6 healthy control mice. B6 control mice of this age are considered young adults (Flurkey & Currer 2004) and it is not surprising that $p75NTR^{ECD}$ is detected in urine of these mice, as $p75NTR^{ECD}$ is detectable in the urine of healthy adult humans, though at lower levels than seen during development (DiStefano *et al.* 1991). This is the first time that a biological fluid biomarker has been detected in the urine of pre-symptomatic $SOD1^{G93A}$ mice. One recent study detected pre-symptomatic changes in serum amino acids of $SOD1^{G93A}$ mice approximately 20 days prior to symptom onset (Bame *et al.* 2014). However, the majority of other biological fluid protein biomarker candidates are first detected at later stages of disease in the $SOD1^{G93A}$ mouse, in studies using insufficient mouse numbers. For example in serum, phosphorylated neurofilament heavy chain (pNfH) is significantly elevated from ~10-15 days before symptoms (Boylan *et al.* 2009), or

in late stage symptomatic disease ~25 days before end stage (Lu *et al.* 2012). Other potential protein biomarker candidates, such as blood volatile organic compounds (Jiang *et al.* 2014), are yet to be tested throughout disease progression.

Importantly, $p75NTR^{ECD}$ was detected in the urine of two people with MND for the first time using the IP/WB method, whereas $p75NTR^{ECD}$ was not detected in the urine of two healthy individuals. Urinary $p75NTR^{ECD}$ is not the first protein suggested as a biomarker candidate in the urine of people with MND. Urinary levels of collagen IV, and collagen metabolite glucosylgalactosyl hydroxylysine have been found to be significantly decreased in people with MND (Ono *et al.* 1999, Ono *et al.* 2001) in small, preliminary studies, but these candidates have not been researched further. In comparison, a large number of protein biomarker candidates have been detected in the CSF or serum of people with MND, requiring invasive procedures for collection and testing. Such candidates most recently include the soluble monocyte receptor CD14 (Süssmuth *et al.* 2010), the astrocytic calcium binding protein S100β (Süssmuth *et al.* 2010), tau (Süssmuth *et al.* 2010, Grossman *et al.* 2014), cystatin C (Ranganathan *et al.* 2005, Pasinetti *et al.* 2006, Ranganathan *et al.* 2007, Wilson *et al.* 2010, Ganesalingam *et al.* 2011), complement C3 (Goldknopf *et al.* 2006, Ganesalingam *et al.* 2011), neurofilament light chain (NfL) (Zetterberg *et al.* 2007, Tortelli *et al.* 2012, Gaiottino *et al.* 2013) and phosphorylated heavy chain (pNfH) (Brettschneider *et al.* 2006, Boylan *et al.* 2009, Ganesalingam *et al.* 2011, Levine *et al.* 2012, Boylan *et al.* 2013).

The detection of $p75NTR^{ECD}$ in urine of $SOD1^{G93A}$ MND mice and people living with MND is reasonable in light of the literature. Following neuronal injury, p75NTR is re-expressed in motor neurons (Ernfors *et al.* 1989, Saika *et al.* 1991, Seeburger *et al.* 1993, Ferri *et al.* 1997, Lowry *et al.* 2001, Copray *et al.* 2003) and re-expressed, and cleaved, from Schwann cells (Taniuchi *et al.* 1986, DiStefano & Johnson 1988, Kerkhoff *et al.* 1991). The subsequent appearance of $p75NTR^{ECD}$ in urine following injury, i.e., sciatic nerve injury in rats (Zupan *et al.* 1989), has also been documented previously. It is important to note that the presence of $p75NTR^{ECD}$ in urine in MND is not due to degeneration of the motor neurons controlling bladder function, as these are spared in MND until very late stages (Kihira *et al.* 1997, Valdez *et al.* 2012, Brockington *et al.* 2013). In addition, the presence of $p75NTR^{ECD}$ is theoretically plausible, as, at 50kDa in size, it is small

enough to pass from the glomerulus to the Bowman's capsule of the kidney during filtration (Haraldsson *et al.* 2008). The results of this study are the first time that these separate findings have been drawn together, showing that p75NTR^{ECD} is detectable in urine following neuronal injury in MND.

Mass Spectrometry was used to validate the detection of p75NTR^{ECD} in the urine of people with MND, and only peptides from the extracellular domain of p75NTR were detected. Using Orbitrap-MS, seven unique peptides from p75NTR^{ECD} were identified using the enzyme GluC, and two unique peptides were identified using Trypsin Gold. When the same IP procedure was followed by Triple TOF-MS, peptides from p75NTR^{ECD} were detected in urine samples using a second MS machine, with nine and three unique p75NTR^{ECD} peptides detected following Trypsin Gold or GluC digestion, respectively.

Trypsin Gold is typically used for digestion of samples prior to Mass Spectrometry analysis (Baldwin 2004). However, analysis of the hypothetical peptide cleavage sites of p75NTR^{ECD} found that Trypsin Gold cleavage resulted in limited peptides within the detection range of the Orbitrap-MS; between 600 and 2,000Da, with peptides between 2,000 and 2,500Da in mass also possible to fragment (Perry *et al.* 2008). As a result, GluC was also utilised for p75NTR^{ECD} detection in MS. This resulted in the detection of p75NTR^{ECD} peptides in the urine of people with MND using GluC digestion in addition to Trypsin Gold. In comparison, sample analysis using a Triple TOF-MS resulted in a more unique peptides detected using Trypsin Gold digestion than GluC digestion, highlighting the need to develop protocols specific for both the protein of interest and the MS machine used. This finding, regarding the enzymatic cleavage of p75NTR^{ECD}, increases the knowledge base regarding this receptor. Since Trypsin is typically used in shotgun approaches for biomarker detection (Pang *et al.* 2002, Kearney & Thibault 2003, Adachi *et al.* 2006), and this enzyme does not produce many sufficiently sized peptides from digestion of p75NTR^{ECD} for MS machines such as Orbitrap-MS, it may explain the lack of literature regarding p75NTR^{ECD}.

A sensitive, high-throughput, easily quantifiable method is required in order to determine any significant differences in p75NTR^{ECD} levels in SOD1^{G93A} MND model mice and people living with MND, and their respective controls. IP/WB and IP/MS methods are not feasible to quantify p75NTR^{ECD} in a large number of

samples. For both methods, large initial volumes of urine are needed for analysis, a small number of samples (IP/WB) or one sample (IP/MS) can be tested at any one time, and, using the particular protocols employed here, cannot be used to quantify $p75NTR^{ECD}$ with sensitivity. As such, other methods should be developed for $p75NTR^{ECD}$ quantification, such as enzyme-linked immunosorbent assays (ELISAs).

In summary, this chapter reports the presence of $p75NTR^{ECD}$ in the urine of $SOD1^{G93A}$ mice and people with MND for the first time, using two novel techniques; IP/WB and IP/MS, and paves the way for further investigation into $p75NTR^{ECD}$ as a biomarker for MND.

Chapter 4. ELISA development for quantification of p75NTR^{ECD}

4.1. Introduction

Having confirmed the presence of $p75NTR^{ECD}$ in urine of the $SOD1^{G93A}$ MND mouse model and people with MND, the next aim of the study was to quantify urinary $p75NTR^{ECD}$ levels in a large number of samples from mice and humans. In order to do this, a method that allows for high-throughput, multi-sample quantification of small sample volumes, with specificity and sensitivity, was required. To address this need, an enzyme-linked immunosorbent assay (ELISA) was developed to quantify mouse and human $p75NTR^{ECD}$, as none were commercially available.

ELISAs, reported separately by Van Weeman and Schuurs (1971), and Engvall and Perlmann (1972), were first established following the development of immunoassays using radioactively labelled components. Immunosorbent assays exploit the specific reactions between antigens and their respective antibodies and use a colourmetric reaction to quantify this reaction (Crowther 2001), and have been used in nervous system research for the detection and quantitative measurement of neurotrophins, for over 3 decades (see Zhang *et al.* 2001 for review). ELISAs have supplanted radioimmunoassays, which use the specificity of antigen-antibody reactions but also rely on radioactivity to detect the antigen-antibody complex and require specific precautions and licensing. ELISAs also have advantages over Immunoprecipitation (IP) techniques. Although IP and ELISA procedures have specificity as they rely on antigen-antibody reactions, ELISAs provide simple quantification and high-throughput capacities, while maintaining small sample volume requirements (Crowther 2001).

Two-site/sandwich ELISAs are mostly commonly used for measuring an antigen in solution, and use two antibodies against different epitopes of an antigen. ELISAs can also be used for measuring the affinity of antibodies for a specific antigen in a one-site ELISA (Crowther 2001).

A one-site, direct ELISA is the simplest ELISA setup, with the smallest number of components. This ELISA measures antibody affinity, relies on an antigen binding to a surface, and uses one antibody for detection, itself conjugated to a signalling peptide (**Figure 4.1.A**). One step up from this is the one-site, indirect ELISA, which again relies on an antigen binding to a surface, but uses two antibodies for

detection; the primary antibody to bind to the antigen of interest, and the secondary antibody conjugated to a signalling peptide, which binds to the primary antibody and increases signal amplification (**Figure 4.1.B**). These simple assays, although quick to perform, can be limited by their signal detection limit; this can be rectified by using the biotin-streptavidin signalling complex (**Figure 4.1.C**) which has the advantage of multiple signalling peptides attached to each secondary conjugated antibody.

Two-site/sandwich ELISAs (indirect; **Figure 4.1.D**) are used to detect and quantify antigens from a sample in a direct or indirect setup. Due to their specificity and sensitivity, sandwich ELISAs are used in a multitude of areas from basic laboratory research to clinical applications, such as infectious disease and clinical endocrinology testing, and are the most common diagnostic approach for testing protein changes using antibodies (see Bowser *et al.* 2011 for review). Sandwich ELISAs have increased specificity due to the use of two primary antibody binding steps; these primary antibodies are normally two different antibodies, which recognise different epitopes of the same antigen. Sandwich ELISAs rely on the passive binding of the first primary antibody (capture antibody) to the solid phase, and its subsequent ability to bind the antigen of interest, the use of a second primary antibody (detection antibody) then greatly increases antigen specificity (Crowther 2001). A secondary antibody conjugated to a signalling peptide, which binds to the primary antibody used for detection, then amplifies the signal. Secondary antibodies, anti-immunoglobulins raised against the animal species of the detecting antibody, bind directly to the constant region of the detecting antibody. For example, injection of a goat immunoglobulin into cows will result in the production of bovine anti-goat immunoglobulin antibodies. As such, secondary antibodies are useful in immunoassays because they are conjugated or labelled with enzymes, such as horseradish peroxidase, and determine the extent of binding of an antigen to detection and capture antibodies (Crowther 2001).

The aim of this chapter is to develop an indirect sandwich ELISA to quantify mouse and human p75NTR^{ECD} in order to test urinary p75NTR^{ECD} as a biomarker of MND in the SOD1^{G93A} MND mouse model and people living with MND.

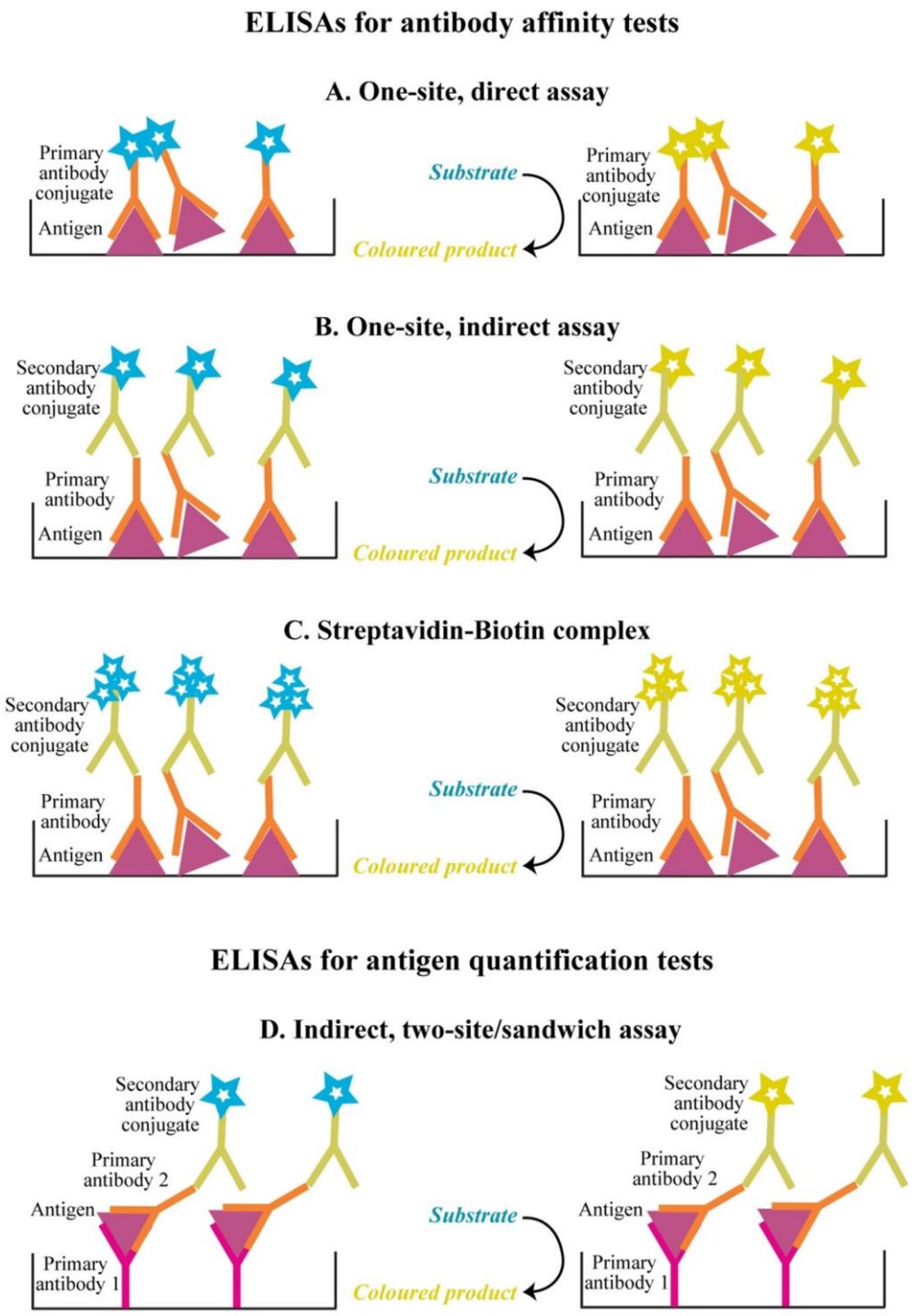

Figure 4.1: Different ELISA configurations

A. One-site, direct ELISAs, using one antibody, are used to quantify the interaction between antibodies and antigen by coating plates with a known quantity of antigen. **B.** The use of a secondary conjugated antibody in a one-site, indirect ELISA has increased signal amplification over direct assays. **C.** Further signal amplification is possible using the specific streptavidin-biotin complex. **D.** Two-site/sandwich ELISAs are used to quantify antigens in a sample using two primary antibodies against different, non-overlapping epitopes, which allows for increased specificity.

4.2. Indirect sandwich ELISA development

A successful indirect sandwich ELISA, to detect an antigen in biological fluids such as urine, requires two antibodies that bind to an antigen at different, non-overlapping epitopes (Crowther 2001). As described previously, the antibody pairs mouse anti-human p75NTR (MLR1) with goat anti-mouse $p75NTR^{ECD}$, and mouse anti-human p75NTR (MLR2) with goat anti-mouse $p75NTR^{ECD}$, detect both mouse- and human-derived $p75NTR^{ECD}$ in IP/WB. For $p75NTR^{ECD}$ quantification, an antibody pair that can detect mouse and human $p75NTR^{ECD}$ in an ELISA was required, and so the antibody pairs used in IP/WB were tested in ELISA, along with a number of other antibody combinations.

4.2.1. Antigen testing

One-site ELISAs were employed to test the binding affinity of antibodies to $p75NTR^{ECD}$ using recombinant mouse and human $p75NTR^{ECD}$ (r-$p75NTR^{ECD}$) antigens. However, the available r-$p75NTR^{ECD}$ antigens contained a human-derived –Fc fragment (Fc-part of human IgG1, 230 amino acids). As a result, before testing the binding affinity of antibodies to r-$p75NTR^{ECD}$-Fc, testing was required to examine if there was any cross reactivity between the human derived -Fc part of the antigen and 1. anti-human primary antibodies, or 2. secondary antibodies used to detect antibody binding to $p75NTR^{ECD}$.

As presented in **Table 4.1**, the addition of anti-human antibodies (anti-CD46, **Table 4.1**, **row 3** and anti-NT4, **Table 4.1**, **row 1**) to plates coated with 2µg/ml mouse r-p75NTR-Fc antigen resulted in absorbance readings that were not significantly different to those obtained using secondary antibodies alone (**Table 4.1**, **rows 2** and **4**). These results show that there is no binding between the human derived -Fc fragment of the antigen and anti-human primary antibodies.

The addition of secondary antibodies alone (Donkey anti-rabbit HRP, **Table 4.1**, **row 2** /Donkey anti-mouse HRP, **row 4**), or the addition of a primary antibody and secondary antibody that do not interact (Mouse anti-human p75NTR (MLR2) and Donkey anti-rabbit HRP, **Table 4.1**, **row 6**) to plates coated with 2µg/ml mouse r-p75NTR-Fc antigen resulted in low absorbance readings, below 0.09. This shows

that there is no cross-reactivity between the human derived -Fc fragment and secondary antibodies.

In addition, the low absorbance readings of 0.058 obtained when the secondary antibody Donkey anti-mouse HRP was added to mouse r-p75NTR^{ECD}-Fc antigen showed a lack of mouse-mouse interaction in these one-site ELISAs (**Table 4.1**, **row 4**). These results are in contrast to the absorbance readings obtained by adding a specific anti-p75NTR antibody and its corresponding secondary antibody to mouse r-p75NTR^{ECD}-Fc; when mouse anti-human p75NTR (MLR2) and donkey anti-mouse HRP antibodies are used, absorbance readings are significantly higher than zero at 0.30 (**Table 4.1**, **row 5**).

After determining that the human-derived -Fc fragment of the recombinant proteins does not cross-react with anti-human antibodies and secondary antibodies, mouse and human r-p75NTR^{ECD}-Fc fusion proteins (R&D Systems) were used to determine antibody affinity in one-site ELISAs, and produce standard curves for p75NTR^{ECD} quantification in sandwich ELISAs.

Table 4.1: Antibody combinations testing cross-reactivity of mouse r-p75NTR^{ECD}-Fc in a one-site, indirect ELISA

Primary antibody		Secondary antibody		Purpose	Abs.
Conc.	**Type**	**Conc.**	**Type**		
5µg/ml	Rabbit anti-human NT4	0.8µg/ml	Donkey anti-rabbit HRP	Cross-reactivity	0.088
10µg/ml					0.100
-	-	0.8µg/ml	Donkey anti-rabbit HRP	Background/ cross-reactivity	0.068
2µg/ml	Mouse anti-human CD46	0.8µg/ml	Donkey anti-mouse HRP	Cross-reactivity test	0.057
4µg/ml					0.058
-	-	0.8µg/ml	Donkey anti-mouse HRP	Background/ cross-reactivity	0.058
2µg/ml	Mouse anti-human p75NTR	0.8µg/ml	Donkey anti-mouse HRP	Positive control	0.307
4µg/ml					0.308
2µg/ml	Mouse anti-human p75NTR	0.8µg/ml	Donkey anti-rabbit HRP	Negative control	0.070
4µg/ml					0.079

Conc. - concentration; Abs. - Absorbance at 450nm, average of 3 wells

4.2.2. Antibody testing

A number of different primary antibodies were tested in one-site ELISAs to determine their relative affinity to mouse- and human-derived p75NTR^{ECD}. As presented in **Table 4.2**, plates were coated with 2µg/ml r-p75NTR^{ECD}-Fc and detected with 1µg/ml primary antibody and 0.8µg/ml HRP-conjugated secondary antibody.

Antibody affinity for mouse and human r-p75NTR^{ECD}-Fc was determined by comparing the absorbance readings of wells with antigen, to wells without antigen present (zero/background), and calculating the resultant signal to noise (S/N) ratio (absorbance with antigen divided by absorbance without antigen).

The antibodies that displayed sufficient affinity to both mouse and human r-p75NTR^{ECD}-Fc were mouse anti-human p75NTR (MLR1 and MLR2) and goat anti-mouse p75NTR^{ECD}; these antibodies were then tested in indirect, sandwich ELISAs using a method based on that developed by Zhang and colleagues (Zhang *et al.* 1999, Zhang *et al.* 2000).

Table 4.2: Antibody binding to mouse and human r-p75NTR^{ECD}-Fc in a one-site, indirect ELISA

Primary antibody	Mouse r-p75NTR^{ECD}-Fc			Human r-p75NTR^{ECD}-Fc		
	Abs.	**Zero**	**S/N**	**Abs.**	**Zero**	**S/N**
Mouse anti-human p75NTR (MLR1)	0.74	0.05	**13.90**	2.59	0.05	**49.27**
Mouse anti-human p75NTR (MLR2)	0.69	0.05	**12.96**	2.55	0.06	**46.31**
Goat anti-mouse p75NTR^{ECD}	3.70	0.08	**45.15**	1.33	0.06	**21.43**
Goat anti-human p75NTR^{ECD}	*0.42*	*0.05*	***7.52***	*0.62*	*0.06*	***11.18***
Mouse anti-human p75NTR (ME20.4)	*0.19*	*0.18*	***1.05***	0.48	0.01	**48.00**

Abs. - Absorbance at 450nm, average of 6 wells; S/N - signal to noise ratio; Zero - background, Abs. reading in wells with no antigen; Secondary antibodies: for mouse derived primary antibodies, Donkey anti-mouse HRP, for goat derived primary antibodies, Bovine anti-goat HRP.

The suitability of antibody pairs in indirect sandwich ELISAs was evaluated by calculating the r^2 values and signal to noise (S/N) ratios of the standard curves produced. The r^2 values were calculated by the fit of a linear regression model (Prism6). Similar to one-site ELISAs, S/N ratios in sandwich ELISAs were calculated by dividing the absorbance readings of the highest r-p75NTR^{ECD}-Fc concentration on a standard curve, by the absorbance readings from wells with no antigen present.

The mouse anti-human p75NTR (MLR1 and MLR2) antibodies are monoclonal antibodies, which bind to one specific p75NTR epitope, having come from one B cell. In contrast, the goat anti-mouse p75NTR^{ECD} antibody is polyclonal, and can bind many different epitopes of p75NTR^{ECD}, as the serum of goats immunised with p75NTR^{ECD} will contain immunoglobulins from many different B cells, each producing antibodies to different epitopes of p75NTR^{ECD} (Harlow & Lane 1988). Due to these inherent characteristics, the use of a monoclonal antibody for antigen capture will produce a superior assay to one that utilises a polyclonal antibody for antigen capture. A monoclonal capture antibody has an inherent monospecificity towards a single epitope of an antigen, such that once the plate is washed, the antibody is binding to one epitope. A polyclonal detection antibody can then bind various epitopes of the antigen that will be different to the monoclonal, and so increase the detection, and allow quantification of small difference in antigen. This is the case with the mouse anti-human p75NTR (MLR1 or MLR2) antibodies and the goat anti-mouse p75NTR antibody combination. Concentration dependent standard curves are produced for mouse and human r-p75NTR^{ECD}-Fc using monoclonal mouse anti-human p75NTR (MLR1 or MLR2) antibodies for p75NTR^{ECD} capture and the polyclonal goat anti-mouse p75NTR^{ECD} antibody for p75NTR^{ECD} detection. However, a concentration dependent standard curve is not produced when the antibody set is reversed i.e., the polyclonal goat anti-mouse p75NTR^{ECD} antibody is used for p75NTR^{ECD} capture (data not shown).

Following this result, the mouse anti-human p75NTR antibodies (MLR1 and MLR2) were compared for p75NTR^{ECD} capture. **Figure 4.2** illustrates that no significant differences are seen between the mouse anti-human p75NTR antibodies in this role, and as such, mouse anti-human p75NTR (MLR2) was used for sandwich ELISAs throughout ELISA optimisation.

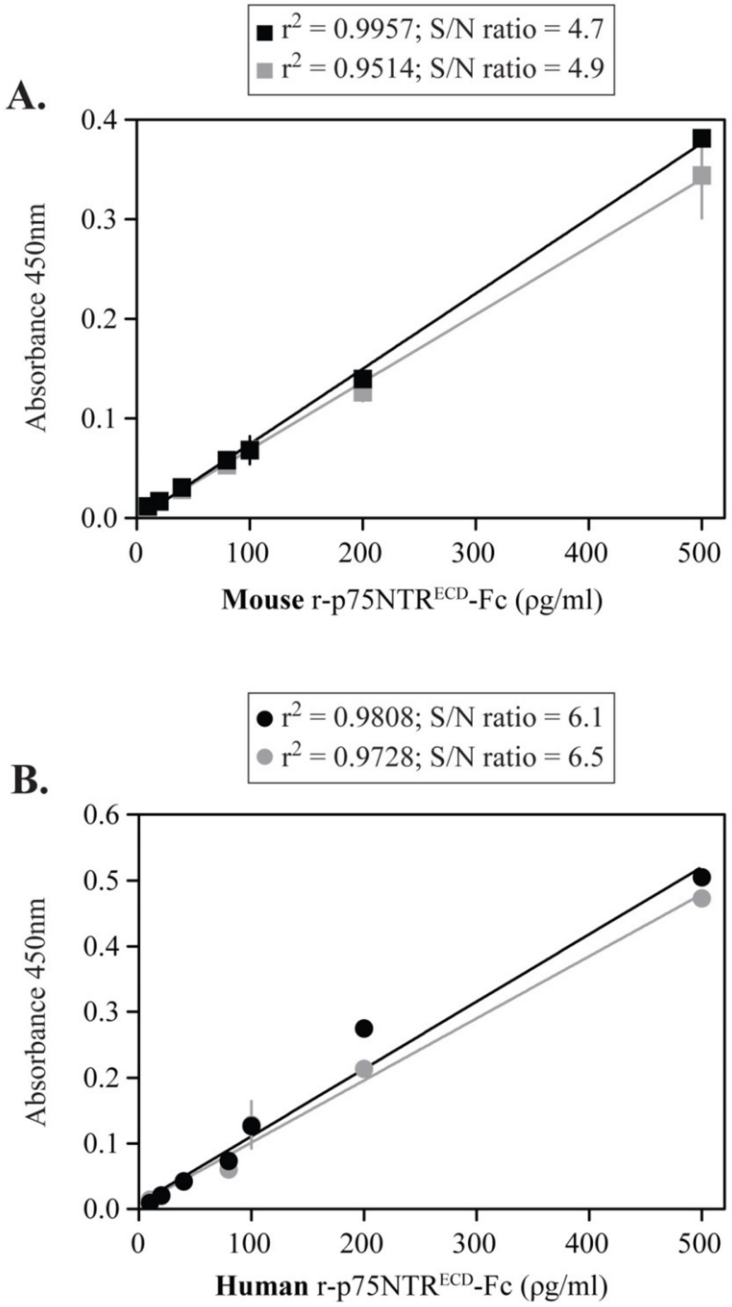

Figure 4.2: Test of different mouse anti-human p75NTR antibodies for r-p75NTR^{ECD}-Fc capture

Mouse anti-human p75NTR antibodies MLR1 (■/●) and MLR2 (■/●) at 2µg/ml were tested as capture antibodies for **A.** mouse and **B.** human r-p75NTR^{ECD}-Fc using 1µg/ml goat anti-mouse p75NTR^{ECD} and bovine anti-goat HRP (0.8µg/ml) detection antibodies in an indirect sandwich ELISA protocol with a 24 hour sample incubation (3 replicates per ELISA, 2 ELISAs). Standard curves are plotted as mean ± SEM with linear regression after removal of background readings (Prism6), and error bars are shown when greater than the symbol. Signal to noise ratios (S/N) were calculated from the absorbance readings of 500ρg/ml in relation to background.

4.3. Indirect sandwich ELISA optimisation

An optimal ELISA will achieve four goals, one, specificity for a particular antigen; two, the best signal to noise ratio (S/N) for the sensitivity required; three, be robust and reproducible for the sample tested; and four, measure an antigen over a biologically relevant range. As such, the ideal conditions for each assay component need to be determined empirically (Crowther 2001). These components include the choice of plate; standard antigen; buffers, including a coating buffer, wash buffer, and sample buffer; and the method used to produce and measure the colourimetric signal.

4.3.1. Unchanged components

4.3.1.1. Assay Plate

Plates used in ELISAs are typically made of polyvinyl chloride (flexible) or polystyrene (inflexible). Other materials such as polypropylene, polycarbonate, and nylon are occasionally used, and plates of different colours are available for different methods of signal detection (Crowther 2001). A clear, flat-bottomed, polyvinyl chloride 96-well ELISA plate which is compatible with colourimetric signal detection, was chosen for sandwich ELISAs.

4.3.1.2. Coating Buffer

The most common technique for attachment of protein (e.g., antibody) to an assay plate is passive adsorption, which is primarily mediated by hydrophobic interactions, although some electrostatic forces may contribute (Crowther 2001). The coating buffer must have a high pH to allow maximum antibody binding; to achieve this, the carbonate-bicarbonate buffer (0.2M Sodium carbonate/bicarbonate pH 9.6) is frequently used (Crowther 2001). The high pH of this buffer aids the solubility of proteins and peptides and ensures that most proteins are unprotonated with an overall negative charge, which helps in binding to a positively charged plate.

The mouse anti-human p75NTR antibodies used for $p75NTR^{ECD}$ capture bound to the 96-well plates using the carbonate-bicarbonate buffer, so the assay plates and

the coating buffer did not change throughout the optimisation of the indirect sandwich ELISA for p75NTR^{ECD}.

An enzymatic detection agent (3,3′,5,5′-tetramethylbenzidine, TMB) was used for colourimetric detection of the horseradish peroxidase (HRP) conjugated to the secondary antibody. TMB is a chromogen that yields a blue colour when oxidized, typically because of oxygen radicals produced by the hydrolysis of hydrogen peroxide by HRP. The colour then changes to yellow with the addition of sulphuric acid with maximum absorbance at 450nm (Crowther 2001). The TMB reagent was used in ELISAs as specified by the manufacturer (i.e., 1 part Reagent B to nine parts Reagent A, 50µl per well for 15 minutes, then 50µl 2M Sulphuric acid per well, with the plate read at 450nm), and did not change during ELISA optimisation.

The optimised mouse and human p75NTR^{ECD} indirect sandwich ELISA was achieved by testing a number of buffer recipes, and the antibody concentrations, empirically.

4.3.2. Buffer testing

4.3.2.1. Blocking agent

Blocking agents are used to block unoccupied sites on plates, thus inhibiting any non-specific binding of antigens and antibodies to the plate (Crowther 2001). The usefulness of a blocking agent is determined by both the background readings, and the resulting standard curve S/N ratios. Three different blocking agents, bovine serum albumin (BSA; **Figures 4.3** and **4.4**), supermarket brand Diploma milk powder (**Figure 4.3**), and a BioRad blocking agent (**Figure 4.4**), all in a bicarbonate-based blocking buffer, were compared using the human p75NTR^{ECD}-Fc standard.

Regardless of blocking agent concentration, the Diploma milk powder and BioRad blocking powder resulted in much higher background readings than seen with 2% BSA (**Figures 4.3.A** and **4.4.A**) and were unable to produce concentration-dependent standard curves with sufficient repeatability after removal of the

background readings (**Figures 4.3.B** and **4.4.B**). As a result, 2% BSA was chosen as the optimum blocking agent.

4.3.2.2. Wash buffer

The purpose of a wash buffer is to remove unbound reagents, without eluting antibodies or antigens from the plate (Crowther 2001); the usefulness of a wash buffer is determined using S/N ratios of the resultant standard curve. Tris buffered saline (TBS)- and Phosphate buffered saline (PBS)-based buffers of similar salt concentrations (1xTBS, 1xPBS) and higher salt concentrations (2xPBS, 0.5M NaCl PBS) were tested as wash buffers as seen in **Figure 4.5**. Buffers with higher salt concentrations decreased the sensitivity of the sandwich ELISAs for both mouse (**Figure 4.5.A**) and human (**Figure 4.5.B**) r-p75NTR^{ECD}-Fc. The 1xPBS buffer resulted in the highest S/N ratios for mouse and human r-p75NTR^{ECD}-Fc standards, and so was chosen as the optimum wash buffer.

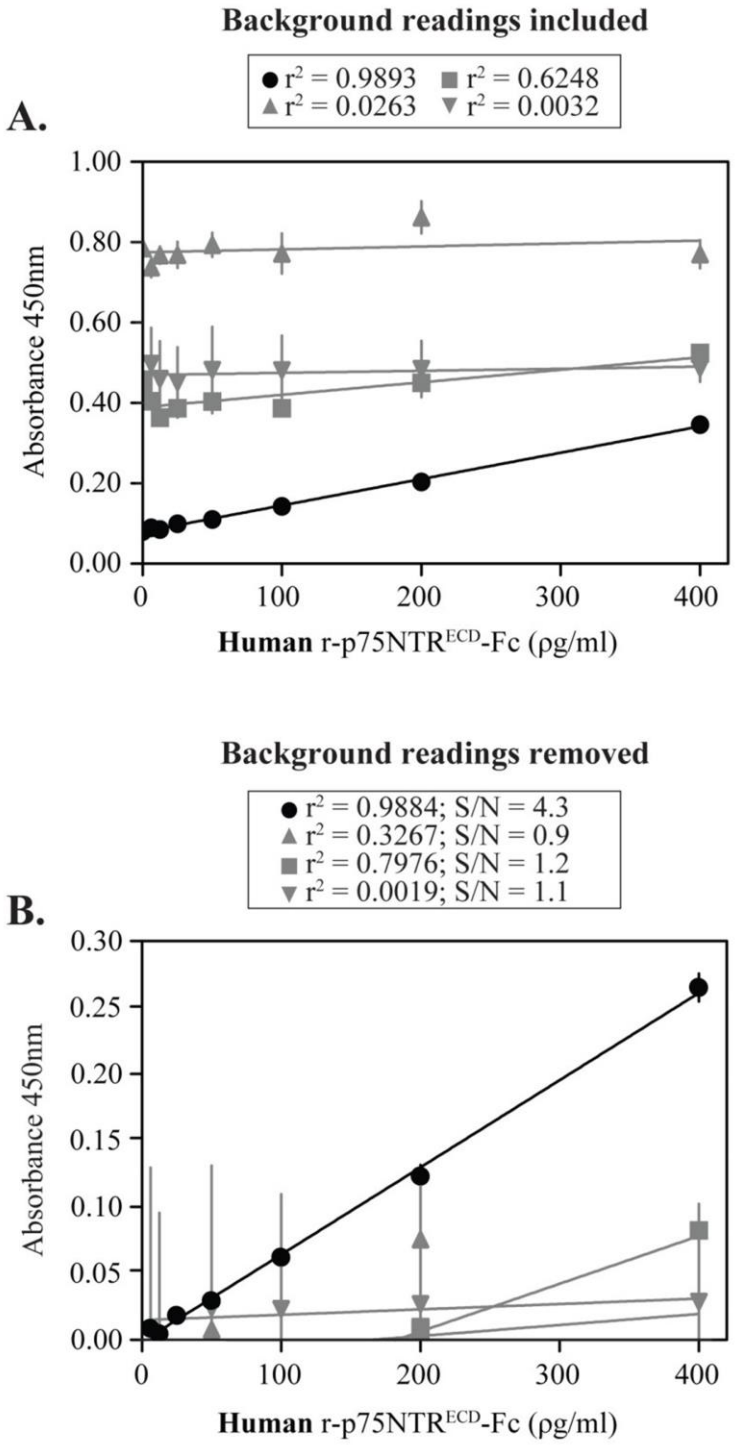

Figure 4.3: Test of blocking agents Diploma milk powder and bovine serum albumin for the detection of human r-p75NTR^{ECD}-Fc

Supermarket brand Diploma milk powder at 5% (▲), 2% (■), and 1% (▼), and 2% bovine serum albumin (BSA; ●) were tested as blocking agents for detection of human r-p75NTR^{ECD}-Fc in an indirect sandwich ELISA protocol with a 24 hour sample incubation (3 replicates per ELISA, 2 ELISAs). Standard curves are plotted as mean ± SEM with linear regression, with **A.** background readings included, or **B.** background readings removed (Prism6), and error bars are shown when greater than the symbol. Signal to noise ratios (S/N) were calculated from the absorbance readings at 400ρg/ml in relation to background.

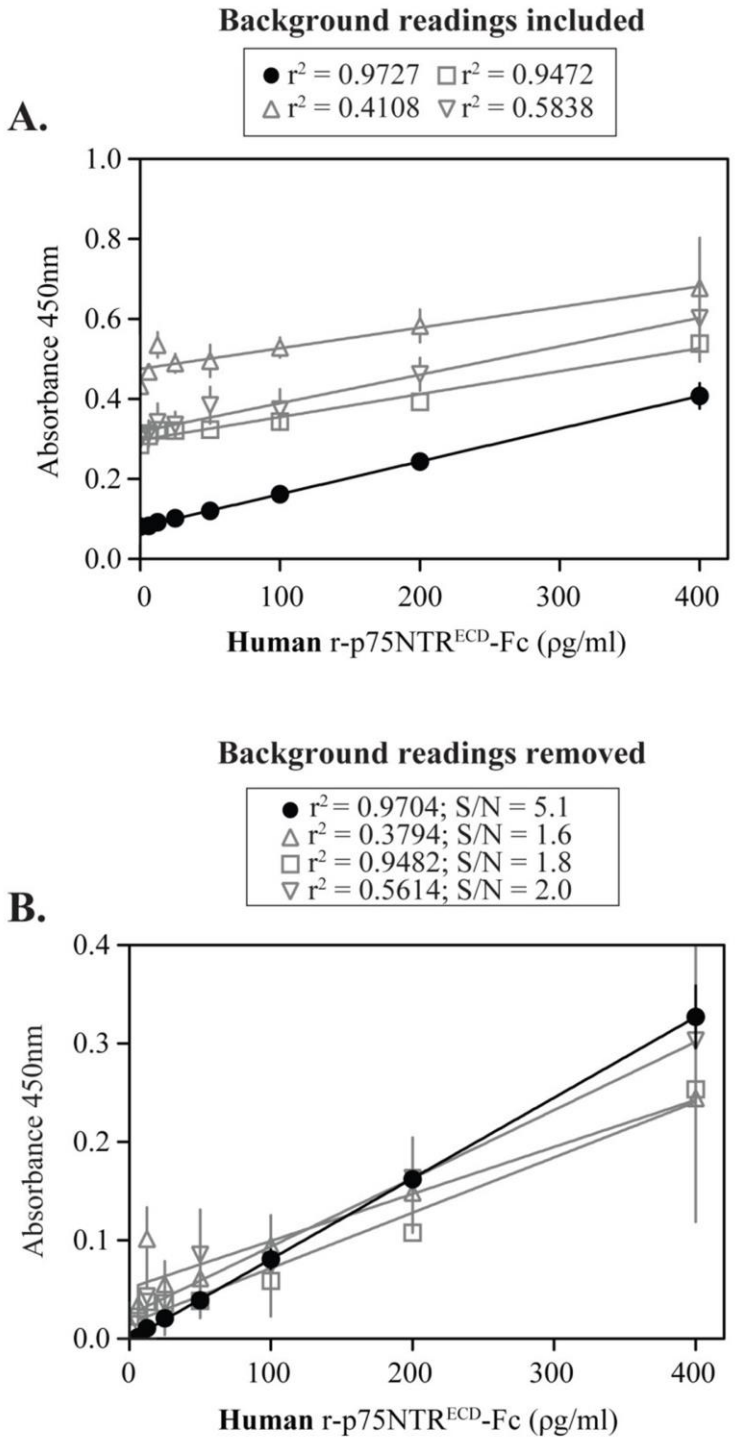

Figure 4.4: Test of blocking agents BioRad blocking powder and bovine serum albumin for the detection of human r-p75NTR^{ECD}-Fc

BioRad blocking powder at 5% (△), 2% (□), and 1% (▽), and 2% bovine serum albumin (BSA; ●) were tested as blocking agents for detection of human r-p75NTR^{ECD}-Fc in an indirect sandwich ELISA protocol with a 24 hour sample incubation (3 replicates per ELISA, 2 ELISAs). Standard curves are plotted as mean ± SEM with linear regression, with **A.** background readings included, or **B.** background readings removed (Prism6), and error bars are shown when greater than the symbol. Signal to noise ratios (S/N) were calculated from the absorbance readings at 400ρg/ml in relation to background.

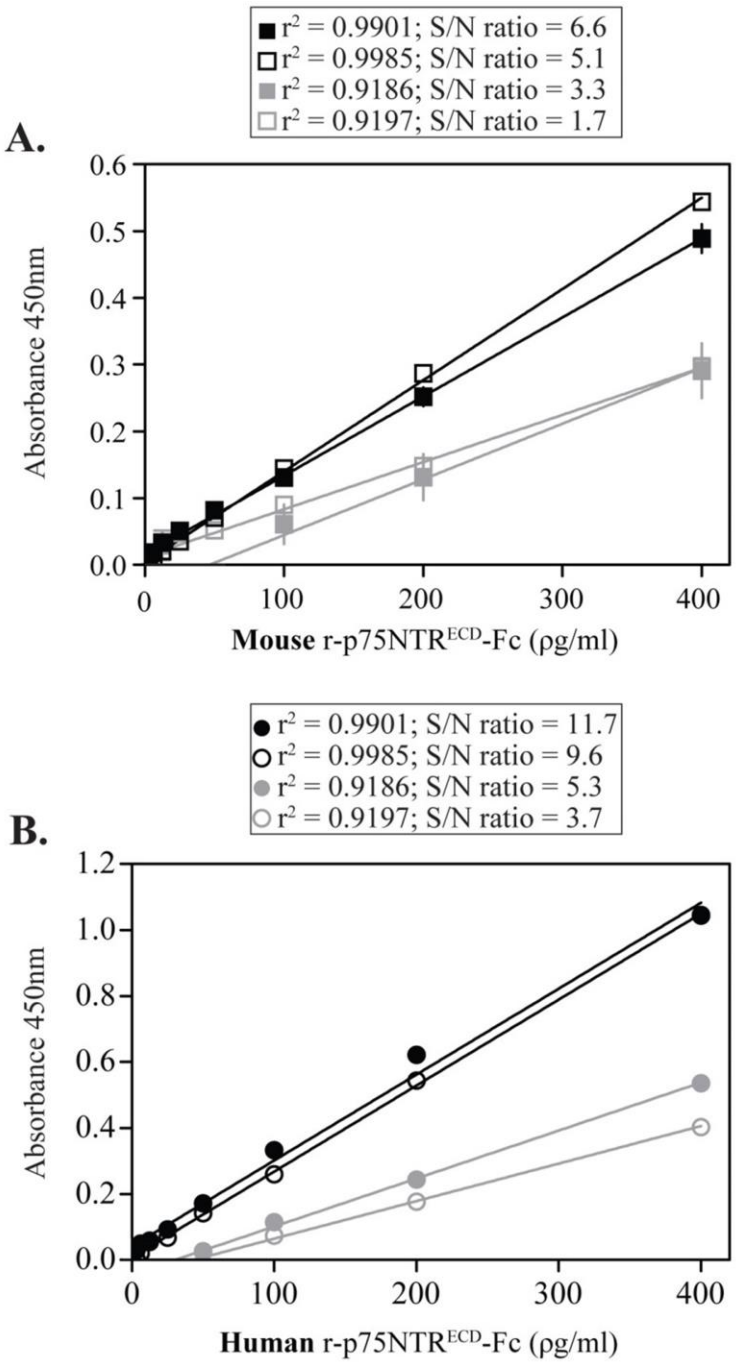

Figure 4.5: Test of TBS and PBS based buffers as wash buffer for the detection of r-p75NTR^{ECD}-Fc

Four different buffers were tested as wash buffers for **A.** mouse and **B.** human r-p75NTR^{ECD}-Fc using an indirect sandwich ELISA protocol with a 16 hour sample incubation; 1xPBS (■/●), 1xTBS (□/○), 2xPBS (■/●), and 0.5M NaCl PBS (□/○)(3 replicates per ELISA, 2 ELISAs). Standard curves are plotted as mean ± SEM with linear regression after removal of background readings (Prism6), and error bars are shown when greater than the symbol. Signal to noise (S/N) ratios were calculated from the absorbance readings at 400ρg/ml in relation to background.

4.3.2.3. Sample buffer

A sample buffer is used when adding the antigen and detection antibodies to an ELISA, and must allow for antigen-antibody reactions without interference (Crowther 2001). Four different buffers were tested for use as sample buffers and compared based upon the resultant S/N ratios. As presented in **Figure 4.6**, two PBS-based, and two TBS-based sample buffers, using either Triton-X or Tween-20 detergents produced standard curves for both mouse and human r-p75NTR^{ECD}-Fc standards. The use of PBS-based sample buffers resulted in higher S/N ratios for the detection of r-p75NTR^{ECD}-Fc standards, and the use of Tween-20 as a detergent resulted in higher absorbance readings at 400ρg/ml when compared to Triton-X. As a result, the PBS-based buffer with 0.05% Tween-20 was chosen as the optimal sample buffer.

4.3.2.4. Blocking buffer

In addition to the blocking agent, the other components of a blocking buffer can affect the performance of an ELISA (Crowther 2001). Using 2% BSA as the blocking agent, two buffers, a carbonate-bicarbonate-based buffer, at pH 9.6, and a PBS-based buffer, at pH 7.4, were tested for use as the blocking buffer and compared by the resultant S/N ratios. An increased S/N ratio was seen for both mouse (**Figure 4.7.A**) and human (**Figure 4.7.B**) r-p75NTR^{ECD}-Fc using the PBS-based buffer as compared to the carbonate-bicarbonate buffer. As a result, PBS-based buffer with 2% BSA was chosen as the optimal blocking buffer.

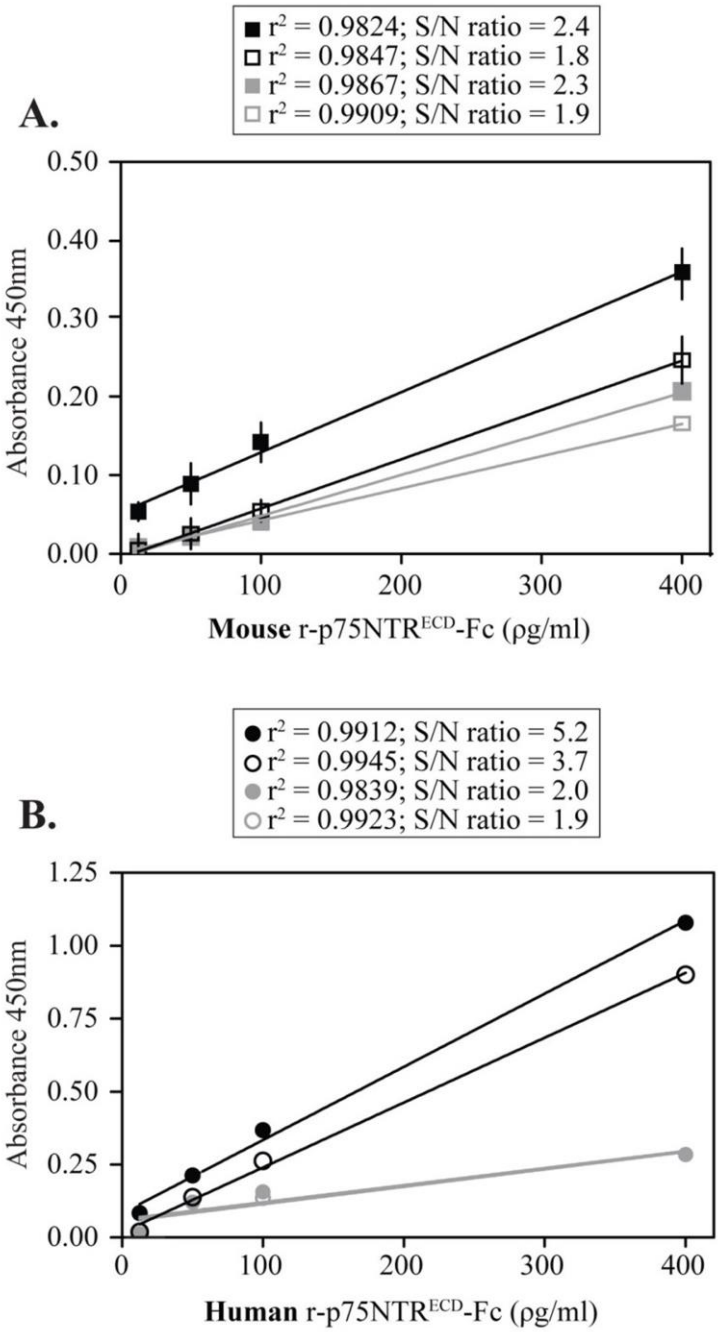

Figure 4.6: Test of TBS and PBS based buffers as sample buffer for the detection of r-p75NTR^{ECD}-Fc

Four different buffers were tested as sample buffers for **A.** mouse and **B.** human r-p75NTR^{ECD}-Fc using an indirect sandwich ELISA protocol with a 16 hour sample incubation; PBS with 0.05% Tween-20 (■/●), PBS with 0.01% Triton-X (□/○), TBS with 0.05% Tween-20 (■/●), and TBS with 0.01% Triton-X (□/○) (3 replicates per ELISA, 2 ELISAs). Standard curves are plotted as mean ± SEM with linear regression after removal of background readings (Prism6), and error bars are shown when greater than the symbol. Signal to noise (S/N) ratios were calculated from the absorbance readings at 400ρg/ml in relation to background.

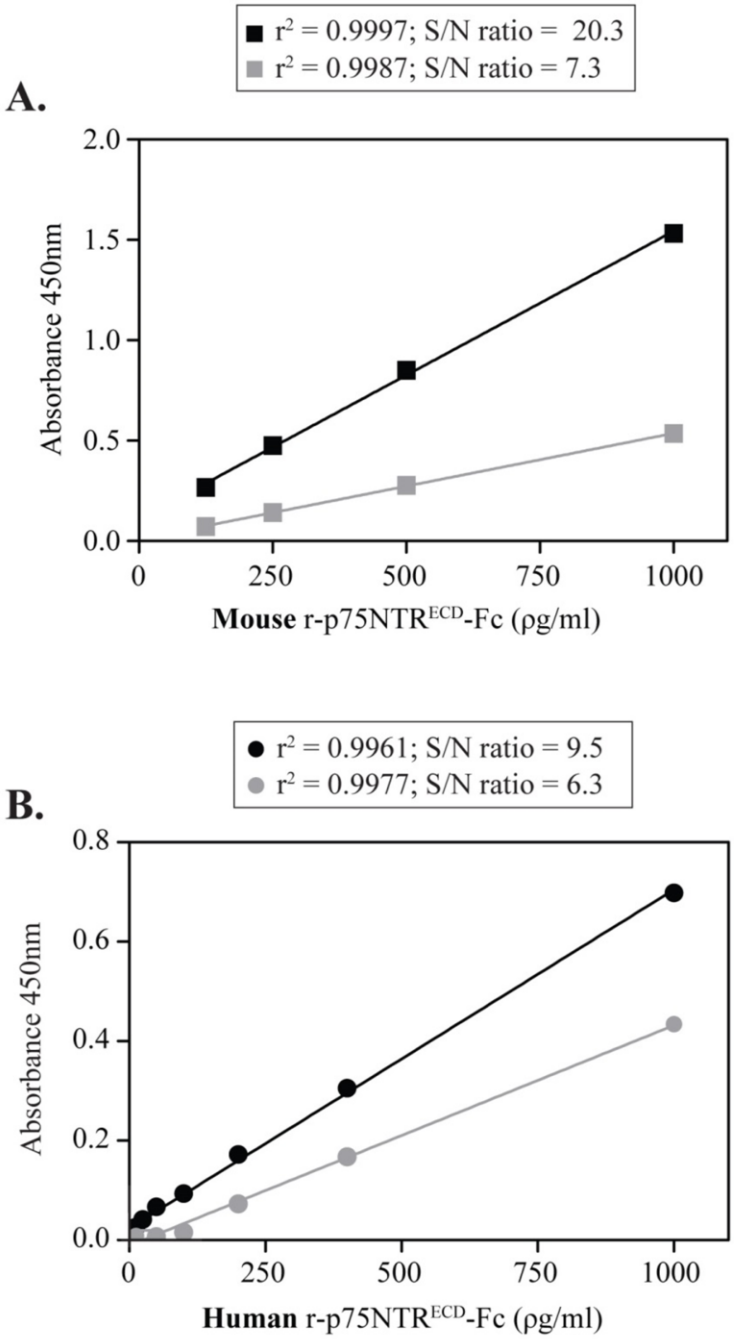

Figure 4.7: Test of bicarbonate buffer and PBS based buffer for the blocking buffer for detection of r-p75NTR^{ECD}-Fc

PBS based buffer (■/●) and bicarbonate buffer (■/●) were tested as blocking buffers for **A.** mouse and **B.** human r-p75NTR^{ECD}-Fc using an indirect sandwich ELISA protocol with a 20 hour sample incubation (3 replicates per ELISA, 2 ELISAs). Standard curves are plotted as mean ± SEM with linear regression after removal of background readings (Prism6), and error bars are shown when greater than the symbol. Signal to noise (S/N) ratios were calculated from the absorbance readings at 1000ρg/ml in relation to background.

4.3.3. Antibody concentrations

Following the optimisation of buffer recipes for the indirect sandwich ELISA for p75NTR^{ECD}, the antibodies were tested further to determine the optimal concentrations for p75NTR^{ECD} quantification. This was determined by comparing resultant S/N ratios when changing the concentrations of the capture and detection antibodies, keeping the secondary HRP conjugated antibody constant at 0.8µg/ml.

As presented in bold text in **Table 4.3.A**, the antibody concentrations of 4.0µg/ml mouse anti-human p75NTR (MLR2) capture antibody and 1.0µg/ml goat anti-mouse p75NTR^{ECD} detection antibody resulted in the highest S/N ratios for quantification of mouse r-p75NTR^{ECD}-Fc. For quantification of human r-p75NTR^{ECD}-Fc, 4.0µg/ml mouse anti-human p75NTR (MLR2) capture antibody and 1.0µg/ml goat anti-mouse p75NTR^{ECD} detection antibody also resulted in the highest S/N ratios (highlighted in bold; **Table 4.3.B**). As a result, ELISAs for mouse- and human-derived p75NTR^{ECD} can be performed using the same setup, with antibody concentrations of 4.0µg/ml mouse anti-human p75NTR (MLR2) capture antibody, 1µg/ml goat anti-mouse p75NTR^{ECD} detection antibody and 0.8µg/ml bovine anti-goat HRP secondary antibody.

Table 4.3.A: Signal to noise ratios of standard curves produced using different antibody concentrations for mouse r-p75NTR^{ECD}-Fc

		Goat anti-mouse p75NTR^{ECD} detection antibody	
		0.5µg/ml	1.0µg/ml
Mouse anti-human p75NTR (MLR2) capture antibody	0.5µg/ml	11.59	12.87
	1.0µg/ml	14.45	14.88
	2.0µg/ml	15.38	16.85
	4.0µg/ml	16.25	**17.88**

Table 4.3.B: Signal to noise ratios of standard curves produced using different antibody concentrations for human r-p75NTR^{ECD}-Fc

		Goat anti-mouse p75NTR^{ECD} detection antibody	
		0.5µg/ml	1.0µg/ml
Mouse anti-human p75NTR (MLR2) capture antibody	0.5µg/ml	6.86	9.58
	1.0µg/ml	7.19	10.25
	2.0µg/ml	7.73	11.38
	4.0µg/ml	9.08	**12.97**

4.3.4. Final comparison of p75NTR^{ECD} capture antibodies

After empirical testing of buffer recipes and antibody concentrations, the two mouse anti-human p75NTR antibodies (MLR1 and MLR2) able to capture mouse and human p75NTR^{ECD} used in combination with goat anti-mouse p75NTR^{ECD} detection antibody, were compared using the final ELISA protocol. As presented in **Figure 4.8**, using mouse anti-human (MLR1) p75NTR antibody for p75NTR^{ECD} capture resulted in standard curves with higher S/N ratios than that produced using mouse anti-human (MLR2) p75NTR. As such, the final indirect sandwich ELISA used mouse anti-human p75NTR (MLR1) capture antibody with goat anti-mouse p75NTR^{ECD} detection antibody.

4.3.5. Storage effects

Following optimisation of the indirect sandwich ELISA, long-term storage effects were tested to determine if multiple plates could be coated and blocked, then stored for later sample analysis without a reduction in sensitivity (**Figure 4.9**). No significant differences were seen in the sensitivity of the ELISA when human r-p75NTR^{ECD}-Fc was tested on freshly coated plates and those stored for up to 6 weeks at -20°C after the blocking step.

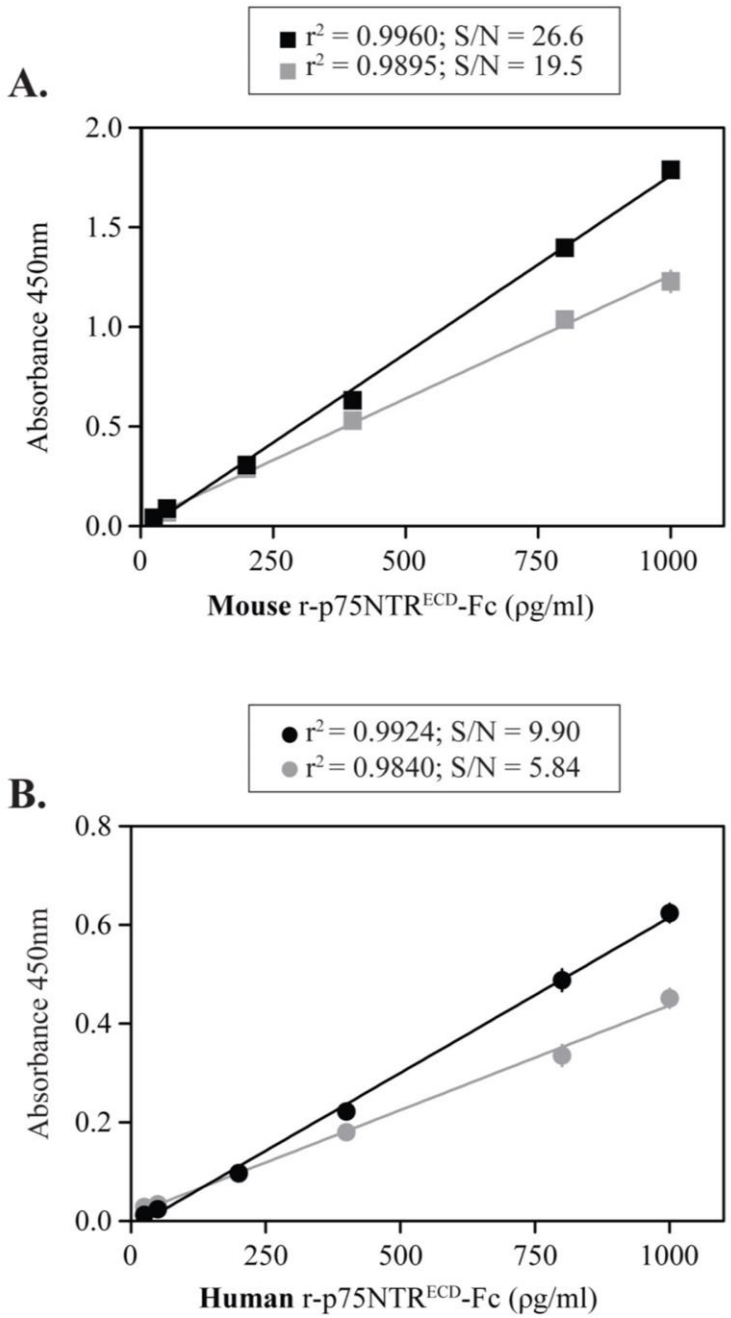

Figure 4.8: Test of different mouse anti-human p75NTR antibodies for r-p75NTR^{ECD}-Fc capture

Mouse anti-human p75NTR antibodies MLR1 (■/●) and MLR2 (■/●) at 4µg/ml were tested as capture antibodies for **A.** mouse and **B.** human r-p75NTR^{ECD}-Fc using 1µg/ml goat anti-mouse p75NTR^{ECD} and bovine anti-goat HRP (0.8µg/ml) antibodies for detection in an indirect sandwich ELISA protocol with a 20 hour sample incubation (3 replicates per ELISA, 2 ELISAs). Standard curves are plotted as mean ± SEM with linear regression after removal of background readings (Prism6), and error bars are shown when greater than the symbol. Signal to noise (S/N) ratios were calculated from the absorbance readings at 1000ρg/ml in relation to background.

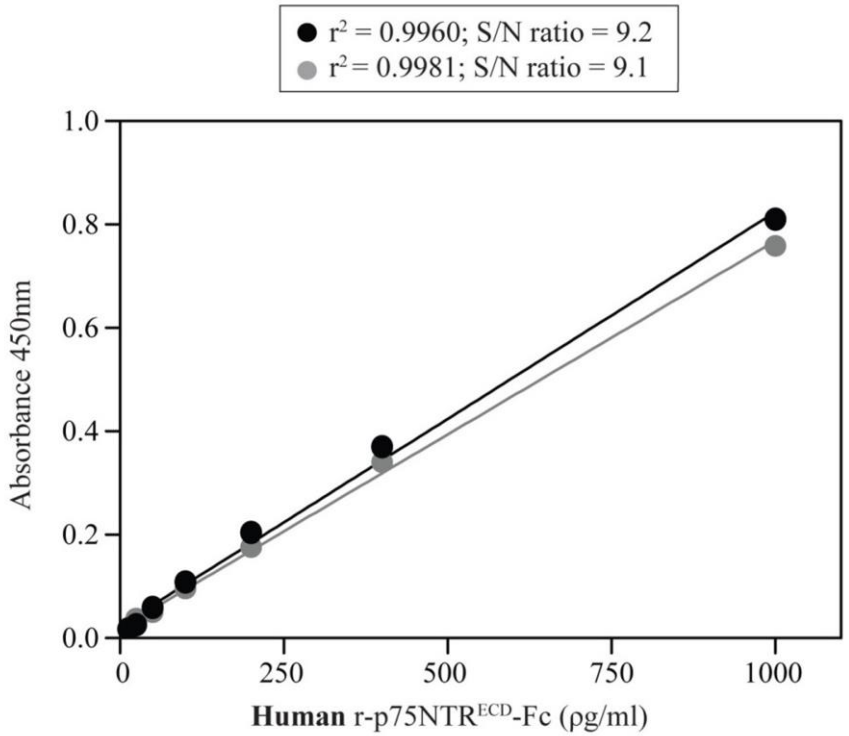

Figure 4.9: Test of long-term plate storage on the detection of human r-p75NTR^{ECD}-Fc

Human r-p75NTR^{ECD}-Fc standards were tested on plates using an indirect sandwich ELISA protocol with a 20 hour sample incubation, either straight after blocking (●) or on plates that had been stored at -20°C for 6 weeks following blocking (●) (3 replicates per ELISA, 2 ELISAs). Standard curves are plotted as mean ± SEM with linear regression after removal of background readings (Prism6), and error bars are shown when greater than the symbol Signal to noise (S/N) ratios were calculated from the absorbance readings at 1000ρg/ml in relation to background.

4.4. Final indirect sandwich ELISA protocol

The optimised protocol for the detection of p75NTR^{ECD} (**Table 4.4** and **Figure 4.10**), using mouse anti-human p75NTR (MLR1) antibody for capture and goat anti-mouse p75NTR^{ECD} with bovine anti-goat HRP for detection, detected both mouse- and human-derived r-p75NTR^{ECD}-Fc over a wide range of concentrations.

Mouse r-p75NTR^{ECD}-Fc was detectable from 5ng/ml down to 0.01ng/ml (**Figure 4.11.A**). In particular, the optimised protocol resulted in concentration dependent absorbance readings fitting a linear regression model between 1ng/ml and 0.01ng/ml with an r^2 value of 0.9959 (**Figure 4.11.B**). By plotting the standard curve between 1ng/ml and 0.01ng/ml with a $\log_{10}$ x-axis, it was determined that the lowest reliable value of detection for mouse r-p75NTR^{ECD}-Fc was 0.05ng/ml (**Figure 4.11.C**).

Additionally, the same optimised protocol could detect human r-p75NTR^{ECD}-Fc from 10ng/ml down to 0.01ng/ml with similar characteristics (**Figure 4.12.A**). A linear regression model fit human r-p75NTR^{ECD}-Fc absorbance readings between 1ng/ml and 0.01ng/ml with an r^2 value of 0.9996 (**Figure 4.12.B**), and the detection limit for human r-p75NTR^{ECD}-Fc was 0.05ng/ml (**Figure 4.12.C**).

Table 4.4: Final protocol for p75NTR^{ECD} sandwich ELISA

Description		Buffer	Volume /well	Incubation time
Primary capture antibody	4μg/ml mouse anti-human p75NTR (MLR1)	25mM sodium bicarbonate buffer, pH 9.6	100μl	18hr, 4°C, agitating
Block	-	PBS with 2% BSA, 0.05% Tween-20, pH 7.3	180μl	1hr, 37°C
Antigen	mouse / human r-p75NTR^{ECD}-Fc standards &/or samples		100μl	20hr, RT, agitating
Primary detection antibody	1μg/ml goat anti-mouse p75NTR^{ECD}		100μl	1hr, RT, agitating
Secondary HRP antibody	0.8μg/ml bovine anti-goat HRP		100μl	1hr, RT, agitating
Substrate	TMB Peroxidase kit		50μl	15min, RT, agitating
Stop	Sulphuric Acid	2M	50μl	

Washing buffer after antigen and antibody incubations: PBS with 0.05% Tween-20; RT: room temperature

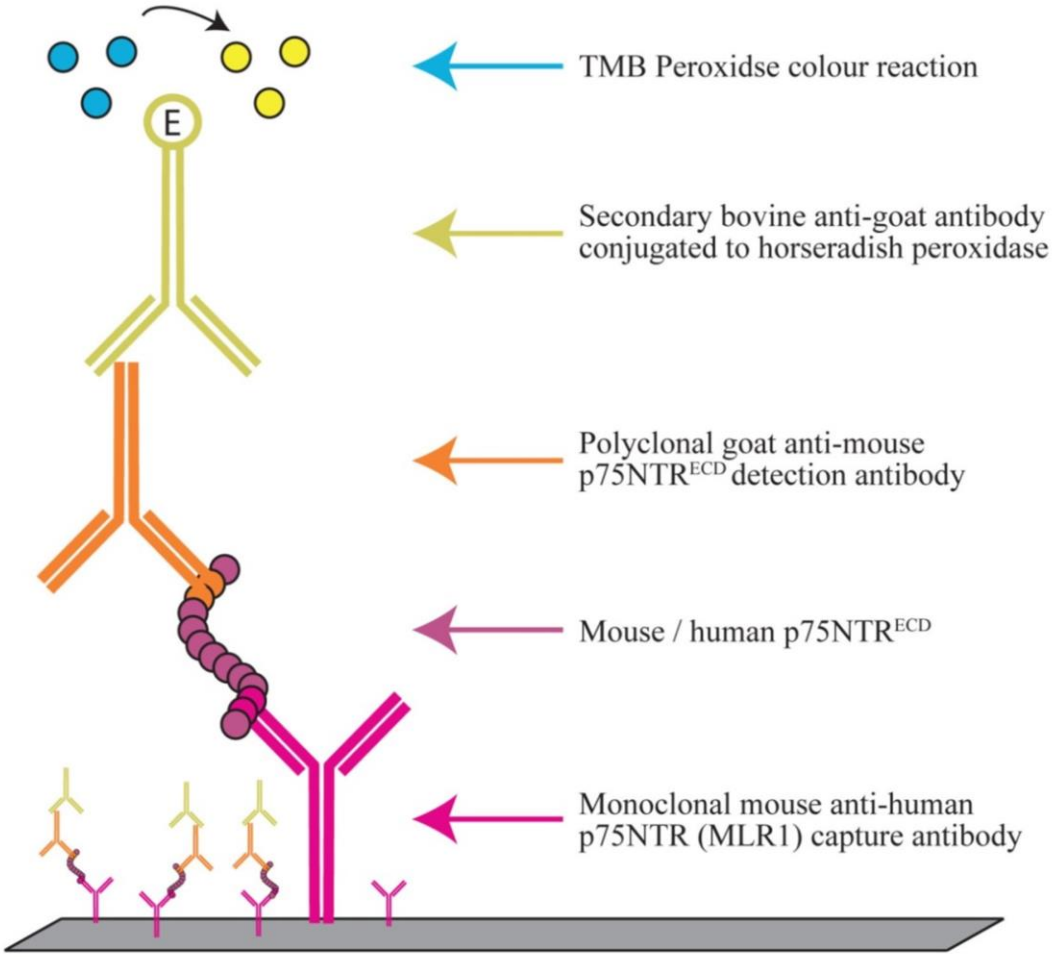

Figure 4.10: Schematic of optimised indirect sandwich ELISA setup for p75NTR^{ECD}

Mouse anti-human p75NTR (MLR1) primary antibody was used to capture p75NTR^{ECD}, and polyclonal goat anti-mouse p75NTR^{ECD} antibody was used for detection. A secondary antibody, conjugated to horseradish peroxidase, bovine anti-goat HRP, and a 3,3',5,5'-tetramethylbenzidine (TMB) colour substrate kit were used for p75NTR^{ECD} visualisation.

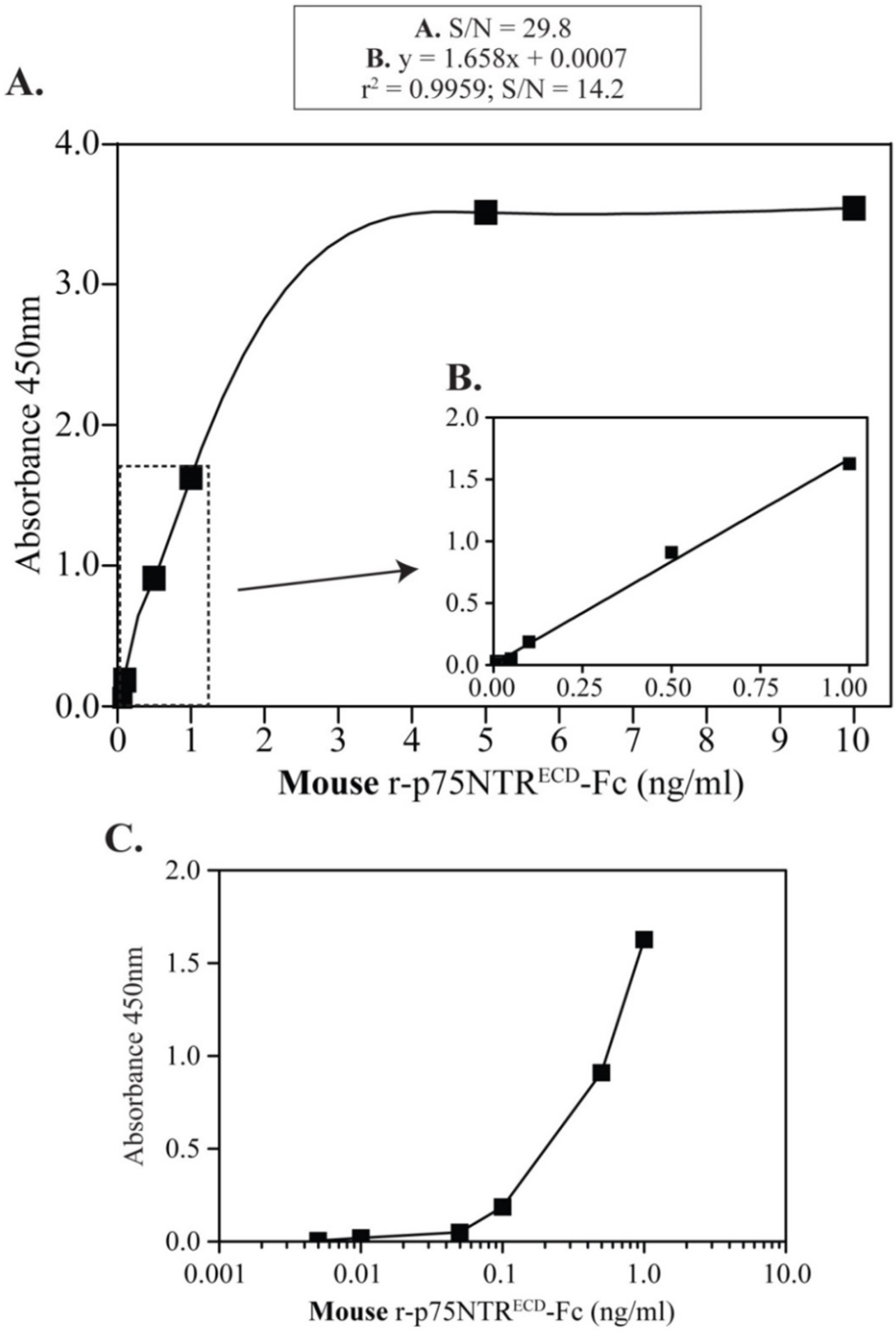

Figure 4.11: Final indirect sandwich ELISA for mouse r-p75NTR^{ECD}-Fc

Mouse r-p75NTR^{ECD}-Fc (■) was detected using an indirect sandwich ELISA protocol with a 20 hour sample incubation (3 replicates per ELISA, 2 ELISAs). **A.** 4µg/ml mouse anti-human p75NTR (MLR1) capture, and 1µg/ml goat anti-mouse p75NTR^{ECD} with 0.8µg/ml bovine anti-goat HRP detection antibodies were used to detect mouse r-p75NTR^{ECD}-Fc across a wide range of concentrations. **B.** The indirect sandwich ELISA is sensitive to 0.01ng/ml fitting a linear regression from 1ng/ml to 0.01ng/ml (Prism6). **C.** Plotting the standard curve with a $\log_{10}$ x-axis shows the detection limit of this antibody set at 0.05ng/ml (50ρg/ml). Absorbance readings are plotted, after removal of background readings, as the mean ± SEM (Prism6). Signal to noise (S/N) ratios achieved were calculated from the absorbance readings at the highest concentration of each curve, in relation to background.

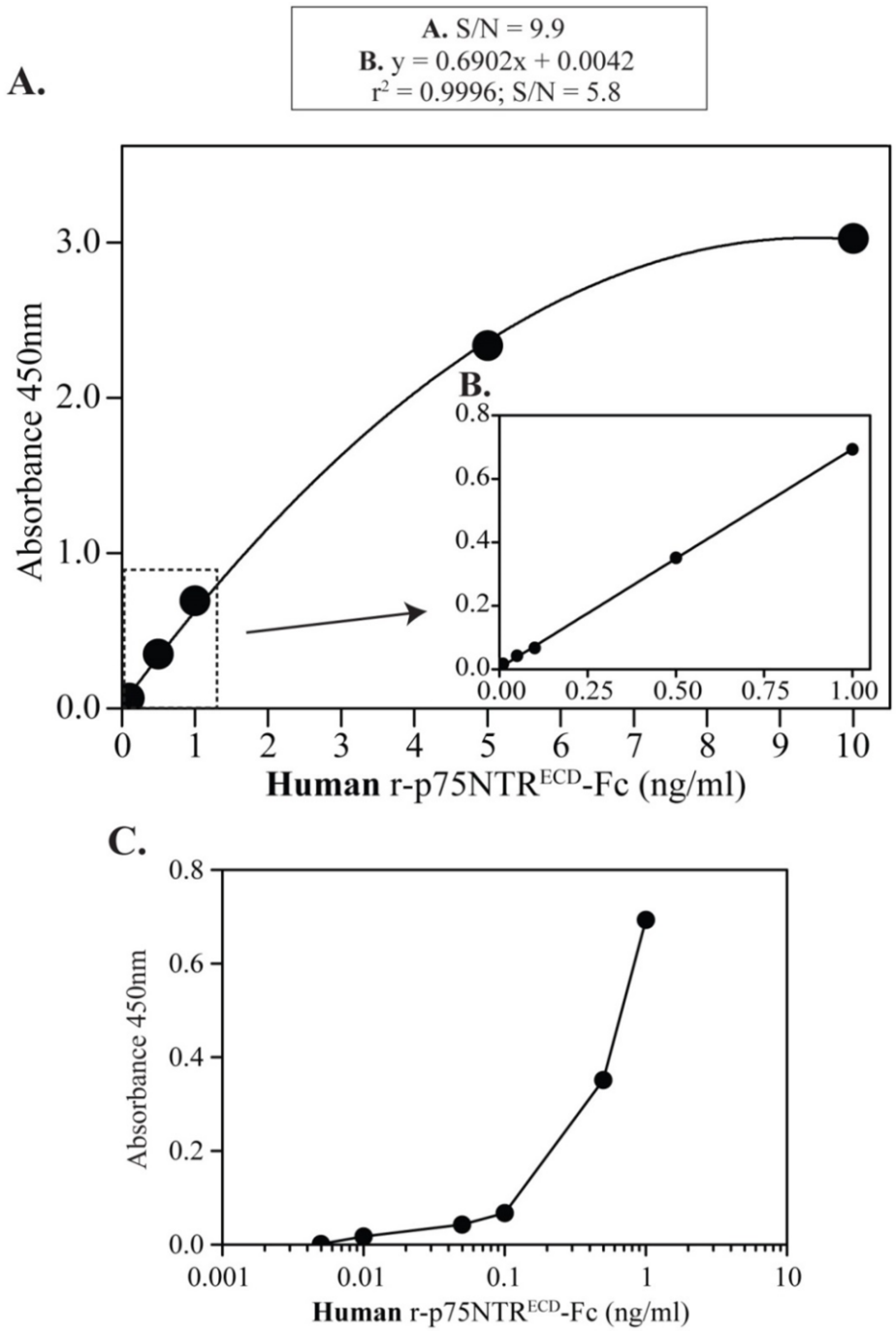

Figure 4.12: Final indirect sandwich ELISA for human r-p75NTR^{ECD}-Fc

Human r-p75NTR^{ECD}-Fc (●) was detected using an indirect sandwich ELISA protocol with a 20 hour sample incubation (3 replicates per ELISA, 2 ELISAs). **A.** 4µg/ml mouse anti-human p75NTR (MLR1) capture, and 1µg/ml goat anti-mouse p75NTR^{ECD} with 0.8µg/ml bovine anti-goat HRP detection antibodies were used to detect mouse r-p75NTR^{ECD}-Fc across a wide range of concentrations. **B.** The indirect sandwich ELISA is sensitive to 0.01ng/ml fitting a linear regression from 1ng/ml to 0.01ng/ml (Prism6). **C.** Plotting the standard curve with a $\log_{10}$ x-axis shows the detection limit of this antibody set at 0.05ng/ml (50ρg/ml). Absorbance readings are plotted, after removal of background readings, as the mean ± SEM (Prism6). Signal to noise (S/N) ratios achieved were calculated from the absorbance readings at the highest concentration of each curve, in relation to background.

4.5. Optimisation of urinary sample treatment

After optimising the indirect sandwich ELISA for the detection of mouse and human p75NTR^{ECD}, the next step was to determine optimal treatment protocols for urinary samples from mice and humans for sensitive p75NTR^{ECD} detection and quantification.

To test the feasibility of using diluted mouse urine in the p75NTR^{ECD} ELISA, samples from SOD1^{G93A} MND model mice, B6 healthy controls (**Figure 4.13.A** and **4.13.B**), and p75NTR^{ECD} Exon III knockout mice (**Figure 4.13.B**) were diluted from 20% to 1.25%. Additionally, SOD1^{G93A} and B6 mouse urine samples were spiked with a 250pg of r-p75NTR^{ECD}-Fc (**Figure 4.13.C**). p75NTR^{ECD} estimates in urine from p75NTR Exon III knock-out mice were below background for all concentrations. In contrast, p75NTR^{ECD} was detectable in serially diluted urine samples from SOD1^{G93A} and B6 mice, but did not have a linear relationship to urine dilution at higher urine concentrations (**Figure 4.13.A**) and recovery of 250pg r-p75NTR^{ECD}-Fc was decreased at higher urine concentrations (**Figure 4.13.C**). In comparison, lower concentrations of mouse urine resulted in linear p75NTR^{ECD} estimates (**Figure 4.13.B**) and higher spiked recovery (**Figure 4.13.C**), suggesting interference at higher concentrations. To address this, neat diluted mouse urine was tested against urinary samples that had been diafiltered with PBS. However, diafiltration produced variable results, significantly decreasing the calculated p75NTR^{ECD} for some, but not all samples (data not shown). As a result, mouse urine was not diafiltered before analysis and neat mouse urine samples were diluted on ELISA plates at low urine concentrations of 1.25% for p75NTR^{ECD} calculation.

To test the feasibility of using diluted human urine in the p75NTR^{ECD} ELISA, samples from people with MND and healthy individuals were diluted from 20% to 1.25% (**Figure 4.14.A**). Additionally, urine samples were spiked with a 250pg of r-p75NTR^{ECD}-Fc (**Figure 4.14.B**). p75NTR^{ECD} estimates and recovery of spiked r-p75NTR^{ECD}-Fc was consistent over the range of human urine concentrations, suggesting no interference in p75NTR^{ECD} quantification. As a result, human urine was not diafiltered before analysis using indirect sandwich ELISAs, and was diluted on plates from a maximum of 20% for p75NTR^{ECD} calculation.

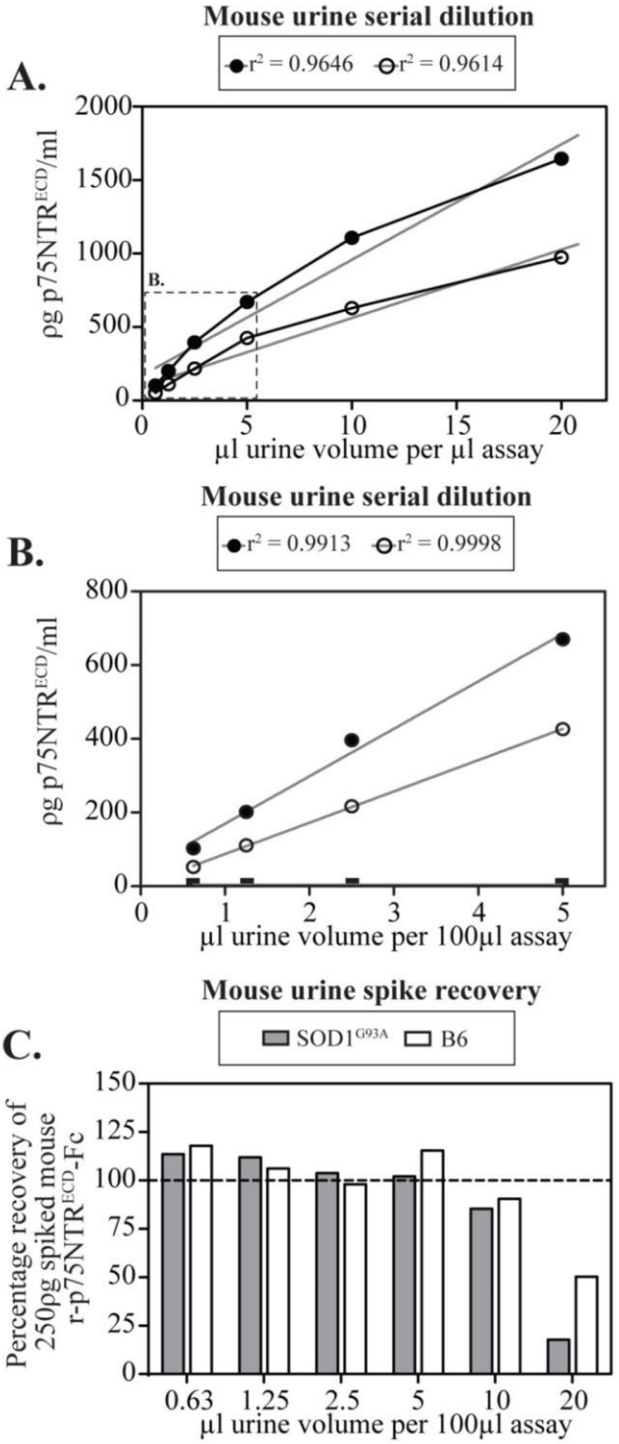

Figure 4.13: Feasibility testing of using neat mouse urine samples for p75NTR^{ECD} estimates by serial dilution and spiking

Urine samples from end stage SOD1^{G93A}, B6 healthy control, and p75NTR Exon III knock-out mice were tested using an indirect sandwich ELISA with a 20 hour sample incubation (4 replicates per ELISA, 2 ELISAs). **A.** Serial dilutions of neat urine samples from SOD1^{G93A} (●) and B6 healthy control (○) mice from 20–1.625%. **B.** Serial dilutions of neat urine samples from SOD1^{G93A} (●), B6 healthy control (○), and p75NTR Exon III knock-out (■) mice from 5-1.625%. **C.** Percentage recovery of 250ρg mouse r-p75NTR^{ECD}-Fc standard spiked into urine samples from SOD1^{G93A} (■) and B6 healthy control (□) mice. Calculated ρg/ml p75NTR^{ECD}/ml and percentage recovery values are plotted as mean ± SEM (Prism6).

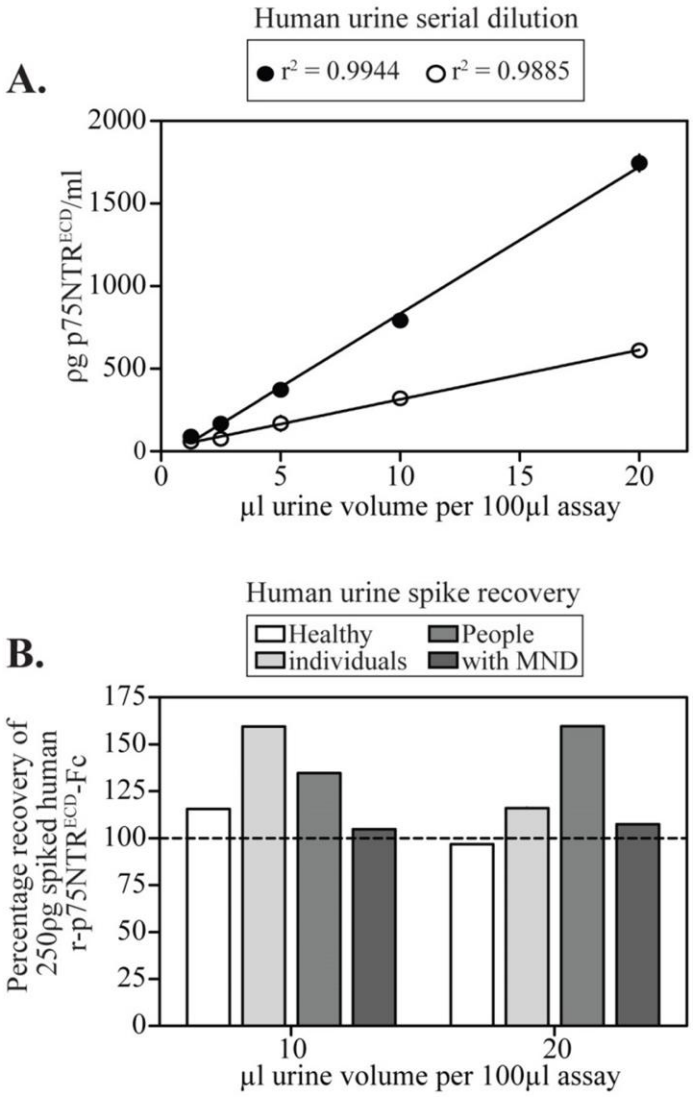

Figure 4.14: Feasibility testing of using neat human urine samples for p75NTR^{ECD} estimates by serial dilution and spiking

Urine samples from people with MND and healthy individuals were tested using an indirect sandwich ELISA with a 20 hour sample incubation (4 replicates per ELISA, 2 ELISAs). **A.** Serial dilutions of neat urine samples from people with MND (●) and healthy individuals (○) from 20-1.625%. **B.** Percentage recovery of 250ρg human r-p75NTR^{ECD}-Fc standard spiked into urine samples from people with MND (□/▫) and healthy individuals (■/■). Calculated ρg/ml p75NTR^{ECD}/ml and percentage recovery values are plotted as mean ± SEM.

A number of human urine samples were tested on all plates as experiment controls to measure the intra- and inter-plate variability for p75NTR^{ECD} quantification. As shown in **Table 4.5**, the variability of p75NTR^{ECD} measurements in these samples, as tested using the coefficient of variance (ratio of the standard deviation to the mean), was lower for replicates on individual plates (intra-assay), but higher between plates (inter-assay). In general, intra-assay variability scores of less than 10% are acceptable, as are inter-assay scores below 15%. Using these guidelines, mouse urine variability was within a normal and acceptable range, showing similar variability between different plates and within an individual plate. Human urine samples showed higher variability between plates than within individual plates, showing inter-assay variability of greater than 15%.

Table 4.5: Inter- and intra- plate variability of mouse and human sandwich ELISAs calculated using covariate of variation

r-p75NTR^{ECD}-Fc	Sample	Intra-assay	Inter-assay	Repeats
Mouse	145_4/10	7.68%	6.18%	3
	185_4/10	6.53%	6.67%	3
Human	MNDU23	4.79%	19.1%	17
	MNDU37/5	5.65%	19.2%	18

4.6. Comparison to a commercial human p75NTR ELISA

Late in the development of the p75NTR^{ECD} indirect sandwich ELISA, a commercial indirect sandwich ELISA kit became available through R&D Systems for detection of human-derived p75NTR. As such, the performance of the in-house ELISA was compared to the R&D Systems kit.

As seen in **Figure 4.15.A**, the R&D Systems human p75NTR indirect sandwich ELISA (R&D Systems kit) resulted in higher absorbance readings for the human r-p75NTR^{ECD}-Fc standard than those seen with the in-house indirect sandwich ELISA (in-house ELISA). However, the R&D Systems kit also had higher background readings, and as a result, had a lower S/N ratio than that produced by the in-house ELISA.

Both indirect sandwich ELISAs were also performed using the incubation times of the R&D Systems kit and the in-house ELISA, resulting in the direct comparison of the two antibody sets (**Figure 4.15.A**). Both setups recorded higher S/N ratios when run over the longer incubation times of the in-house ELISA (total 41.25 hours, standard/sample incubation 20 hours) than that of the R&D Systems kit (total 23.6 hours, standard/sample incubation 2 hours).

Although the R&D Systems kit resulted in standard curves with higher S/N ratios than the in-house ELISA using the in-house incubation times, p75NTR^{ECD} estimates from human urine samples were not significantly different between the two setups (**Figure 4.15.B**).

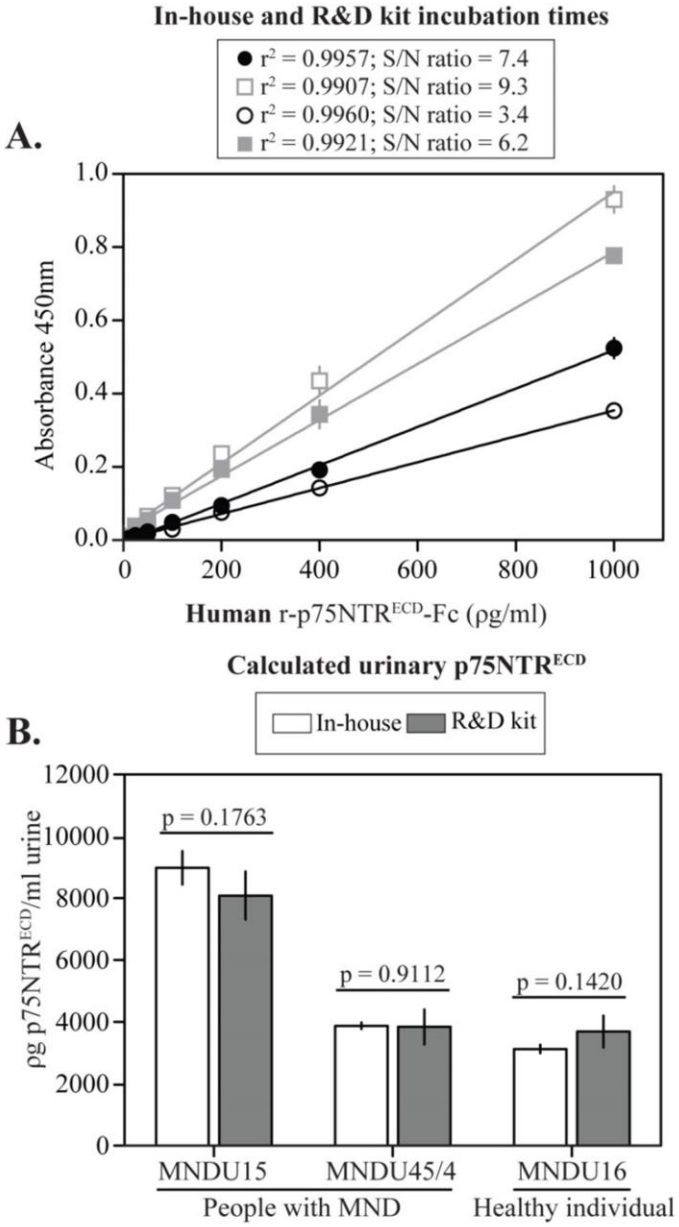

Figure 4.15: Comparison of the in-house p75NTR^{ECD} indirect sandwich ELISA to a commercial human p75NTR indirect sandwich ELISA kit

A. Indirect sandwich ELISAs were tested using the optimum incubation protocols for the in-house ELISA (in-house ●; R&D Systems □), or as recommended by the R&D systems kit (in-house ○; R&D Systems ■) (3 replicates per ELISA, 2 ELISAs). **B.** Neat human urine samples from people with MND and a healthy individual were diluted to 10% urine in sample buffer, and tested with the in-house p75NTR^{ECD} indirect sandwich ELISA (□) and the R&D Systems kit for human p75NTR (■), using in-house ELISA incubation times (4 replicates per ELISA, 2 ELISAs). Standard curves of human r-p75NTR^{ECD}-Fc are plotted as mean ± SEM with linear regression after removal of background readings. Signal to noise (S/N) ratios were calculated from the absorbance readings at 1000ρg/ml in relation to background, and error bars are shown when greater than the symbol. Calculated p75NTR^{ECD} levels are plotted in ng/ml of urine as mean ± SEM. Statistical significance determined using independent t-tests (Prism6).

4.7. Discussion

The aim of this chapter was to develop and optimise an ELISA for the quantification of p75NTR^{ECD}. In order to achieve this, an indirect sandwich ELISA configuration was chosen, as it allows for specific detection of p75NTR^{ECD} by using two different primary antibodies against two different p75NTR^{ECD} epitopes, and shows greater signal amplification over direct ELISAs by using a secondary HRP-conjugated antibody. Development and optimisation of the ELISA required empirical testing of different components in this setup including different antibody combinations and concentrations, and buffer recipes. The optimised p75NTR^{ECD} ELISA allows for the detection and quantification of mouse- and human-derived p75NTR^{ECD} using one setup.

As the aim of developing the ELISA was for quantification of p75NTR^{ECD} in urine, urine sample preparation was also optimised. Higher concentrations of urine from SOD1^{G93A} MND model mice and B6 healthy control mice showed interference with p75NTR^{ECD} estimations, as evident by a decrease in the recovery of spiked r-p75NTR^{ECD}-Fc, and lower estimates of p75NTR^{ECD}/ml. This interference may be due to the large volume of proteins in mouse urine, including the major urinary protein/α2u-globulin subfamily, which is important in scent communication, constitutes 99% of mouse urinary protein (Finlayson *et al.* 1963, Humphires *et al.* 1999) and is highly conserved across strains (Cheetham *et al.* 2009). In comparison, p75NTR^{ECD} estimates in urine from p75NTR Exon III knock-out mice were below zero for all urine concentrations tested. These p75NTR knock-out mice, developed by Lee and colleagues (1992) are produced by the targeted disruption of the third exon encoding the cysteine-rich repeats 2, 3, and 4 of p75NTR^{ECD}. Mice homozygous for this mutation are viable but lack p75NTR mRNA and the p75NTR^{ECD}. Thus, absorbance readings for p75NTR^{ECD} in urine samples from these mice are expected to be below background, and these results highlight the specificity of the ELISA.

In contrast to mouse urine, human urine did not show any interference with p75NTR^{ECD} estimations at higher concentrations, perhaps because human urine contains little protein, with under 100mg released per day (Adachi *et al.* 2006). These results highlight the fact that an ELISA needs to be optimised for the

particular sample source it will be used for, and suggests that the p75NTR^{ECD} ELISA setup would require further optimisation for use in biological samples containing a high abundance of proteins, such as blood or CSF.

ELISAs are used for a wide range of diagnostic tests and urinary analyses, and the p75NTR^{ECD} indirect sandwich ELISA is comparable to ELISAs used for these purposes. For example, in the p75NTR^{ECD} ELISA, urinary samples do not require treatment before analysis; only a small volume (180µl) of urine is required per test; the assay is specific (as shown by testing of urine from p75NTR Exon III knock-out mice); and, using the concentrations optimised here, recovery following spiking of a known amount of p75NTR^{ECD} standard is at or close to 100%. In addition, the p75NTR^{ECD} ELISA has an assay range of 10.0-0.01ng/ml with a reliable detection limit of 0.05ng/ml. These characteristics are comparable to other sandwich ELISA kits used in MND biomarker research, for example, an ELISA for human CSF-derived phosphorylated neurofilament H (pNfH) has an assay calibration range of 4.0-0.062ng/ml with a detection limit of .0235ng/ml (BioVendor Research and Diagnostic Products; Ganesalingam *et al.* 2011), and a serum-derived pNfH ELISA has an assay calibration range of 12.5-0.025ng/ml (EnCor Biotechnology Inc.; Boylan *et al.* 2009, Ganesalingam *et al.* 2011). The p75NTR^{ECD} ELISA is also similar to recently studied urine-based sandwich ELISA kits. For example, a matrix metalloproteinase 3 (MMP-3) ELISA has a calibration range of 10-0.156ng/ml and detection limit of 0.054ng/ml (Cusabio; El-Sharkawi *et al.* 2014), and an MMP-9 ELISA has an assay calibration range of 20-0.312ng/ml with a detection limit of 0.156ng/ml (R&D Systems; El-Sharkawi *et al.* 2014).

One limitation of this ELISA is the length of the protocol. The optimised incubation time for urinary samples for the p75NTR^{ECD} ELISA is 20 hours, resulting in an overall ELISA protocol of 42 hours, or ~23 hours from the addition of samples. In comparison, the above-mentioned CSF or serum-based pNfH, and urine-based MMP-3 or MMP-9 sandwich ELISAs are much shorter with sample incubation times of 1 or 2 hours.

The need for a p75NTR ELISA is shown by the fact that a kit (R&D Systems) became available during development of the in-house p75NTR^{ECD} ELISA. A direct comparison of the in-house and R&D Systems indirect sandwich ELISAs showed no significant differences in p75NTR estimations of human urine samples despite

the fact that the R&D Systems kit produced standard curves with greater S/N ratios, when using the longer incubation times of the in-house ELISA protocol. These greater S/N ratios may be explained by the use of the biotin-streptavidin complex in the R&D Systems ELISA kit, which has the advantage of multiple signalling peptides attached to each secondary conjugated antibody, allowing for more sensitivity. However, a significant advantage of the in-house developed ELISA is the ability to detect and quantify p75NTR^{ECD} from both mouse- and human-derived samples using the same setup.

A limitation of the optimised ELISA is the use of a polyclonal antibody for p75NTR^{ECD} detection. As Crowther (2001) explains, polyclonal antibodies are derived from the serum of an immunised animal, and the resulting immune response produces antibodies from different clones of B cells. As such, the immune response differs across different animals, so different batches of polyclonal antibodies may be heterogeneous and behave differently in experiments. This was encountered during p75NTR^{ECD} ELISA development, as seen between **Figure 4.6** and **Figure 4.7**, where only the batch of the polyclonal goat anti-mouse p75NTR^{ECD} antibody was changed, and the sensitivity of the ELISA decreased for human r-p75NTR^{ECD}-Fc and increased for mouse r-p75NTR^{ECD}-Fc. It is likely that future experiments using this ELISA, requiring a constant source of polyclonal antibody, will encounter the same situation, and so this needs to be taken into account.

In summary, the indirect sandwich ELISA developed and optimised in this chapter is the first reported ELISA for the detection of both mouse- and human-derived p75NTR^{ECD} using the one ELISA setup. The development of the p75NTR^{ECD} ELISA allows for p75NTR^{ECD} quantification in a large number of urine samples from the SOD1^{G93A} MND mouse model and people with MND, which enables sensitive, high-throughput testing of urinary p75NTR^{ECD} as a biomarker for MND.

Chapter 5. Urinary p75NTR^{ECD} as a biomarker of disease in SOD1^{G93A} mice

5.1. Introduction

Following the development of an indirect sandwich ELISA for high-throughput $p75NTR^{ECD}$ quantification, the next aim of this study was to test urinary $p75NTR^{ECD}$ as a biomarker in a pre-clinical MND model. To do this, the ELISA was used to quantify urinary $p75NTR^{ECD}$ levels in the high-copy number $SOD1^{G93A}$ mouse, the only pre-clinical MND model used in pharmaceutical trials. To determine the time course and usefulness of $p75NTR^{ECD}$ change, urinary $p75NTR^{ECD}$ levels in $SOD1^{G93A}$ mice needed to be quantified prior to disease onset and throughout disease progression, and compared to levels in healthy, age-matched C57BL/6J (B6) control mice.

The only way to test urinary $p75NTR^{ECD}$ as a disease progression biomarker in the $SOD1^{G93A}$ mouse is in comparison to survival and behavioural tests, as no objective biomarkers of disease progression exist (Weydt *et al.* 2003, Miana-Mena *et al.* 2005). In order to monitor disease progression throughout the life span of mice, non-invasive survival and behavioural tests were required. In pre-clinical trials, such tests include Kaplan-Meier survival analysis and behavioural tests including weight measurements, a neurological scoring test designed specifically for SOD1 mice (Leitner *et al.* 2010), the grip duration test, and the rotarod test (Klivenyi *et al.* 1999, Weydt *et al.* 2003, Miana-Mena *et al.* 2005).

In order to test urinary $p75NTR^{ECD}$ as a biomarker of treatment effectiveness, $SOD1^{G93A}$ mice needed to be given MND treatments. For this study, cohorts of mice were given one of two MND treatments; riluzole, or c29.

Riluzole (6-(trifluoromethoxy)benzothiazol-2-amine), the only FDA-approved treatment for MND, is a glutamate antagonist (Wokke 1996), which inhibits glutamate release (Cheramy *et al.* 1992). Riluzole has multiple modes of action depending on the concentration at which it is given, and can affect neuronal firing and membrane properties, specific ion channels, neurotransmission, protein kinases, two-pore domain potassium channels, and heat shock properties (see Bellingham 2011 for review). In the $SOD1^{G93A}$ pre-clinical MND mouse, riluzole treatment resulted in a modest increase in survival in small treatment groups (Gurney *et al.* 1996, Gurney *et al.* 1998, Waibel *et al.* 2004, Del Signore *et al.* 2009), but had no significant effect on survival when re-tested using rigorous criteria and more

animals (Scott *et al.* 2008). In people with MND, riluzole treatment results in an increased survival of 2-3 months (Miller *et al.* 2012). C29 is a potential MND treatment developed at the University of Queensland, which interacts with the TrkA cell receptor and facilitates increased nerve growth factor (NGF) binding, thus enhancing the response to NGF in superior cervical ganglia neurons and PC12 cells (Matusica *et al.* 2013). In motor neurons, c29 has a protective role, reducing motor neuron death in cell culture and the $SOD1^{G93A}$ mouse (Matusica *et al.* 2015, manuscript under preparation).

The aim of this chapter is to quantify urinary $p75NTR^{ECD}$ levels in untreated, riluzole-treated, and c29-treated $SOD1^{G93A}$ and B6 healthy control mice, and correlate these levels to disease progression, in order to test urinary $p75NTR^{ECD}$ as a biomarker of disease and treatment effectiveness in the pre-clinical $SOD1^{G93A}$ MND model mouse.

5.2. Quantification of urinary p75NTR^{ECD} levels in untreated SOD1^{G93A} mice

Using the p75NTR^{ECD} indirect sandwich ELISA and standardising urine dilution using urinary creatinine, urinary p75NTR^{ECD} was detected and quantified at all ages tested in SOD1^{G93A} mice.

In female SOD1^{G93A} mice (n=8-12), urinary p75NTR^{ECD} levels trended higher than B6 healthy females (n=2-9) throughout disease, and were significantly higher at 60 ($p<0.05$) and 120 days of age ($p<0.05$), and at end stage of disease ($p<0.01$) (**Figure 5.1.A**; two-way ANOVA, Bonferroni's post-hoc analysis, and for all future analyses unless otherwise stated). In male SOD1^{G93A} mice (n=4-7) urinary p75NTR^{ECD} levels were significantly higher at 40 ($p<0.05$), 60 ($p<0.01$), 100 ($p<0.001$), and 120 days of age ($p<0.001$), and end stage of disease ($p<0.0001$), as compared to male B6 healthy controls (n=7-10; **Figure 5.1.B**).

Overall, urinary p75NTR^{ECD} levels were significantly higher in untreated SOD1^{G93A} mice (n=13-21) than B6 healthy controls (n=11-16) throughout disease. This was seen from 40 days of age were levels were increased by 31.7ng p75NTR^{ECD}/mg creatinine, through to end stage of disease where levels were increased by 54.8ng/mg creatinine (40 days, $p<0.01$; 60 days, $p<0.001$; 80 days, $p<0.01$; 100 days, 120 days and end stage, $p<0.0001$; **Figure 5.1.C**).

Urine samples from p75NTR Exon III knock-out mice (Lee *et al.* 1992) were also tested for p75NTR^{ECD}, acting as negative controls. Across all ages, estimated urinary p75NTR^{ECD} levels in p75NTR Exon III knock-out mice (n=2; 0-5.2ng/mg creatinine), were significantly lower than B6 healthy controls (22.1-35.1ng/mg creatinine; 40 days–end stage, $p<0.0001$; n=11-16) and SOD1^{G93A} mice (60.3-87.9ng/mg creatinine; 40 and 120 days, $p<0.01$; 60-100 days, $p<0.05$; end stage, $p<0.001$; n=13-21, **Figure 5.1.C**).

As urine dilution was standardised using urinary creatinine, urinary creatinine levels were measured in SOD1^{G93A} and B6 healthy control mice throughout disease. Average urinary creatinine levels were significantly lower in SOD1^{G93A} mice than B6 healthy controls at 120 days of age ($p<0.01$), but did not correlate to disease progression (data not shown).

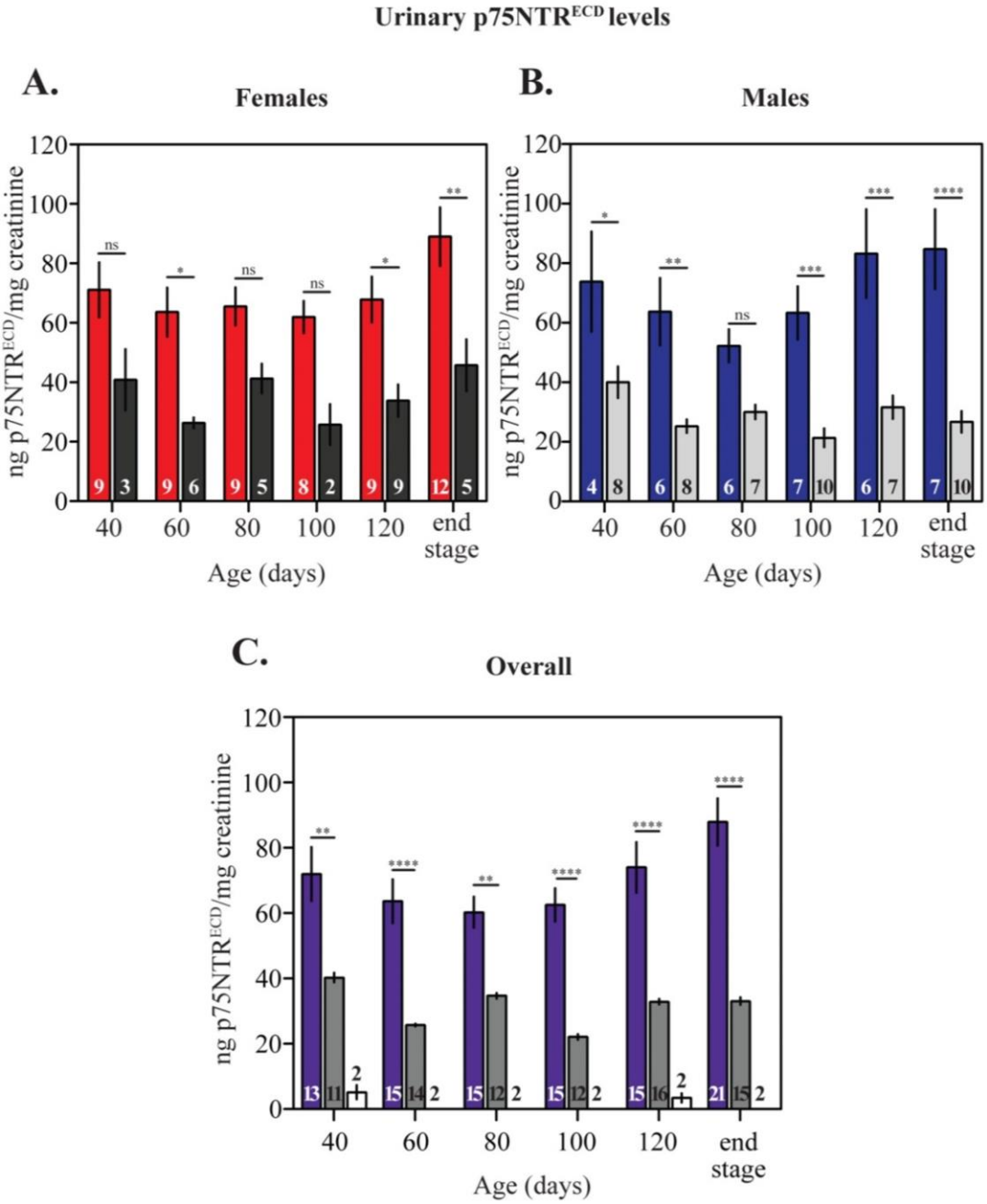

Figure 5.1: Urinary p75NTR^{ECD} levels in untreated SOD1^{G93A}, B6 healthy controls, and p75NTR Exon III knock-out mice

Urinary samples from SOD1^{G93A}, B6 healthy control, and p75NTR Exon III knock-out mice were tested using a p75NTR^{ECD} indirect sandwich ELISA. **A.** Urinary p75NTR^{ECD} levels in female SOD1^{G93A} mice (■, n=8-12), as compared to female B6 healthy controls (■, n=2-9). **B.** Urinary p75NTR^{ECD} levels in male SOD1^{G93A} mice (■, n=4-7), as compared to male B6 healthy controls (■, n=7-10), and **C.** the overall cohort of SOD1^{G93A} mice (■, n=13-21) as compared to B6 healthy controls (■, n=11-16) and p75NTR Exon III knock-out mice (□, n=2). Statistical significance determined using two-way ANOVAs with Bonferroni's post-hoc analyses (*p<0.05; **p<0.01; ***p<0.001; ****p<0.0001, Prism6). Ns: not significant.

5.3. Behavioural analysis of untreated SOD1^{G93A} mice

In order to monitor disease in SOD1^{G93A} mice, a combination of survival analysis and three behavioural tests, weight measurements, neurological scoring, and grip duration, were used. All of these non-invasive tests have been used previously in SOD1^{G93A} mice studies to monitor symptom onset, duration, and disease progression (Weydt *et al.* 2003, Miana-Mena *et al.* 2005, Leitner *et al.* 2010).

5.3.1. Survival analysis

The survival of untreated SOD1^{G93A} mice was analysed using Kaplan-Meier survival curves. On average, untreated female SOD1^{G93A} mice reached end stage at 157 days of age (151-165 days; n=17). In contrast, untreated male SOD1^{G93A} mice reached end stage of disease at 149.5 days of age (144-162 days; n=18), which was significantly earlier than their female counterparts (p=0.015, Log-rank test; **Figure 5.2.A**). Overall, untreated SOD1^{G93A} mice had a significantly shorter life span than B6 healthy controls (p<0.0001, Log-rank test). SOD1^{G93A} mice reached end stage of disease at 155 days of age (144-165 days; n=35), whereas B6 healthy controls remained alive and healthy until the end of experiments (n=20, 10 female, 10 male; **Figure 5.2.B**).

5.3.2. Weight

Mouse weight was recorded to track overall muscle degeneration. SOD1^{G93A} females were significantly lighter than SOD1^{G93A} males throughout life from 40 days of age until end stage (40 days, p<0.05; 60 days, p<0.01; 80-140 days, 20 day intervals, p<0.0001; end stage, p<0.001; two-way ANOVA, Bonferroni's post-hoc analysis, and for all future analyses unless otherwise stated).

On average, SOD1^{G93A} females were heaviest at 100 days of age (20.0g; n=17), then decreased in weight by 19%, by time of euthanasia. Male SOD1^{G93A} mice were also heaviest at 100 days of age (23.6g; n=18) and decreased in weight by 19% by the time of euthanasia (**Figure 5.2.C**). In comparison, B6 healthy control mice of

both genders increased in weight until euthanasia. On average, B6 females (n=10) measured a peak weight of 21.3g and were significantly lighter than B6 males (n=10; peak weight 26.2g) from 60 days of age (60 days, $p<0.05$; 80 and 100 days, $p<0.01$; 120 days-end stage $p<0.0001$).

Using weight measurements to track disease symptoms showed that female $SOD1^{G93A}$ mice were significantly lighter than healthy B6 females at 140 days of age ($p<0.0001$) and through to end stage of disease (150 days; $p< 0.0001$). A similar pattern was seen in males, with $SOD1^{G93A}$ males weighing significantly less than B6 male controls at 120 days of age ($p<0.05$), 140 days of age ($p<0.0001$) and end stage of disease ($p<0.0001$; **Figure 5.2.C**). **Figure 5.2.D** shows that, overall, $SOD1^{G93A}$ mice were significantly lighter than B6 healthy control mice from 120 days of age (120 days $p<0.05$; 140 days-end stage, $p<0.0001$).

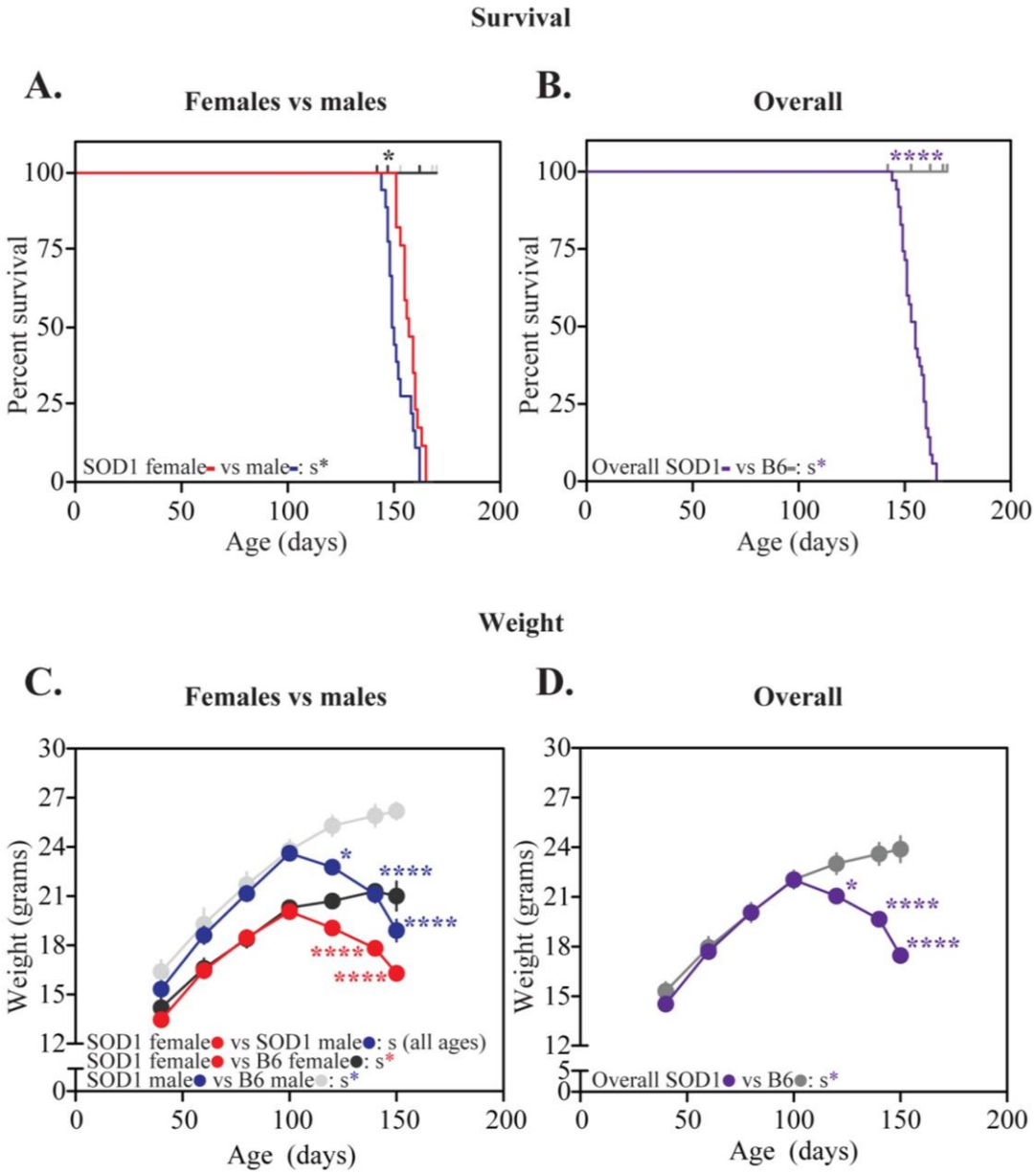

Figure 5.2: Survival and weight measurements in untreated SOD1^{G93A} and B6 healthy control mice

Kaplan-Meier survival curves of **A**. female (—, n=17) as compared to male (—, n=18) SOD1^{G93A} mice, or **B.** the overall cohort of SOD1^{G93A} mice (—, n=35) as compared to B6 healthy controls (female —, n=9; male —, n=11; overall —, n=20). Weight measurements of **C**. female (●) and male (●), or **D.** the overall cohort of SOD1^{G93A} mice (●) as compared to B6 healthy controls (female ●, male ●, overall ●). Statistical significance determined using log-rank tests for Kaplan-Meier survival curves and two-way ANOVAs with Bonferroni's post-hoc analyses for weight measurements (*p<0.05; ****p<0.0001, Prism6). S: significant.

5.3.3. Neurological scores

A neurological score test, specifically developed for SOD1 mice, allows for subjective but accurate detection of motor deficits by analysis of hind limb movement and overall walking capacity (see **2.7.2**; Leitner *et al.* 2010). Using this test, the first detectable symptoms of disease were seen from 125 days of age in $SOD1^{G93A}$ females and males, with no significant difference in disease progression between genders ($p=0.1029$, two-way ANOVA with Bonferroni's post-hoc analysis, and for all future analyses unless otherwise stated; **Figure 5.2.A**). Overall, untreated $SOD1^{G93A}$ mice showed significantly less movement capacity, and thus higher neurological scores, than healthy B6 controls from 135 days of age until end stage of disease (135 days, $p<0.001$; 140 days-165 days, 5 day intervals, $p<0.0001$; **Figure 5.2.B**).

5.3.4. Grip duration

First disease symptoms were detected in $SOD1^{G93A}$ mice by the grip duration test, which measures fore limb and hind limb strength by allowing mice to hang upside down from a cage lid (see **2.7.4**; Miana-Mena *et al.* 2005). A decrease in grip duration was first recorded at 120 days of age in $SOD1^{G93A}$ females, with significantly shorter hanging times than those seen in healthy B6 females from 130 days of age (130 days–160 days, 10 day intervals, $p<0.0001$). The same pattern of disease symptoms was seen in males (130 days–160 days, 10 day intervals, $p<0.0001$; **Figure 5.3.C**). Overall, the hanging time recorded in $SOD1^{G93A}$ mice was significantly shorter than healthy B6 controls from 120 days of age until end stage of disease (120 days-160 days, 10 day intervals, $p<0.0001$; **Figure 5.3.D**).

As summarised in **Figure 5.4**, urinary $p75NTR^{ECD}$ levels were significantly higher in untreated $SOD1^{G93A}$ mice than B6 healthy controls prior to detectable signs of disease using behavioural tests. Urinary $p75NTR^{ECD}$ levels were significantly increased from 40 days of age and through disease at all ages, to end stage. In comparison, the first signs of disease were detected at 120 days of age by significant weight decreases, and a shortening of grip duration times (significant at 130 days of age), followed by a decrease in neurological scores at 125 days of age (significant at 135 days of age).

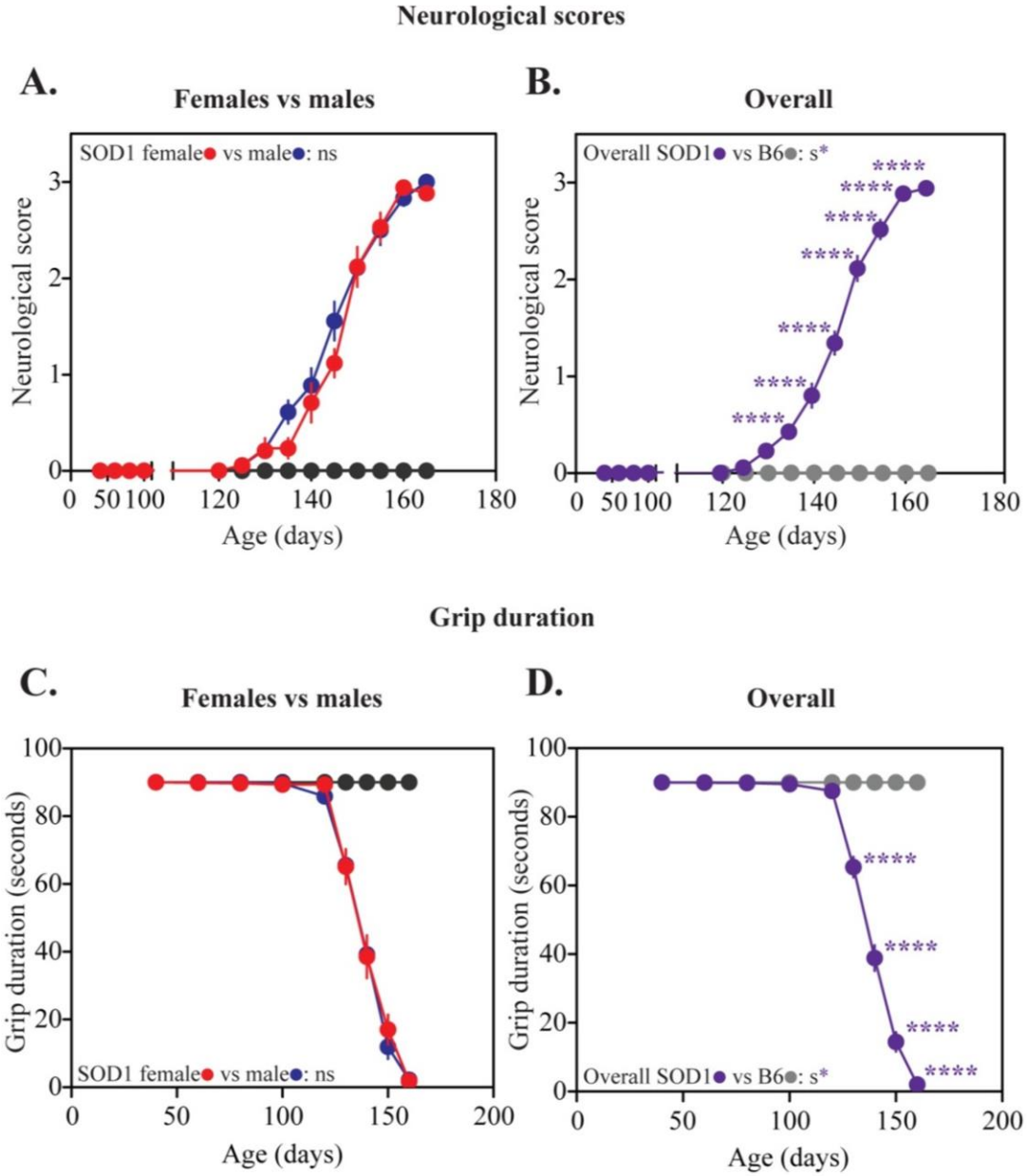

Figure 5.3: Neurological score and grip duration changes in untreated SOD1^{G93A} and B6 healthy control mice

Neurological scores of **A**. female (●, n=17) as compared to male (●, n=18) SOD1^{G93A} mice, or **B.** the overall cohort of SOD1^{G93A} mice (●, n=35) as compared to B6 healthy controls (female ●, n=9; male ●, n=11; overall ●, n=20). Grip duration measurements of **C**. female (●) as compared to male (●) SOD1^{G93A} mice, or **D.** the overall cohort of SOD1^{G93A} mice (●) compared to B6 healthy controls (female ●, male ●, overall ●). Statistical significance determined using two-way ANOVAs with Bonferroni's post-hoc analyses (****p<0.0001, Prism6). Ns: not significant, s: significant.

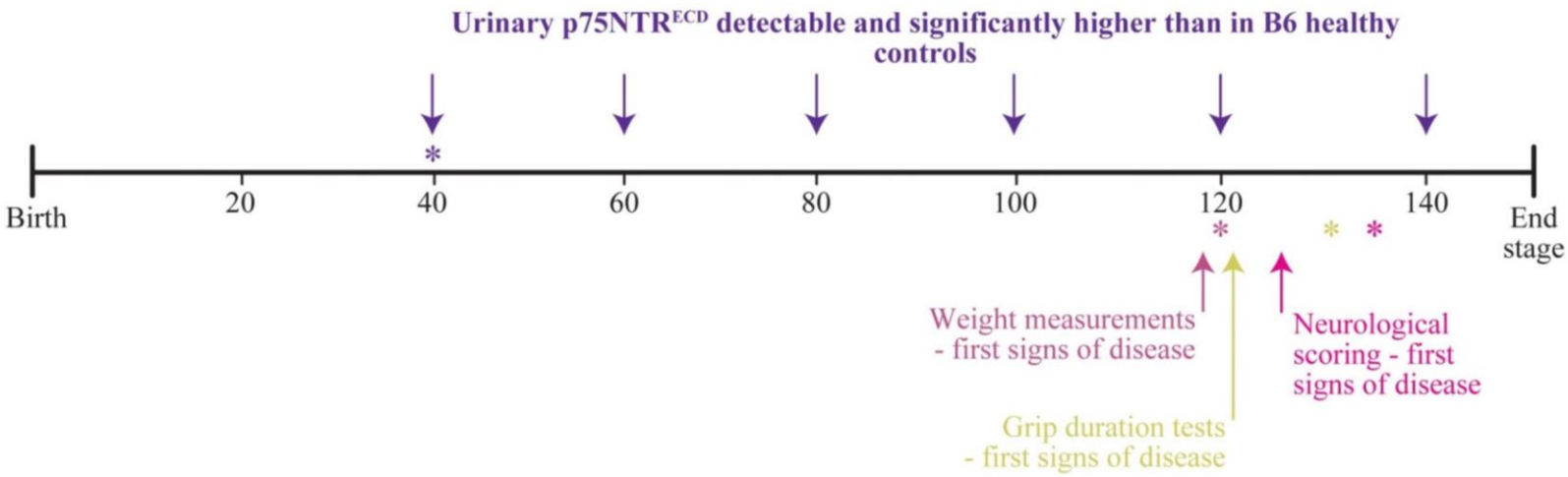

Figure 5.4: Timeline of urinary p75NTR^{ECD} levels and behavioural test analyses in untreated SOD1^{G93A} mice

Urinary p75NTR^{ECD} levels were significantly higher in SOD1^{G93A} mice (*) than B6 healthy controls pre-symptomatically from 40 days of age through to end stage of disease. In comparison, weight measurements showed the first signs of disease at 120 days of age and weight was significantly lower (*) in SOD1^{G93A} mice than B6 controls from 120 days through to end stage. Grip duration testing showed first signs of disease at 120 days of age and resulted in significant lower scores (*) in SOD1^{G93A} mice than B6 healthy controls at 130 days of age. Neurological scoring first showed signs of disease at 125 days of age, with significantly lower scores (*) in SOD1^{G93A} mice than B6 healthy controls recorded from 135 days of age.

5.4. Quantification of urinary p75NTR^{ECD} levels in response to treatments

The usefulness of urinary p75NTR^{ECD} as a biomarker of treatment effectiveness was analysed. To determine the response of urinary p75NTR^{ECD} to treatments, two MND treatments were given to separate cohorts of mice. The first cohort consisted of SOD1^{G93A} and B6 healthy control mice which were given riluzole, the only FDA-approved MND treatment, or vehicle control, via oral gavage at a dosage of 30mg/kg/day from 30 days of age until end stage of disease (neurological score of 3).

The second cohort consisted of SOD1^{G93A} mice were given c29, a 29 amino acid sequence of p75NTR juxtamembrane 'Chopper' domain (treatment administered and samples obtained by Associate Professor Lizzie Coulson and colleagues, University of Queensland) or a vehicle control. C29/vehicle treatment was via subcutaneous osmotic minipump, at a dosage of 5mg/kg/day from 9 weeks of age (~60 days) until end stage of disease (20% decrease in body weight).

Urinary p75NTR^{ECD} levels were then tested in both mice cohorts using the p75NTR^{ECD} indirect sandwich ELISA, and levels were compared to survival and behavioural tests of disease.

5.4.1. The effect of riluzole treatment on urinary p75NTR^{ECD} levels and disease

Urinary p75NTR^{ECD} levels in riluzole-treated female (**Figure 5.5.A**), male (**Figure 5.5.B**), or the overall cohort, of SOD1^{G93A} mice (**Figure 5.5.C**) were not significantly different from urinary p75NTR^{ECD} levels measured in untreated SOD1^{G93A} mice at all ages (two-way ANOVA, Bonferroni's post-hoc analyses, and for all future analyses unless otherwise stated). However, overall, there was a trend towards a decrease in urinary p75NTR^{ECD} levels in riluzole-treated SOD1^{G93A} mice at 40, 60, 100, and 120 days of age, and end stage of disease. Additionally, urinary p75NTR^{ECD} levels in B6 healthy controls were not significantly changed with a riluzole dosage of 30mg/kg/day. Riluzole treatment also had no effect on urinary

creatinine levels, with no significant differences seen between riluzole treated and untreated SOD1^{G93A} mice at all ages throughout disease (data not shown).

In line with the results of urinary p75NTR^{ECD} level analysis, riluzole treatment did not have a significant effect on SOD1^{G93A} mice survival compared to untreated SOD1^{G93A} animals. However, a trend towards an increase in survival was detected (females, p=0.476; males, p=0.095; overall p=0.179, Log-rank test; **Figure 5.6.A**, **B**, and **C**). Additionally, riluzole treatment did not result in significant changes in the other behavioural tests used. Weight loss in riluzole-treated SOD1^{G93A} females (**Figure 5.7.A**), males (**Figure 5.7.B**), or the overall cohort (**Figure 5.7.C**) was not significantly changed from untreated SOD1^{G93A} mice. The same patterns were observed in neurological scores (**Figure 5.8.A**, **B**, and **C**), and grip duration measurements (**Figure 5.9.A**, **B**, and **C**).

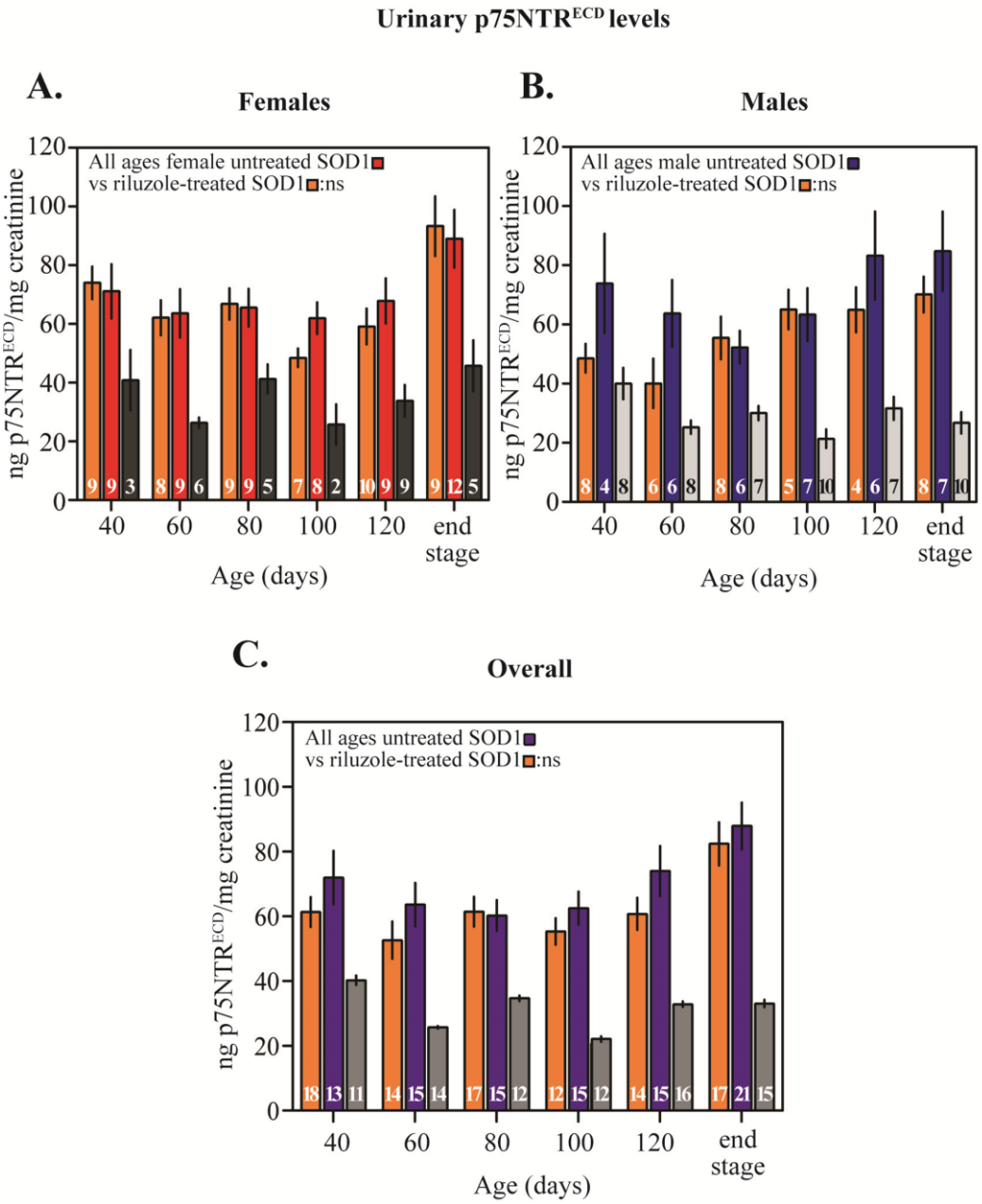

Figure 5.5: Urinary p75NTR^{ECD} levels of riluzole-treated and untreated SOD1^{G93A} and B6 healthy control mice

Urinary samples from untreated and riluzole-treated SOD1^{G93A} and B6 healthy control mice were tested using a p75NTR^{ECD} indirect sandwich ELISA. **A.** Urinary p75NTR^{ECD} levels in female riluzole-treated SOD1^{G93A} mice (■, n=8-10) as compared to female untreated SOD1^{G93A} mice (■, n=8-12) and B6 healthy controls (■, n=2-9), **B.** urinary p75NTR^{ECD} levels in male riluzole-treated SOD1^{G93A} mice (■, n=4-8) as compared to male SOD1^{G93A} mice (■, n=4-7) and B6 healthy controls (■, n=7-10), and **C.** the overall cohort of to riluzole-treated SOD1^{G93A} mice (■, n=12-18) as compared to untreated SOD1^{G93A} mice (■, n=13-21) and B6 healthy controls (■, n=11-16). Statistical significance determined using two-way ANOVAs with Bonferroni's post-hoc analyses, Prism6. Ns: not significant.

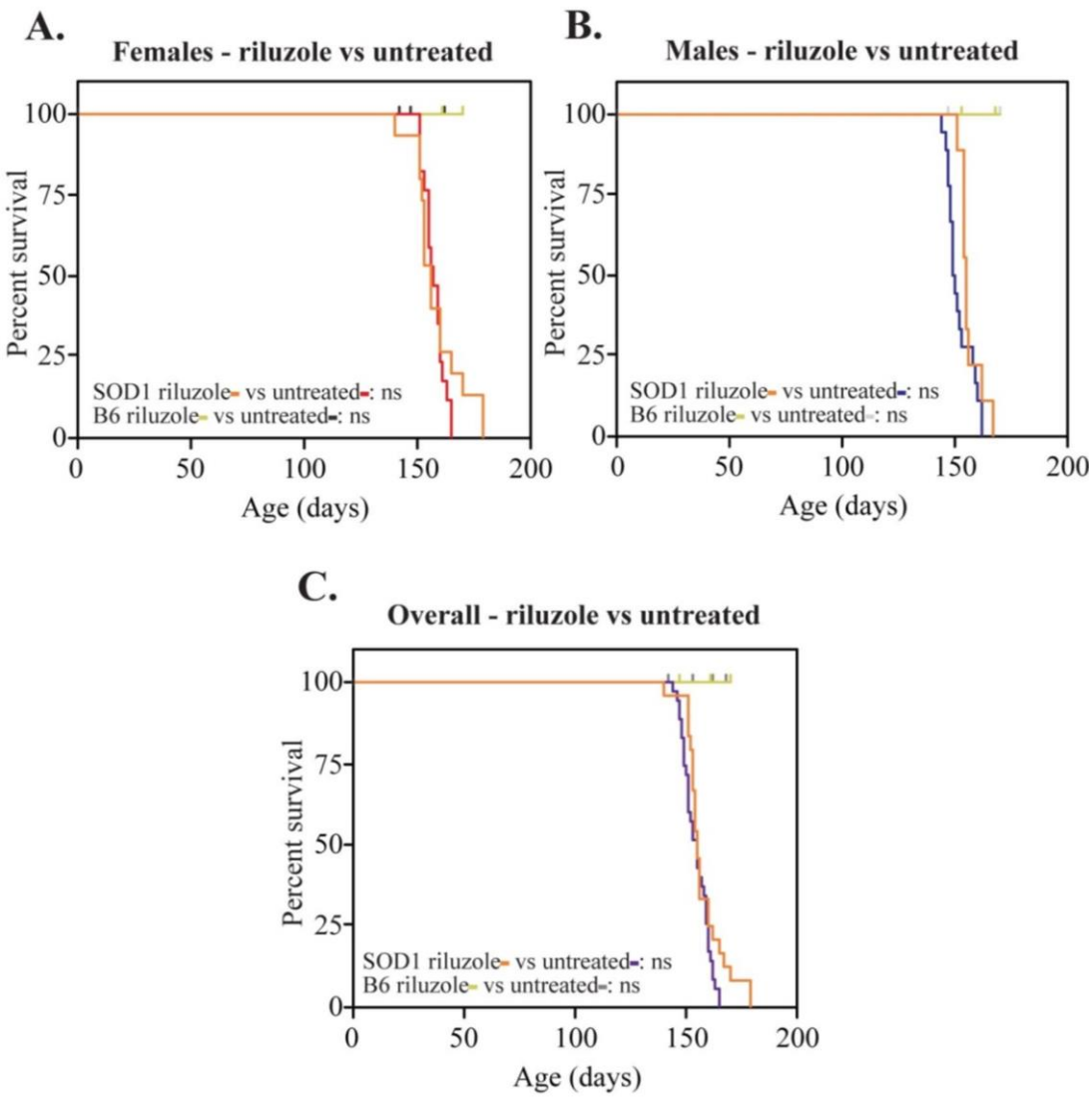

Figure 5.6: Survival of riluzole-treated and untreated SOD1^{G93A} and B6 healthy control mice

Kaplan-Meier survival curves of **A**. female riluzole-treated SOD1^{G93A} mice (, n=15) as compared to untreated SOD1^{G93A} females (, n=17), **B.** male riluzole-treated SOD1^{G93A} mice (, n=9) as compared to untreated SOD1^{G93A} males (, n=18), and **C**. the overall cohort of riluzole-treated SOD1^{G93A} mice (, n=24) as compared to overall cohort of untreated SOD1^{G93A} mice (, n=35) and B6 healthy controls (riluzole-treated female/male , n=10/gender; untreated female , n=9; untreated male , n=11; untreated overall , n=20). Statistical significance determined using Log-rank tests, Prism6. Ns: not significant.

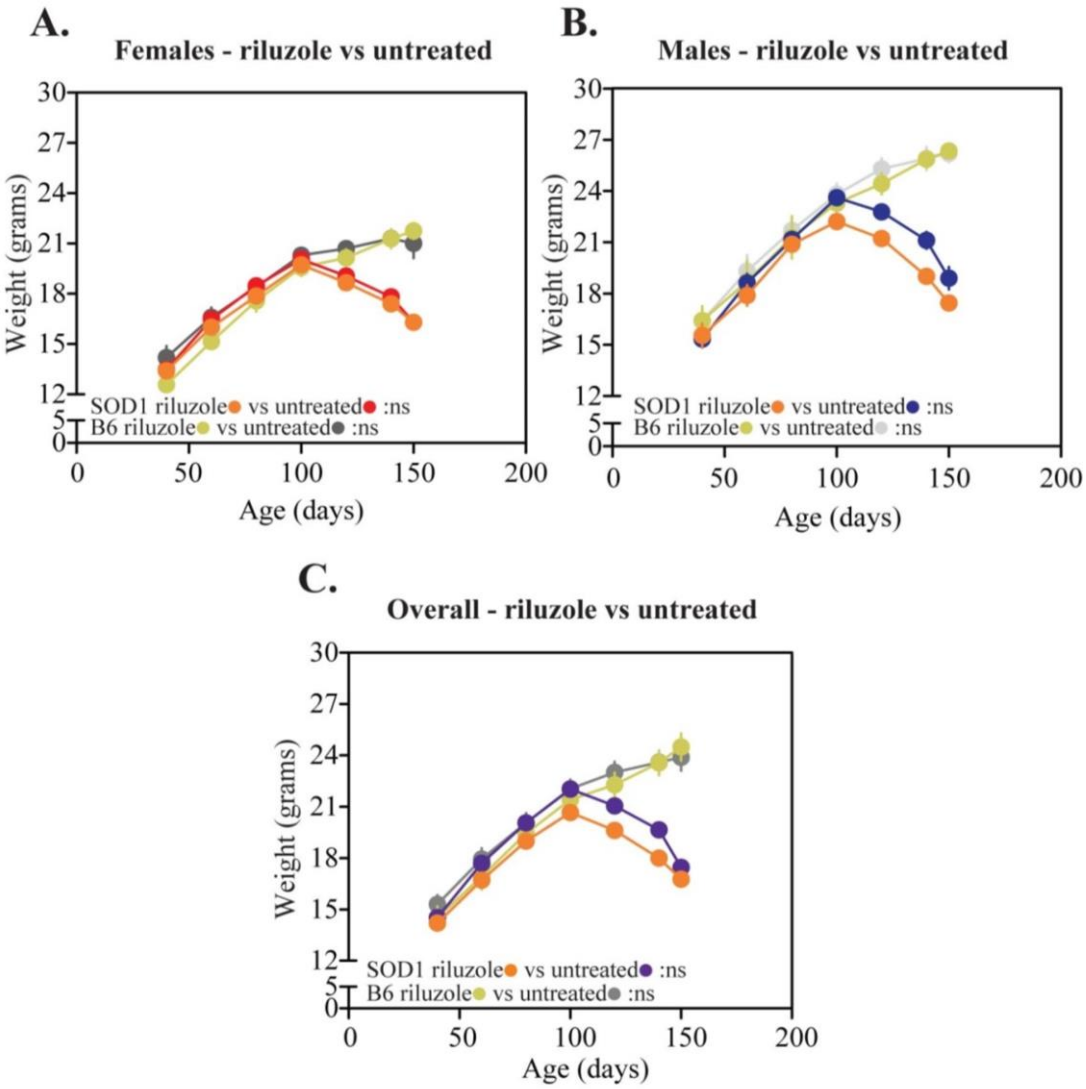

Figure 5.7: Weight of riluzole-treated and untreated SOD1^{G93A} and B6 healthy control mice

Weight measurements of **A**. female riluzole-treated SOD1^{G93A} mice (●, n=15) as compared to untreated SOD1^{G93A} females (●, n=17), **B.** male riluzole-treated SOD1^{G93A} mice (●, n=9) as compared to untreated SOD1^{G93A} males (●, n=18), and **C**. the overall cohort of riluzole-treated SOD1^{G93A} mice (●, n=24) as compared to overall cohort of untreated SOD1^{G93A} mice (●, n=35) and B6 healthy controls (riluzole-treated female/male ●, n=10/gender; untreated female ●, n=9; untreated male ●, n=11; untreated overall ●, n=20). Statistical significance determined using two-way ANOVAs with Bonferroni's post-hoc analyses, Prism6. Ns: not significant.

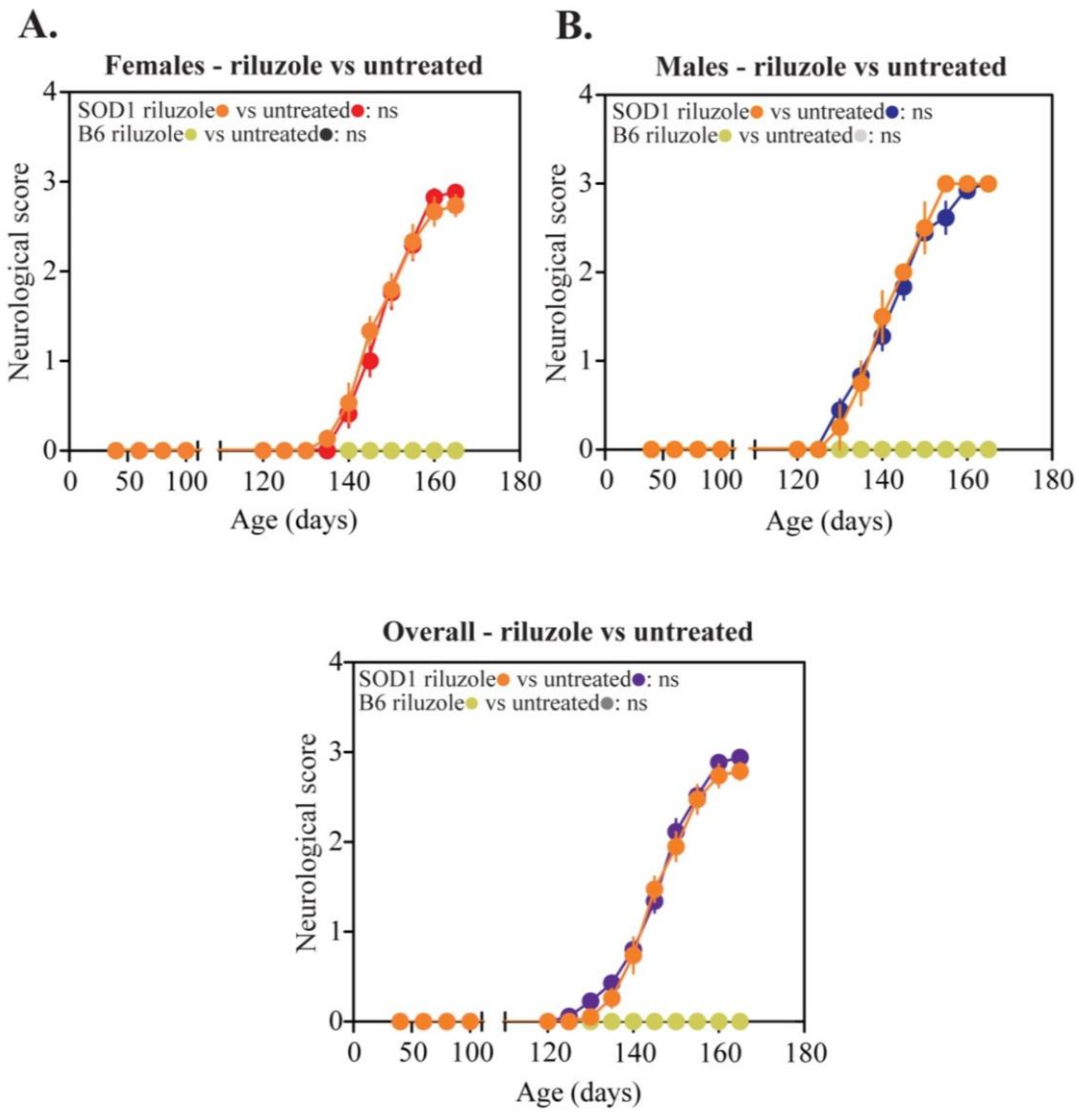

Figure 5.8: Neurological scores of riluzole-treated and untreated SOD1^{G93A} and B6 healthy control mice

Neurological scores of **A**. female riluzole-treated SOD1^{G93A} mice (●, n=15) as compared to untreated SOD1^{G93A} females (●, n=18), **B.** male riluzole-treated SOD1^{G93A} mice (●, n=9) as compared to untreated SOD1^{G93A} males (●, n=18), and **C**. the overall cohort of riluzole-treated SOD1^{G93A} mice (●, n=24) as compared to overall cohort of untreated SOD1^{G93A} mice (●, n=35) and B6 healthy controls (riluzole-treated female/male ●, n=10/gender; untreated female ●, n=9; untreated male ●, n=11; untreated overall ●, n=20). Statistical significance determined using two-way ANOVAs with Bonferroni's post-hoc analyses, Prism6. Ns: not significant.

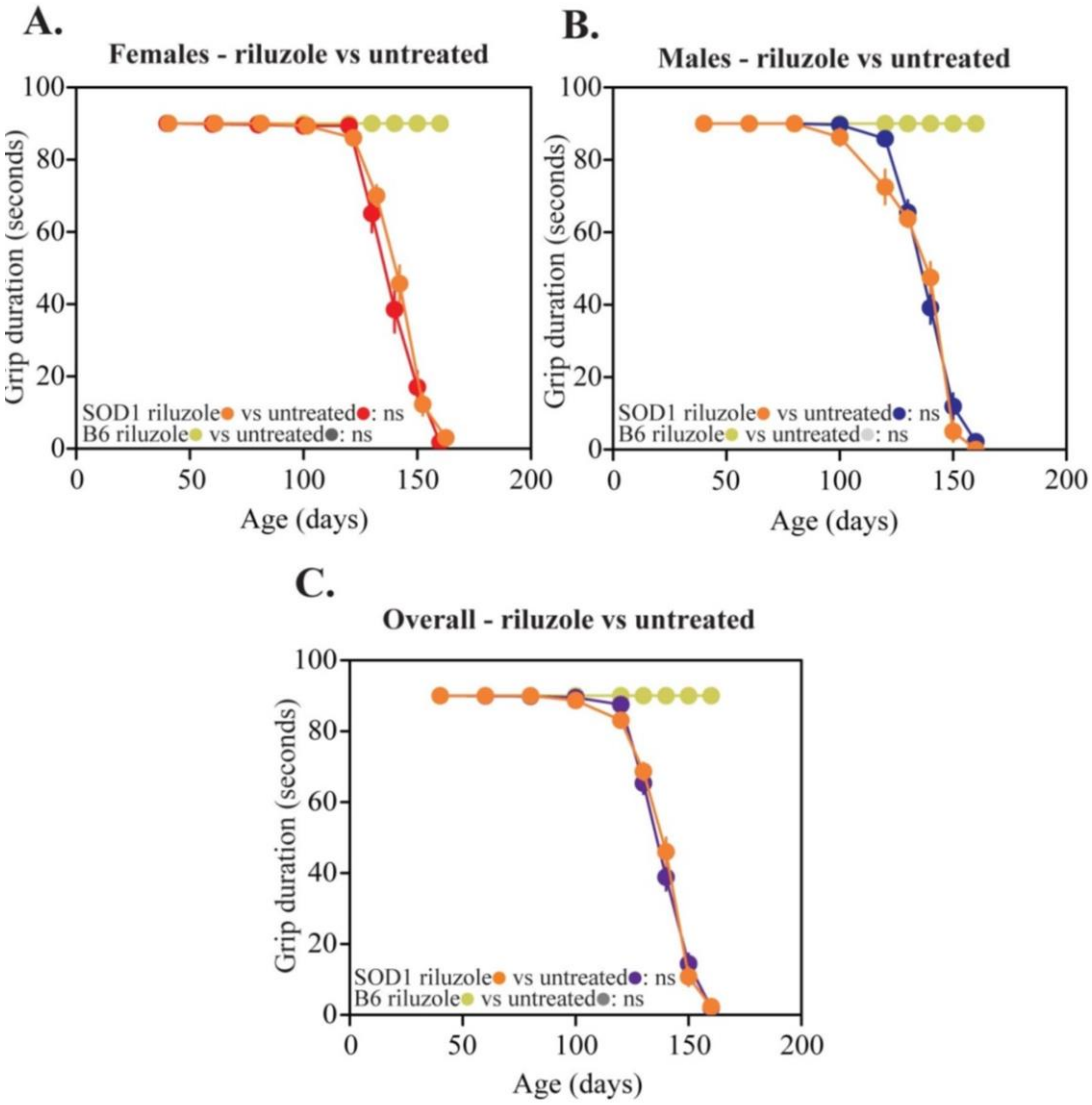

Figure 5.9: Grip duration of riluzole-treated and untreated SOD1^{G93A} and B6 healthy control mice

Grip duration measurements of **A**. female riluzole-treated SOD1^{G93A} mice (●, n=15) as compared to untreated SOD1^{G93A} females (●, n=18), **B.** male riluzole-treated SOD1^{G93A} mice (●, n=9) as compared to untreated SOD1^{G93A} males (●, n=18), and **C**. the overall cohort of riluzole-treated SOD1^{G93A} mice (●, n=24) as compared to overall cohort of untreated SOD1^{G93A} mice (●, n=35) and B6 healthy controls (riluzole-treated female/male ●, n=10/gender; untreated female ●, n=9; untreated male ●, n=11; untreated overall ●, n=20). Statistical significance determined using two-way ANOVAs with Bonferroni's post-hoc analyses, Prism6. Ns: not significant.

5.4.2. The effect of c29 treatment on urinary p75NTR^{ECD} levels and disease

Urinary p75NTR^{ECD} levels in SOD1^{G93A} mice treated with a 29 amino acid peptide from the p75NTR juxtamembrane 'Chopper' domain, called c29, were significantly lower than levels seen in untreated SOD1^{G93A} mice from first measurement at 80 days of age, through until 125 days of age (**Figure 5.10**; two-way ANOVA, Bonferroni's post-hoc analyses, and for all future analyses unless otherwise stated). As urinary dilution was standardised using urinary creatinine, urinary creatinine levels were also measured. No significant differences were seen in urinary creatinine levels between untreated and c29-treated SOD1^{G93A} mice at any age (data not shown).

Treatment with c29 resulted in a significant improvement in disease symptoms at 112 and 119 days of age as compared to untreated SOD1^{G93A} mice (non-linear regression (curve fit) function, Prism6), the same time frame over which urinary p75NTR^{ECD} levels were significantly decreased. Performance during the rotarod test was maintained at 112 and 119 days of age, with an average increased rotarod time of 46 and 52 seconds in c29-treated SOD1^{G93A} mice, as compared to untreated SOD1^{G93A} mice who continued to decline in performance over this period (**Figure 5.11.A**). However, c29-treatment showed no significant changes to lifespan, with the average life expectancy of untreated and c29-treated SOD1^{G93A} mice differing by 2 days (162.5 days and 164.5 days; p=0.395, Log-rank test; **Figure 5.11.B**). Additionally, weight measurements were not significantly different between untreated and c29-treated SOD1^{G93A} mice (p=0.3206, **Figure 5.11.C**).

Figure 5.12 summarises the effect of the two MND treatments on urinary p75NTR^{ECD} levels and behavioural tests in SOD1^{G93A} mice. Riluzole treatment had no significant effect on urinary p75NTR^{ECD} levels or disease onset, duration, or severity, in comparison to untreated SOD1^{G93A} mice. In comparison, c29 treatment of SOD1^{G93A} mice resulted in significantly decreased levels of urinary p75NTR^{ECD} between 80 and 125 days of age, and significantly improved rotarod performance as compared to untreated SOD1^{G93A} mice over the same period at 112 and 119 days of age.

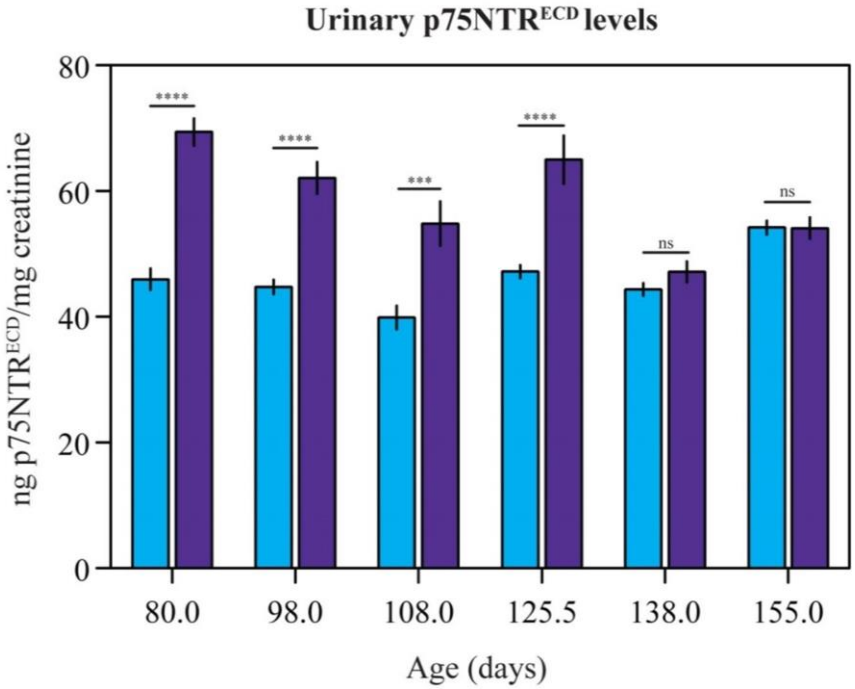

Figure 5.10: Urinary p75NTR^{ECD} levels in c29-treated and untreated SOD1^{G93A} mice

Urinary samples from c29-treated (■, n=8) and untreated (■, n=8) SOD1^{G93A} mice were tested using a p75NTR^{ECD} indirect sandwich ELISA (8 replicates per ELISA, 2 ELISAs per sample). Statistical significance determined using two-way ANOVAs with Bonferroni's post-hoc analysis, Prism6 (***p<0.001; ****p<0.0001). Ns: not significant.

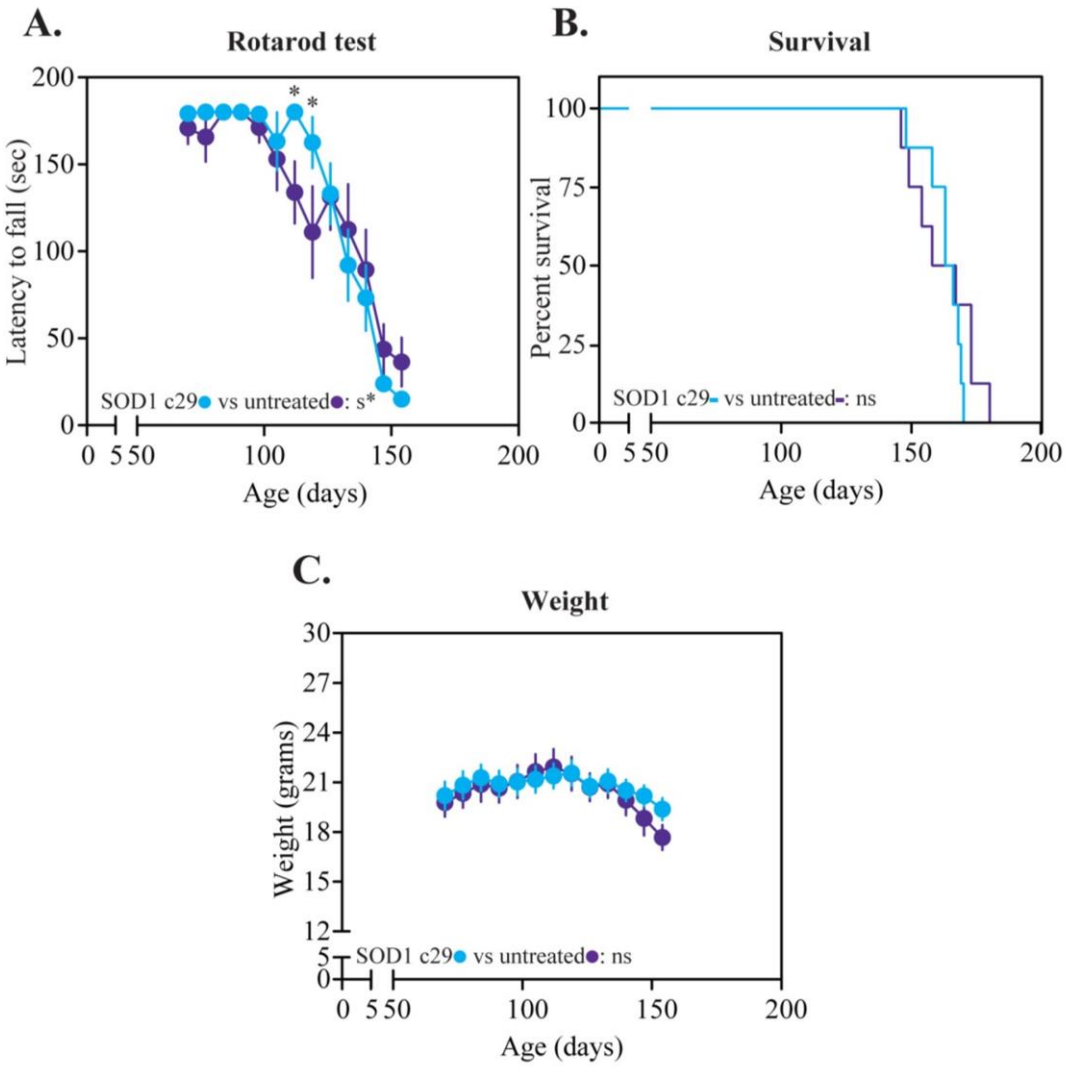

Figure 5.11: Behavioural analysis of c29-treated and untreated SOD1^{G93A} mice

A cohort of SOD1^{G93A} mice was treated with a potential MND treatment, c29 (–/●, n=8) and compared to an untreated SOD1^{G93A} cohort (–/●, n=8), using **A.** rotarod performance, **B.** Kaplan-Meier curves, and **C.** weight measurements. Statistical significance determined using Log-rank tests for Kaplan-Meier survival curves, two-way ANOVA with Bonferroni's post-hoc analysis for weight measurements, and non-linear (curve fit) function for rotarod measurements, Prism6 (*$p<0.05$). Ns: not significant, s: significant.

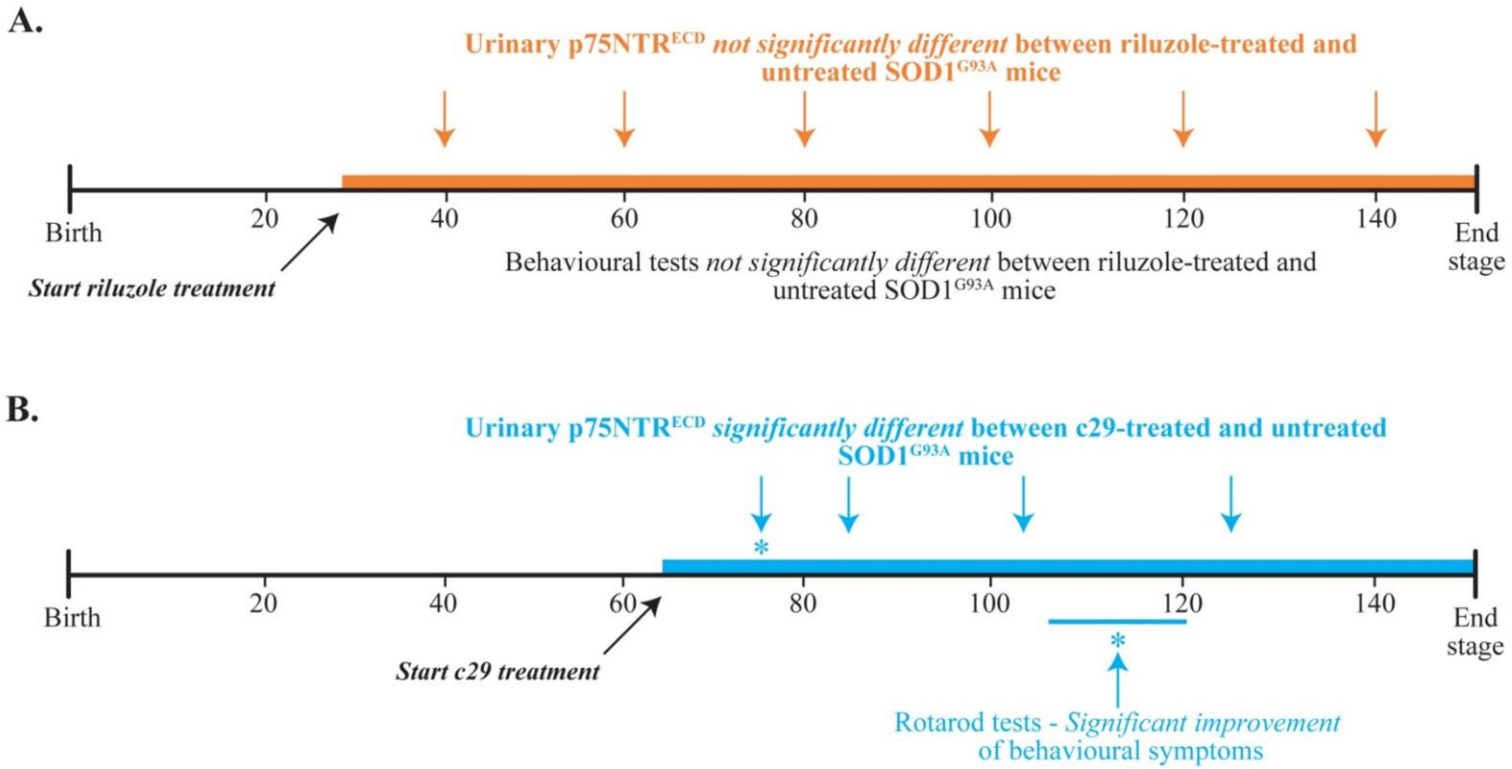

Figure 5.12: Timeline of urinary p75NTR^{ECD} levels and behavioural test analyses in riluzole-treated and c29-treated SOD1^{G93A} mice

Urinary p75NTR^{ECD} levels were compared to behavioural tests of disease in response to treatments. **A.** Urinary p75NTR^{ECD} levels were not significantly different between riluzole-treated and untreated SOD1^{G93A} mice. Similarly, behavioural tests did not show differences in disease onset, severity, or duration between riluzole-treated and untreated SOD1^{G93A} mice. **B.** Urinary p75NTR^{ECD} levels were significantly lower (*) in c29-treated than untreated SOD1^{G93A} mice at 75, 85, 102 and 125 days of age. Similarly, latency to fall during rotarod testing was significantly longer in c29-treated SOD1^{G93A} mice than untreated SOD1^{G93A} mice between 105 and 120 days of age.

5.5. Discussion

The aim of this chapter was to test urinary p75NTR^{ECD} as a biomarker in pre-clinical MND. To do this, urinary p75NTR^{ECD} levels were tested in the well-characterised pre-clinical MND model, the SOD1^{G93A} mouse, using the p75NTR^{ECD} indirect sandwich ELISA. First, urinary p75NTR^{ECD} levels were measured and compared to survival and behavioural tests to determine if urinary p75NTR^{ECD} levels are a biomarker of disease progression. Second, urinary p75NTR^{ECD} levels were measured in mice given one of two different MND treatments, riluzole, or c29, to test urinary p75NTR^{ECD} levels as a biomarker of treatment effectiveness.

Using IP/WB, p75NTR^{ECD} was first detected in the urine of SOD1^{G93A} mice pre-symptomatically from 60 days of age and was continuously detected throughout disease progression (see **Figure 3.3**). In comparison, quantitative measurement of urinary p75NTR^{ECD} in a larger number of SOD1^{G93A} mice using the p75NTR^{ECD} indirect sandwich ELISA, and standardising urine dilution using urinary creatinine, showed significantly higher levels of urinary p75NTR^{ECD} in SOD1^{G93A} mice at every age tested, from 40 days of age. Significantly higher urinary p75NTR^{ECD} levels were detected both prior to the detection of symptoms using behavioural tests, and after symptom onset, throughout disease progression. It is important to note that urinary creatinine, used to standardise urine dilution, did not change throughout disease. As such, it is valid to use urinary creatinine to standardise for urine dilution (Arndt 2009).

The SOD1^{G93A} model used in this study has a C57BL/6J background (Jackson laboratory Cat. # 004435, B6.Cg-Tg(SOD1*G93A)1Gur/J), which has a longer average survival than mice bred on a mixed C57BL/6J*B6SJL background (Heiman-Patterson *et al.* 2005). The detection of a significant increase in urinary p75NTR^{ECD} levels at 40 days of age, approximately 100 days before end stage of disease, is earlier than the first signs of underlying degeneration detected by other studies in SOD1^{G93A} mice with a C57BL/6J background, and the shorter-surviving mixed C57BL/6J*B6SJL background.

One biological biomarker study found significant pre-symptomatic changes in the serum amino acid profiles in SOD1^{G93A} mice at two ages measured, 50 and 70 days. In these mixed background SOD1^{G93A} mice, the changes were detectable a

maximum of 20 days prior to symptom onset and 80 days prior to end stage, with three amino acids, asparate, cysteine and phosphoenthanolamine, consistently different at both ages compared to wild type mice (Bame *et al.* 2014). However, longitudinal analysis following the onset of symptoms was not performed.

Other 'non-invasive' studies have found pre-symptomatic changes that persist throughout disease progression. In mixed C57BL/6J*B6SJL background $SOD1^{G93A}$ mice, Evans and colleagues (2014) used T_2 weighted-MRI and found changes in brainstem nuclei from 60 days of age, approximately 10-30 days before symptom onset and 70 days before end stage, which increased with disease. Using electrical impedance myography 50Hz phase (EIM), Li and colleagues (2013) showed that significant signs of muscle decline were also detectable ~10-30 days before symptom onset and 70 days prior to end stage, and continued to decline throughout disease progression. In C57BL/6J background $SOD1^{G93A}$ mice, Hayworth and Gonzalez-Lima (2009), found motor performance deficits in free roaming mice from 45 days of age, muscle girth measurement in three hind limb muscles was an accurate predictor of genotype at approximately 55 days of age, and that both of these parameters persisted with disease progression.

The use of urinary $p75NTR^{ECD}$ levels as a biomarker in $SOD1^{G93A}$ mice has significant advantages over other candidates studied. Although first detectable around the same time period as motor performance deficits (Hayworth & Gonzalez-Lima 2009), urinary $p75NTR^{ECD}$ measurements are objective, and urine sample collection is less invasive than muscle girth, EIM and T_2-weighted MRI measurements; although these techniques are termed 'non-invasive', all require anaesthesia.

After the massive increase in urinary $p75NTR^{ECD}$, there was no further rise across disease progression in $SOD1^{G93A}$ mice. However, this does not mean that urinary $p75NTR^{ECD}$ levels do not increase with disease progression. In this respect, one limitation of the high-copy $SOD1^{G93A}$ mouse is the rapid disease onset, progression, and short pre-symptomatic period. It is possible that urinary $p75NTR^{ECD}$ levels increase with disease progression earlier in disease than was examined in this study, but that such changes are masked by the rapid disease progression in the high-copy $SOD1^{G93A}$ model; testing this would require urinary $p75NTR^{ECD}$ level measurement very early in this model, and/or tracking in the low-copy $SOD1^{G93Adl}$ mouse.

A number of tests were used to monitor disease progression in untreated and treated SOD1^{G93A} and healthy B6 control mice. The use of a number of parameters allowed for accurate detection of changes due to disease progression and ruled out any events not related to MND. The average survival, weight changes, and behavioural test results from this cohort of SOD1^{G93A} mice are comparable to the disease progression changes seen in other cohorts of the SOD1^{G93A} mouse model with a C57BL/6J background (Heiman-Patterson *et al.* 2005). However, some differences were observed between the two cohorts of SOD1^{G93A} mice tested in this study. For example, the average life expectancy in the University of Queensland-based SOD1^{G93A} mice cohort was 8 days longer than that seen in the Flinders University-based SOD1^{G93A} mice cohort regardless of whether or not mice were administered treatments. Such differences could be due to cohort sizes, the University of Queensland-based cohort consisted of eight untreated, and eight c29-treated SOD1^{G93A} mice as compared to the Flinders University-based cohort, which consisted of 35 untreated and 24 riluzole-treated SOD1^{G93A} mice; or copy numbers of the mutant *SOD1* gene.

This study found that riluzole treatment does not have an effect on disease onset, progression, or survival at a dosage of 30mg/kg/day. These results are in line with previous studies in the SOD1^{G93A} mouse which used lower (8mg/kg/day, Li *et al.* 2013) or higher (~22 or 44mg/kg/day, Scott *et al.* 2008) riluzole doses. However, urinary p75NTR^{ECD} levels trended lower in riluzole-treated SOD1^{G93A} mice at different ages throughout disease, suggesting a beneficial effect of riluzole on the underlying pathology of MND, which does not result in improved behavioural outcomes. These results suggest that urinary p75NTR^{ECD} levels may be sensitive to a subclinical effect of riluzole treatment.

In contrast, this study found that c29-treatment shows a significant decrease in urinary p75NTR^{ECD} between 80 and 125 days of age in SOD1^{G93A} mice, correlating to a significant improvement in rotarod performance in c29-treated SOD1^{G93A} mice over the same period (112-119 days of age). These results suggest that urinary p75NTR^{ECD} levels are sensitive to the effect of c29 treatment. This is plausible as c29 is a 29 amino acid peptide of the juxtamembrane 'Chopper' domain of p75NTR^{ICD}. Previous studies have found that c29 treatment enhances the response of the TrkA receptor to NGF in superior cervical ganglia neurons and PC12 cells

(Matusica *et al.* 2013) and increases motor neuron survival *in vitro* in the presence of BDNF, and *in vivo* (Matusica *et al.* 2015, manuscript under preparation). This beneficial effect may be due to c29-mediated enhancement of ligand-binding to Trk receptors, changing the balance from p75NTR apoptotic signalling, to Trk receptor survival signalling (Matusica *et al.* 2015, manuscript under preparation). However, the use of c29 as a treatment for MND in the $SOD1^{G93A}$ mouse requires further study.

Typically, potential treatments and potential biomarkers are tested separately in pre-clinical models of MND and their usefulness is determined by comparison to survival, and subjective behavioural analyses. In contrast, this study tested urinary $p75NTR^{ECD}$, a potential biomarker, simultaneously with riluzole, the only FDA-approved treatment for MND, and c29, a potential MND treatment. Bame and colleagues (Bame *et al.* 2014) also recently used this approach, testing the changes in the serum amino acid profile of $SOD1^{G93A}$ mice to treatment with methionine sulfoximine (MSO). As seen with c29 treatment and behavioural analysis in this study, MSO improved behavioural symptoms and changed the serum amino acid profiles of $SOD1^{G93A}$ towards levels seen in WT mice (Bame *et al.* 2014). As such, the method of using potential treatments, or other drugs, to test candidate biological biomarkers is a promising way forward.

In summary, this chapter details the testing of urinary $p75NTR^{ECD}$ as a biomarker in a pre-clinical model of MND, the $SOD1^{G93A}$ mouse, for the first time. Importantly, significantly higher urinary $p75NTR^{ECD}$ levels were detected pre-symptomatically in $SOD1^{G93A}$ mice as compared to B6 healthy controls and continued at significantly higher levels throughout disease progression. Additionally, as shown by measurements in response to the MND treatments riluzole and c29, urinary $p75NTR^{ECD}$ levels may be useful as a biomarker of treatment effectiveness in the $SOD1^{G93A}$ mouse.

Chapter 6. Urinary p75NTR^{ECD} as a biomarker in people with MND

6.1. Introduction

Following the study of urinary p75NTR^{ECD} levels in the pre-clinical SOD1^{G93A} model of MND, the next aim was to test urinary p75NTR^{ECD} as a biomarker in human disease. To do this, urinary p75NTR^{ECD} levels were quantified in a large cohort of people with MND using the p75NTR^{ECD} indirect sandwich ELISA.

The aim of testing urine from a large cohort of people with MND is two-fold. First, to determine if urinary p75NTR^{ECD} levels can be used to distinguish people with MND from people who do not have MND, in which case, levels need to be measured in comparison to healthy individuals, and in comparison to people with other neurological conditions. Second, to determine if urinary p75NTR^{ECD} levels are indicative of disease progression and prognosis in people with MND, in which case, levels need to be measured within individuals longitudinally, and compared to currently available measures of disease progression.

Current biomarker candidates for MND include genetic, neurophysiological, neuroimaging, and tissue/fluid sources. However, none of these candidates are routinely used in the clinic (see Turner *et al.* 2009, Bowser *et al.* 2011 for reviews), and no objective disease progression biomarkers exist. One of the most promising biological biomarkers, cerebrospinal fluid (CSF)-derived phosphorylated neurofilament heavy chain (pNfH), distinguishes between people with MND and healthy individuals alone (Brettschneider *et al.* 2006) and in combination with complement C3 (Ganesalingam *et al.* 2011), and has been linked to prognosis (Brettschneider *et al.* 2006, Levine *et al.* 2012). In addition, serum pNfH levels also show promise as a diagnostic and prognostic biomarker (Boylan *et al.* 2009, Boylan *et al.* 2013). However, although CSF pNfH was suggested as a progression biomarker (Brettschneider *et al.* 2006), this has not been confirmed, and pNfH levels in the serum are also not useful in disease progression (Lu *et al.* 2015).

The only disease progression measure that has been tested for validity and reliability is the subjective questionnaire-based Amyotrophic Lateral Sclerosis Functional Rating Scale-revised (ALSFRS-r) (Kaufmann *et al.* 2005, Kaufmann *et al.* 2007). Using 12 multiple choice questions, the ALSFRS-r scale measures physical function in carrying out every-day activities such as eating, walking and sleeping (full ALSFRS-r scale in **Appendix A**) (Cedarbaum *et al.* 1999, Kaufmann

et al. 2005, Kaufmann *et al.* 2007, Kollewe *et al.* 2008). Thus, the ALSFRS-r was used to monitor disease progression longitudinally in people with MND in this study, and time from symptom onset, and time from diagnosis, were used as additional measures of disease progression.

This chapter focuses on the measurement of urinary p75NTR^{ECD} in people diagnosed with MND, pre-symptomatic people carrying mutant *SOD1* mutations who will develop MND symptoms, healthy individuals, and people with other neurological diseases. The comparison of urinary p75NTR^{ECD} levels to clinical characteristics in these groups will determine the usefulness of p75NTR^{ECD} in discriminating MND from healthy individuals and other conditions, and its value as a prognostic and disease progression biomarker of MND.

6.2. Urinary p75NTR^{ECD} levels in MND and healthy individuals

6.2.1. Clinical characteristics of people with MND and healthy individuals

Forty-one people with MND were recruited in Adelaide through the MND clinic at the Repatriation General Hospital, Daw Park and the neurological wards of Flinders Medical Centre, consisting of 15 women (36.6%) and 26 men (63.4%) (**Table 6.1**). As outlined in **Figure 6.1**, 23 participants provided multiple urine samples throughout the study.

Twenty-seven people with MND presented with limb onset, and 14 presented with bulbar onset disease. The majority of participants, 92.6%, had sporadic disease, and the average age of symptom onset in the whole cohort was 67.5 years. Time from symptom onset to MND diagnosis varied between 0 and 41 months, with a mean of 11.5 months. Additionally, 16 people with MND passed away during the study, with disease length from symptom onset an average of 27.6 months (range 13.3-50.8 months).

Twenty-four people carrying known *SOD1* genetic mutations, who did not show symptoms of disease at the time of first sample collection (pre-symptomatic at baseline), were recruited through the *pre-fALS* study by Dr. Michael Benatar and Joanne Wuu at the Miller School of Medicine, University of Miami, Florida. This cohort of people, termed pre-familial MND (pre-fMND), consisted of 21 females and three males, with an average age of 49 years (22-67) at baseline. Throughout the study, 3 females phenoconverted, showing first signs of MND symptoms at 44, 17, and 22 months after baseline (aged 45, 45, and 46 respectively).

Twelve healthy individuals were recruited in Adelaide through the MND clinic at the Repatriation General Hospital, the neurological ward of Flinders Medical Centre and the School of Medicine, Flinders University. Additionally, 11 healthy individuals were recruited in Miami through the *pre-fALS* study. The average age of the 23 healthy individuals was 51.0 years, consisting of 13 female and 10 male participants.

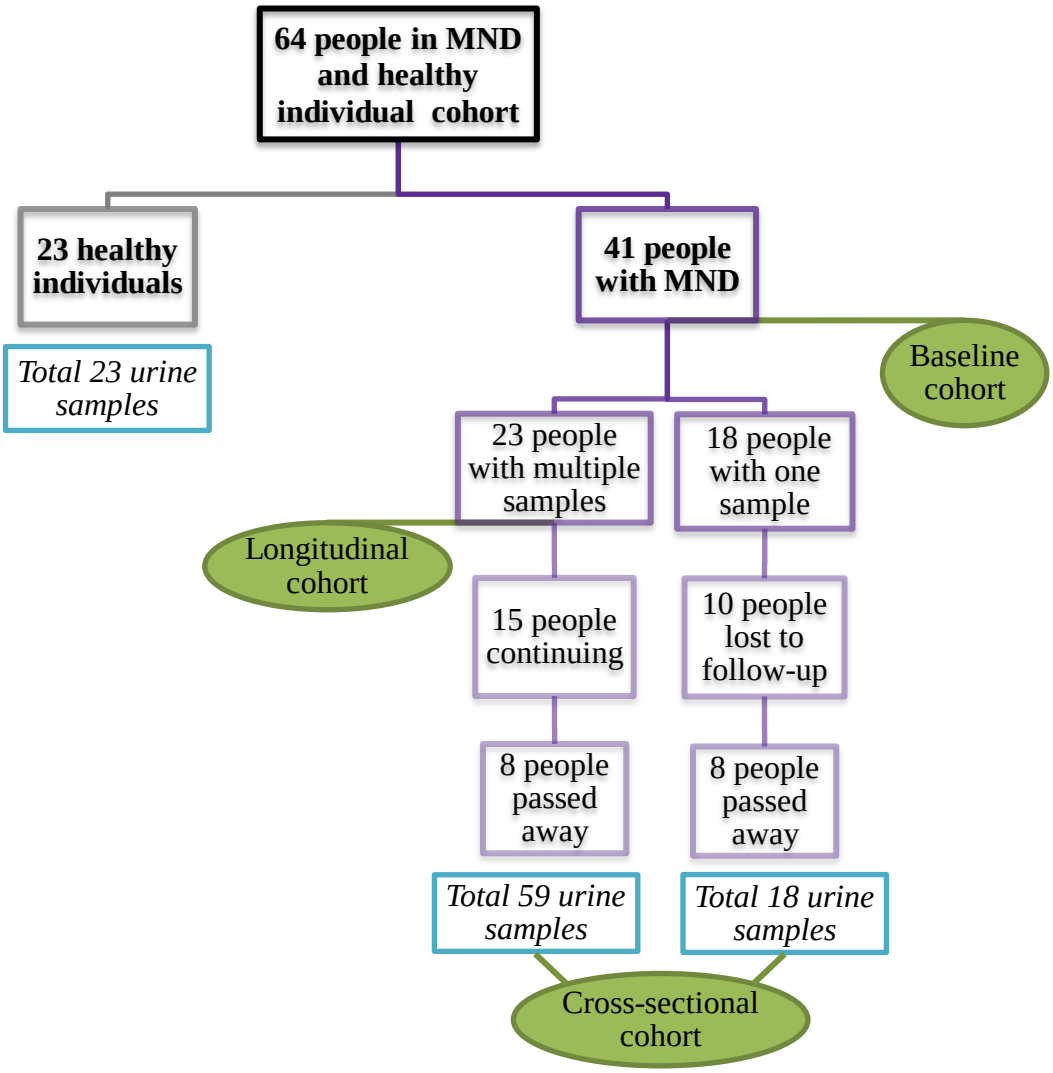

Figure 6.1: Flowchart of people with MND and healthy individuals recruited, and urine samples collected

Table 6.1: Baseline clinical characteristics of people with MND and healthy individuals

Characteristic	MND (n=41)	HI (n=23)
Gender	15 female, 26 male	10 female, 13 male
Age at symptom onset	67.5 (41.6-85.7)	N/A
Age at diagnosis	68.4 (42.5-86.3)	N/A
Diagnostic delay (months)	11.5 (0.0-40.9)	N/A
Age at baseline	68.9 (43.3-86.4)	51.0 (29.0-72.0)*
ALSFRS-r score at baseline	39 (22-47)	N/A
Disease genotype	38 sporadic, 3 familial	N/A
Disease onset site	14 bulbar, 27 limb	N/A
Riluzole treatment	26 yes, 15 no	N/A

Values presented as average (range). Diagnostic delay: time from symptom onset to diagnosis, Baseline: recruitment date, HI: Healthy individuals. *Age difference p=0.024, significant at 0.05 level, independent t-test (Prism6)

As the disease course and average survival can differ between bulbar and limb onset disease (Chiò *et al.* 2009), the clinical characteristics of people with bulbar and limb onset MND were compared. The average ALSFRS-r score at baseline was significantly lower, with bulbar onset participants recruited, on average, with an ALSFRS-r score of 37, 3 points lower than people with limb onset. However, all other clinical characteristics tested in people with bulbar and limb onset MND showed no significant differences (**Table 6.2**).

Table 6.2: Comparison of clinical characteristics of bulbar versus limb onset MND

Characteristic	Bulbar (n=14)	Limb (n=27)	p value
Gender	6 female, 8 male	9 female, 18 male	N/A
Age at symptom onset	64.6 (41.6-85.7)	68.9 (42.9-84.2)	0.240
Age at diagnosis	65.4 (42.5-86.3)	70.0 (43.3-84.8)	0.222
Diagnostic delay (months)	9.9 (2.6-35.3)	12.4 (0.0-41.0)	0.412
Age at baseline	66.3 (44.6-86.4)	70.4 (43.3-84.9)	0.277
ALSFRS-r score at baseline	37 (22-45)	40 (31-47)	0.018*
Disease genotype	13 sporadic, 1 familial	25 sporadic, 2 familial	N/A

Values presented as mean (range). Baseline: recruitment date for each patient, diagnostic delay: time from symptom onset to diagnosis. Independent samples t-tests (SPSS). * ALSFRS-r score at baseline significant at the 0.05 level.

6.2.2. Urinary characteristics of people with MND and healthy individuals

In addition to analysis of the clinical characteristics, the general urinary characteristics were analysed in order to rule out potential confounding factors. A comparison of urinary creatinine levels in people with MND and healthy individuals is particularly important, as urine dilution was standardised using urinary creatinine.

As presented in **Table 6.3**, urinary creatinine, protein, and urea levels were not significantly different between people with MND and healthy individuals. Additionally, no significant differences were seen between the urinary creatinine, protein, and urea levels based on MND disease onset site (bulbar vs limb onset; creatinine p=0.969, protein p=0.437 independent t-tests, and urea p=0.082 Welch's t-test).

Table 6.3: Urinary characteristics of baseline samples from people with MND and healthy individuals

Characteristic	MND (n=41)	HI (n=23)	p value
Creatinine mg/ml	0.97 (0.09-2.72)	1.31 (0.11-3.88)	$^{\beta}$0.114
Protein mg/ml	0.10 (0.02-0.44)	0.11 (0.01-0.32)	$^{\alpha}$0.854
Urea mol/L	0.29 (0.05-0.59)	0.29 (0.35-0.63)	$^{\alpha}$0.881

Values presented as mean (range). HI: Healthy individuals, p value: $^{\alpha}$independent t-test, $^{\beta}$Welch's t-test (SPSS)

6.2.3. Urinary p75NTR^{ECD} in MND versus healthy individuals

Following characterisation of study participants and their urine samples, the utility of urinary p75NTR^{ECD} as a diagnostic biomarker was investigated. To do this, urinary p75NTR^{ECD} levels in people with MND were compared to levels in healthy individuals using the p75NTR^{ECD} indirect sandwich ELISA.

Figure 6.2.A shows that urinary p75NTR^{ECD} levels were significantly higher in people with MND after standardisation of urine dilution using urinary creatinine. People with MND had an average of 5.94 ± 0.39ng urinary p75NTR^{ECD}/mg

creatinine (average ± SEM, n=41) compared to healthy individuals, with an average reading of 2.57 ± 0.20ng/mg creatinine (n=23; p<0.0001, independent t-test).

To investigate this difference further, the ability of urinary p75NTR^{ECD} levels to discriminate between people with MND and healthy individuals was assessed using Receiver Operating Characteristic (ROC) curves. An ideal diagnostic test would produce a discriminatory accuracy of 1 (100%), as determined by measuring the area under the curve (AUC) in a ROC analysis, and each level of the dependent variable (i.e. urinary p75NTR^{ECD} value) would accurately detect all true positives while excluding all false positives, and simultaneously detecting true negatives and excluding false negatives. In comparison, a poor diagnostic test shows the same discriminatory accuracy of the toss of a coin (50%) (Fawcett 2006, Hayworth & Gonzalez-Lima 2009).

ROC curves of urinary p75NTR^{ECD} levels in people with MND and healthy individuals shows a 96% probability of a random person with MND having a higher test result than that of a randomly selected healthy individual i.e. a discriminatory accuracy of 96% (**Figure 6.2.B**, Area Under Curve 0.957 ± 0.02). Additionally, a cut-off value of 3.865ng urinary p75NTR^{ECD}/mg creatinine resulted in the highest sensitivity and specificity scores, achieving 80.5% sensitivity and 95.7% specificity (ROC curve analysis).

Urinary p75NTR^{ECD} levels were then compared between bulbar and limb onset MND as one characteristic of an ideal biomarker would be the ability to distinguish between patterns of regional involvement (Otto *et al.* 2012). **Figure 6.2.C** shows that urinary p75NTR^{ECD} levels were not significantly different in bulbar and limb onset disease (p=0.8987; independent t-test).

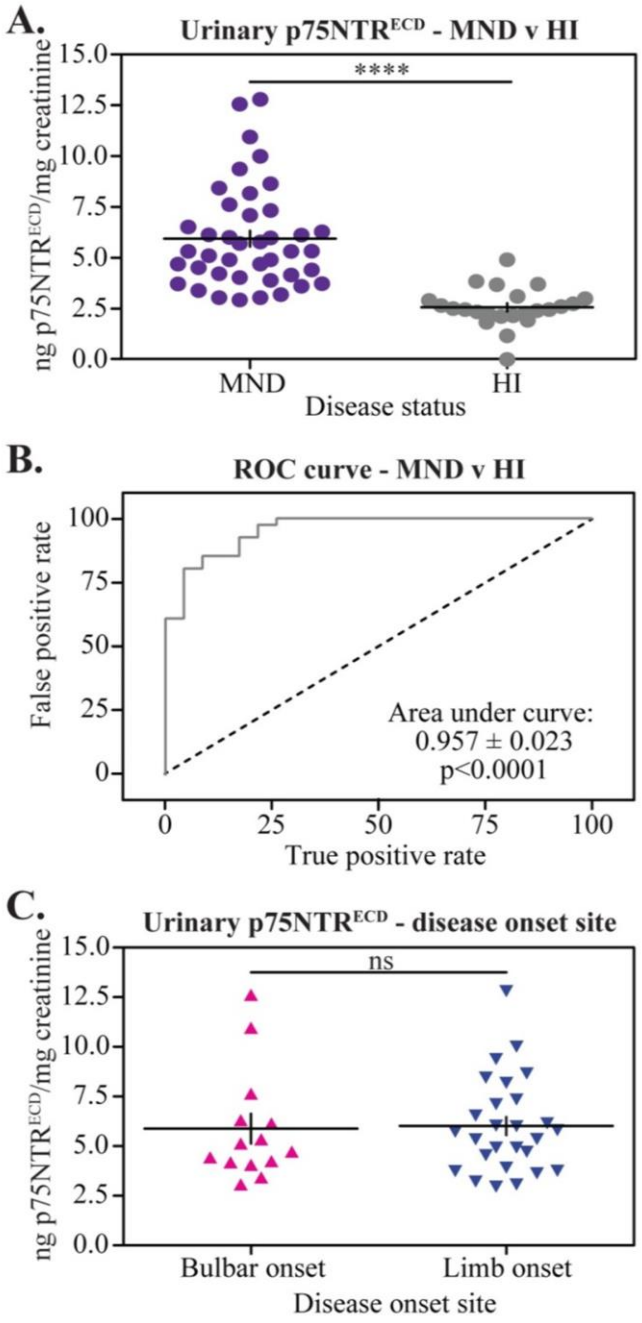

Figure 6.2: Urinary p75NTR^{ECD} levels in people with MND and healthy individuals

Urinary p75NTR^{ECD} levels were quantified in samples from people with MND (●; n=41) and healthy individuals (HI, ●; n=21) using the p75NTR^{ECD} indirect sandwich ELISA (n=8 replicates per ELISA, 4 ELISAs per sample). **A.** Calculated urinary p75NTR^{ECD} levels from people with MND and HI. **B.** Receiver Operating Characteristic curve using urinary p75NTR^{ECD} levels to discriminate between people with MND and HI. A discriminatory power of 50% (that equal to a flip of a coin) is shown by the dotted line. **C.** Comparison of urinary p75NTR^{ECD} levels in bulbar (▲, n=14) and limb (▼, n=27) onset MND. Calculated urinary p75NTR^{ECD} levels were standardised to urinary creatinine to account for urine dilution. Statistical significance determined using t-tests and ROC curve analysis, Prism6 (****p<0.0001). Ns: not significant.

Urinary p75NTR^{ECD} levels were then tested to determine if they could distinguish between different clinical characteristics. As outlined in **Table 6.4**, urinary p75NTR^{ECD} levels were not correlated with age at symptom onset or diagnosis, the diagnostic delay, genetic involvement of disease, or treatment with riluzole, the only FDA-approved treatment for MND. However, significant correlations were found between urinary p75NTR^{ECD} levels and age, and ALSFRS-r score, in people with MND. Importantly, urinary p75NTR^{ECD} levels were not correlated to age or gender in healthy individuals.

Table 6.4: Correlation of baseline urinary p75NTR^{ECD} to clinical characteristics

Characteristic	p value
Age: MND	$^{\kappa}$0.047*
Age: HI	$^{\kappa}$0.279
ALSFRSr score	$^{\kappa}$0.030*
Diagnosis: time from	$^{\kappa}$0.490
Diagnosis: age	$^{\kappa}$0.054
Diagnostic delay	$^{\kappa}$0.319
Gender: MND	$^{\beta}$0.941
Gender: HI	$^{\beta}$0.837
Genetic involvement - familial vs sporadic	$^{\beta}$0.737
Riluzole administered	$^{\beta}$0.933
Symptom onset: time from	$^{\kappa}$0.216
Symptom onset: age	$^{\kappa}$0.062

$^{\kappa}$Pearson's correlation, $^{\beta}$Independent t-test (SPSS)
*Age in MND, and ALSFRS-r score significant at the 0.05 level

6.3. Urinary p75NTR^{ECD} levels in other neurological conditions

6.3.1. Clinical characteristics of people with other neurological conditions

In order to determine the disease specificity of increased urinary p75NTR^{ECD} levels, urinary p75NTR^{ECD} levels in people with MND needed to be tested against other neurological conditions. To do this, urine samples were collected from a cohort of people with Multiple Sclerosis or Parkinson's disease (**Figure 6.3**). As outlined in **Table 6.5**, seven females and two males with Multiple Sclerosis, and seven females and three males with Parkinson's disease were recruited.

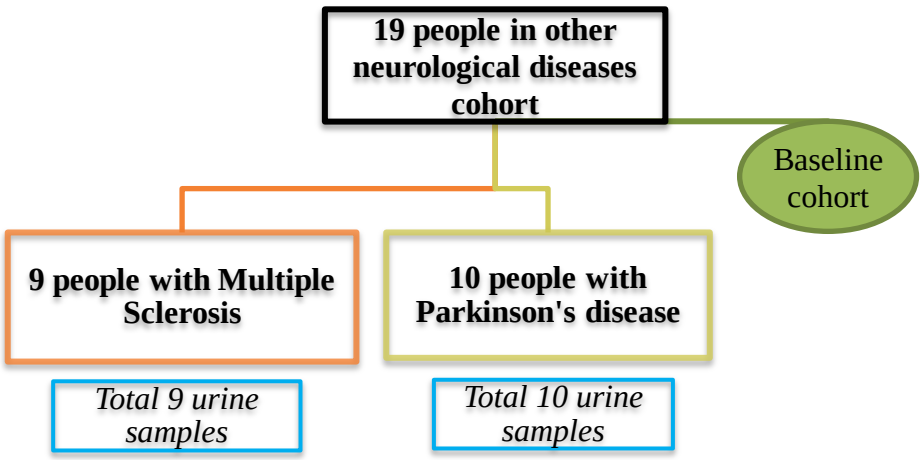

Figure 6.3: Flowchart of people with Multiple Sclerosis and Parkinson's disease recruited, and urine samples collected

Table 6.5: Overall clinical characteristics of people with other neurological conditions

Characteristic	Multiple Sclerosis	Parkinson's disease
Gender	7 female, 2 male	7 female, 3 male
Age at baseline	47.5 (34.5-61.9)	69.7 (62.3-68.7)
Age different?	p<0.0001****	
Age different to MND?	p<0.0001****	p=0.995
Age different to HI?	p=0.739	p<0.0001****

Values presented as average (range). p-value: one-way ANOVA, with Bonferroni's post-hoc analysis (Prism6). ****Ages significantly different at 0.0001 level.

6.3.2. Urinary characteristics of people with other neurological conditions

The general urinary characteristics of samples from people with Multiple Sclerosis and Parkinson's disease were analysed in order to identify potential confounding factors. As presented in **Table 6.6**, urinary creatinine, protein, and urea levels were not significantly different between people with MND and Multiple Sclerosis or Parkinson's disease.

In comparison to healthy individuals, urinary creatinine, urea, and protein levels were not significantly different in people with Parkinson's disease (p=0.161, 0.573, 0.524 respectively, independent t-tests). Urinary creatinine levels in people with Multiple Sclerosis were significantly lower than healthy individuals by 0.85mol/L (p=0.017, independent t-test), and urinary protein levels were significantly lower by 0.04mg/ml (p=0.038, independent t-test), but urea levels were not significantly changed (p=0.143, independent t-test).

Table 6.6: Urinary characteristics of baseline samples from people with MND, Multiple Sclerosis, and Parkinson's disease

Characteristic	MND (n=41)	MS (n=9)	p value
Creatinine mg/ml	0.97 (0.09-2.72)	0.71 (0.34-1.73)	0.171
Protein mg/ml	0.10 (0.02-0.44)	0.06 (0.03-0.12)	0.144
Urea mol/L	0.29 (0.05-0.59)	0.21 (0.07-0.36)	0.055
Characteristic	**MND (n=41)**	**PD (n=10)**	**p value**
Creatinine mg/ml	0.97 (0.09-2.72)	1.00 (0.59-1.44)	0.858
Protein mg/ml	0.10 (0.02-0.44)	0.09 (0.03-0.17)	0.627
Urea mol/L	0.29 (0.05-0.59)	0.26 (0.16-0.40)	0.364

Values presented as mean (range). MS: Multiple Sclerosis, PD: Parkinson's disease. p value: independent t-test

6.3.3. Urinary p75NTR^{ECD} in MND versus other neurological conditions

As shown in **Figure 6.4**, urinary p75NTR^{ECD} levels in Multiple Sclerosis were significantly lower than in MND (MS: 3.86 ± 0.33ng/mg creatinine versus MND: 5.94 ± 0.39ng/mg creatinine, p=0.023; one-way ANOVA with Bonferroni's post-hoc analysis, and all future analyses unless otherwise stated), and in Parkinson's disease, urinary p75NTR^{ECD} levels trended lower than in MND (PD: 4.30 ± 0.87 ng/mg creatinine versus MND: 5.94 ± 0.39ng/mg creatinine). In comparison, urinary p75NTR^{ECD} levels in people with Multiple Sclerosis and Parkinson's disease were not significantly higher than in healthy individuals (2.56 ± 0.96ng/mg creatinine, p=0.310 and 0.084 respectively).

In order to determine the discriminatory power of urinary p75NTR^{ECD} levels when comparing MND to Multiple Sclerosis or Parkinson's disease, Receiver Operating Characteristic curves were generated. **Figure 6.5** shows the results obtained from ROC analyses; urinary p75NTR^{ECD} levels distinguish between people with MND and Multiple Sclerosis with 79% accuracy (**Figure 6.5.A**, Area Under Curve 0.789 ± 0.074) and people with MND or Parkinson's disease with 71% accuracy (Figure **6.5.B**, Area Under Curve 0.707 ± 0.074).

For MND versus Multiple Sclerosis, a cut-off value of 5.23ng urinary p75NTR^{ECD}/mg creatinine resulted in the highest sensitivity and specificity

combination, of 53.6% sensitivity and 88.89% specificity (ROC curve analysis, Prism6). The highest sensitivity and specificity scores for distinction between people with MND and Parkinson's disease showed an optimum sensitivity of 56.3% and 90% specificity using a cut-off value of 5.25ng urinary $p75NTR^{ECD}$/mg creatinine (ROC curve analysis).

A.

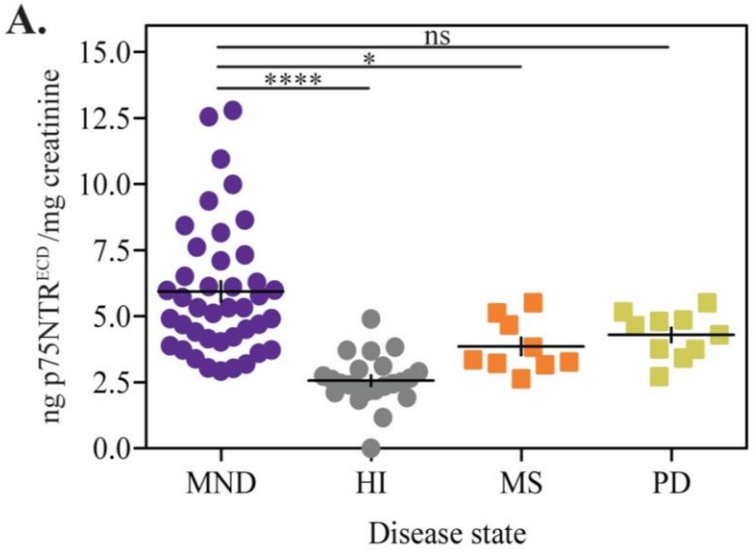

B.

Comparison of urinary p75NTR^{ECD} levels between disease states and healthy individuals

Comparison	Mean difference (ng/mg creatinine)	Significant	p value
MND versus HI	+3.38 ± 0.49	Yes	<0.0001
MND versus MS	+2.08 ± 0.70	Yes	0.023
MND versus PD	+1.65 ± 0.67	No	0.097
MS versus HI	+1.30 ± 0.75	No	0.514
PD versus HI	+1.73 ± 0.72	No	0.111
MS versus PD	-0.43 ± 0.88	No	1.000

Figure 6.4: Urinary p75NTR^{ECD} levels in people with MND versus Multiple Sclerosis and Parkinson's disease

Urinary p75NTR^{ECD} levels were quantified in samples from people with MND (●; n=41), Multiple Sclerosis (MS, ■; n=9), Parkinson's disease (PD, ■; n=10) and healthy individuals (HI, ●; n=23) using the p75NTR^{ECD} indirect sandwich ELISA (n=8 replicates per ELISA, 4 ELISAs per sample). **A.** Calculated urinary p75NTR^{ECD} comparisons between people with MND, MS, PD, and HI. **B.** Table of urinary p75NTR^{ECD} comparisons between people with MND, MS, PD, and HI. Calculated urinary p75NTR^{ECD} levels were standardised to urinary creatinine to account for urine dilution. Statistical significance determined using one-way ANOVA with Bonferroni's post-hoc analysis, SPSS (*p<0.05, ****p<0.0001). Ns: not significant.

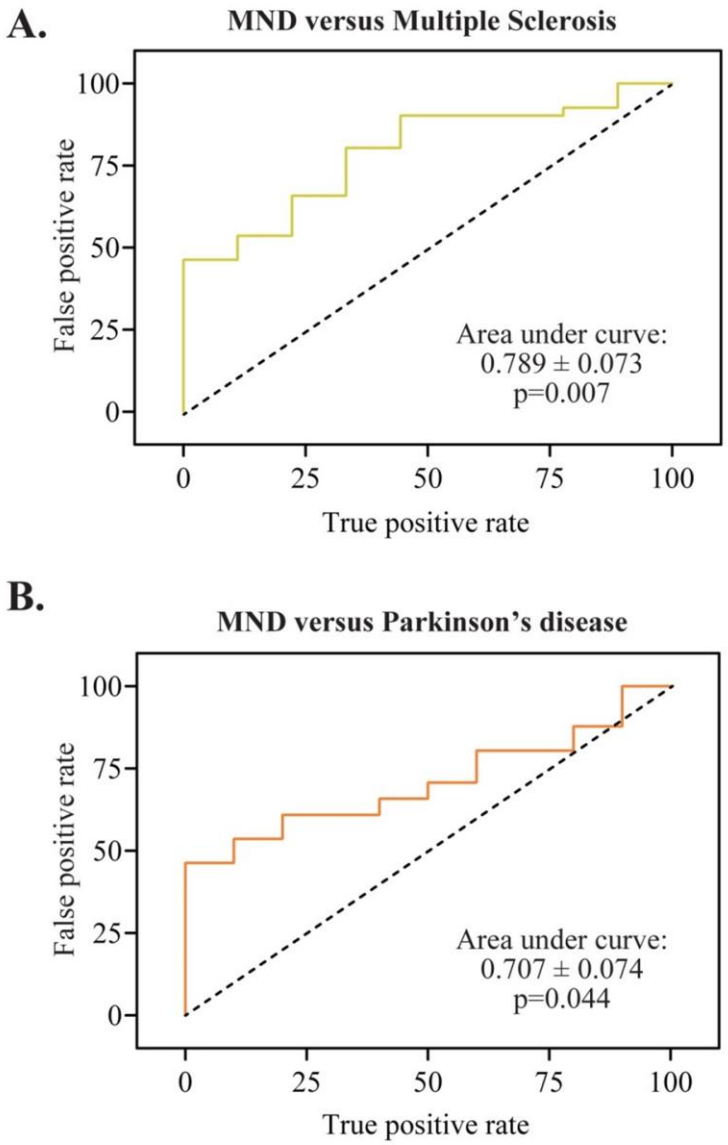

Figure 6.5: Receiver Operating Characteristic curves of urinary p75NTR^{ECD} levels in people with MND versus Multiple Sclerosis and Parkinson's disease

Receiver Operating Characteristic curves using urinary p75NTR^{ECD} levels to discriminate between people with MND and **A.** Multiple Sclerosis (—), or **B.** Parkinson's disease (—). A discriminatory power of 50% (that equal to a flip of a coin) is shown by the dotted line. Calculated urinary p75NTR^{ECD} levels were standardised to urinary creatinine to account for urine dilution. Statistical significance determined using ROC curve analysis, Prism6.

6.4. Urinary p75NTR^{ECD} levels in pre-symptomatic MND

6.4.1. Clinical characteristics of people with pre-symptomatic MND

Following the finding that urinary p75NTR^{ECD} levels are increased in people with MND, urinary p75NTR^{ECD} was investigated pre-symptomatically, to determine at what time point levels increase. To do this, urinary samples from people carrying mutant *SOD1* genes, but who did not show disease symptoms at the time of baseline sample collection, termed pre-familial MND (pre-fMND), were obtained through the *pre-fALS* study (**Figure 6.6**).

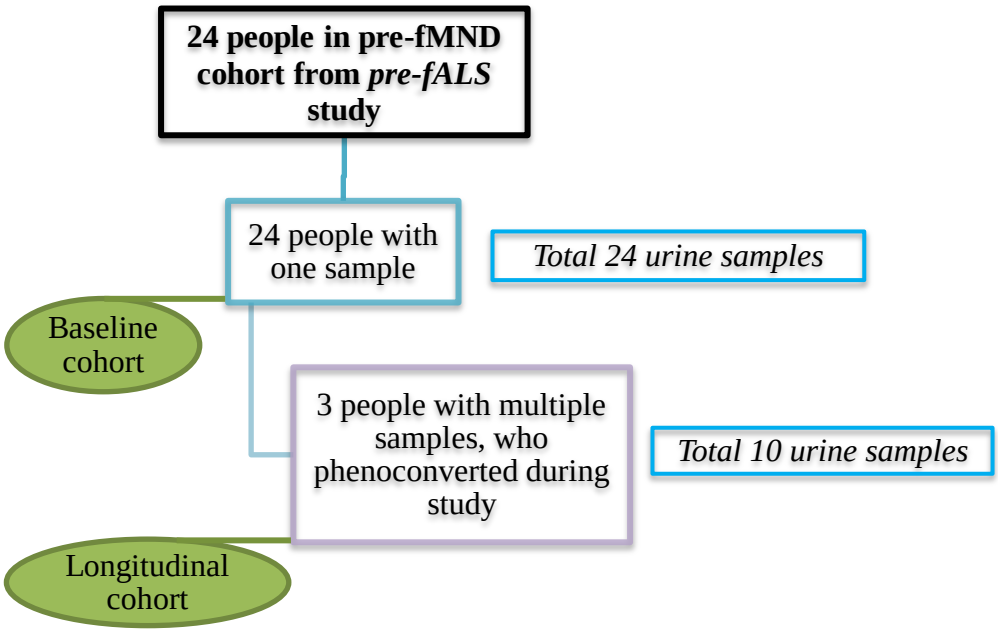

Figure 6.6: Flowchart of people with pre-fMND recruited, and urine samples collected

6.4.2. Urinary characteristics of people with pre-symptomatic MND

The general urinary characteristics of samples from people with pre-fMND were analysed in order to identify potential confounding factors. As presented in **Table 6.7**, urinary creatinine and protein levels were not significantly different between people with pre-fMND and MND. However urea levels were significantly lower in people with pre-fMND by 0.09mol/L (p=0.002, Welch's t-test).

In comparison to healthy individuals, creatinine and protein levels were not significantly different in people with pre-fMND, but urea levels were significantly lower in people with pre-fMND by 0.09mol/L (p=0.018, Welch's t-test).

Table 6.7: Urinary characteristics of baseline samples from people with MND and pre-fMND

Characteristic	MND (n=41)	Pre-fMND (n=24)	p value
Creatinine mg/ml	0.97 (0.09-2.72)	0.91 (0.24-2.01)	$^{\alpha}$0.661
Protein mg/ml	0.10 (0.02-0.44)	0.11 (0.02-0.37)	$^{\alpha}$0.542
Urea mol/L	0.29 (0.05-0.59)	0.20 (0.05-0.37)	$^{\alpha}$0.002**
Characteristic	**HI (n=23)**	**Pre-fMND (n=24)**	**p value**
Creatinine mg/ml	1.31 (0.11-3.88)	0.91 (0.24-2.01)	$^{\beta}$0.077
Protein mg/ml	0.11 (0.01-0.32)	0.11 (0.02-0.37)	$^{\alpha}$ 0.724
Urea mol/L	0.29 (0.35-0.63)	0.20 (0.05-0.37)	$^{\beta}$0.018*

Values presented as mean (range). HI: Healthy individuals, p value: $^{\alpha}$independent t-test, $^{\beta}$Welch's t-test (SPSS). * Urea significant at the 0.05 level, ** Urea significant at the 0.01 level

6.4.3. Urinary p75NTR^{ECD} in MND versus pre-symptomatic MND

Urinary p75NTR^{ECD} levels in the pre-symptomatic (pre-fMND) cohort were compared to those seen in already diagnosed people with MND and healthy individuals (**Figure 6.7**). The average urinary p75NTR^{ECD} level in people with pre-fMND (n=24; 2.99 ± 0.12ng/mg creatinine) was significantly lower than in people with MND (n=41, 5.94 ± 0.39ng/mg creatinine), and was not significantly different to that seen in healthy individuals (n=23, 2.56 ± 0.20ng/mg creatinine; one-way ANOVA with Bonferroni's post-hoc analysis).

A.

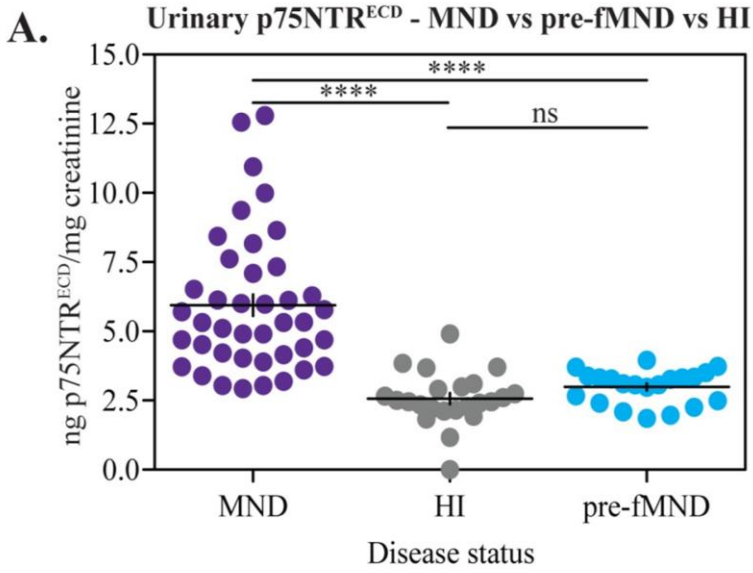

B.

Comparison of urinary p75NTR^{ECD} levels between pre-fMND, MND and healthy individuals

Comparison	Mean difference (ng/mg creatinine)	Significant	p value
pre-fMND versus MND	-2.95 ± 0.47	Yes	<0.0001
pre-fMND versus HI	+0.42 ± 0.53	No	1.000
MND versus HI	+3.38 ± 0.48	Yes	<0.0001

Figure 6.7: Urinary p75NTR^{ECD} levels in pre-fMND individuals versus people with MND and healthy individuals

Urinary p75NTR^{ECD} levels were quantified in samples from people with pre-fMND (●; n=24), MND (●; n=41) and healthy individuals (HI, ●; n=23) using the p75NTR^{ECD} indirect sandwich ELISA (n=8 replicates per ELISA, 4 ELISAs per sample). **A.** Calculated urinary p75NTR^{ECD} levels from people with pre-fMND, MND and HI. **B.** Table of urinary p75NTR^{ECD} comparisons between people with pre-fMND, MND, and HI. Calculated urinary p75NTR^{ECD} levels were standardised to urinary creatinine to account for urine dilution. Statistical significance determined using one-way ANOVA with Bonferroni's post-hoc analysis, SPSS (****p<0.0001). Ns: not significant.

6.5. Cross-sectional urinary p75NTR^{ECD} levels

6.5.1. Clinical characteristics of cross-sectional MND cohort

An important need in MND is a biomarker that can be used to track disease. An ideal biomarker in this area would change in a predictable way with disease progression (Otto *et al.* 2012), and thus be used for prognosis, and measuring the effectiveness of treatments in people already diagnosed with MND, and also in those people at genetic risk of developing MND symptoms (pre-fMND).

To determine whether urinary p75NTR^{ECD} could be used as a prognostic and disease progression biomarker, p75NTR^{ECD} levels were measured longitudinally in people diagnosed with MND, and compared to currently available measures of disease progression. Cross-sectional cohort analyses included baseline samples from 18 people living with MND who provided one sample, and 59 baseline and repeat samples from 23 individuals, totalling a cohort of 77 urine samples.

6.5.2. Prognosis

An objective prognostic biomarker, which would allow for accurate determination of life expectancy in MND, is desperately needed. The average life expectancy following diagnosis with MND is just 3 years (see Robberecht & Philips 2013 for review). However, 5% of people diagnosed with MND will survive over a decade (see Turner *et al.* 2013a for review), and the ability to distinguish between people with these differing life expectancies has been identified as one of the eight characteristics of an ideal biomarker for MND (Otto *et al.* 2012).

As presented in **Table 6.8**, 16 people with MND passed away during the course of this study (**Figure 6.1**). As a result, a correlation analysis between urinary p75NTR^{ECD} levels and time to death was performed, to determine the usefulness of urinary p75NTR^{ECD} as a prognostic biomarker.

Table 6.8: Clinical characteristics of people with MND who passed away during the course of the study

Characteristic	MND (n=16)
Gender	5 female, 11 male
Age at symptom onset	67.3 (41.6-85.7)
Age at diagnosis	68.3 (42.5-86.3)
Symptom onset to diagnosis (months)	12.0 (2.6-34.0)
Age at baseline	68.9 (44.6-86.4)
ALSFRS-r score at baseline	36 (22-45)
Disease genotype	16 sporadic
Disease onset site	9 bulbar, 7 limb
Riluzole treatment	8 yes, 8 no

As presented in **Figure 6.8.A**, urinary p75NTR^{ECD} levels were correlated to time to death, with urinary p75NTR^{ECD} levels increasing as disease progressed and time to death decreased (p=0.017, Pearson's correlation).

To investigate the relationship between urinary p75NTR^{ECD} levels and survival further, Kaplan-Meier survival curves were generated for 78 urinary samples from all 41 people with MND. Samples were separated by whether the urinary p75NTR^{ECD} levels were higher or lower than estimated urinary p75NTR^{ECD} levels at different times to death, as calculated by the linear regression curve in **Figure 6.8.A**. At 12 months to death, estimated urinary p75NTR^{ECD} levels equated to 5.327ng/mg creatinine, at 6 months, 7.355ng/mg creatinine, and at 3 months, 8.369ng/mg creatinine ($y = -0.3380*x + 9.383$, linear regression). No significant differences in projected survival times were found using these values to separate people with MND (12 months, p=0.418; 6 months, p=0.482; 3 months, p=0.974, log-rank tests, Prism6; **Figure 6.8.B**, **C**, and **D**).

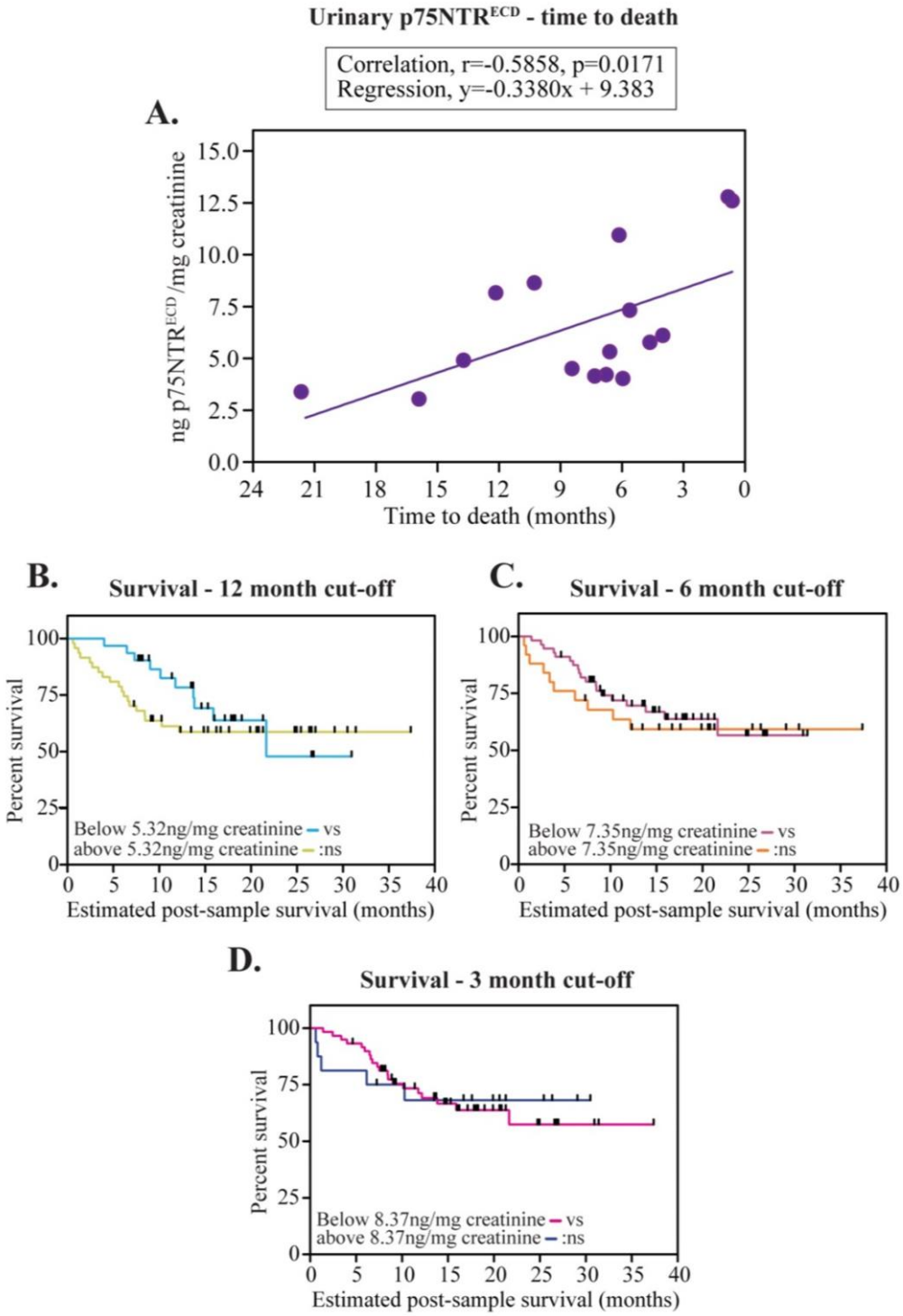

Figure 6.8: Correlation of urinary p75NTR^{ECD} levels to time of death and estimation of survival in people with MND

Urinary p75NTR^{ECD} levels were quantified in samples from people with MND using the p75NTR^{ECD} indirect sandwich ELISA (n=8 replicates per ELISA, 4 ELISAs per sample) and **A.** compared to time to death in 16 people. Calculated urinary p75NTR^{ECD} levels at **B.** 12 months, **C.** 6 months, and **D.** 3 months to death, were used to model estimated survival from MND urinary sample p75NTR^{ECD} levels (n=41 people, 77 samples). Statistical significance determined using Pearson's correlation for urinary p75NTR^{ECD} levels and time to death, and Log-rank tests for Kaplan-Meier survival curves (Prism6). Ns: not significant.

6.5.3. Disease progression

An objective disease progression biomarker is lacking in MND, with no current candidate biomarkers measured changing in a predictable way with disease progression (Turner & Benatar 2014). As outlined in **Table 6.9**, overall longitudinal urinary p75NTR^{ECD} levels at the cohort level (n=77) were significantly correlated to ALSFRS-r score, time from symptom onset, and time from diagnosis, but not other clinical characteristics. The significant correlations were then explored further, as these are the only measures of disease progression currently available in clinical trials and the clinic.

Table 6.9: Correlation of urinary p75NTR^{ECD} to clinical characteristics in the longitudinal MND cohort

Characteristic	p value
Age	$^{\kappa}$0.294
ALSFRS-r score	$^{\kappa}$0.002**
Diagnosis: time from	$^{\kappa}$0.017*
Diagnosis: age	$^{\kappa}$0.361
Diagnostic delay	$^{\kappa}$0.512
Gender	$^{\alpha}$0.599
Genetic involvement familial vs sporadic	$^{\alpha}$0.089
Riluzole taken vs not taken	$^{\alpha}$0.950
Symptom onset: time from	$^{\kappa}$0.029*
Symptom onset: age	$^{\kappa}$0.379
Site of symptom onset	$^{\alpha}$0.110

$^{\kappa}$Pearson's correlation, $^{\alpha}$independent t-test (SPSS). **ALSFRS-r score significant at the 0.01 level, *time from diagnosis, and symptom onset significant at the 0.05 level.

Figure 6.9.A plots urinary p75NTR^{ECD} levels against ALSFRS-r scores for the 77 urine samples in the cross-sectional MND cohort. Additionally, as urine dilution was standardised to urinary creatinine, urinary creatinine levels were tested against ALSFRS-r scores (**Figure 6.9.B**). A maximum score of 48 on the ALSFRS-r scale represents no signs of paralysis or inhibition of everyday activities, and as the score decreases, symptoms of disease progressively worsen (Cedarbaum *et al.* 1999). Overall, there was a significant correlation between urinary p75NTR^{ECD} levels and

ALSFRS-r score (p=0.0016, Pearson's correlation) with increased levels of urinary p75NTR^{ECD} detected with worsening signs of disease (**Figure 6.9.A**). In comparison, no significant correlation was found between urinary creatinine levels and ALSFRS-r scores (p=0.5454, Pearson's correlation; **Figure 6.9.B**).

The correlation between urinary p75NTR^{ECD} levels and ALSFRS-r scores was then investigated further, by plotting values based on the site of symptom onset. Although no significant differences were seen in urinary p75NTR^{ECD} levels based on disease onset site (p=0.106, independent t-test, **Table 6.9**), a significant correlation was seen between urinary p75NTR^{ECD} levels and ALSFRS-r scores in limb onset (**Figure 6.10.A**), but not bulbar onset, MND (**Figure 6.10.B**).

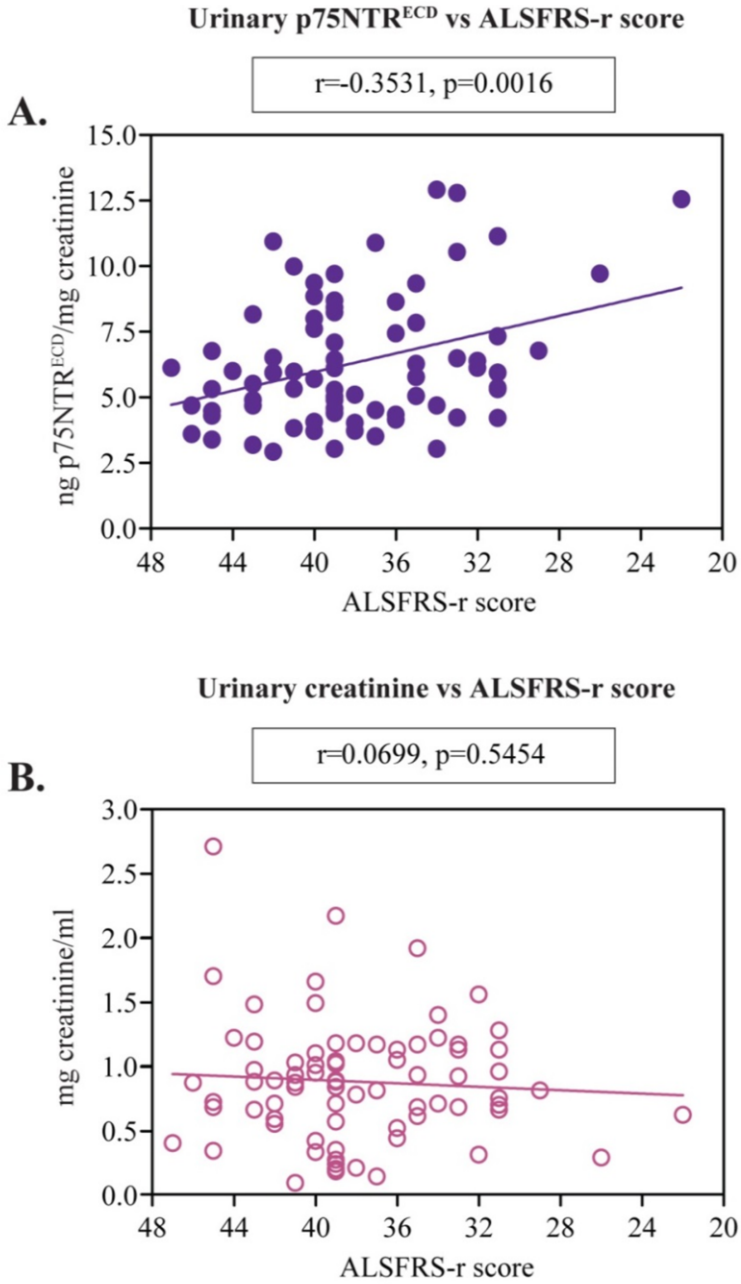

Figure 6.9: Correlation of urinary p75NTR^{ECD} and creatinine levels to ALSFRS-r scores in the longitudinal MND cohort

Urinary p75NTR^{ECD} levels were quantified in samples from people with MND (●; n=41 people, 77 samples) using the p75NTR^{ECD} indirect sandwich ELISA (n=8 replicates per ELISA, 4 ELISAs per sample). Urinary creatinine levels were quantified in samples from people with MND (○; n=41, 77 samples) using enzymatic analysis in a Roche/Hitachi Modular analyser. **A.** Correlation of urinary p75NTR^{ECD} levels to the questionnaire-based ALSFS-r scale. **B.** Correlation of urinary creatinine levels to the questionnaire-based ALSFRS-r scale. Statistical significance determined using Pearson's correlations (Prism6).

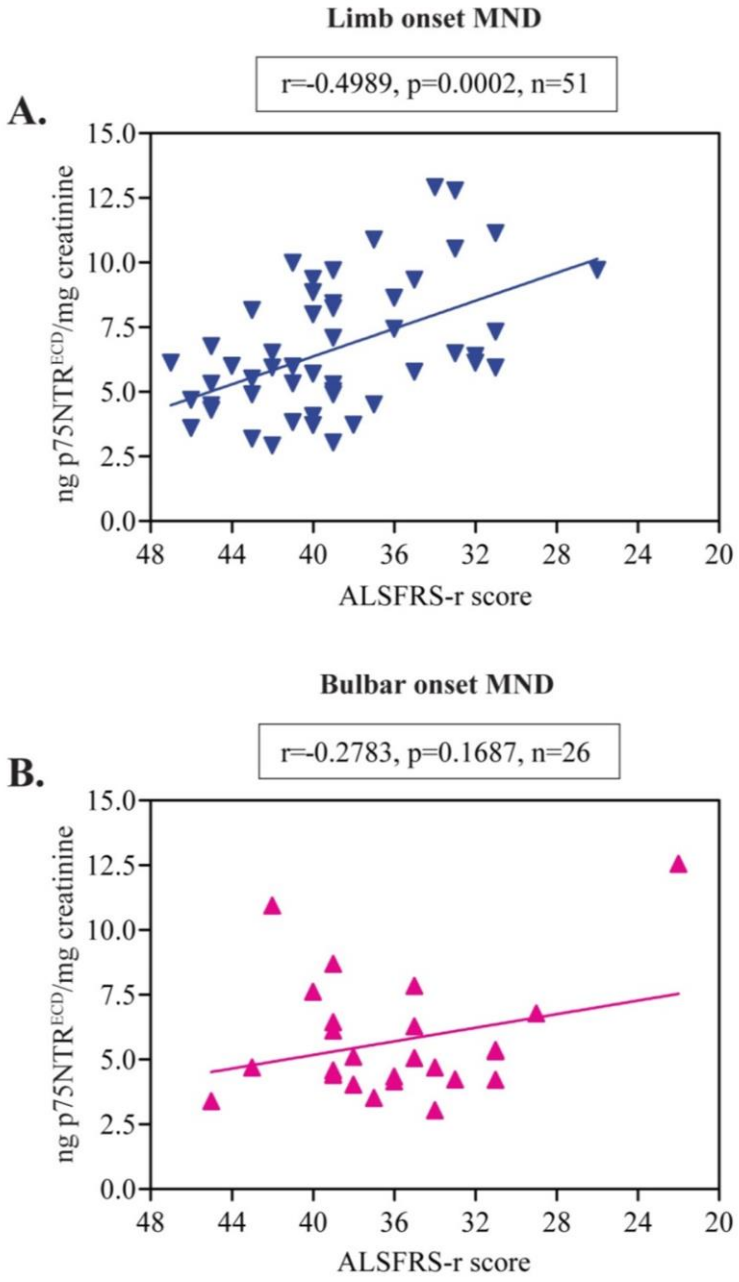

Figure 6.10: Correlation of urinary p75NTR^{ECD} to ALSFRS-r scores based on disease onset site in the longitudinal MND cohort

Urinary p75NTR^{ECD} levels were quantified in samples from people with limb onset (▼; n=27 people, 51 samples) or bulbar onset (▲; n=14 people, 26 samples) MND using the p75NTR^{ECD} indirect sandwich ELISA (n=8 replicates per ELISA, 4 ELISAs per sample). **A.** Correlation of urinary p75NTR^{ECD} levels in people with limb onset MND to the questionnaire-based ALSFS-r scale. **B.** Correlation of urinary p75NTR^{ECD} levels in people with bulbar onset MND to the questionnaire-based ALSFRS-r scale. Statistical significance determined using Pearson's correlations (Prism6).

Urinary p75NTR^{ECD} levels of the cross-sectional MND cohort were then compared to time from symptom onset (**Figure 6.11**) and time from diagnosis (**Figure 6.12**). Overall, urinary p75NTR^{ECD} levels were significantly higher in people with MND than healthy individuals at all time points from symptom onset (**Figure 6.11.A**) and diagnosis (**Figure 6.12.A**). Urinary p75NTR^{ECD} levels trended towards increasing levels as disease progressed until later stages; after 37 months since symptom onset overall urinary p75NTR^{ECD} levels decreased (**Figure 6.11A**), and after 25 months since diagnosis, the variation in urinary p75NTR^{ECD} levels increased (**Figure 6.12.A**). However, this could be due to smaller numbers at these later time points.

Separating samples based upon disease onset site also showed significant increases in urinary p75NTR^{ECD} levels in most time points from symptom onset (**Figure 6.11.B**) and diagnosis (**Figure 6.12.B**) compared to healthy individuals, and where analyses were not significant, urinary p75NTR^{ECD} levels in people with MND trended higher than healthy individuals. Additionally, in the majority of time points from symptom onset and diagnosis, urinary p75NTR^{ECD} levels were not significantly different between people with bulbar and limb onset MND (**Figure 6.11.B** and **Figure 6.12.B**).

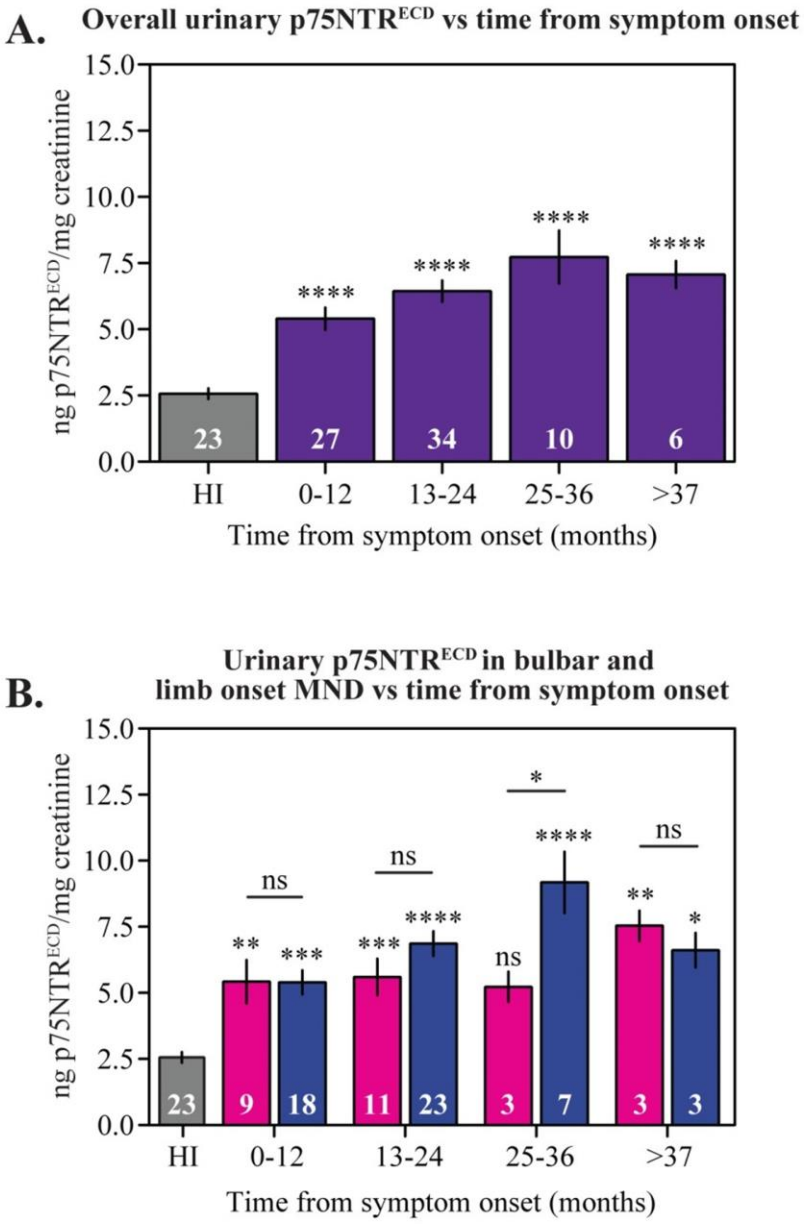

Figure 6.11: Correlation of urinary p75NTR^{ECD} to time from symptom onset overall and based on disease onset site in the longitudinal MND cohort

Urinary p75NTR^{ECD} levels were quantified in samples from people with MND (■; n=41 people, 77 samples) and healthy individuals (HI, ■; n=23) using the p75NTR^{ECD} indirect sandwich ELISA (n=8 replicates per ELISA, 4 ELISAs per sample).**A.** Urinary p75NTR^{ECD} levels in people with MND at 0-12 (n=27), 13-24 (n=34), 35-36 (n=10) and over 27 (n=6) months from symptom onset, compared to HI. **B.** Comparison of urinary p75NTR^{ECD} levels in people with bulbar (■; n=14) and limb (■; n=27) onset MND at 0-12 (bulbar n=9, limb n=18), 13-24 (n=11, 23), 25-46 (n=3, 7), and over 27 (n=3, 3) months from symptom onset, compared to HI. Statistical significance determined using one-way ANOVA with Bonferroni's post-hoc analysis (Prism6). (*p<0.05; **p<0.01; ***p<0.001; ****p<0.0001). Ns: not significant.

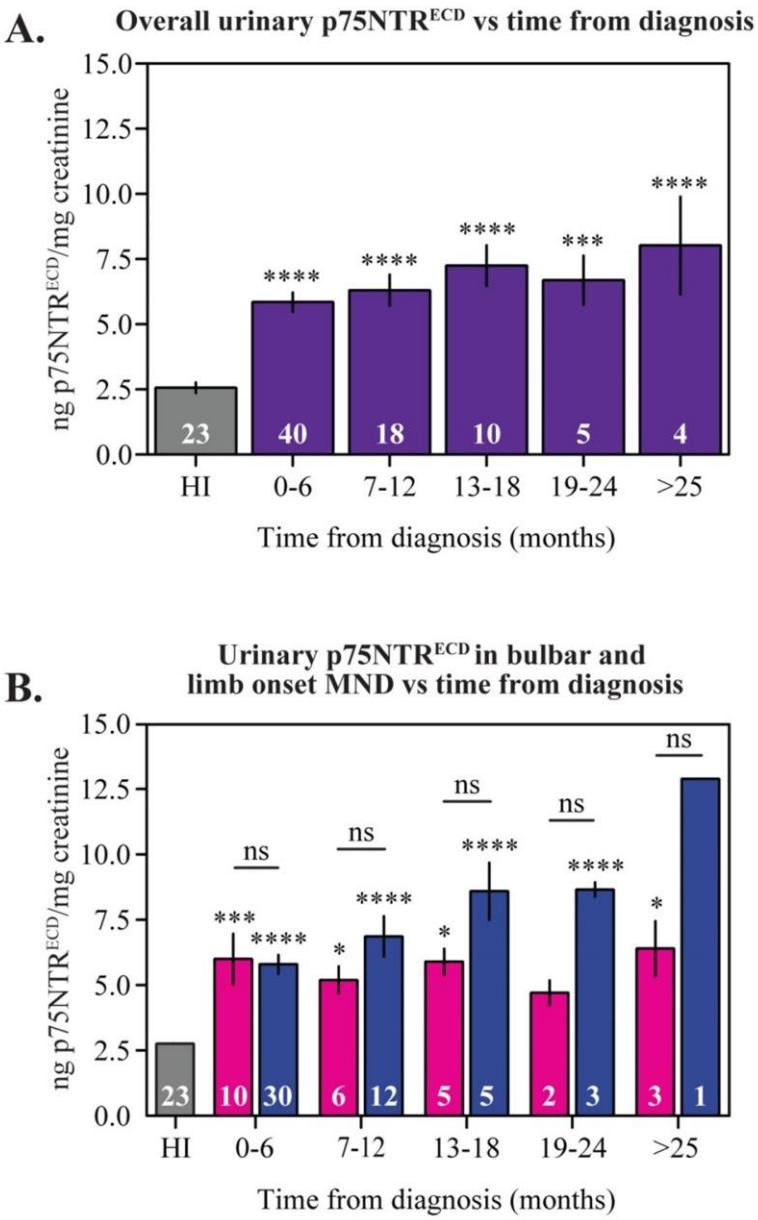

Figure 6.12: Correlation of urinary p75NTR^{ECD} to time from diagnosis overall and based on disease onset site in the longitudinal MND cohort

Urinary p75NTR^{ECD} levels were quantified in samples from people with MND (■; n=41 people, 77 samples) and healthy individuals (HI, ■; n=23) using the p75NTR^{ECD} indirect sandwich ELISA (n=8 replicates per ELISA, 4 ELISAs per sample). **A.** Urinary p75NTR^{ECD} levels in people with MND at 0-6 (n=40), 7-12 (n=18), 13-18 (n=10) 19-24 (n=5) and over 25 (n=4) months from disease onset, compared to HI. **B.** Comparison of urinary p75NTR^{ECD} levels in people with bulbar (■; n=14) and limb (■; n=27) onset MND at 0-6 (bulbar n=10, limb n=30), 7-12 (n=6, 12), 13-18 (n=5, 5), 19-24 (n=2, 3) and over 25 (n=3, 1) months from diagnosis, compared to HI. Statistical significance determined using one-way ANOVA with Bonferroni's post-hoc analysis (Prism6). (*p<0.05; **p<0.01; ***p<0.001; ****p<0.0001). Ns: not significant.

6.6. Longitudinal urinary p75NTR^{ECD} levels in individuals

6.6.1. Clinical characteristics of the longitudinal MND and pre-fMND cohorts

As urinary p75NTR^{ECD} levels were not significantly increased in the pre-fMND cohort but were significantly increased in people diagnosed with MND (**Figure 6.7**), longitudinal analysis of people with pre-fMND was performed. Three individuals from the pre-fMND cohort developed symptoms during the course of the study (**Table 6.10**). Longitudinal changes in ALSFRS-r scores in pre-fMND individuals are plotted in **Figure 6.13.A**.

Table 6.10: Clinical characteristics of longitudinal pre-fMND cohort

Characteristic	Pre-fMND (n=3)
Gender	3 female
Age at symptom onset	49 (44-56)
Age at diagnosis	49 (44-56)
Symptom onset to diagnosis (months)	0
Age at baseline	47 (43-52)
ALSFRS-r score at baseline	48
ALSFRS-r score at last sample	43 (39-46)
Rate of ALSFRS-r decline (first to last sample)	0.16 points/month (0.11-0.20)
Rate of ALSFRS-r decline (symptom onset to last sample)	0.84 points/month (0.00-1.65)
Disease genotype	3 familial
Number of samples collected	Two samples: 1 Four samples: 2

Values presented as average (range). Baseline = recruitment date for each individual.

The correlations seen between urinary p75NTR^{ECD} levels and ALSFRS-r scores, time from symptom onset, and time from diagnosis in people already diagnosed with MND at the cohort level were investigated longitudinally in 23 individual people diagnosed with MND, to determine if cohort level analyses were relevant to individuals.

Twenty-three people with MND provided multiple urine samples with samples collected, on average, every 4.91 months (range 2.8-16.8; **Table 6.11**). Urinary

p75NTR^{ECD} levels in these samples were then correlated to measures of disease progression, including longitudinal changes in the ALSFRS-r scale in individual people with MND (**Figure 6.13.B**).

Table 6.11: Clinical characteristics of longitudinal MND cohort

Characteristic	MND (n=23)
Gender	11 female, 12 male
Age at symptom onset	66.6 (43.0-85.7)
Age at diagnosis	67.5 (43.3-86.3)
Symptom onset to diagnosis (months)	10.3 (0.0-35.3)
Age at baseline	67.9 (43.3-86.4)
ALSFRS-r score at baseline	40 (31-46)
ALSFRS-r score at last sample	36 (26-45)
Rate of ALSFRS-r decline (first to last sample)	0.82 points/month (-0.34-3.01)
Disease genotype	2 familial, 21 sporadic
Disease onset site	8 bulbar, 15 limb
Riluzole administered	16 yes, 7 no
Number of samples collected	Two samples: 14 Three samples: 6 Four samples: 3

Values presented as average (range). Baseline = recruitment date for each individual.

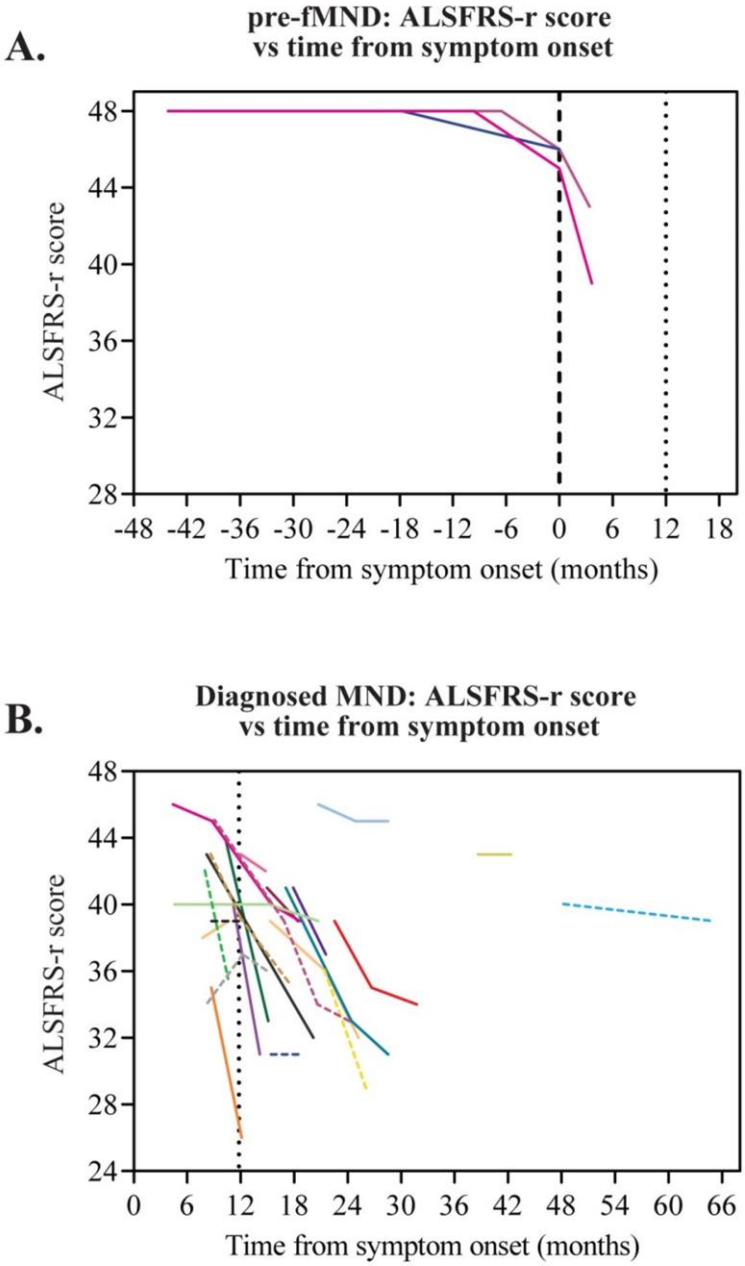

Figure 6.13: Longitudinal changes in ALSFRS-r score in individual people with pre-fMND and MND

ALSFRS-r scores were recorded at the time of collection of multiple samples from individual people. Each different coloured line represents a different individual with **A.** pre-fMND who developed symptoms (phenoconverted) during the study (n=3), and **B.** MND (- - -, bulbar onset, n=8; ▬, limb onset, n=15). Dashed line at 12 months equate to average time to diagnosis after symptom onset.

6.6.2. Longitudinal urinary p75NTR^{ECD} levels

6.6.2.1. Pre-familial MND

To determine what stage of disease progression urinary p75NTR^{ECD} levels increase, urinary p75NTR^{ECD} was measured longitudinally in three people in the pre-symptomatic (pre-fMND) cohort, beginning before symptom onset, through to phenoconversion, and after symptoms became clinically apparent. This is represented in **Figure 6.14**, where each different coloured line represents separate individuals who provided multiple urine samples. In this small number of people, urinary p75NTR^{ECD} levels were lower pre-symptomatically, and increased at the time of symptom onset (time 0). In the two individuals who provided urinary samples after symptom onset, urinary p75NTR^{ECD} levels were higher at four months post symptom onset than the average reading in healthy individuals (patient 1: 4.76ng urinary p75NTR^{ECD}/mg creatinine, patient 2: 4.27ng/mg creatinine, HI: n=23, 2.56 ± 0.20ng/mg creatinine).

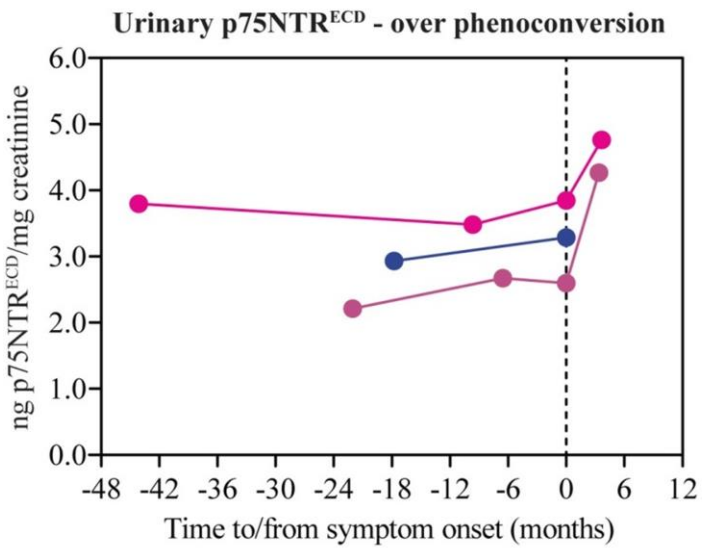

Figure 6.14: Longitudinal urinary p75NTR^{ECD} levels in people with pre-fMND compared to time to/from symptom onset

Urinary p75NTR^{ECD} levels were quantified in samples from people with pre-fMND (●/●/●, n=3) using the p75NTR^{ECD} indirect sandwich ELISA (n=8 replicates per ELISA, 4 ELISAs per sample). Each different colour represents a different individual who developed MND symptoms, phenoconverting to MND (time 0, dotted line).

6.6.2.2. Diagnosed MND

The overall increase in urinary p75NTR^{ECD} throughout disease progression at the cohort level was also seen in the majority of individuals with MND. This is presented in the spaghetti plots of **Figure 6.15** and **Figure 6.16**, where each different coloured line represents separate individuals who provided multiple urine samples. As seen in **Figure 6.15**, the majority of individuals with MND showed an increase in urinary p75NTR^{ECD} levels as ALSFRS-r scores decreased and disease symptoms worsened. Analysis of all individuals together resulted in a significant correlation between urinary p75NTR^{ECD} levels and ALSFRS-r scores (p=0.0058) despite not all individuals following the same trend.

Figure 6.16.A shows a significant correlation of urinary p75NTR^{ECD} levels in individuals as compared to the time since symptom onset. The majority of individuals gave multiple samples between 6 and 24 months since symptom onset and showed increased urinary p75NTR^{ECD} levels as time from symptom onset increased (p=0.0060). The same trend was seen when analysing urinary p75NTR^{ECD} levels from time of diagnosis (**Figure 6.16.B**); the majority of individuals showed increased levels as time progressed, and a significant correlation was seen between group urinary p75NTR^{ECD} levels and time since diagnosis (p=0.0046).

When combining all three analyses of disease progression, two of the 23 individuals showed different urinary p75NTR^{ECD} level changes to the rest of the cohort, showing an overall decrease in urinary p75NTR^{ECD} levels over time. One of these individuals reported a rapid 8-point decrease in ALSFRS-r scores over a 2-month period and urinary p75NTR^{ECD} levels decreased by 3.1ng/mg creatinine over the same period, while the other reported no change in ALSFRS-r over a 4-month period and showed a urinary p75NTR^{ECD} decrease of 2.65ng/mg creatinine.

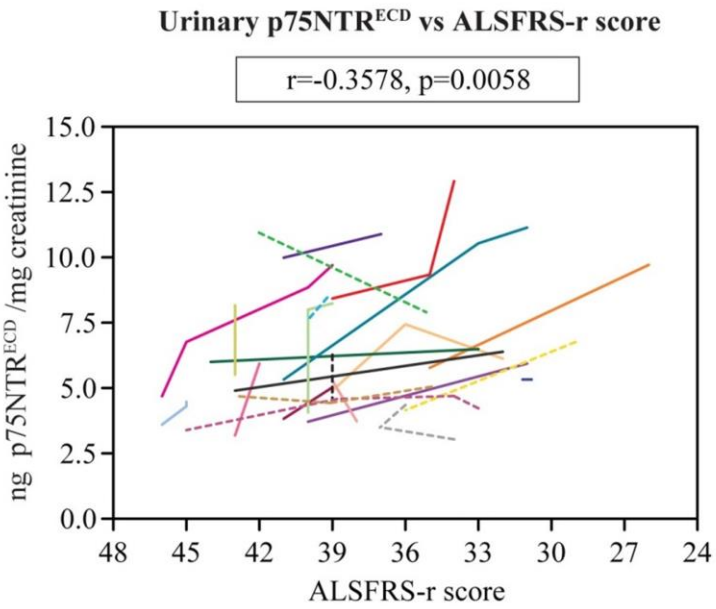

Figure 6.15: Longitudinal urinary p75NTR^{ECD} levels in individual people with MND compared to ALSFRS-r score

Urinary p75NTR^{ECD} levels were quantified in multiple samples from individual people with MND (- - -, bulbar onset, n=8; ▬, limb onset, n=15; each different colour represents a different individual) using the indirect p75NTR^{ECD} sandwich ELISA (n=8 replicates per ELISA, 4 ELISAs per sample) and compared to ALSFRS-r scores. Statistical significance determined using Pearson's correlation on group data (Prism6).

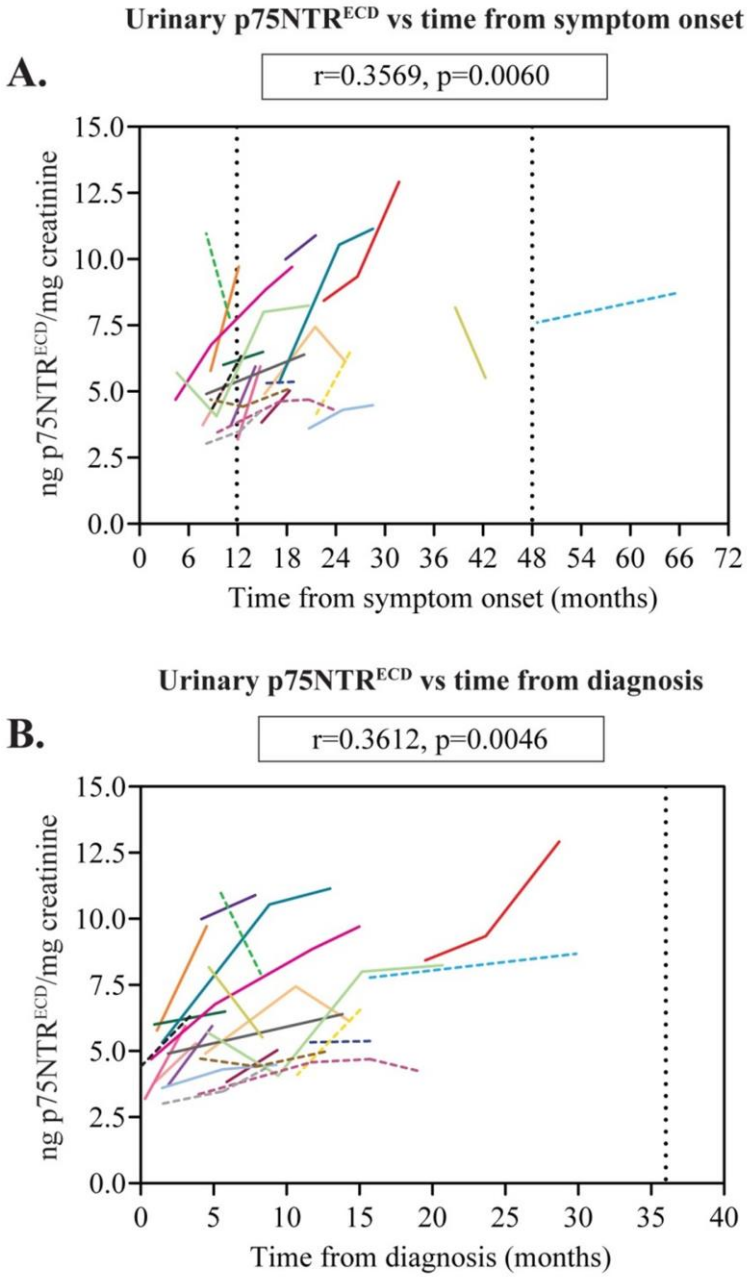

Figure 6.16: Correlation of urinary p75NTR^{ECD} in individual people with MND to time from symptom onset and diagnosis

Urinary p75NTR^{ECD} levels were quantified in multiple samples from individual people with MND (- - -, bulbar onset, n=8; ▬, limb onset, n=15; each different colour represents a different individual) using the p75NTR^{ECD} indirect sandwich ELISA (n=8 replicates per ELISA, 4 ELISAs per sample). **A.** Urinary p75NTR^{ECD} levels from individual people with MND compared to time from symptom onset. Dashed line at 12 months equate to average time to diagnosis, at 48 months, average life expectancy following diagnosis (36 months between diagnosis and death). **B.** Urinary p75NTR^{ECD} levels from individual people with MND compared to time from diagnosis. Dashed line at 36 months is the average life expectancy following diagnosis. Statistical significance determined using Pearson's correlations on group data (Prism6).

6.7. Discussion

The aim of this chapter was to test urinary p75NTR^{ECD} as a biomarker in people with MND. To do this, urinary samples from people were tested using the p75NTR^{ECD} indirect sandwich ELISA. First, urinary p75NTR^{ECD} levels were measured in people with MND, and compared to healthy individuals, to determine if levels were significantly changed during MND. Following this, urinary p75NTR^{ECD} levels were tested in people with other neurological conditions, to determine the specificity of increased urinary p75NTR^{ECD} and its usefulness as a diagnostic biomarker. The utility of urinary p75NTR^{ECD} as a prognostic biomarker was then examined, by testing levels from people with MND, who passed away during the study. Last, urinary p75NTR^{ECD} was tested as a disease progression biomarker; first by testing pre-symptomatic individuals at genetic risk of MND (pre-fMND), to determine at what stage of disease urinary p75NTR^{ECD} levels first increase, and second, longitudinal samples from symptomatic individuals diagnosed with MND, to compare urinary p75NTR^{ECD} levels with current measures of disease progression.

The MND cohort in this study consisted of 41 people diagnosed with bulbar or limb onset MND**,** with an average age at symptom onset of 67.5 years, an average age of 68.9 years at baseline, and a diagnostic delay of 11.5 months. The characteristics of this cohort are similar to other published studies, where peak symptom onset has been recorded as 60-75 years of age (Logroscino *et al.* 2010, Chiò *et al.* 2013b) and the delay between symptom onset and diagnosis is ~1 year (Mitchell 2000, Cellura *et al.* 2012, Nzwalo *et al.* 2014).

Using IP/WB, urinary p75NTR^{ECD} was detectable in people with MND but not healthy individuals (see **Figure 3.4**). In line with this, quantitative measurement of urinary p75NTR^{ECD} in people with MND and healthy individuals using the p75NTR^{ECD} ELISA, and correcting for urine dilution using urinary creatinine, detected significantly higher levels of urinary p75NTR^{ECD} in people with MND.

Urinary p75NTR^{ECD} levels were not significantly different between bulbar and limb onset disease, suggesting that urinary p75NTR^{ECD} would not be useful in discriminating between these differing sites of onset for diagnosis or progression. However, the validity of discriminating between onset sites for diagnosis has been

questioned previously, as there may be no difference in the underlying pathogenesis (Otto *et al.* 2012).

Candidate biomarkers in human disease are typically tested in their ability to discriminate between MND and healthy individuals, and other diseases. In this study, urinary p75NTR^{ECD} levels differentiated between MND and healthy individuals with 96% accuracy, and Multiple Sclerosis and Parkinson's disease with 79% and 71% accuracy, respectively. In MND, only two other studies have identified candidate biomarkers in urine (Ono *et al.* 1999, Ono *et al.* 2001). However, the ability of these candidate biomarkers to discriminate between MND and healthy individuals was not determined.

In comparison to biomarker candidates from other biological sources, the discriminatory power of urinary p75NTR^{ECD} between MND and healthy individuals is superior to CSF pNfH levels (diagnostic accuracy 87%; Brettschneider *et al.* 2006), and similar to NfL levels in the CSF (diagnostic accuracy 92%; Zetterberg *et al.* 2007) and serum (diagnostic accuracy not recorded, similar ROC curve sensitivity and specificity; Gaiottino *et al.* 2013). However, it is inferior to biomarker panels such as a three protein mix from the CSF including cystatin C and a proteolytic fragment of VEGF (Pasinetti *et al.* 2006), and a panel of 14 proteins in peripheral blood mononuclear cells (Nardo *et al.* 2011).

It could be argued that the need for a diagnostic biomarker of MND is limited, as MND can be diagnosed in the clinic using the El Escorial criteria (de Carvalho *et al.* 2008a). However, symptom heterogeneity and similarity to other diseases at this early stage makes it difficult to differentiate pure MND (Brooks *et al.* 2000). Therefore, it may be more important to differentiate MND from other neurodegenerative diseases than from healthy individuals.

This study detected a non-significant increase in urinary p75NTR^{ECD} people with Multiple Sclerosis or Parkinson's disease as compared to healthy individuals, for the first time. Re-expression of p75NTR has previously been detected in brain plaques in people with Multiple Sclerosis (Dowling *et al.* 1999) and some basal forebrain cholinergic neurons in Parkinson's disease (Mufson *et al.* 1991). However, the level of urinary p75NTR^{ECD} in these neurological conditions is significantly less than that seen in MND. This may be because the re-expression of

p75NTR in these conditions is limited to CNS motor neurons (Mufson *et al.* 1991, Dowling *et al.* 1999), and does not include peripheral Schwann cells, as seen in MND (Kerkhoff *et al.* 1991). In addition, $p75NTR^{ECD}$ has also been detected in the urine of people with Alzheimer's disease (Lindner *et al.* 1993).

The fact that urinary $p75NTR^{ECD}$ levels trend towards an increase in other neurological conditions compared to healthy individuals suggests that urinary $p75NTR^{ECD}$ cannot discriminate between MND and other diseases for sensitive diagnosis. In keeping with this, the discriminatory power of urinary $p75NTR^{ECD}$ levels is inferior to other biological biomarkers comparing MND to other diseases, including CSF pNfH (Brettschneider *et al.* 2006, Ganesalingam *et al.* 2011, Ganesalingam *et al.* 2013), CSF tau (Brettschneider *et al.* 2006), the ratio of CSF phosphorylated tau to total tau (Grossman *et al.* 2014), and a two protein panel in in peripheral blood mononuclear cells (Nardo *et al.* 2011). However, similar values were seen when using CSF NfL to compare MND to disease controls in two studies (Zetterberg *et al.* 2007, Tortelli *et al.* 2012), and urinary $p75NTR^{ECD}$ was superior to individual proteins identified in peripheral blood mononuclear cells (Nardo *et al.* 2011).

Measuring urinary $p75NTR^{ECD}$ in a small cohort of 16 individuals that passed away during the study, and measuring the correlation of urinary $p75NTR^{ECD}$ to the ALSFRS-r score in all samples, allowed for analysis of the prognostic potential of urinary $p75NTR^{ECD}$ levels in people with MND. To date, the majority of candidate prognostic biomarkers correlate to the intensity of the MND disease process, e.g., the rate of the degeneration process as measured by the ALSFRS-r. This includes higher CSF and serum pNfH levels (Boylan *et al.* 2009, Boylan *et al.* 2013) and higher CSF NfL levels (Tortelli *et al.* 2012, Tortelli *et al.* 2014), associated with faster disease progression, and lower CSF cystatin C levels correlating to shorter survival times (Wilson *et al.* 2010). In contrast, this study found that urinary $p75NTR^{ECD}$ levels positively correlate to time of death and ALSFRS-r score, which is indicative of disease stage, as opposed to disease rate. Two other biomarker candidates also correlate to disease stage in the CSF; CD14 levels are inversely correlated to survival, and S100β is positively correlated to survival (Süssmuth *et al.* 2010).

The identification of disease progression biomarkers is also important for MND (Benatar & Wuu 2012, Otto *et al.* 2012, Benatar *et al.* 2013, Turner *et al.* 2013b). In this study, urinary p75NTR^{ECD} levels were not significantly increased before symptom onset in 24 pre-symptomatic mutant *SOD1* gene carrying individuals, but increased at time of symptom onset, and continued to increase throughout disease progression in people diagnosed with MND. In symptomatic MND cross-sectional cohort analyses, urinary p75NTR^{ECD} levels had significant correlations to the time from symptom onset and diagnosis, and also the only validated clinical measure of disease, the ALSFRS-r score. These correlations also appeared in the majority of people with MND when analyses were performed within individuals longitudinally. Increases in urinary p75NTR^{ECD} over time are not linked to age but disease progression. This is shown by the fact that there was no significant correlation between urinary p75NTR^{ECD} levels and age in the healthy individuals, which is in line with other studies (Zupan *et al.* 1989, DiStefano *et al.* 1991).

In comparison, most other biological biomarker studies have been performed on single samples from a number of individuals, and as a result, any claims to usefulness as markers of disease progression, pre- or post-symptomatic, are limited by cross-sectional trends. In fact, it has recently been proposed that longitudinal studies should be the gold standard for biomarker validation (Turner & Benatar 2014), as such, longitudinal changes in urinary p75NTR^{ECD} levels are the only identified biomarker that correlates to disease progression, to date.

Only two other studies have investigated a potential biological biomarker prior to the onset of symptoms. Freischmidt and colleagues found a significant down regulation of 24 miRNAs in pre-symptomatic mutation carriers in comparison to healthy individuals, independent of the causative gene. Interestingly, 30 miRNAs were down regulated in people with diagnosed MND, 22 of which were also down regulated in pre-symptomatic people, but to a lesser extent (Freischmidt *et al.* 2014). Carew and colleagues measured significantly decreased CSF ratios of N-acetylaspartate/creatine and N-acetylaspartate/myo-inositol in pre-symptomatic mutant *SOD1* carriers and people with MND in comparison to healthy individuals, and, a significantly decreased myo-insotol/creatine ratio in pre-symptomatic mutant *SOD1* carriers, but not people with MND, in comparison to healthy individuals (Carew *et al.* 2011). Although promising, these studies were not conducted

longitudinally, and so the time point at which these changes become significant before symptom onset is unknown. Although not a biological biomarker, motor unit number estimation (MUNE), detected an abrupt loss of motor neurons in two pre-symptomatic MND mutation carriers who developed symptoms, beginning to decrease 10 and 15 months before symptom onset (Aggarwal & Nicholson 2002).

One other study has performed longitudinal analysis of potential biological biomarkers in individual people with MND, finding that the levels of three proteins, CypA, ERp57, and TDP-43, in peripheral blood mononuclear cells, increased longitudinally (Nardo *et al.* 2011). However, these levels were measured over a 6-month period and were not compared to clinical indicators of disease progression, such as the length of disease i.e. time from symptom onset or diagnosis, or to the level of disability i.e., ALSFRS-r score.

Recently, serum creatinine levels, indicative of muscle mass (Baxmann *et al.* 2008), have been identified as a candidate biomarker for MND; serum creatinine was significantly lower in people with MND than healthy individuals, and baseline levels were indicative of disease progression and survival (Ikeda *et al.* 2012, Atassi *et al.* 2014, Chen *et al.* 2014, Chiò *et al.* 2014). However, creatinine levels in urine have not been investigated in MND. In this study, urinary creatinine was used to standardise urine dilution. No significant difference was seen in urinary creatinine levels between people with MND and healthy individuals, and urinary creatinine levels in people with MND were not correlated to ALSFRS-r score (**Figure 6.9.B**), time to death, time from symptom onset or time from diagnosis, and did not change as disease progressed (results not shown). This suggests that urinary creatinine levels alone are not useful as a biomarker of MND, and it is valid to use urinary creatinine to standardise for urine dilution. However, it is possible that urinary creatinine levels are indicative of muscle mass in MND below levels of statistical significance. As such, urine dilution could be standardised using other parameters, such as cystatin C (Conti *et al.* 2005, Baxmann *et al.* 2008) or osmolarity (Chadha *et al.* 2001, Richmond *et al.* 2005). A small study of urinary p75NTR^{ECD} using osmolarity to standardise urine dilution has been conducted in our laboratory, and shows similar trends and significance between people with MND and healthy individuals to that of urinary p75NTR^{ECD} measurements when creatinine is used to standardise urine dilution.

In summary, this chapter tests urinary p75NTR^{ECD} as a biomarker in people with MND for the first time. Importantly, significantly higher levels of urinary p75NTR^{ECD} were detected in people with MND in comparison to healthy individuals. Urinary p75NTR^{ECD} levels in MND were also significantly higher than in people with Multiple Sclerosis and levels trended higher than in people with Parkinson's disease. Additionally, significant correlations were found between urinary p75NTR^{ECD} levels and time from symptom onset; time from diagnosis; ALSFRS-r score; and, time to death. These significant correlations, along with a post-symptomatic increase in p75NTR^{ECD} levels, suggest that urinary p75NTR^{ECD} levels show utility as a marker of disease progression in people with symptomatic MND.

Chapter 7. Discussion

7.1. Overview

In describing the general situation in MND research and the clinic, **Chapter 1** highlighted that some of the biggest challenges in MND are monitoring and managing disease progression in the clinic, and translating useful findings from pre-clinical models, such as effective treatments, into benefits for people living with MND (Otto *et al.* 2012). One way to address this issue is to identify objective biomarkers of disease.

As outlined by the Volcano group, an ideal biomarker for MND would: allow for sensitive and specific diagnosis of MND prior to significant weakness; discriminate between clinical phenotypes and predict regional involvement in advance; change in a predictable way with disease progression; and judge therapeutic response. In addition, the ideal biomarker would perform these functions while being practical to measure in physically disabled people with MND, using accessible and affordable technology (Otto *et al.* 2012).

The current approach to biological biomarker discovery, using invasive CSF or serum sampling, poses challenges to the development of objective biomarkers of disease progression, as longitudinal sampling from these fluids is not practical. In order to overcome this, potential biological biomarkers need to be tested from sources that are easily accessible and allow for longitudinal sampling, such as urine.

In order for an objective biological biomarker to be useful, it needs to be indicative of the underlying pathological process of MND. Re-expression of p75NTR by adult motor neurons (Seeburger *et al.* 1993, Lowry *et al.* 2001, Copray *et al.* 2003) and Schwann cells (DiStefano & Johnson 1988, Kerkhoff *et al.* 1991), occurs when motor neurons are dying, retracting, and losing neurotrophic support, and Schwann cells are denervated. Additionally, the cleavage of $p75NTR^{ECD}$ following signalling (Chao 2003), and the subsequent appearance of $p75NTR^{ECD}$ in urine has previously been documented as an indicator of underlying injury (DiStefano & Johnson 1988).

The central aims of this study were to determine if $p75NTR^{ECD}$ is *detectable* and *quantifiable* in the urine of the $SOD1^{G93A}$ MND mouse model and people with MND. From these findings, the hypothesis that the presence of $p75NTR^{ECD}$ in urine is an objective biomarker for MND could be elucidated (**Figure 7.1**).

7.1.1. Urinary p75NTR^{ECD} detection

First, urine samples were tested to determine if p75NTR^{ECD} was detectable in SOD1^{G93A} MND model mice, and people with MND. As described in **Chapter 3**, a combined Immunoprecipitation/Western Blot (IP/WB) procedure resulted in p75NTR^{ECD} detection in the urine of SOD1^{G93A} mice and people with MND. Importantly, urinary p75NTR^{ECD} was not seen in B6 healthy control mice until the equivalent of end stage of disease (approx. 145-160 days), and was not detected in healthy people. The presence of p75NTR^{ECD} in urine was then confirmed using a second procedure, where peptides specifically from the extracellular domain of p75NTR were detected and sequenced from urine of people with MND using Immunoprecipitation/ Mass Spectrometry (IP/MS).

7.1.2 Urinary p75NTR^{ECD} quantification

Chapter 4 describes the development of a novel indirect sandwich ELISA for urinary p75NTR^{ECD} quantification. The optimised ELISA for p75NTR^{ECD} used mouse anti-human p75NTR (MLR1) monoclonal antibody for p75NTR^{ECD} capture, and goat anti-mouse p75NTR^{ECD} polyclonal antibody with bovine anti-goat HRP antibody for p75NTR^{ECD} detection. Using one setup, the optimised ELISA could detect mouse- and human-derived p75NTR^{ECD} with high sensitivity and specificity.

In **Chapter 5,** urinary p75NTR^{ECD} was measured in the SOD1^{G93A} mouse model of MND using the ELISA. In this model, urinary p75NTR^{ECD} was significantly higher than healthy controls prior to symptom onset. Additionally, urinary p75NTR^{ECD} levels remained increased throughout disease progression in SOD1^{G93A} mice, and trended towards an increase with disease progression. Following on from this, urinary p75NTR^{ECD} levels correlated with treatment effectiveness showing no response to the ineffective riluzole, but decreasing in c29-treated SOD1^{G93A} mice over the same period that behavioural symptoms of disease were improved.

The usefulness of urinary p75NTR^{ECD} as a biomarker in people with MND was investigated in **Chapter 6**. Urinary p75NTR^{ECD} levels were significantly increased in people with MND in comparison to healthy individuals and people with Multiple Sclerosis and MND urinary p75NTR^{ECD} trended higher than levels in Parkinson's

disease. However, urinary p75NTR^{ECD} levels were not increased before symptom onset in people at genetic risk of MND. Cross-sectional and longitudinal analysis showed increased urinary p75NTR^{ECD} levels at the time of symptom onset, which continued to increase in people diagnosed with MND as disease progressed, correlating with time, and ALSFRS-r scores.

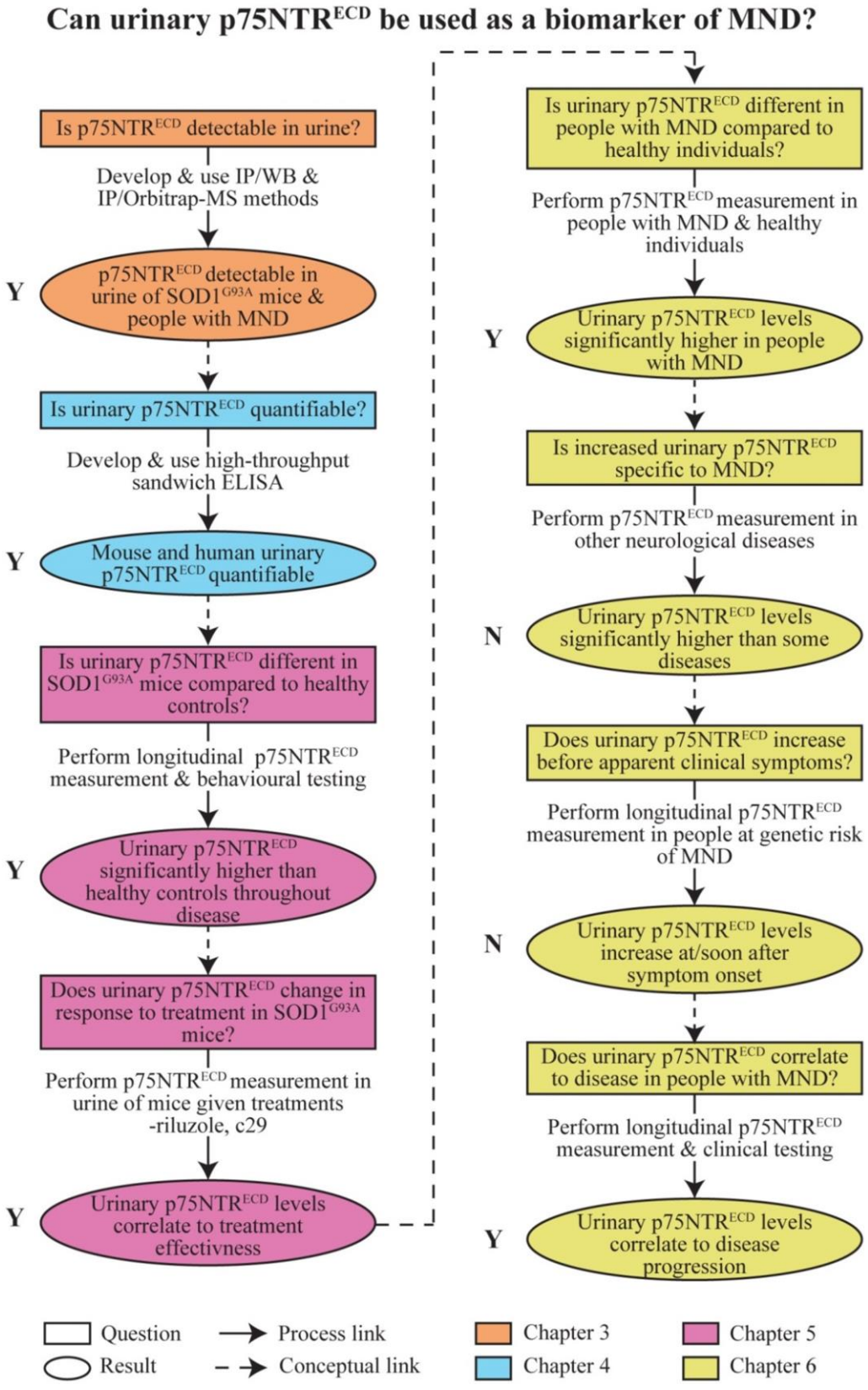

Figure 7.1: Chapter summary flowchart

7.2. Study limitations

It is widely accepted that a minimum of 24 mice (Scott *et al.* 2008), or a sufficient number as determined by power analysis (Ludolph *et al.* 2010) is required for pre-clinical testing using the $SOD1^{G93A}$ mouse model. Although longitudinal survival and behavioural analyses was performed on 35 untreated $SOD1^{G93A}$ mice and 24 riluzole-treated $SOD1^{G93A}$ mice, it proved difficult to collect and test urine samples from at least 24 mice at each time point in this study. Mouse urine samples were often of small volume, and were insufficient to allow for testing of urinary $p75NTR^{ECD}$ levels and creatinine; this was exacerbated by the size of the $SOD1^{G93A}$ mouse colony and availability of the large number of mice required. As a result, the number of urine samples tested at each time point in the study did not reach 24, but ranged between 13 and 21 for untreated $SOD1^{G93A}$ mice, and 12 and 18 for riluzole treated $SOD1^{G93A}$ mice.

To a lesser extent than in the $SOD1^{G93A}$ mouse, sample acquisition was also a limitation in studying urinary $p75NTR^{ECD}$ levels in people. However, in people, the limitation was in sourcing urinary samples from healthy people at the same age as people with MND. In this study, the average age of the MND cohort was 68.9, and in theory, urine samples from healthy people were to be sourced from family members of people with sporadic MND. However, at this age, a large number of family members had illnesses that may have confounded analyses, and so were precluded from participating. This included such illnesses as diabetes, in which the full-length, and intracellular and extracellular domains of p75NTR, has been detected in the plasma (Chilton *et al.* 2004) and as a result, may be detectable in urine. As such, healthy individuals recruited to this study were younger than people with MND. Although urinary $p75NTR^{ECD}$ levels were not correlated with age in healthy individuals in this, or other studies (Zupan *et al.* 1989, DiStefano *et al.* 1991), an ideal study would have age-matched controls.

The study of urinary $p75NTR^{ECD}$ as a biomarker of disease progression as determined by changes in the ALSFRS-r score also has limitations. The ALSFRS-r is a subjective measurement with a maximum score of 48, and minimum of 0, reflecting the ability of an individual to perform everyday tasks (full ALSFRS-r scale in **Appendix A**). Within this cohort, scores increased over time in some

individuals, this is not theoretically possible as MND is a progressive neurodegenerative disease and symptoms do not improve. However, variations in ALSFRS-r scores within individuals have been seen in other studies (Fournier & Glass 2015). Additionally, the ALSFRS-r score attributes one score to three distinct domains of disease, that of bulbar, limb, and respiratory function, and so two people with the same ALSFRS-r score may have different levels of weakness in different areas (Franchignoni *et al.* 2013). These limitations highlight the need for objective markers of disease progression.

Another potential limitation of this study is that participants were recruited close to the time of diagnosis and the majority reported ALSFRS-r scores at the higher end of the scale. Although this is beneficial for determining the usefulness of urinary $p75NTR^{ECD}$ at earlier stages of disease, the disease period over which urinary $p75NTR^{ECD}$ levels could be measured was limited, and the relationship between urinary $p75NTR^{ECD}$ and later stages of disease was not explored extensively, as has been investigated in other candidate biomarker studies (Hwang *et al.* 2013, Tortelli *et al.* 2014).

7.3. Future directions

This study shows that urinary p75NTR^{ECD} is an objective biomarker of MND. However, further testing might well be conducted in order to address the limitations of this study and further test the feasibility of using urinary p75NTR^{ECD} to determine prognosis, track disease progression, and test treatment effectiveness in pre-clinical models, clinical trials, and in the clinic.

Analysis of urinary p75NTR^{ECD} levels in additional pre-clinical MND models would provide further information regarding the usefulness of urinary p75NTR^{ECD} as a pre-clinical biomarker. For example, studying urinary p75NTR^{ECD} levels in the low-copy SOD1^{G93Adl} mouse model, which has a slower disease progression than the high-copy, rapidly progressing SOD1^{G93A} mouse (Acevedo-Arozena *et al.* 2011), would give a clearer picture of whether and/or when urinary p75NTR^{ECD} levels change throughout disease progression in SOD1^{G93A} mice.

Urinary p75NTR^{ECD} levels could also be measured during the testing of new potential treatments in pre-clinical models. This would allow for further testing of urinary p75NTR^{ECD} as a biomarker of treatment effectiveness, and give an objective indication of how effective a treatment is in delaying disease onset and/or progression.

Identifying MND earlier may improve the effectiveness of the only available treatment, riluzole, thus improving the quality, and length, of life in human disease. As such, testing of urinary p75NTR^{ECD} levels could be conducted in people suspected of having MND, as this would allow for more robust testing of diagnostic use; some of these people will go on to develop MND and others will not, thus providing true disease mimics for biomarker testing (Turner & Benatar 2014). Additionally, further longitudinal study of urinary p75NTR^{ECD} in people with pre-fMND may prove useful to pinpoint the time at which urinary p75NTR^{ECD} levels first increase, and further longitudinal studies in people already diagnosed with MND would determine the urinary p75NTR^{ECD} trends in later stages of disease.

This study is only the second to investigate urine as a source of biomarkers in MND and has proven that this is a feasible biological fluid for non-invasive, longitudinal study. Although requiring more invasive collection procedures, serum as a

biomarker source is widely studied, and p75NTR^{ECD} levels in serum may be useful in MND, alone, or as a ratio to urinary p75NTR^{ECD}.

In this study, increased levels of urinary p75NTR^{ECD} were not specific to MND. This lack of specificity has also been seen in other promising biological biomarkers of MND. For example, CSF pNfH is increased in MND (Brettschneider *et al.* 2006, Ganesalingam *et al.* 2011, Boylan *et al.* 2013, Ganesalingam *et al.* 2013, Lehnert *et al.* 2014), and also in Guillan-Barré syndrome (Dujmovic *et al.* 2013), dementia, late onset Alzheimer's disease, and frontotemporal lobe degeneration (de Jong *et al.* 2007). Changed levels of pNfH in serum is also seen in other diseases, including Multiple Sclerosis (Gresle *et al.* 2014), and optic neuropathy (Guy *et al.* 2008). Rather than detracting from the usefulness of urinary p75NTR^{ECD} in MND, these results suggest that urinary p75NTR^{ECD} could also be useful as an objective biomarker in other neurological diseases. This has been postulated previously, with urinary p75NTR levels increased in rats following sciatic nerve injury (DiStefano & Johnson 1988) and in mildly demented people with Alzheimer's disease (Lindner *et al.* 1993).

Increased urinary p75NTR^{ECD} in pre-clinical SOD1^{G93A} mice and people with MND provides the basis for further investigations into p75NTR re-expression. It is suggested that the presence of p75NTR^{ECD} in urine seen in this study, follows the re-expression of p75NTR on motor neurons (Seeburger *et al.* 1993, Lowry *et al.* 2001, Copray *et al.* 2003) and Schwann cells (DiStefano & Johnson 1988, Kerkhoff *et al.* 1991) following injury, and cleavage of the extracellular domain following signalling (Chao 2003). However, the source of urinary p75NTR^{ECD} and the mechanism by which it ends up in urine could be investigated further.

In mice, the source of urinary p75NTR^{ECD} could be investigated through conditional knock-out models. In this study, p75NTR Exon III knock-out mice that do not express p75NTR in any cells (Lee *et al.* 1992), were used as a urinary p75NTR^{ECD} negative control. This could be taken further, by testing urinary p75NTR^{ECD} levels following injury in conditional knock-out mice that express p75NTR only in motor neurons or Schwann cells, and by cross-breeding conditional p75NTR knock-out mice with SOD1^{G93A} mice or other MND models. Additionally, comparing urinary p75NTR^{ECD} levels in people with only lower motor neuron damage, e.g., progressive muscular atrophy (PMA) and only upper

motor neuron damage, e.g., primary lateral sclerosis (PLS) to levels in people with MND could provide information about the source of p75NTR^{ECD} in human disease. In order to study the mechanisms behind the presence of p75NTR^{ECD} in urine, labelled p75NTR^{ECD} could be injected into the central or peripheral nervous system of models, and traced to determine if it is detectable in urine.

A recent opinion piece estimates that less than 0.01% of papers describing multiple potential biomarkers for human disease have been translated to everyday clinical use, and blames a lack of large scale collaborations, standardisation of protocols, and sufficient funding (Poste 2011). Evidence to support this claim is no clearer than the findings of Lehnert and colleagues, who showed that a number of promising biological biomarkers in the CSF, including tau, cystatin C and S100β, showed contradictory results across laboratories, and only one tested potential biomarker, CSF pNfH, consistently showed an increase in people with MND (Lehnert *et al.* 2014). As such, if urinary p75NTR^{ECD} levels were to be implemented as a biomarker in pre-clinical models, clinical trials, and in the clinic, rigorous testing across multiple sites is required. This could be achieved through the formation of large initiatives such as the Alzheimer's Disease Neuroimaging Initiative, which has been validating potential biomarkers for the last 10 years (Hua *et al.* 2008, Ott *et al.* 2010, Kennedy *et al.* 2012, Liang *et al.* 2014).

It is likely that a single biomarker would not capture the complex biology of MND (Turner & Benatar 2014) and meet all the criteria of the 'ideal biomarker of MND' (Otto *et al.* 2012), as such, combining potential biomarkers could produce stronger discriminatory power (Otto et al. 2012). This is evident in MND in the high discriminatory power achieved by combining multiple proteins in the CSF (Pasinetti *et al.* 2006) and blood (Nardo *et al.* 2011), and the discriminatory power of biomarker panels in other diseases such as Alzheimer's disease (Wang *et al.* 2014, Olazarán *et al.* 2015) and Multiple Sclerosis (Ottervald *et al.* 2010).

An ideal biomarker panel that includes urinary p75NTR^{ECD} levels could use urinary p75NTR^{ECD} for prognosis, the identification of the stage of disease progression, and treatment effectiveness, along with other biomarkers, such as biological, clinical, genetic, physiological, neurophysiological, and neuroimaging parameters, to strengthen these associations. Additional biomarkers that appear before symptom onset, are sensitive to diagnosis, and/or the rate of disease progression could also be

included, to address all biomarker needs of MND (Otto *et al.* 2012). Such biomarker panels have been identified in other neurological conditions, such as Alzheimer's disease, where verification of treatment engagement with its target can be measured using Aβ and amyloid precursor, whereas the evidence that a treatment ameliorates neurodegeneration can be measured using CSF tau and MRI volumetry (Blennow *et al.* 2014).

7.4. Conclusions

This study describes the first time that urinary p75NTR^{ECD} has been hypothesised and tested as a candidate biomarker for MND in the pre-clinical SOD1^{G93A} MND mouse model, and in people with MND. In the SOD1^{G93A} MND model mouse, urinary p75NTR^{ECD} levels discriminate between SOD1^{G93A} mice and healthy control mice before the onset of behavioural symptoms, and are an objective biomarker of treatment effectiveness. In people, urinary p75NTR^{ECD} levels discriminate between people with MND and healthy individuals and other neurological diseases after the onset of symptoms, and are an objective prognostic and disease progression biomarker.

The positive results of this study provide solid groundwork on which to perform larger scale testing of urinary p75NTR^{ECD} as a novel, objective biomarker of MND. It is hoped that the results presented in this study are used to implement urinary p75NTR^{ECD} as an objective biomarker of MND in pre-clinical studies, clinical trials, and in the clinic. Alone, or as part of a bigger biomarker panel which addresses all the biomarker needs of MND, the use of urinary p75NTR^{ECD} as a biomarker paves the way to more effective identification, testing, and implementation of potential treatments.

The importance of MND biomarkers for the development of treatments is summarised neatly by Ludolph (Ludolph 2011):

> ‘through the successful development of MND biomarkers, no MND drug trial should be ‘negative’ again, since – if appropriately designed – the results will support or refute an experimental hypothesis, and, therefore, advance knowledge in the field’.

This novel study of urinary p75NTR^{ECD} as an MND biomarker moves research forward to a time in which no MND drug trials will be negative.

Appendix A

Table A1: Amyotrophic Lateral Sclerosis Functional Rating Scale-revised (ALSFRS-r) (Cedarbaum *et al.* 1999)

1	Speech
	4 – Normal speech 3 – Detectable disturbance 2 – Intelligible without repeating 1 – Speech with non-verbal communication 0 – Loss of useful speech
2	Salivation
	4 – Normal 3 – Slight, but definite excess of saliva 2 – Moderate excessive saliva, minimum drooling 1 – Marked excessive saliva, some drooling 0 – Marked drooling, needs constant tissue
3	Swallowing
	4 – Normal eating habits 3 – Early eating problems, occasional choking 2 – Dietary consistency changes 1 – Needs supplemental tube feeding 0 – Nil orally
4	Handwriting
	4 – Normal 3 – Slow or sloppy, all words legible 2 – Not all words legible 1 – Able to grip pen, but cannot write 0 – Unable to grip pen
5	Cutting food and handling utensils
	4 – Normal 3 – Slow and clumsy, but no help needed 2 – Can cut most foods, although clumsy and needs some help 1 – Food must be cut by somone else 0 – Needs to be fed
6	Dressing and Hygiene
	4 – Normal 3 – Independnet, but decreased efficiency 2 – Some help with closures and fasteners 1 – Provides minimum assistance to caregiver 0 – Unable to perform any task

7	Turning in bed
	4 – Normal 3 – Slow and clumsy 2 – Can turn along with difficulty 1 – Can initiate but cannot turn or adjust sheets 0 – Total dependence
8	Walking
	4 – Normal 3 – Early ambulation difficulties 2 – Walks with assistance 1 – Non-ambulatory, functional movement 0 – No purposeful leg movement
9	Climbing stairs
	4 – Normal 3 – Early ambulation difficulties 2 – Walks with assistance 1 – Non ambulatory, functional movement 0 – No purposeful leg movement
10	Dyspnoea
	4 – None 3 – Occurs when walking 2 – Occurs when eating, bathing, or dressing 1 – Occurs at rest 0 – Considerable difficulty
11	Orthopnoea
	4 – None 3 – Some difficulty, does not routinely use more than two pillows 2 – Needs extra pillows to sleep 1 – Only sleep sitting up 0 – Unable to sleep
12	Respiratory insufficiency
	4 – None 3 – Intermittent use of non-invasive ventilation 2 – Continuous use of non-invasive ventilation at night 1 - Continuous use of non-invasive ventilation , day and night 0 – Mechanical ventialtion via tracheostomy

Appendix B

Table B.1: Theoretical peptides from Trypsin Gold cleavage of human p75NTR^{ECD} (Swissprot online databases 2014)

Position of cleavage site	Resulting peptide sequence	Peptide length [aa]	Peptide mass [Da]	Within detection limit?
1	K	1	146.189	No
17	EACPTGLYTHSGECCK	16	1698.901	Yes
80	ACNLGEGVAQPCGANQTV CEPCLDSVTFSDVVSATEP CKPCTECVGLQSMSAPCVE ADDAVCR	63	6411.220	No
93	CAYGYYQDETTGR	13	1526.597	Yes
98	CEACR	5	580.675	No
113	VCEAGSGLVFSCQDK	15	1542.742	Yes
147	QNTVCEECPDGTYSDEAN HVDPCLPCTVCEDTER	34	3774.021	No
150	QLR	3	415.493	Yes
154	ECTR	4	507.562	Yes
166	WADAECEEIPGR	12	1375.475	Yes
170	WITR	4	574.680	Yes
217	STPPEGSDSTAPSTQEPEAP PEQDLIASTVAGVVTTVMG SSQPVVTR	47	4710.112	No
222	GTTDN	5	506.470	No
Seven peptides within detection limit				

Table B2: Theoretical peptides from GluC cleavage of human p75NTR^{ECD}
(Swissprot online databases 2014)

Position of cleavage site	Peptide sequence	Peptide length [aa]	Peptide mass [Da]	Within detection limit?
2	KE	2	275.305	No
14	ACPTGLYTHSGE	12	1235.334	Yes
23	CCKACNLGE	9	940.115	Yes
37	GVAQPCGANQTVCE	14	1376.522	Yes
53	PCLDSVTFSDVVSATE	16	1669.821	Yes
60	PCKPCTE	7	776.921	Yes
73	CVGLQSMSAPCVE	13	1323.560	Yes
89	ADDAVCRCAYGYYQDE	16	1841.941	Yes
95	TTGRCE	6	665.719	Yes
101	ACRVCE	6	679.807	Yes
119	AGSGLVFSCQDKQNTVCE	18	1886.082	Yes
120	E	1	147.131	No
129	CPDGTYSDE	9	985.975	Yes
143	ANHVDPCLPCTVCE	14	1500.723	Yes
146	DTE	3	363.324	No
151	RQLRE	5	700.796	Yes
159	CTRWADAE	8	951.022	Yes
161	CE	2	250.270	No
162	E	1	147.131	No
175	IPGRWITRSTPPE	13	1509.728	Yes
186	GSDSTAPSTQE	11	1079.042	Yes
188	PE	2	244.247	No
192	APPE	4	412.443	No
222	QDLIASTVAGVVTTVMGSS QPVVTRGTTDN	30	3005.347	No
Sixteen peptides within detection limit				

Table B3: Theoretical peptides from Trypsin Gold cleavage of mouse p75NTR^{ECD} (Swissprot online databases 2014)

Position of cleavage site	Resulting peptide sequence	Peptide length [aa]	Peptide mass [Da]	Within detection limit?
1	K	1	146.189	No
17	ETCSTGMYTHSGECCK	16	1736.922	Yes
80	ACNLGEGVAQPCGANQTV CEPCLDSVTFSDVVSATEP CKPCTECLGLQSMSAPCVE ADDAVCR	63	6425.247	No
93	CSYGYYQDEETGR	13	1570.607	Yes
113	CEACSVCGVGSGLVFSCQD K	20	1992.282	Yes
147	QNTVCEECPEGTYSDEANH VDPCLPCTVCEDTER	34	3788.048	No
150	QLR	3	415.493	No
166	ECTPWADAECEEIPGR	16	1805.952	Yes
170	WITR	4	574.680	No
193	STPPEGSDVTTPSTQEPEAP PER	23	2409.503	Possible
217	DLIASTVADTVTTVMGSSQ PVVTR	24	2448.771	Possible
225	GTADNLIP	8	799.879	Yes
Five peptides within detection limit				

Table B4: Theoretical peptides from GluC cleavage of mouse p75NTR^{ECD}
(Swissprot online databases 2014)

Position of cleavage site	Peptide sequence	Peptide length [aa]	Peptide mass [Da]	Within detection limit?
2	KE	2	275.305	No
14	TCSTGMYTHSGE	12	1273.355	Yes
23	CCKACNLGE	9	940.115	Yes
37	GVAQPCGANQTVCE	14	1376.522	Yes
53	PCLDSVTFSDVVSATE	16	1669.821	Yes
60	PCKPCTE	7	776.921	Yes
73	CLGLQSMSAPCVE	13	1337.587	Yes
89	ADDAVCRCSYGYYQDE	16	1857.941	Yes
90	E	1	147.131	No
95	TGRCE	5	564.614	No
119	ACSVCGVGSGLVFSCQDK QNTVCE	24	2434.754	Possible
120	E	1	147.131	No
123	CPE	3	347.386	No
129	GTYSDE	6	670.631	Yes
143	ANHVDPCLPCTVCE	14	1500.723	Yes
146	DTE	3	363.324	No
151	RQLRE	5	700.796	Yes
159	CTPWADAE	8	891.951	Yes
161	CE	2	250.270	No
162	E	1	147.131	No
175	IPGRWITRSTPPE	13	1509.728	Yes
186	GSDVTTPSTQE	11	1121.123	Yes
188	PE	2	244.247	No
192	APPE	4	412.443	No
225	RDLIASTVADTVTTVMGSS QPVVTRGTADNLIP	33	3386.823	No
Thirteen peptides within detection limit				

Peptide sequence SAPC[CAM]VEADDAVC[CAM]R				
Residue	**b**	**b+2**	**y**	**y+2**
S	88.0	44.5	1449.6	725.3
A	159.1	80.04	1362.6	681.8
P	256.1	128.6	1291.5	646.3
C[CAM]	416.2	208.6	1194.5	597.8
V	515.2	258.1	1034.5	517.7
E	644.3	322.6	935.4	468.2
A	715.3	358.2	806.3	403.7
D	830.3	415.7	735.3	368.2
D	945.4	473.2	620.3	310.7
A	1016.4	508.7	505.3	253.1
V	1115.5	558.2	434.2	217.6
C[CAM]	1275.5	638.3	335.2	168.1
R	1431.6	716.3	175.1	88.1

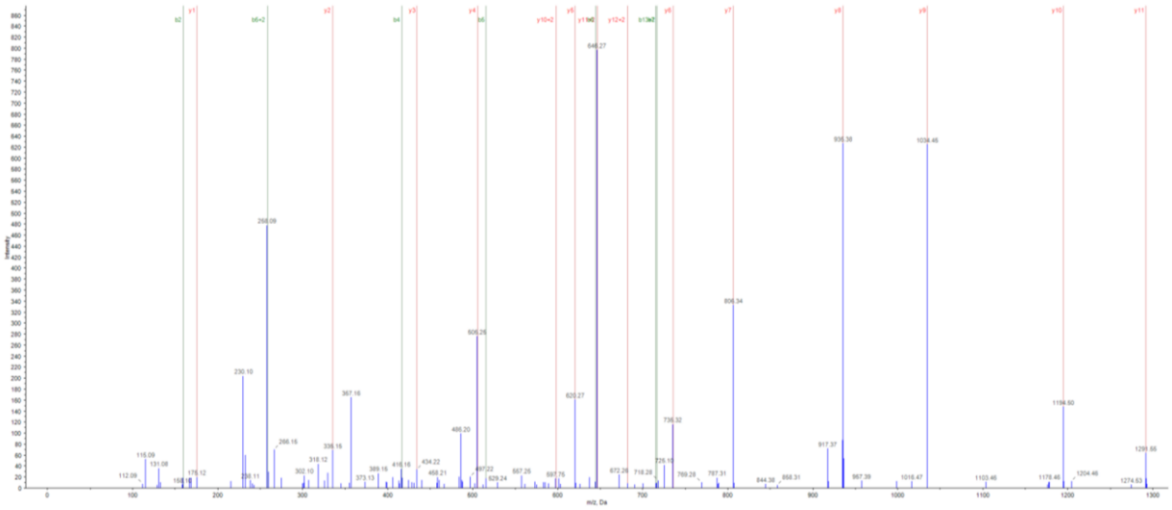

FigureC1.A: Representative spectra from Trypsin Gold digestion of urinary sample MNDU22/2 using Triple TOF-MS
Following IP/Triple TOF-MS, peptide sequences were analysed using Protein Pilot software. The expected b, b+2, y and y+2 ions from peptide sequence SAPCVEADDAVCR are shown in the table, and detected ions are highlighted green.

Peptide sequence WADAEC[CAM]EEIPGR				
Residue	**b**	**b+2**	**y**	**y+2**
W	187.1	94.0	1432.6	716.8
A	258.1	129.6	1246.5	623.8
D	373.2	187.1	1175.5	588.3
A	444.2	222.6	1060.5	530.7
E	573.2	287.1	989.4	495.2
C[CAM]	733.3	367.1	860.4	430.7
E	862.3	431.7	700.4	350.7
E	991.3	496.2	571.3	286.2
I	1104.4	552.7	442.3	221.7
P	1201.5	601.2	329.2	165.1
G	1258.5	629.8	232.1	116.6
R	1414.6	707.8	175.1	88.1

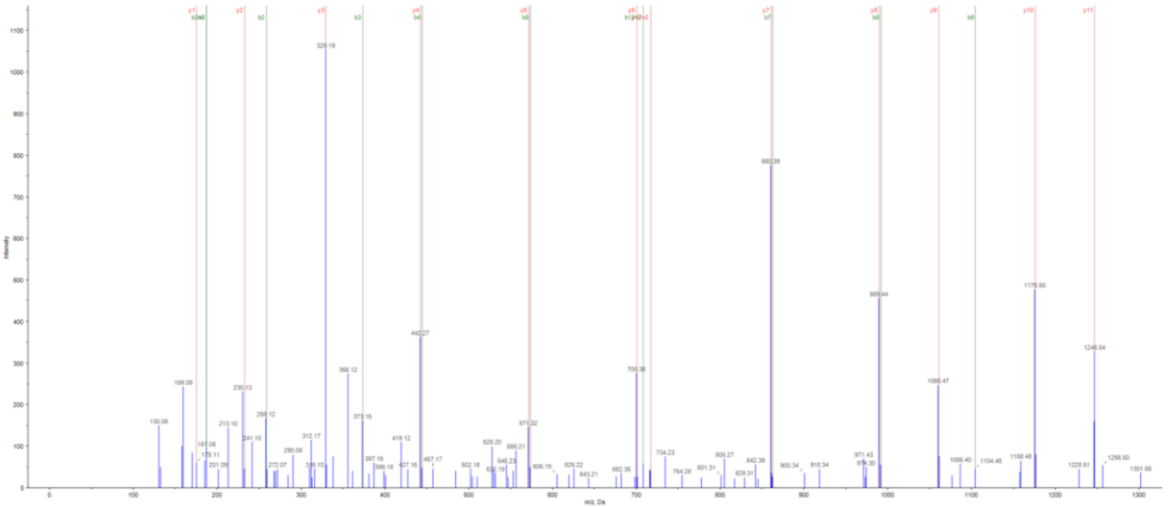

Figure C1.B: Representative spectra from Trypsin Gold digestion of urinary sample MNDU22/2 using Triple TOF-MS
Following IP/Triple TOF-MS, peptide sequences were analysed using Protein Pilot software. The expected b, b+2, y and y+2 ions from peptide sequence WADAEC[CAM]EEIPGR are shown in the table, and detected ions are highlighted green.

References

Abel O. 2015. *Amyotrophic Lateral Sclerosis online Database (6.0)* [Online]. King's College London, Institute of Psychiatry. Available: http://alsod.iop.kcl.ac.uk/ 2015].

Acevedo-Arozena A, Kalmar B, Essa S, Ricketts T, Joyce P, *et al.* 2011, 'A comprehensive assessment of the SOD1G93A low-copy transgenic mouse, which models human amyotrophic lateral sclerosis', *Disease Models & Mechanisms,* **4**(5): 686-700.

Adachi J, Kumar C, Zhang Y, Olsen JV & Mann M 2006, 'The human urinary proteome contains more than 1500 proteins, including a large proportion of membrane proteins', *Genome Biology,* **7**(9): R80.

Aggarwal A & Nicholson G 2002, 'Detection of preclinical motor neurone loss in SOD1 mutation carriers using motor unit number estimation', *Journal of Neurology, Neurosurgery, and Psychiatry,* **73**(2): 199-201.

Aggarwal S & Cudkowicz M 2008, 'ALS drug development: reflections from the past and a way forward', *Neurotherapeutics,* **5**(4): 516-527.

Ahmed A & Wicklund MP 2011, 'Amyotrophic lateral sclerosis: what role does environment play?', *Neurologic Clinics,* **29**(3): 689-711.

Alami NH, Smith RB, Carrasco MA, Williams LA, Winborn CS, *et al.* 2014, 'Axonal transport of TDP-43 mRNA granules is impaired by ALS-causing mutations', *Neuron,* **81**(3): 536-543.

Albalat A, Mischak H & Mullen W 2011, 'Urine proteomics in clinical applications: technologies, principal considerations and clinical implementation', *Contributions, Macedonian Academy of Science and Arts Section of Biological and Medical Sciences,* **32**(1): 13-44.

Alegria-Schaffer A, Lodge A & Vattem K 2009. Chapter 33 Performing and Optimizing Western Blots with an Emphasis on Chemiluminescent Detection. *In:* Richard, RB & Murray, PD (eds.) *Methods in Enzymology*. Academic Press.

Alexander G, Erwin K, Byers N, Deitch J, Augelli B, *et al.* 2004, 'Effect of transgene copy number on survival in the G93A SOD1 transgenic mouse model of ALS', *Brain Research. Molecular Brain Research,* **130**(1-2): 7-15.

Alonso A, Logroscino G, Jick S & Hernán M 2009, 'Incidence and lifetime risk of motor neuron disease in the United Kingdom: a population-based study', *European Journal of Neurology,* **16**(6): 745-751.

Andersen P, Sims K, Xin W, Kiely R, O'Neill G, *et al.* 2003, 'Sixteen novel mutations in the Cu/Zn superoxide dismutase gene in amyotrophic lateral sclerosis: a decade of discoveries, defects and disputes', *Amyotrophic Lateral Sclerosis and Other Motor Neuron Disorders,* **4**(2): 62-73.

Andersen PM 2006, 'Amyotrophic lateral sclerosis associated with mutations in the CuZn superoxide dismutase gene', *Current Neurology and Neuroscience Reports,* **6**(1): 37-46.

Andersen PM & Al-Chalabi A 2011, 'Clinical genetics of amyotrophic lateral sclerosis: what do we really know?', *Nature Reviews Neurology,* **7**(11): 603-615.

Appel V, Stewart S, Smith G & Appel S 1987, 'A rating scale for amyotrophic lateral sclerosis: description and preliminary experience', *Annals of Neurology*, **22**(3): 328-333.

Arai T, Hasegawa M, Akiyama H, Ikeda K, Nonaka T, *et al.* 2006, 'TDP-43 is a component of ubiquitin-positive tau-negative inclusions in frontotemporal lobar dengeneration and amyotrophic lateral sclerosis', *Biochemical and Biophysical Research Communications,* **351**(3): 602-611.

Arndt T 2009, 'Urine-creatinine concentration as a marker of urine dilution: Reflections using a cohort of 45,000 samples', *Forensic Science International,* **186**(1–3): 48-51.

Arthur-Farraj Peter J, Latouche M, Wilton D, Quintes S, Chabrol E, *et al.* 2012, 'c-Jun Reprograms Schwann Cells of Injured Nerves to Generate a Repair Cell Essential for Regeneration', *Neuron,* **75**(4): 633-647.

Ash P, Bieniek K, Gendron T, Caulfield T, Lin L, *et al.* 2013, 'Unconvential translation of C9ORF72 GGGGCC expansion generates insoluble polypeptides specific to c9FTD/ALS', *Neuron,* **77**(4): 639-646.

Atassi N, Berry J, Shui A, Zach N, Sherman A, *et al.* 2014, 'The PRO-ACT database: Design, initial analyses, and predictive features', *Neurology,* **83**(19): 1719-1725.

Atkinson A, Colburn W, Degruttola V, DeMets D, G D, *et al.* 2001, 'Biomarkers and surrogate endpoints: preferred definitions and conceptual framework', *Clinical Pharmacology and Therapeutics,* **69**(3): 89-95.

Ayala Y, De Conti L, Avendano-Vazquez S, Dhir A, Romano M, *et al.* 2011, 'TDP-43 regulates its mRNA levels through a negative feedback loop', *The EMBO Journal,* **30**(2): 277-288.

Baldwin MA 2004, 'Protein identification by mass spectrometry: issues to be considered', *Molecular & Cellular Proteomics,* **3**(1): 1-9.

Balendra R, Jones A, Jivraj N, Knights C, Ellis C, *et al.* 2014, 'Estimating clinical stage of amyotrophic lateral sclerosis from the ALS Functional Rating Scale', *Amyotrophic Lateral Sclerosis & Frontotemporal Degeneration,* **15**(3-4): 279-284.

Bame M, Grier RE, Needleman R & Brusilow WS 2014, 'Amino acids as biomarkers in the SOD1(G93A) mouse model of ALS', *Biochimica et Biophysica Acta - Molecular Basis of Disease,* **1842**(1): 79-87.

Bannwarth S, Ait-El-Mkadem S, Chaussenot A, Genin EC, Lacas-Gervais S, *et al.* 2014, 'A mitochondrial origin for frontotemporal dementia and amyotrophic lateral sclerosis through CHCHD10 involvement', *Brain,* **137**(Pt 8): 2329-2345.

Bär P 2000, 'Motor neuron disease in vitro: the use of cultured motor neurons to study amyotrophic lateral sclerosis', *European Journal of Pharmacology,* **405**(1-3): 285-295.

Barratt J & Topham P 2007, 'Urine proteomics: the present and future of measuring urinary protein components in disease', *Canadian Medical Association Journal,* **177**(4): 361-368.

Barth SK, Kang HK, Bullman TA & Wallin M 2009, 'Neurological mortality among US veterans of the Persian Gulf War: 13‐year follow‐up', *American Journal of Industrial Medicine,* **52**(9): 663-670.

Bastow E, Gourlay C & Tuite M 2011, 'Using yeast models to probe the molecular basis of amyotrophic lateral sclerosis', *Biochemical Society Transactions,* **39**(5): 1482-1487.

Baxmann AC, Ahmed MS, Marques NC, Menon VB, Pereira AB, *et al.* 2008, 'Influence of muscle mass and physical activity on serum and urinary creatinine and serum cystatin C', *Clinical Journal of the American Society of Nephrology*, **3**(2): 348-354.

Beattie M, Harrington A, Lee R, Kim J, Boyce S, *et al.* 2002, 'ProNGF induces p75-mediated death of oligodendrocytes following spinal cord injury', *Neuron*, **36**(3): 375-386.

Bede P, Bokde AL, Byrne S, Elamin M, McLaughlin RL, *et al.* 2013, 'Multiparametric MRI study of ALS stratified for the C9orf72 genotype', *Neurology*, **81**(4): 361-369.

Beers D, Henkel J, Xiao Q, Zhao W, Wang J, *et al.* 2006, 'Wild-type microglia extend survival in PU.1 knockout mice with familial amyotrophic lateral sclerosis', *Proceedings of the National Academy of Sciences, USA*, **103**(43): 16021-16026.

Belli S & Vanacore N 2005, 'Proportionate mortality of Italian soccer players: Is amyotrophic lateral sclerosis an occupational disease?', *European Journal of Epidemiology*, **20**(3): 237-242.

Bellingham M 2011, 'A Review of the Neural Mechanisms of Action and Clinical Efficiency of Riluzole in Treating Amyotrophic Lateral Sclerosis: What have we Learned in the Last Decade?', *CNS Neuroscience & Therapeutics*, **17**(1): 4-31.

Belzil VV, Bauer PO, Prudencio M, Gendron TF, Stetler CT, *et al.* 2013, 'Reduced C9orf72 gene expression in c9FTD/ALS is caused by histone trimethylation, an epigenetic event detectable in blood', *Acta Neuropathologica*, **126**(6): 895-905.

Benatar M & Wuu J 2012, 'Presymptomatic studies in ALS: Rationale, challenges, and approach', *Neurology*, **79**(16): 1732-1739.

Benatar M, Wuu J & Ravits J 2013, 'Opportunity and Innovation in Studying Pre-symptomatic Amyotrophic Lateral Sclerosis', *Muscle & Nerve*, **47**(5): 629-631.

Benda P, Lightbody J, Sato G, Levine L & Sweet W 1968, 'Differentiated rat glial cell strain in tissue culture', *Science*, **161**(3839): 370-371.

Bensimon G, Lacomblez L & Meininger V 1994, 'A controlled trial of riluzole in amyotrophic lateral sclerosis. ALS/Riluzole Study Group.', *New England Journal of Medicine*, **330**(9): 585-591.

Benussi L, Ghidoni R, Pegoiani E, Moretti D, Zanetti O, *et al.* 2009, 'Progranulin Leu271LeufsX10 is one of the most common FTLD and CBS associated mutations worldwide', *Neurobiology of Disease*, **33**(3): 379-385.

Bergomi M, Vinceti M, Nacci G, Pietrini V, Brätter P, *et al.* 2002, 'Environmental exposure to trace elements and risk of amyotrophic lateral sclerosis: a population-based case-control study', *Environmental Research* **89**(2): 116-123.

Bibel M, Hoppe E & Barde YA 1999, 'Biochemical and functional interactions between the neurotrophin receptors trk and p75NTR', *The EMBO Journal*, **18**(3): 616-622.

Bilican B, Serio A, Barmada SJ, Nishimura AL, Sullivan GJ, *et al.* 2012, 'Mutant induced pluripotent stem cell lines recapitulate aspects of TDP-43 proteinopathies and reveal cell-specific vulnerability', *Proceedings of the National Academy of Sciences, USA*, **109**(15): 5803-5808.

Birktoft JJ & Breddam K 1994, 'Glutamyl endopeptidases', *Methods in Enzymology*, **244**: 114-26.

Blackburn D, Sargsyan S, Monk PN & Shaw P 2009, 'Astrocyte function and role in motor neuron disease: A future therapeutic target?', *Glia*, **57**(12): 1251-1264.

Blair I, Williams K, Warraich S, Durnall J, Thoeng A, *et al.* 2010, 'FUS mutations in amyotrophic lateral sclerosis: clinical, pathological, neurophysiological and genetic analysis', *Journal of Neurology, Neurosurgery, and Psychiatry*, **81**(6): 639-645.

Blauw HM, Barnes CP, van Vught PWJ, van Rheenen W, Verheul M, *et al.* 2012, 'SMN1 gene duplications are associated with sporadic ALS', *Neurology*, **78**(11): 776-780.

Blennow K, Hampel H & Zetterberg H 2014, 'Biomarkers in amyloid-beta immunotherapy trials in Alzheimer's disease', *Neuropsychopharmacology*, **39**(1): 189-201.

Blokhuis A, Groen E, Koppers M, van den Berg LH & Pasterkamp R 2013, 'Protein aggregation in amyotrophic lateral sclerosis', *Acta Neuropathologica*, **125**(6): 777-794.

Boillée S, Yamanaka K, Lobsiger C, Copeland N, Jenkins N, *et al.* 2006, 'Onset and Progression in Inherited ALS Determined by Motor Neurons and Microglia', *Science*, **312**(5778): 1389-1392.

Borghero G, Floris G, Cannas A, Marrosu M, Murru M, *et al.* 2011, 'A patient carrying a homozygous p.A382T TARDBP missense mutation shows a syndrome including ALS, extrapyramidal symptoms, and FTD', *Neurobiology of Aging*, **32**(12): 2327.e1-2327.e5.

Bosco D, Morfini G, Karabacak N, Song Y, Gros-Louis F, *et al.* 2010, 'Wild-type and mutant SOD1 share an aberrant conformation and a common pathogenic pathway in ALS', *Nature Neuroscience*, **13**(11): 1396-1403.

Bowser R, Cudkowicz M & Kaddurah-Daouk R 2006, 'Biomarkers for amyotrophic lateral sclerosis', *Expert Review of Molecular Diagnostics*, **6**(3): 387-398.

Bowser R, Turner MR & Shefner J 2011, 'Biomarkers in amyotrophic lateral sclerosis: opportunities and limitations', *Nature Reviews Neurology*, **7**(11): 631-638.

Boylan K, Glass J, Crook J, Yang C, Thomas C, *et al.* 2013, 'Phosphorylated neurofilament heavy subunit (pNF-H) in peripheral blood and CSF as a potential prognostic biomarker in amyotrophic lateral sclerosis', *Journal of Neurology, Neurosurgery, and Psychiatry*, **84**(4): 467-472.

Boylan K, Yang C, Crook J, Overstreet K, Heckman M, *et al.* 2009, 'Immunoreactivity of the phosphorylated axonal neurofilament H subunit (pNF-H) in blood of ALS model rodents and ALS patients: evaluation of blood pNF-H as a potential ALS biomarker', *Journal of Neurochemistry*, **111**(5): 1182-1191.

Bozik M, Mather J, Krammer W, Gribkoff V & Ingersholl E 2011, 'Safety, tolerability and pharmacokinetics of KNS-760704 (Dexpramipexole) in healthy adult subjects', *Journal of Clinical Pharmacology*, **51**(8): 1177-1185.

Brettschneider J, Libon D, Toldeo J, Xie S, McCluskey L, *et al.* 2012a, 'Microglial activation and TDP-43 pathology correlate with executive dysfunction in amyotrophic lateral sclerosis', *Acta Neuropathologica*, **123**(3): 395-407.

Brettschneider J, Petzold A, Süssmuth S, Ludolph A & Tumani H 2006, 'Axonal damage markers in cerebrospinal fluid are increased in ALS', *Neurology*, **66**(6): 852-856.

Brettschneider J, Toledo J, Van Deerlin V, Elman L, McCluskey L, *et al.* 2012b, 'Microglial Activation Correlates with Disease Progression and Upper Motor Neuron Clinical Symptoms in Amyotrophic Lateral Sclerosis', *PLoS One,* **7**(6): e39216.

Brinkham J, Andres P, Mendoza M & Sanjak M 1997, 'Guidelines for the use and performance of quantitative outcome measures in ALS clinical trials', *Journal of the Neurological Sciences,* **147**(1): 97-111.

Brockington A, Ning K, Heath P, Wood E, Kirby J, *et al.* 2013, 'Unravelling the enigma of selective vulnerability in neurodegeneration: motor neurons resistant to degeneration in ALS show distinct gene expression characteristics and decreased susceptibility to excitotoxicity', *Acta Neuropathologica,* **125**(1): 95-109.

Broich K 2007, 'Outcome measures in clinical trials on medicinal products for the treatment of dementia: a European regulatory perspective', *International Psychogeriatrics,* **19**(3): 509-524.

Brooks BR 1994, 'El Escorial World Federation of Neurology Criteria for the Diagnosis of Amyotrophic Lateral Sclerosis', *Journal of Neurological Sciences,* **124**: 96-107.

Brooks BR, Miller RG, Swash M & Munsat T 2000, 'El Escorial revisited: revised criteria for the diagnosis of amyotrophic lateral sclerosis', *Amyotrophic Lateral Sclerosis and Other Motor Neuron Disorders,* **1**(5): 293-299.

Bruijn LI, Becher MW, Lee MK, Anderson KL, Jenkins NA, *et al.* 1997, 'ALS-linked SOD1 mutant G85R mediates damage to astrocytes and promotes rapidly progressive disease with SOD1-containing inclusions', *Neuron,* **18**(2): 327-338.

Bruijn LI, Miller TM & Cleveland D 2004, 'Unraveling the mechanisms involved in motor neuron degeneration in ALS', *Annual Review of Neuroscience,* **27**: 723-749.

Brunello N, Reynolds M, Wrathall J & Mocchetti I 1990, 'Increased nerve growth factor receptor mRNA in contused rat spinal cord', *Neuroscience Letters,* **118**(2): 238-240.

Buratti E & Baralle F 2008, 'Multiple roles of TDP-43 in gene expression, splicing regulation and human disease', *Frontiers in Bioscience,* **13**: 867-878.

Buratti E & Baralle F 2010, 'The multiple roles of TDP-43 in pre-mRNA processing and gene expression regulation', *RNA Biology,* **7**(4): 420-429.

Burke RE, Levine DN, Tsairis P & Zajac FE, 3rd 1973, 'Physiological types and histochemical profiles in motor units of the cat gastrocnemius', *Journal of Physiology,* **234**(3): 723-748.

Byrne S, Elamin M, Bede P, Shatunov A, Walsh C, *et al.* 2012, 'Cognitive and clinical characteristics of patients with amyotrophic lateral sclerosis carrying a C9orf72 repeat expansion: a population-based cohort study', *Lancet Neurology,* **11**(3): 232-240.

Byrne S, Walsh C, Lynch C, Bede P, Elamin M, *et al.* 2011, 'Rate of familial amyotrophic lateral sclerosis: a systematic review and meta-analysis', *Journal of Neurology, Neurosurgery, and Psychiatry,* **82**(6): 623-627.

Callaghan B, Feldman D, Gruis K & Feldman E 2011, 'The Association of Exposure to Lead, Mercury, and Selenium and the Development of Amyotrophic Lateral Sclerosis and the Epigenetic Implications', *Neurodegenerative Diseases,* **8**(1-2): 1-8.

Cannon A, Yang B, Knight J, Farnham I, Zhang Y, *et al.* 2012, 'Neuronal sensitivity to TDP-43 overexpression is dependent on timing of induction', *Acta Neuropathologica*, **123**(6): 807-823.

Carew J, Nair G, Andersen P, Wuu J, Gronka S, *et al.* 2011, 'Presymptomatic spinal cord neurometabolic findings in SOD1-positive people at risk for familial ALS', *Neurology*, **77**(14): 1370-1375.

Carriedo S, Yin H & Weiss J 1996, 'Motor neurons are selectively vulnerable to AMPA/kainite receptor-mediated injury in vitro', *Journal of Neuroscience*, **16**(13): 4069-4079.

Cashman NR, Durham HD, Blusztajn JK, Oda K, Tabira T, *et al.* 1992, 'Neuroblastoma × spinal cord (NSC) hybrid cell lines resemble developing motor neurons', *Developmental Dynamics*, **194**(3): 209-221.

Cedarbaum JM, Stambler N, Malta E, Fuller C, Hilt D, *et al.* 1999, 'The ALSFRS-R: a revised ALS functional rating scale that incorporates assessments of respiratory function', *Journal of Neurological Sciences*, **169**(1-2): 13-21.

Cellura E, Spataro R, Taiello A & La Bella V 2012, 'Factors affecting the diagnostic delay in amyotrophic lateral sclerosis', *Clinical Neurology and Neurosurgery*, **114**(6): 550-554.

Chadha V, Garg U & Alon US 2001, 'Measurement of urinary concentration: a critical appraisal of methodologies', *Pediatric Nephrology*, **16**(4): 374-382.

Chambers D, Peters J & Abbott C 1998, 'The lethal mutation of the mouse wasted (*wst*) is a deletion that abolishes expression of a tissue-specific isoform of translation elongation factor 1α, encoded by the Eef1α2 gene', *Proceedings of the National Academy of Sciences, USA*, **95**(8): 4463-4468.

Chang Y, Kong Q, Shan X, Tian G, Ilieva H, *et al.* 2008, 'Messenger RNA oxidation occurs early in disease pathogenesis and promotes motor neuron degeneration in ALS', *PLoS One*, **3**(8): e2849.

Chao M 2003, 'Neurotrophins and their receptors: A convergence point for many signalling pathways', *Nature Reviews Neuroscience*, **4**(4): 299-309.

Charcot J 1874, 'Amyotrophies spinales deuteropathiques scle´rose late´rale amyotrophique & Scle´rose late´rale amyotrophique', *Bureaux du Progre`s Me´dical* **2**: 234-266.

Charcot JM & Joffory A 1869, ' Deux cas d'atrophie musculaire progressive avec lesions de la substance grise et des faisceaux antero-lateraux de la moelle epiniere', *Archives of Physiology Neurology & Pathology*, **2**: 744–754

Chaussenot A, Le Ber I, Ait-El-Mkadem S, Camuzat A, de Septenville A, *et al.* 2014, 'Screening of CHCHD10 in a French cohort confirms the involvement of this gene in frontotemporal dementia with amyotrophic lateral sclerosis patients', *Neurobiology of Aging*, **35**(12): 2884 e1- 2884 e4.

Cheah BC, Vucic S, Krishnan AV, Boland R & Kiernan M 2011, 'Neurophysiological index as a biomarker for ALS progression: Validity of mixed effects models', *Amyotrophic Lateral Sclerosis*, **12**(1): 33-38.

Cheetham S, Smith A, Armstrong S, Beynon R & Hurst J 2009, 'Limited variation in the major urinary proteins of laboratory mice', *Physiology & Behavior*, **96**(2): 253-261.

Chen A, Weimer L, Brannagan Tr, Colin M, Andrews J, *et al.* 2010, 'Experience with the Awaji Island modifications to the ALS diagnostic criteria', *Muscle & Nerve*, **42**(5): 831-832.

Chen X, Guo X, Huang R, Zheng Z, Chen Y, *et al.* 2014, 'An exploratory study of serum creatinine levels in patients with amyotrophic lateral sclerosis', *Neurological Sciences*, **35**(10): 1591-1597.

Chen YZ, Bennett CL, Huynh HM, Blair IP, Puls I, *et al.* 2004, 'DNA/RNA helicase gene mutations in a form of juvenile amyotrophic lateral sclerosis (ALS4)', *American Journal of Human Genetics,* **74**(6): 1128-1135.

Cheramy A, Barbeito L, Godeheu G & Glowinski J 1992, 'Riluzole inhibits the release of glutamate in the caudate nucleus of the cat in vivo', *Neuroscience Letters,* **147**(2): 209-212.

Chilton L, Middlemas A, Gardiner N & Tomlinson DR 2004, 'The p75 neurotrophin receptor appears in plasma in diabetic rats—characterisation of a potential early test for neuropathy', *Diabetologia,* **47**(11): 1924-1930.

Chiò A, Calvo A, Bovio G, Canosa A, Bertuzzo D, *et al.* 2014, 'Amyotrophic lateral sclerosis outcome measures and the role of albumin and creatinine: a population-based study', *JAMA Neurology,* **71**(9): 1134-1142.

Chiò A, Calvo A, Mazzini L, Cantello R, Mora G, *et al.* 2012, 'Extensive genetics of ALS: a population-based study in Italy', *Neurology,* **79**(19): 1983-1989.

Chio A, Calvo A, Mazzini L, Cantello R, Mora G, *et al.* 2012, 'Extensive genetics of ALS: a population-based study in Italy', *Neurology,* **79**(19): 1983-1989.

Chiò A, Calvo A, Moglia C, Mazzini L & Mora G 2011, 'Phenotypic heterogeneity of amyotrophic lateral sclerosis: a population based study', *Journal of Neurology, Neurosurgery, and Psychiatry,* **82**(7): 740-746.

Chiò A, Calvo A, Moglia C, Restagno G, Ossola I, *et al.* 2010, 'Amyotrophic lateral sclerosis-frontotemporal lobar dementia in 3 families with p.Ala382Thr TARDBP mutations', *Archives of Neurology,* **67**(8): 1002-1009.

Chiò A, Hammond E, Mora G, Bonito V & Filippini G 2013a, 'Development and evaluation of a clinical staging system for amyotrophic lateral sclerosis', *Journal of Neurology, Neurosurgery, and Psychiatry,* **86**(1): 38-44.

Chiò A, Logroscino G, Hardiman O, Swingler R, Mitchell D, *et al.* 2009, 'Prognostic factors in ALS: A critical review', *Amyotrophic Lateral Sclerosis,* **10**(5-6): 310-323.

Chiò A, Logroscino G, Traynor BJ, Collins J, Simeone J, *et al.* 2013b, 'Global Epidemiology of Amyotrophic Lateral Sclerosis: A Systematic Review of the Published Literature', *Neuroepidemiology,* **41**(2): 118-130.

Chiò A, Magnani C & Schiffer D 1995, 'Gompertzian analysis of amyotrophic lateral sclerosis mortality in Italy, 1957-1987; application to birth cohorts', *Neuroepidemiology,* **14**(6): 269-277.

Chiu AY, Zhai P, Dal Canto MC, Peters TM, Kwon YW, *et al.* 1995, 'Age-dependent penetrance of disease in a transgenic mouse model of familial amyotrophic lateral sclerosis', *Molecular and Cellular Neurosciences,* **6**(4): 349-362.

Cho E, Kim H, Lee J, Jeong-Ju Y, Choi W, *et al.* 2014, 'Serum insulin-like growth factor-1 predicts disease progression and survival in patients with hepatocellular carcinoma who undergo transarterial chemoembolization', *PloS One,* **9**(3): e90862.

Choudry R & Cudkowicz M 2005, 'Clinical trials in amyotrophic lateral sclerosis: the tenuous past and the promising future', *Journal of Clinical Pharmacology,* **45**(12): 1334-1344.

Chow CY, Landers JE, Bergren SK, Sapp PC, Grant AE, *et al.* 2009, 'Deleterious variants of FIG4, a phosphoinositide phosphatase, in patients with ALS', *American Journal of Human Genetics,* **84**(1): 85-88.

Cima V, Logroscino G, D'Ascenzo C, Palmieri A, Volpe M, *et al.* 2009, 'Epidemiology of ALS in Padova district, Italy, from 1992 to 2005', *European Journal of Neurology,* **16**(8): 920-924.

Clavelou P, Blanquet M, Peyrol F, Ouchchane L & Gerbaud L 2013, 'Rates of progression of weight and forced vital capacity as relevant measurement to adapt amyotrophic lateral sclerosis management for patient Result of a French multicentre cohort survey', *Journal of the Neurological Sciences,* **331**(1-2): 126-131.

Clement A, Nguyen M, Roberts E, Garcia M, Boillée S, *et al.* 2003, 'Wild-Type Nonneuronal Cells Extend Survival of SOD1 Mutant Motor Neurons in ALS Mice', *Science,* **302**(5642): 113-117.

Cleveland DW & Rothstein JD 2001, 'From Charcot to Lou Gehrig: deciphering selective motor neuron death in ALS', *Nature Reviews Neuroscience,* **2**(11): 806-819.

Comte B, Franceschi C, Sadoulet M, Silvy F, Lafitte D, *et al.* 2006, 'Detection of bile salt-dependent lipase, a 110 kDa pancreatic protein, in urines of healthy subjects', *Kidney International,* **69**(6): 1048-1055.

Conte A, Lattante S, Luigetti M, Del Grande A, Romano A, *et al.* 2012, 'Classification of familial amyotrophic lateral sclerosis by family history: effects on frequency of genes mutation', *Journal of Neurology, Neurosurgery, and Psychiatry,* **83**(12): 1201-1203.

Conti M, Zater M, Lallali K, Durrbach A, Moutereau S, *et al.* 2005, 'Absence of circadian variations in urine cystatin C allows its use on urinary samples', *Clinical Chemistry,* **51**(1): 272-273.

Copray J, Jaarsma D, Küst B, Bruggeman R, Mantingh I, *et al.* 2003, 'Expression of the low affinity neurotrophin receptor p75 in spinal motoneurons in a transgenic mouse model for amyotrophic lateral sclerosis', *Neuroscience,* **116**(3): 685-694.

Corcia P, Camu W, Halimi J, Vourc'h P, Antar C, *et al.* 2006, 'SMN1 gene, but not SMN2, is a risk factor for sporadic ALS', *Neurology,* **67**(7): 1147-1150.

Corcia P, Mayeux-Portas V, Khoris J, de Toffol B, Autret A, *et al.* 2002, 'Abnormal SMN1 gene copy number is a susceptibility factor for amyotrophic lateral sclerosis', *Annals of Neurology,* **51**(2): 243-246.

Côté F, Collard J & Julien J 1993, 'Progressive neuronopathy in transgenic mice expressing the human neurofilament heavy gene: a mouse model of amyotrophic lateral sclerosis', *Cell,* **73**(1): 35-46.

Coulson E, Reid K, Baca M, Shipham K, Hulett S, *et al.* 2000, 'Chopper, a New Death Domain of the p75 Neurotrophin Receptor That Mediates Rapid Neuronal Cell Death', *Journal of Biological Chemistry,* **275**(39): 30537-30545.

Coussee E, De Smet P, Bogaert E, Elens I, Van Damme P, *et al.* 2011, 'G37R SOD1 mutant alters mitochondrial complex I activity, Ca (2+) uptake and ATP production', *Cell Calcium,* **49**(4): 217-225.

Couthouis J, Hart M, Shorter J, DeJesus-Hernandez M, Erion R, *et al.* 2011, 'A yeast functional screen predicts new candidate ALS disease genes', *Proceedings of the National Academy of Sciences, USA,* **108**(52): 20881-20890.

Cox LE, Ferraiuolo L, Goodall EF, Heath PR, Higginbottom A, *et al.* 2010, 'Mutations in CHMP2B in lower motor neuron predominant amyotrophic lateral sclerosis (ALS)', *PLoS One,* **5**(3): e9872.

Cox P, Richer R, Metcalf J, Banack S, Codd G, *et al.* 2009, 'Cyanobacteria and BMAA exposure from desert dust: a possible link to sporadic ALS among Gulf War veterans', *Amyotrophic Lateral Sclerosis* **Suppl2**: 109-117.

Crisp M, Beckett J, Coates J & Miller T 2013, 'Canine degenerative myelopathy: biochemical characterization of superoxide dismutase 1 in the first naturally occuring non-human amyotrophic lateral sclerosis model', *Experimental Neurology*, **248**: 1-9.

Crowther J 2001. *The ELISA guidebook*, Totowa, New Jersey, USA, Humana Press.

Cudkowicz M, Bozik ME, Ingersoll EW, Miller R, Mitsumoto H, *et al.* 2011, 'The effects of dexpramipexole (KNS-760704) in individuals with amyotrophic lateral sclerosis', *Nature Medicine*, **17**(12): 1652-1656.

Cudkowicz M, McKenna-Yasek D, Sapp P, Chin W, Geller B, *et al.* 1997, 'Epidemiology of mutations in superoxide dismutase in amyotrophic lateral sclerosis', *Annals of Neurology*, **41**(2): 210-221.

Cudkowicz M, van den Berg L, Shefner J, Mitsumoto H, Mora J, *et al.* 2013, 'Dexpramipexole versus placebo for patients with amyotrophic lateral sclerosis (EMPOWER): a randomised, double-blind, phase 3 trial', *Lancet Neurology*, **12**(11): 1059-1067.

Czaplinski A, Yen AA & Appel SH 2006, 'Forced vital capacity (FVC) as an indicator of survival and disease progression in an ALS clinic population', *Journal of Neurology, Neurosurgery, and Psychiatry*, **77**(3): 390-392.

Danzeisen R, Schwalenstöcker B, Gillardon F, Buerger E, Krzykalla V, *et al.* 2006, 'Targeted antioxidative and neuroprotective properties of the dopamine agonist pramipexole and its nondopamergic enantiomer SND919CL2x [(+)2-amino-4,5,6,7-tetrahydro-6-Lpropylamino-benzathiazole dyhydrochloride]', *Journal of Pharmacology and Experimental Therapeutics*, **316**(1): 189-199.

Daoud H, Zhou S, Noreau A, Sabbagh M, Belzil V, *et al.* 2012, 'Exome sequencing reveals SPG11 mutations causing juvenile ALS', *Neurobiology of Aging*, **33**(4): 839.e5-839.e9.

de Carvalho M, Dengler R, Eisen A, England J, Kaji R, *et al.* 2008a, 'Electrodiagnostic criteria for diagnosis of ALS', *Clinical Neurophysiology*, **119**(3): 497-503.

de Carvalho MA, Pinto S & Swash M 2008b, 'Paraspinal and limb motor neuron involvement within homologous spinal segments in ALS', *Clinical Neurophysiology*, **119**(7): 1607-1613.

de Jong D, Jansen RW, Pijnenburg YA, van Geel WJ, Borm GF, *et al.* 2007, 'CSF neurofilament proteins in the differential diagnosis of dementia', *Journal of Neurology Neurosurgery, and Psychiatry*, **78**(9): 936-938.

de Munck E, Muñoz-Sáez E, Miguel BG, Solas MT, Ojeda I, *et al.* 2013, 'β-N-methylamino-l-alanine causes neurological and pathological phenotypes mimicking Amyotrophic Lateral Sclerosis (ALS): The first step towards an experimental model for sporadic ALS', *Environmental Toxicology and Pharmacology*, **36**(2): 243-255.

De Vos K, Chapman A, Tennant M, Manser C, Tudor E, *et al.* 2007, 'Familal amyotrophic lateral sclerosis-linked SOD1 mutants perturb fast axonal transport to reduce axonal mitochondrial content', *Human Molecular Genetics*, **16**(22): 2720-2728.

Dechant G & Barde YA 1997, 'Signalling through the neurotrophin receptor p75NTR', *Current Opinion in Neurobiology*, **7**(3): 413-418.

DeJesus-Hernandez M, Mackenzie Ian R, Boeve Bradley F, Boxer Adam L, Baker M, *et al.* 2011, 'Expanded GGGGCC Hexanucleotide Repeat in Noncoding Region of C9ORF72 Causes Chromosome 9p-Linked FTD and ALS', *Neuron*, **72**(2): 245-256.

Del Signore SJ, Amante DJ, Kim J, Stack EC, Goodrich S, *et al.* 2009, 'Combined riluzole and sodium phenylbutyrate therapy in transgenic amyotrophic lateral sclerosis mice', *Amyotrophic Lateral Sclerosis*, **10**(2): 85-94.

Della-Bianca V, Rossi F, Armato U, Dal-Pra I, Constantini C, *et al.* 2001, 'Neurotrophin p75 receptor is involved in neuronal damage by prion peptide-(106-126)', *Journal of Biological Chemistry*, **276**(42): 38929-38933.

Deng H-X, Zhai H, Bigio E, Yan J, Fecto F, *et al.* 2010, 'FUS-immunoreactive inclusions are a common feature in sporadic and non-SOD1 familial amyotrophic lateral sclerosis', *Annals of Neurology*, **67**(6): 739-748.

Deng HX, Chen W, Hong ST, Boycott KM, Gorrie GH, *et al.* 2011, 'Mutations in UBQLN2 cause dominant X-linked juvenile and adult-onset ALS and ALS/dementia', *Nature*, **477**(7363): 211-215.

Dengler R, Konstanzer A, Küther G, Hesse S, Wolf W, *et al.* 1990, 'Amyotrophic lateral sclerosis: macro-EMG and twitch forces of single motor units', *Muscle & Nerve*, **13**(6): 545-550.

Dewil M, dela Cruz V, Van Den Bosch L & Robberect W 2007, 'Inhibition of p38 mitogen activated protein kinase activation and mutant SOD1(G93A)-induced motor neuron death', *Neurobiology of Disease*, **26**(2): 332-341.

Dimos J, Rodolfa K, Niakan K, Weisenthal L, Mitsumoto H, *et al.* 2008, 'Induced pluripotent stem cells generated from patients with ALS can be differentiated into motor neurons', *Science*, **321**(5893): 1218-1221.

DiStefano P & Johnson E 1988, 'Identification of a truncated form of the nerve growth factor receptor', *Proceedings of the National Academy of Sciences, USA*, **85**(1): 270-274.

DiStefano PS, Clagett-Dame M, Chelsea D & Loy R 1991, 'Developmental regulation of human truncated nerve growth factor receptor', *Annals of Neurology*, **29**(1): 13-20.

Doble A & Kennel P 2000, 'Animal models of amyotrophic lateral sclerosis', *Amyotrophic Lateral Sclerosis and Other Motor Neuron Diseases*, **1**(5): 301-312.

Dobrowolny G, Aucello M, Rizzuto E, Beccafico S, Mammucari C, *et al.* 2008, 'Skeletal muscle is a primary target of SOD1G93A-mediated toxicity', *Cell Metabolism*, **8**(5): 425-436.

Donnelly C, Zhang P, Pham J, Haeusler A, Mistry N, *et al.* 2013, 'RNA toxicity from the ALS/FTD C9ORF72 expansion is mitigated by antisense intervention', *Neuron*, **80**(2): 415-428.

Douglass C, Kandler R, Shaw P & McDermott C 2010, 'An evaluation of neurophysiological criteria used in the diagnosis of motor neuron disease', *Journal of Neurology, Neurosurgery, and Psychiatry*, **81**(6): 646-649.

Dowling P, Ming X, Raval S, Husar W, Casaccia-Bonnefil P, *et al.* 1999, 'Up-regulated p75NTR neurotrophin receptor on glial cells in MS plaques', *Neurology*, **53**(8): 1676-1682.

Drachman D, Frank K, Dkyes-Hoberg M, Teismann P, Almer G, *et al.* 2002, 'Cycloosygenase 2 inhibition protects motor neurons and prolongs survival in a transgenic mouse model of ALS', *Annals of Neurology*, **52**(6): 771-778.

Duan W, Li X, Shi J, Gou Y, Li Z, *et al.* 2010, 'Mutant TAR DNA-binding protein-43 induces oxidative injury in motor neuron-like cell', *Neuroscience*, **169**(4): 1621-1629.

Dujmovic I, Lunn MP, Reilly MM & Petzold A 2013, 'Serial cerebrospinal fluid neurofilament heavy chain levels in severe Guillain-Barre syndrome', *Muscle Nerve*, **48**(1): 132-134.

Dunlop R, Cox P, Banack S & Rodgers K 2013, 'The non-protein amino acid BMAA is misincorporated into human proteins in place of L-serine causing protein misfolding and aggregation', *PLoS One*, **8**(9): e75376.

Eisen A, Kiernan M, Mitsumoto H & Swash M 2014, 'Amyotrophic lateral sclerosis: a long preclinical period?', *Journal of Neurology, Neurosurgery, and Psychiatry*, **85**(11): 1232-1238.

Ekegren T, Hanrieder J & Bergquist J 2008, 'Clinical perspectives of high-resolution mass spectrometry-based proteomics in neuroscience: exemplified in amyotrophic lateral sclerosis biomarker discovery research', *Journal of Mass Spectrometry*, **43**(5): 559-571.

Ekestern E 2004, 'Neurotrophic factors and amyotrophic lateral sclerosis', *Neurodegenerative Diseases*, **1**(2-3): 88-100.

El-Sharkawi F, El Sabah M, Hassan Z & Khaled H 2014, 'The biochemical value of urinary metalloproteinases 3 and 9 in diagnosis and prognosis of bladder cancer in Egypt', *Journal of Biomedical Science*, **21**(72).

Elden AC, Kim HJ, Hart MP, Chen-Plotkin AS, Johnson BS, *et al.* 2010, 'Ataxin-2 intermediate-length polyglutamine expansions are associated with increased risk for ALS', *Nature*, **466**(7310): 1069-1075.

Engvall E & Perlmann P 1972, 'Enzyme-linked immunosorbent assay (ELISA) Quantitative assay of immunoglobulin G', *Immunohistochemistry*, **8**: 871-874.

Ernfors P, Henschen A, Olson L & Persson H 1989, 'Expression of nerve growth factor receptor mRNA is developmentally regulated and increased after axotomy in rat spinal cord motoneurons', *Neuron*, **2**(6): 1605-1613.

Esmaeili M, Panahi M, Yadav S, Hennings L & Kiaei M 2013, 'Premature death of TDP-43 (A315T) transgenic mice due to gastrointestinal complications prior to development of full neurological symptoms of amyotrophic lateral sclerosis', *International Journal of Experimental Pathology*, **94**(1): 56-64.

Evans MC, Serres S, Khrapitchev AA, Stolp HB, Anthony DC, *et al.* 2014, 'T(2)-weighted MRI detects presymptomatic pathology in the SOD1 mouse model of ALS', *Journal of Cerebral Blood Flow & Metabolism*, **34**(5): 785-93.

Fawcett T 2006, 'An introduction to ROC analysis', *Pattern Recognition Letters*, **27**(8): 861-874.

Fecto F, Yan J, Vemula SP, Liu E, Yang Y, *et al.* 2011, 'SQSTM1 mutations in familial and sporadic amyotrophic lateral sclerosis', *Archives of Neurology*, **68**(11): 1440-1446.

Ferraiuolo L, Higginbottom A, Heath P, Barber S, Greenald D, *et al.* 2011a, 'Dysregulation of astrocyte-motoneuron cross-talk in mutant superoxide dismutase 1-related amyotrophic lateral sclerosis', *Brain*, **134**(Pt 9): 2627-2641.

Ferraiuolo L, Kirby J, Grierson AJ, Sendtner M & Shaw PJ 2011b, 'Molecular pathways of motor neuron injury in amyotrophic lateral sclerosis', *Nature Reviews Neurology*, **7**(11): 616-630.

Ferri CC, Moore FA & Bisby MA 1997, 'Effects of facial nerve injury on mouse motoneurons lacking the p75 low-affinity neurotrophin receptor', *Journal of Neurobiology*, **34**(1): 1-9.

Fiala M, Mizwicki MT, Weitzman R, Magpantay L & Nishimoto N 2013, 'Tocilizumab infusion therapy normalizes inflammation in sporadic ALS patients', *American Journal of Neurodegenerative Disease*, **2**(2): 129-139.

Figlewicz DA, Krizus A, Martinoli MG, Meininger V, Dib M, *et al.* 1994, 'Variants of the heavy neurofilament subunit are associated with the development of

amyotrophic lateral sclerosis', *Human Molecular Genetics,* **3**(10): 1757-1761.

Finehout EJ & Lee KH 2004, 'An introduction to mass spectrometry applications in biological research', *Biochemistry and Molecular Biology Education,* **32**(2): 93-100.

Finlayson J, Potter M & Runner C 1963, 'Electrophoretic variation and sex dimorphism of the Major Urinary Protein complex in inbred mice: a new genetic marker', *Journal of the National Cancer Institute,* **31**: 91-107.

Fitzmaurice P, Shaw I, Kleiner H, Miller R, Monks T, *et al.* 1996, 'Evidence for DNA damage in amyotrophic lateral sclerosis', *Muscle & Nerve,* **19**(6): 797-798.

Floyd A, Yu Q, Piboolnurak P, Tang M, Fang Y, *et al.* 2009, 'Transcranial magnetic stimulation in ALS: utility of central motor conduction tests', *Neurology,* **72**(6): 498-504.

Flurkey K & Currer JM 2004, 'Pitfalls of animal model systems in ageing research', *Best Practice & Research Clinical Endocrinology & Metabolism,* **18**(3): 407-421.

Fombonne J, Rabizadeh S, Banawit S, Mehlen P & Bredesen D 2009, 'Selective vulnerability in Alzheimer's disease: amyloid precursor protein and p75(NTR) interaction', *Annals of Neurology,* **65**(3): 294-303.

Fornai F, Longone P, Cafaro L, Kastsiuchenka O, Ferrucci M, *et al.* 2008, 'Lithium delays progression of amyotrophic lateral sclerosis', *Proceedings of the National Academy of Sciences, USA,* **105**(6): 2052-2057.

Fournier C & Glass JD 2015, 'Modeling the course of amyotrophic lateral sclerosis', *Nature Biotechnology,* **33**(1): 45-47.

Frade J, Rodríguez-Tébar A & Barde Y 1996, 'Induction of cell death by endogenous nerve growth factor through its p75 receptor', *Nature,* **383**(6596): 166-168.

Frakes A, Ferraiuolo L, Haidet-Phillips AM, Schmelzer L, Braun L, *et al.* 2014, 'Microglia Induce Motor Neuron Death via the Classical NF-κB Pathway in Amyotrophic Lateral Sclerosis', *Neuron,* **81**(5): 1009-1023.

Franchignoni F, Mora G, Giordano A, Volanti P & Chiò A 2013, 'Evidence of multidimensionality in the ALSFRS-R Scale: a critical appraisal on its measurement properties using Rasch analysis', *Journal of Neurology, Neurosurgery, and Psychiatry,* **84**(12): 1340-1345.

Freischmidt A, Muller K, Zondler L, Weydt P, Volk AE, *et al.* 2014, 'Serum microRNAs in patients with genetic amyotrophic lateral sclerosis and pre-manifest mutation carriers', *Brain,* **137**(Pt 11): 2938-2950.

Frey D, Schneider C, Xu L, Borg J, Spooren W, *et al.* 2000, 'Early and selective loss of neuromuscular synapse subtypes with low sprouting competence in motoneuron diseases', *Journal of Neuroscience,* **20**(7): 2534-2542.

Fridovich I 1986, 'Superoxide dismutases', *Advances in Enzymology and Related Areas of Molecular Biology,* **58**: 61-97.

Friedman WJ, Olson L & Persson H 1991, 'Temporal and spatial expression of NGF receptor mRNA during postnatal rat brain development analyzed by *in situ* hybridization', *Brain Research. Developmental Brain Research,* **63**(1-2): 43-51.

Gaiottino J, Norgren N, Dobson R, Topping J, Nissim A, *et al.* 2013, 'Increased neurofilament light chain blood levels in neurodegenerative neurological diseases', *PLoS One,* **8**(9): e75091.

Ganesalingam J, An J, Bowser R, Andersen PM & Shaw CE 2013, 'pNfH is a promising biomarker for ALS', *Amyotrophic Lateral Sclerosis & Frontotemporal Degeneration,* **14**(2): 146-149.

Ganesalingam J, An J, Shaw CE, Shaw G, Lacomis D, *et al.* 2011, 'Combination of neurofilament heavy chain and complement C3 as CSF biomarkers for ALS', *Journal of Neurochemistry,* **117**(3): 528-537.

Giard DJ, Aaronson SA, Todaro GJ, Arnstein P, Kersey JH, *et al.* 1973, 'In vitro cultivation of human tumors: establishment of cell lines derived from a series of solid tumors', *Journal of the National Cancer Institute,* **51**(5): 1417-1423.

Gitcho M, Baloh R, Chakraverty S, Mayo K, Norton J, *et al.* 2008, 'TDP-43 A315T mutation in familial motor neuron disease', *Annals of Neurology,* **63**(4): 535-538.

Glaser V, Nazari E, Müller Y, Feksa L, Wannmacher C, *et al.* 2010, 'Effects of inorganic selenium administration in methylmercury-induced neurotoxicity in mouse cerebral cortex', *International Journal of Developmental Neuroscience* **28**(7): 631-637.

Goldknopf I, Sheta E, Bryson J, Folsom B, Wilson C, *et al.* 2006, 'Complement C3c and related protein biomarkers in amyotrophic lateral sclerosis and Parkinson's disease', *Biochemical and Biophysical Research Communications,* **342**(4): 1034-1039.

Gomes C, Palma A, Almeida R, Regalla M, McCluskey L, *et al.* 2008, 'Establishment of a cell model of ALS disease: Golgi apparatus disruption occurs independently from apoptosis', *Biotechnology Letters,* **30**(4): 603-610.

Gong YH, Parsadanian AS, Andreeva A, Snider WD & Elliott JL 2000, 'Restricted expression of G86R Cu/Zn superoxide dismutase in astrocytes results in astrocytosis but does not cause motoneuron degeneration', *Journal of Neuroscience,* **20**(2): 660-665.

Good D, Thongboonkerd V, Novak J, Bascands J, Schanstra J, *et al.* 2007, 'Body fluid proteomics for biomarker discovery: lessons from the past hold the key to success in the future', *Journal of Proteome Research,* **6**(12): 4549-4555.

Gordon P 2011, 'Amyotrophic Lateral Sclerosis: Pathophysiology, Diagnosis and Management', *CNS Drugs,* **25**(1): 1-15.

Gordon PH & Meininger V 2011, 'How can we improve clinical trials in amyotrophic lateral sclerosis?', *Nature Reviews Neurology,* **7**(11): 650-654.

Gordon PH, Miller RG & Moore DH 2004, 'ALSFRS‐R', *Amyotrophic Lateral Sclerosis and Other Motor Neuron Diseases,* **5**(Suppl 1): 90-93.

Grad L & Cashman C 2013, 'Prion-like activity of Cu/Zn superoxide dismutatse: Implications for amyotrophic lateral sclerosis', *Prion,* **8**(1): 33-41.

Greenway MJ, Andersen PM, Russ C, Ennis S, Cashman S, *et al.* 2006, 'ANG mutations segregate with familial and 'sporadic' amyotrophic lateral sclerosis', *Nature Genetics,* **38**(4): 411-413.

Gresle MM, Liu Y, Dagley LF, Haartsen J, Pearson F, *et al.* 2014, 'Serum phosphorylated neurofilament-heavy chain levels in multiple sclerosis patients', *Journal of Neurology, Neurosurgery, and Psychiatry,* **85**(11): 1209-1213.

Gros-Louis F, Kriz J, Kabashi E, McDearmid J, Millecamps S, *et al.* 2008, 'Als2 mRNA splicing variants detected in KO mice rescue severe motor dysfunction phenotype in Als2 knock-down zebrafish', *Human Molecular Genetics,* **17**(17): 2691-2702.

Gros-Louis F, Larivière R, Gowing G, Laurent S, Camu W, *et al.* 2004, 'A frameshift deletion in peripherin gene associated with amyotrophic lateral sclerosis', *Journal of Biological Chemistry,* **279**(44): 45951-45956.

Grossman M, Elman L, McCluskey L, McMillan C, Boller A, *et al.* 2014, 'Phosphorylated Tau as a candidate biomarker for amyotrophic lateral sclerosis', *JAMA Neurology,* **71**(4): 442-448.

Gunnarsson L, Dahlbom K & Strandman E 1991, 'Motor neuron disease and dementia reported among 13 members of a single family', *Acta Neurologica Scandinavica,* **84**(5): 429-433.

Guo Y, Wang Q, Zhang K, An T, Shi P, *et al.* 2012, 'HO-1 induction in motor cortex and intestinal dysfunction in TDP-43 A315T transgenic mice', *Brain Research,* **1460**: 88-95.

Gurney M, Cutting F, Zhai P, Doble A, Taylor C, *et al.* 1996, 'Benefit of vitamin E, riluzole, and gabapentin in a transgenic model of familal amyotrophic lateral sclerosis', *Annals of Neurology,* **39**(2): 147-157.

Gurney M, Fleck T, Himes C & Hall E 1998, 'Riluzole preserves motor function in a transgenic model of familial amyotrophic lateral sclerosis', *Neurology,* **50**(1): 62-66.

Gurney ME, Pu H, Chiu AY, Dal Canto MC, Polchow C, *et al.* 1994, 'Motor neuron degeneration in mice that express a human Cu, Zn superoxide dismutase mutation', *Science,* **264**(5166): 1772-1775.

Guy J, Shaw G, Ross-Cisneros FN, Quiros P, Salomao SR, *et al.* 2008, 'Phosphorylated neurofilament heavy chain is a marker of neurodegeneration in Leber hereditary optic neuropathy (LHON)', *Molecular Vision,* **14**: 2443-2450.

Haastert K, Grosskreutz J, Jaeckel M, Laderer C, Bufler J, *et al.* 2005, 'Rat embryonic motoneurons in long-term co-culture with Schwann cells--a system to investigate motoneuron diseases on a cellular level in vitro', *Neuroscience Methods,* **142**(2): 275-284.

Hadano S, Hand C, Osuga H, Yanagisawa Y, Otomo A, *et al.* 2001, 'A gene encoding a putative GTPase regulator is mutated in familial amyotrophic lateral sclerosis 2', *Nature Genetics,* **29**(2): 166-173.

Hafezparast M, Klocke R, Ruhrburg C, Marquardt A, Ahmad-Annuar A, *et al.* 2003, 'Mutations in dynein link motor neuron degeneration to defects in retrograde transport', *Science,* **300**(5620): 808-812.

Haley R 2003, 'Excess incidence of ALS in young Gulf War veterans', *Neurology,* **61**(6): 750-756.

Hall E, Oostveen J & Gurney M 1998, 'Relationship of microglial and astrocytic activation to disease onset and progression in a transgenic model of familial ALS', *Glia,* **23**(3): 249-256.

Hand CK, Khoris J, Salachas F, Gros-Louis F, Lopes AA, *et al.* 2002, 'A novel locus for familial amyotrophic lateral sclerosis, on chromosome 18q', *American Journal of Human Genetics,* **70**(1): 251-256.

Haraldsson B, Nyström J & Deen WM 2008, 'Properties of the Glomerular Barrier and Mechanisms of Proteinuria', *Physiological Reviews,* **88**(2): 451-487.

Harlow E & Lane D 1988. *Antibodies: A Laboratory Manual,* Cold Spring Harbor, NY, Cold Spring Harbor Laboratory Press.

Harraz M, Marden J, Zhou W, Zhang Y, Williams A, *et al.* 2008, 'SOD1 mutations disrupt redox-sensitive Rac regulation of NADPH oxidase in a familial ALS model', *Journal of Clinical Investigation,* **118**(2): 659-670.

Hatzpetros T, Bogdanik L, Tassinari V, Kidd J, Moreno A, *et al.* 2013, 'C57BL/6J congenic Prp-TDP43A315T mice develop progressive neurodegeneration in the myenteric plexus of the colon without exhibiting key features of ALS', *Brain Research,* 10.1016/j.brainres.2013.10.013.

Hayworth C & Gonzalez-Lima F 2009, 'Pre-symptomatic detection of chronic motor deficits and genotype prediction in congenic B6.SOD1(G93A) ALS mouse model', *Neuroscience,* **164**(3): 975-985.

He X 2004, 'Structure of Nerve Growth Factor Complexed with the Shared Neurotrophin Receptor p75', *Science*, **304**(5672): 870-875.

Heiman-Patterson T, Deitch J, Blankenhorn E, Erwin K, Perreault M, *et al.* 2005, 'Background and gender effects on survival in the TgN(SOD1-G93A)1Gur mouse model of ALS', *Journal of the Neurological Sciences*, **236**(1-2): 1-7.

Hemsptead B, Martin-Zanca D, Kaplan D, Parada L & Chao M 1991, 'High-affinity NGF binding requires coexpression of the trk proto-oncogene and the low-affinity NGF receptor', *Nature*, **350**(6320): 678-683.

Hennigan A, O'Callaghan RM & Kelly AM 2007, 'Neurotrophins and their receptors: roles in plasticity, neurodegeneration and neuroprotection', *Biochemical Society Transactions,* **35**: 424-427.

Herdewyn S, Cirillo C, Van Den Bosch L, Robberecht W, Vanden Berghe P, *et al.* 2014, 'Prevention of intestinal obstruction reveals progressive neurodegeneration in mutant TDP-43 (A315T) mice', *Molecular Neurodegeneration*, **9**(1): 24.

Hillel A, Miller R, Yorkston K, McDonald E, Norris F, *et al.* 1989, 'Amyotrophic lateral sclerosis severity scale', *Neuroepidemiology*, **8**(3): 142-150.

Hirtz D, Thurman D, Gwinn-Hardy K, Mohamed M, Chaudhuri A, *et al.* 2007, 'How common are the "common" neurologic disorders?', *Neurology,* **68**(5): 326-337.

Horner R, Kamins K, Feussner J, Grambow S, Hoff-Lindguist J, *et al.* 2003, 'Occurrence of amyotrophic lateral sclerosis among Gulf War veterans', *Neurology*, **61**(6): 742-749.

Howland D, Liu J, She Y, Goad B, Maragakis N, *et al.* 2002, 'Focal loss of glutamate transporter EAAT2 in a transgenic rat model of SOD1 mutant-mediated amyotrophic lateral sclerosis (ALS)', *Proceedings of the National Academy of Sciences, USA*, **99**(3): 1604-1609.

Hua X, Leow AD, Lee S, Klunder AD, Toga AW, *et al.* 2008, '3D characterization of brain atrophy in Alzheimer's disease and mild cognitive impairment using tensor-based morphometry', *Neuroimage*, **41**(1): 19-34.

Huang C, Tong J, Bi F, Zhou H & Xia X 2010, 'Mutant TDP-43 in motor neurons promotes the onset and progression of ALS in rats', *Journal of Clinical Investigation,* **122**(1): 107-118.

Hugon J, Ludolph A, Roy D, Schaumburg H & Spencer P 1988, 'Studies on the etiology and pathogenesis of motor neuron diseases. II. Clinical and electrophysiologic features of pyramidal dysfunction in macaques fed *Lathryus sativus* and IDPN', *Neurology,* **38**(3): 435-442.

Hugon J & Vallat J 1990, 'Abnormal distribution of phosphorylated neurofilaments in neuronal degeneration induced by kainic acid', *Neuroscience Letters*, **119**(1): 45-48.

Huisman M, Seelen M, de Jong S, Dorresteijn K, van Doormaal P, *et al.* 2013, 'Lifetime physical activity and the risk of amyotrophic lateral sclerosis', *Journal of Neurology, Neurosurgery, and Psychiatry,* **84**(9): 976-981.

Humphires R, Robertson D, Beynon R & Hurst J 1999, 'Unravelling the chemical basis of competitive scent marking in house mice', *Animal Behaviour*, **58**(6): 1177-1190.

Hurtado O, Cárdenas A, Lizasoain I, Boscá L, Leza J, *et al.* 2001, 'Up-regulation of TNF-alpha convertase (TACE/ADAM17) after oxygen-glucose deprivation in rat forebrain slices', *Neuropharmacology*, **40**(8): 1094-1102.

Husi H, Barr J, Skipworth R, Stephens N, Greig C, *et al.* 2013. The human urinary proteome fingerprint dabatase UPdb. *International Journal of Proteomics* [Online], 10.1155/2013/760208.

Hwang CS, Liu GT, Chang MD, Liao IL & Chang HT 2013, 'Elevated serum autoantibody against high mobility group box 1 as a potent surrogate biomarker for amyotrophic lateral sclerosis', *Neurobiology of Disease*, **58**: 13-18.

Hwee DT, Kennedy A, Ryans J, Russell AJ, Jia Z, *et al.* 2014, 'Fast skeletal muscle troponin activator tirasemtiv increases muscle function and performance in the B6SJL-SOD1G93A ALS mouse model', *PLoS One*, **9**(5): e96921.

Ibáñez CF & Simi A 2012, 'p75 neurotrophin receptor signaling in nervous system injury and degeneration: paradox and opportunity', *Trends in Neurosciences*, **35**(7): 431-440.

Igaz L, Kwong L, Lee E, Chen-Plotkin A, Swanson E, *et al.* 2011, 'Dysregulation of the ALS-associated gene TDP-43 leads to neuronal death and degeneration in mice', *Journal of Clinical Investigation*, **121**(2): 726-738.

Igoudjil A, Magrané J, Fischer L, Kim H, Hervias I, *et al.* 2011, 'In Vivo Pathogenic Role of Mutant SOD1 Localized in the Mitochondrial Intermembrane Space', *Journal of Neuroscience*, **31**(44): 15826-15837.

Ikeda K, Hirayama T, Takazawa T, Kawabe K & Iwasaki Y 2012, 'Relationships between disease progression and serum levels of lipid, urate, creatinine and ferritin in Japanese patients with amyotrophic lateral sclerosis: a cross-sectional study', *Internal Medicine*, **51**(12): 1501-1508.

Ilieva H, Polymenidou M & Cleveland D 2009, 'Non-cell autonomous toxicity in neurodegenerative disorders: ALS and beyond', *Journal of Cell Biology*, **187**(6): 761-772.

Ince P, Shaw P, Candy J, Mantle D, Tandon L, *et al.* 1994, 'Iron, selenium and gluthathione peroxidase activity are elevated in sporadic motor neuron disease', *Neuroscience Letters*, **182**(1): 87-90.

Ince P, Stout N, Shaw P, Slade J, Hunziker W, *et al.* 1993, 'Parvalbumin and calbindin D‐28k in the human motor system and in motor neuron disease', *Neuropathology and Applied Neurobiology*, **19**(4): 291-299.

Ito H, Wate R, Zhang J, Ohnishi S, Kaneko S, *et al.* 2008, 'Treatment with edaravone, initiated at symptom onset, slows motor decline and decreases SOD1 deposition in ALS mice', *Experimental Neurology*, **213**(2): 448-455.

Jaarsma D, Teuling E, Haasdijk ED, De Zeeuw CI & Hoogenraad CC 2008, 'Neuron-specific expression of mutant superoxide dismutase is sufficient to induce amyotrophic lateral sclerosis in transgenic mice', *Journal of Neuroscience*, **28**(9): 2075-2088.

Jaiswal M & Keller B 2009, 'Cu/Zn superoxide dismutase typical for familial amyotrophic lateral sclerosis increases the vulnerability of mitochondria and perturbs Ca2+ homeostasis in SOD1G93A mice', *Molecular Pharmacology*, **75**(3): 478-489.

Jiang H, Wang C, Ren M, Yin X, Chi C, *et al.* 2014, 'Blood Volatile Organic Compounds as Potential Biomarkers for Amyotrophic Lateral Sclerosis: an

Animal Study in the SOD1 G93A Mouse', *Journal of Molecular Neuroscience*, 10.1007/s12031-014-0297-4.

Johnson D, Lanahan A, Buck CR, Sehgal A, Morgan C, *et al.* 1986, 'Expression and structure of the human NGF receptor', *Cell*, **47**: 545-554.

Johnson JO, Mandrioli J, Benatar M, Abramzon Y, Van Deerlin VM, *et al.* 2010, 'Exome sequencing reveals VCP mutations as a cause of familial ALS', *Neuron*, **68**(5): 857-864.

Johnson JO, Pioro EP, Boehringer A, Chia R, Feit H, *et al.* 2014, 'Mutations in the Matrin 3 gene cause familial amyotrophic lateral sclerosis', *Nature Neuroscience*, **17**(5): 664-666.

Johnston C, Stanton B, Turner M, Gray R, Blunt A, *et al.* 2006, 'Amyotrophic lateral sclerosis in an urban setting: a population based study of inner city London', *Neurology*, **253**(12): 1642-1643.

Johnstone A & Thorpe R 1988. *Immunochemistry in Practice*, Blackwell Scientific Publications.

Jokic N, Gonzalez de Aguilar J, Pradat P, Dupuis L, Echaniz-Laguna A, *et al.* 2005, 'Nogo expression in muscle correlates with amyotrophic lateral sclerosis severity', *Annals of Neurology*, **57**(4): 553-556.

Jones BJ & Roberts DJ 1968, 'A rotarod suitable for quantitative measurements of motor incoordination in naive mice', *Naunyn-Schmiedebergs Archiv für Experimentelle Pathologie und Pharmakologie*, **259**(2): 211.

Jonsson PA, Ernhill K, Andersen PM, Bergemalm D, Brännström T, *et al.* 2004, 'Minute quantities of misfolded mutant superoxide dismutase-1 cause amyotrophic lateral sclerosis', *Brain*, **127**(Pt 1): 73-88.

Jonsson PA, Graffmo KS, Brännström T, Nilsson P, Andersen PM, *et al.* 2006, 'Motor neuron disease in mice expressing the wild type-like D90A mutant superoxide dismutase-1', *Journal of Neuropathology and Experimental Neurology*, **65**(12): 1126-1136.

Jovičić A & Gitler AD 2014, 'TDP-43 in ALS: stay on target...almost there', *Neuron*, **81**(3): 463-465.

Joyce P, Fratta P, Fisher E & Acevedo-Arozena A 2011, 'SOD1 and TDP-43 animal models of amyotrophic lateral sclerosis: recent advances in understanding disease toward the development of clinical treatments', *Mammalian Genome*, **22**(7-8): 420-448.

Jung C, Higgins C & Xu Z 2002, 'Mitochondrial electron transport chain complex dysfunction in a transgenic mouse model for amyotrophic lateral sclerosis', *Journal of Neurochemistry*, **83**(3): 535-545.

Kabashi E, Bercier V, Lissouba A, Liao M, Brustein E, *et al.* 2011, 'FUS and TARDBP but Not SOD1 Interact in Genetic Models of Amyotrophic Lateral Sclerosis', *PLoS Genetics*, **7**(8): e1002214.

Kabashi E, Valdmanis P, Dion P, Spiegelman D, McConkey B, *et al.* 2008, 'TARDBP mutations in individuals with sporadic and familial amyotrophic lateral sclerosis', *Nature Genetics*, **40**(5): 572-574.

Kaboord B & Perr M 2008, 'Isolation of proteins and protein complexes by immunoprecipitation', *Methods in Molecular Biology*, **424**: 349-364.

Kanning KC, Hudson M, Amieux PS, Wiley J, Bothwell M, *et al.* 2003, 'Proteolytic processing of the p75 neurotrophin receptor and two homologs generates C-terminal fragments with signaling capability', *Journal of Neuroscience*, **23**(13): 5425-5436.

Kanning KC, Kaplan A & Henderson CE 2010, 'Motor Neuron Diversity in Development and Disease', *Annual Review of Neuroscience*, **33**: 409-440.

Kaufmann P, Levy G, Montes J, Buchsbaum R, Barsdorf A, *et al.* 2007, 'Excellent inter-rater, intra-rater, and telephone-administered reliability of the ALFRSR-R in a multicenter clinical trial', *Amyotrophic Lateral Sclerosis,* **8**(1): 42-46.

Kaufmann P, Levy G, Thompson JLP, Delbene ML, Battista V, *et al.* 2005, 'The ALSFRSr predicts survival time in an ALS clinic population', *Neurology,* **64**(1): 38-43.

Kawamura M, Yamasaki R, Kawamura N, Tateishi T, Nagara Y, *et al.* 2012, 'Impaired recruitment of neuroprotective microglia and T cells during acute neuronal injury coincides with increased neuronal vulnerability in an amyotrophic lateral sclerosis model', *Experimental Neurology,* **234**(2): 437-445.

Kearney P & Thibault P 2003, 'Bioinformatics meets Proteomics — Bridging the gap between Mass Spectrometry data analysis and cell biology', *Bioinformatics and Computational Biology,* **1**(1): 183-200.

Keil B 1992. *Specificity of Proteolysis*, Springer Berlin Heidelberg.

Keller A, Gravel M & Kriz J 2009, 'Live imaging of amyotrophic lateral sclerosis pathogenesis: disease onset is characterised by marked induction of GFAP in Schwann cells', *Glia,* **57**(10): 1130-1142.

Kenchappa R, Tep C, Korade Z, Urra S, Bronfman F, *et al.* 2010, 'p75 Neurotrophin Receptor-mediated Apoptosis in Sympathetic Neurons Involves a Biphasic Activation of JNK and Up-regulation of Tumor Necrosis Factor- -converting Enzyme/ADAM17', *Journal of Biological Chemistry,* **285**(26): 20358-20368.

Kenchappa R, Zampieri N, Chao M, Barker P, Teng H, *et al.* 2006, 'Ligand-dependent cleavage of the p75 neurotrophin receptor is necessary for NRIF nuclear translocation and apoptosis in sympathetic neurons', *Neuron,* **50**(2): 219-232.

Kennedy RE, Schneider LS, Cutter GR & Alzheimer's Disease Neuroimaging Initiative 2012, 'Biomarker positive and negative subjects in the ADNI cohort: clinical characterization', *Current Alzheimer Research,* **9**(10): 1135-1141.

Kennel P, Fonteneau P, Martin E, Schmidt J, Azzouz M, *et al.* 1996, 'Electromyographical and motor performance studies in the pmn mouse model of neurodegenerative disease', *Neurobiology of Disease,* **3**(2): 137-147.

Kerkhoff H, Jennekens F, Troost D & Veldman H 1991, 'Nerve growth factor receptor immunostaining in the spinal cord and peripheral nerves in amyotrophic lateral sclerosis', *Acta Neuropathologica,* **81**(6): 649-656.

Kerman A, Liu H-N, Croul S, Bilbao J, Rogaeva E, *et al.* 2010, 'Amyotrophic lateral sclerosis is a non-amyloid disease in which extensive misfolding of SOD1 is unique to the familial form', *Acta Neuropathologica,* **119**(3): 335-344.

Kew J, Leigh P, Playford E, Passingham R, Goldstein L, *et al.* 1993, 'Cortical function in amyotrophic lateral sclerosis: a positron emission tomography study', *Brain,* **116**(Pt 3): 656-680.

Khandelwal P, Herman A & Moussa CE 2011, 'Inflammation in the early stages of neurodegenerative pathology', *Neuroimmunology,* **238**(1-2): 1-11.

Kiaei M, Petri S, Kipiani K, Gardian G, Choi D, *et al.* 2006, 'Thalidomide and lenalidomide extend survival in a transgenic mouse model of amyotrophic lateral sclerosis', *Journal of Neuroscience,* **26**(9): 2467-2473.

Kihira T, Yoshida S, Yoshimasu F, Wakayama I & Yase Y 1997, 'Involvement of Onuf's nucleus in amyotrophic lateral sclerosis', *Journal of Neurological Sciences*, **147**(1): 81-88.

Kim HJ, Kim NC, Wang Y-D, Scarborough EA, Moore J, *et al.* 2013, 'Mutations in prion-like domains in hnRNPA2B1 and hnRNPA1 cause multisystem proteinopathy and ALS', *Nature*, **495**(7442): 467-473.

Kim WK, Liu X, Sandner J, Pasmantier M, Andrews J, *et al.* 2009, 'Study of 962 patients indicates progressive muscular atrophy is a form of ALS', *Neurology*, **73**(20): 1686-1692.

Klivenyi P, Ferrante R, Matthews R, Bodganov M, Klein A, *et al.* 1999, 'Neuroprotective effects of creatine in a transgenic animal model of amyotrophic lateral sclerosis', *Nature Medicine*, **5**(3): 347-350.

Klivenyi P, Kiaei M, Gardian G, Calingasan N & Beal M 2004, 'Additive neuroprotective effects of creatine and cyclooxygenase 2 inhibitors in a transgenic mouse model of amyotrophic lateral sclerosis', *Journal of Neurochemistry*, **88**(3): 576-582.

Ko H, Uehara T, Tsuruma K & Nomura Y 2004, 'Ubiquilin interacts with ubiquitylated proteins and proteasome through its ubiqutin-associated and ubiquitin-like domains', *FEBS Letters*, **566**(1-3): 110-114.

Kokaia Z, Andsberg G, Martinez-Serrano A & Lindvall O 1998, 'Focal cerebral ischemia in rats induces expression of P75 neurotrophin receptor in resistant striatal cholinergic neurons', *Neuroscience*, **84**(4): 1113-1125.

Koliatsos VE, Price DL & Clatterbuck RE 1994, 'Motor neurons in Onuf's nucleus and its rat homologues express the p75 nerve growth factor receptor: sexual dimorphism and regulation by axotomy', *Journal of Comparative Neurology*, **345**(4): 510-527.

Kollewe K, Mauss U, Krampfl K, Petri S, Dengler R, *et al.* 2008, 'ALSFRS-R score and its ratio: a useful predictor for ALS-progression', *Journal of the Neurological Sciences*, **275**(1-2): 69-73.

Koomen J, Li D, Xiao L, Liu T, Coombes K, *et al.* 2005, 'Direct tandem mass spectrometry reveals limitations in protein profiling experiments for plasma biomarker discovery', *Journal of Proteome Research*, **4**(3): 972-981.

Kraemer B, Schuck T, Wheeler J, Robinson L, Trojanowski J, *et al.* 2010, 'Loss of murine TDP-43 disrupts motor function and plays an essential role in embryogenesis', *Acta Neuropathologica*, **119**(4): 409-419.

Krüger T, Lautenschläger J, Grosskreutz J & Rhode H 2013, 'Proteome analysis of body fluids for amyotrophic lateral sclerosis biomarker discovery', *Proteomics. Clinical Applications*, **7**(1-2): 123-135.

Kubota M, Sakakihara Y, Uchiyama Y, Nara A, Nagata T, *et al.* 2000, 'New ocular movement detector system as a communication tool in ventilator-assisted Werdnig-Hoffmann disease', *Developmental Medicine and Child Neurology*, **42**(1): 61-64.

Kuhle J, Lindberg R, Regeniter A, Mehling M, Steck A, *et al.* 2009, 'Increasd levels of inflammatory chemokines in amyotrophic lateral sclerosis', *European Journal of Neurology*, **16**(6): 771-774.

Kurnaz M & Seker H. A framework towards computational discovery of disease sub-types and associated (sub-)biomarkers. Annual International Conference of the IEEE Engineering in Medicine and Biology Society, 2013. 4074-4077.

Kwiatkowski TJ, Bosco D, Leclerc A, Tamrazian E, Vanderburg C, *et al.* 2009, 'Mutations in the FUS/TLS Gene on Chromosome 16 Cause Familial Amyotrophic Lateral Sclerosis', *Science*, **323**(5918): 1205-1208.

Laemmli UK 1970, 'Cleavage of structural proteins during the assembly of the head of bacteriophage T4', *Nature*, **227**(5259): 680-685.

Lagier-Tourenne C & Cleveland D 2009, 'Rethinking ALS: The FUS about TDP-43', *Cell*, **136**(6): 1001-1004.

Lagier-Tourenne C, Polymenidou M, Hutt KR, Vu AQ, Baughn M, *et al.* 2012, 'Divergent roles of ALS-linked proteins FUS/TLS and TDP-43 intersect in processing long pre-mRNAs', *Nature Neuroscience*, **15**(11): 1488-1497.

Lambert E & Mulder D 1957, 'Electromyographic studies in amyotrophic lateral sclerosis', *Proceedings of the Staff Meetings. Mayo Clinic*, **32**(17): 441-446.

Lanka V, Wieland S, Barber J & Cudkowicz M 2009, 'Arimoclomol: a potential therapy under development for ALS', *Expert Opinion on Investigational Drugs*, **18**(12): 1907-1918.

Lasiene J & Yamanaka K. 2011. Glial Cells in Amyotrophic Lateral Sclerosis. *Neurology Research International* [Online], 10.1155/2011/718987.

Lawicki S, Bedkowska G, Gacuta-Szumarksa E & Szmitkowski M 2013, 'The plasma concentration of VEGF, HE4 and CA125 as a new biomarkers panel in different stages and sub-types of epithelial ovarian tumours', *Journal of Ovarian Research*, **6**(1): 45.

Lee KF, Davies AM & Jaenisch R 1994a, 'p75-deficient embryonic dorsal root sensory and neonatal sympathetic neurons display a decreased sensitivity to NGF', *Development*, **120**(4): 1027-1033.

Lee KF, Li E, Huber LJ, Landis S, Sharpe AH, *et al.* 1992, 'Targeted mutation of the gene encoding the low affinity NGF receptor p75 leads to deficits in the peripheral sensory nervous system', *Cell*, **69**(5): 737-749.

Lee M, Marszalek J & Cleveland D 1994b, 'A mutant neurofilament subunit causes massive, selective motor neuron death: implications for the pathogenesis of human motor neuron disease', *Neuron*, **13**(4): 975-988.

Lee R, Kermani P, Teng KK & Hempstead BL 2001, 'Regulation of cell survival by secreted proneurotrophins', *Science*, **294**(5548): 1945-1948.

Lee Y, Morrison BM, Li Y, Lengacher S, Farah MH, *et al.* 2012, 'Oligodendroglia metabolically support axons and contribute to neurodegeneration', *Nature*, **487**(7408): 443-448.

Lehnert S, Costa J, de Carvalho M, Kirby J, Kuzma-Kozakiewicz M, *et al.* 2014, 'Multicentre quality control evaluation of different biomarker candidates for amyotrophic lateral sclerosis', *Amyotrophic Lateral Sclerosis & Frontotemporal Degeneration*, **15**(5-6): 344-350.

Leitner M, Menzies S & Lutz C 2010. Working with ALS Mice: Guidelines for preclinical testing & colony management. Prize4Life, The Jackson Laboratory.

Lemire M, Philibert A, Fillion M, Passos C, Guimarães J, *et al.* 2012, 'No evidence of selenosis from a selenium-rich diet in the Brazilian Amazon', *Environment International* **40**: 128-136.

Lenglet T, Lacomblez L, Abitbol JL, Ludolph A, Mora JS, *et al.* 2014, 'A phase II-III trial of olesoxime in subjects with amyotrophic lateral sclerosis', *European Journal of Neurology*, **21**(3): 529-536.

Lesage S, Le Ber I, Condroyer C, Broussolle E, Gabelle A, *et al.* 2013, 'C9ORF72 repeat expansions are a rare genetic cause of parkinsonism', *Brain*, **136**(Pt2): 385-391.

Leung CL, He CZ, Kaufmann P, Chin SS, Naini A, *et al.* 2004, 'A pathogenic peripherin gene mutation in a patient with amyotrophic lateral sclerosis', *Brain Pathology*, **14**(3): 290-296.

Levine T, Bowser R, Hank N, Gately S, Stephan D, *et al.* 2012. A Pilot Trial of Pioglitazone HCl and Tretinoin in ALS: Cerebrospinal Fluid Biomarkers to Monitor Drug Efficacy and Predict Rate of Disease Progression. *Neurology Research International* [Online], 10.1155/2012/582075.

Levine T, Daniels R, Gatta A, Wong L & Hayes M 2013, 'The product of C9orf72, a gene strongly implicated in neurodegeneration, is structurally related to DENN Rab-GEFs', *Bioinformatics*, **29**(4): 499-503.

Li J, Pan P, Song W, Huang R, Chen K, *et al.* 2012a, 'A meta-analysis of diffusion tensor imaging studies in amyotrophic lateral sclerosis', *Neurobiology of Aging*, **33**(8): 1833-1838.

Li J, Staats W, Spieker A, Sung M & Rutkove SB 2012b, 'A Technique for Performing Electrical Impedance Myography in the Mouse Hind Limb: Data in Normal and ALS SOD1 G93A Animals', *PLoS One*, **7**(9): e45004.

Li J, Sung M & Rutkove SB 2013, 'Electrophysiologic Biomarkers for Assessing Disease Progression and the Effect of Riluzole in SOD1 G93A ALS Mice', *PLoS One*, **8**(6): e65976.

Liang P, Xiang J, Liang H, Qi Z, Li K, *et al.* 2014, 'Altered amplitude of low-frequency fluctuations in early and late mild cognitive impairment and Alzheimer's disease', *Current Alzheimer Research*, **11**(4): 389-398.

Liao B, Zhao W, Beers DR, Henkel JS & Appel SH 2012, 'Transformation from a neuroprotective to a neurotoxic microglial phenotype in a mouse model of ALS', *Experimental Neurology*, **237**(1): 147-152.

Liepinsh E, Ilag L, Otting G & Ibáñez C 1997, 'NMR structure of the death domain of the p75 neurotrophin receptor', *The EMBO Journal*, **16**(16): 4999-5005.

Lindner MD, Gordon DD, Miller JM, Tariot PN, McDaniel K, *et al.* 1993, 'Increased levels of truncated nerve growth factor receptor in urine of mildly demented patients with Alzheimer's disease', *Archives of Neurology*, **50**(10): 1054-1060.

Link AJ & LaBaer J 2011, 'Solution protein digest', *Cold Spring Harbor Protocols*, **2011**(2): pdb.prot5569.

Lino M, Schneider C & Caroni P 2002, 'Accumulation of SOD1 mutant in postnatal motoneurons does not cause motoneuron pathology in motoneuron disease', *Journal of Neuroscience*, **22**(12): 4825-4832.

Liu HN, Tjostheim S, Dasilva K, Taylor D, Zhao B, *et al.* 2012, 'Targeting of monomer/misfolded SOD1 as a therapeutic strategy for amyotrophic lateral sclerosis', *Journal of Neuroscience*, **32**(26): 8791-8799.

Lobsiger C, Boillee S, McAlonis-Downes M, Khan A, Feltri M, *et al.* 2009, 'Schwann cells expressing dismutase active mutant SOD1 unexpectedly slow disease progression in ALS mice', *Proceedings of the National Academy of Sciences, USA*, **106**(11): 4465-4470.

Logroscino G, Traynor B, Hardiman O, Chiò A, Mitchell D, *et al.* 2010, 'Incidence of amyotrophic lateral sclerosis in Europe', *Journal of Neurology, Neurosurgery, and Psychiatry*, **81**(4): 385-390.

López-Bastida J, Perestelo-Pérez L, Montón-Alvarez F, Serrano-Aquilar P & Luis Alfonso-Sanchez J 2009, 'Social economic costs and health-related quality of life in patients with amyotrophic lateral sclerosis in Spain', *Amyotrophic Lateral Sclerosis*, **10**(4): 237-243.

Lowry K, Murray S, McLean C, Talman P, Mathers S, *et al.* 2001, 'A potential role for the p75 low-affinity neurotrophin receptor in spinal motor neuron degeneration in murine and human amyotrophic lateral sclerosis', *Amyotrophic Lateral Sclerosis and Other Motor Neuron Disorders,* **2**(3): 127-134.

Lu C-H, Petzold A, Kalmar B, Dick J, Malaspina A, *et al.* 2012, 'Plasma Neurofilament Heavy Chain Levels Correlate to Markers of Late Stage Disease Progression and Treatment Response in SOD1G93A Mice that Model ALS', *PLoS One*, **7**(7): e40998.

Lu CH, Petzold A, Topping J, Allen K, Macdonald-Wallis C, *et al.* 2015. Plasma neurofilament heavy chain levels and disease progression in amyotrophic lateral sclerosis: insights from a longitudinal study. *Journal of Neurology, Neurosurgery, and Psychiatry* [Online], **86**(5).

Ludolph A, Brettschneider J & Weishaupt J 2012, 'Amyotrophic lateral sclerosis', *Current Opinion in Neurology,* **25**(5): 530-535.

Ludolph AC 2011, 'Motor neuron disease: Urgently needed—biomarkers for amyotrophic lateral sclerosis', *Nature Reviews Neurology*, **7**(1): 13-14.

Ludolph AC, Bendotti C, Blaugrund E, Chio A, Greensmith L, *et al.* 2010, 'Guidelines for preclinical animal research in ALS/MND: A consensus meeting', *Amyotrophic Lateral Sclerosis*, **11**(1-2): 38-45.

Lutsep H & Rodriguez M 1989, 'Ultrastructural, morphometric and immunocytochemical study of anterior horn cells in mice with 'wasted' mutation', *Journal of Neuropathology and Experimental Neurology,* **48**(5): 519-533.

Mackenzie IR, Rademakers R & Neumann M 2010, 'TDP-43 and FUS in amyotrophic lateral sclerosis and frontotemporal dementia', *Lancet Neurology*, **9**(10): 995-1007.

Majounie E, Abramzon Y, Renton A, Perry R, Bassett S, *et al.* 2012a, 'Repeat expansion in C9ORF72 in Alzheimer's disease', *New England Journal of Medicine,* **366**(3): 283-284.

Majounie E, Renton A, Mok K, Dopper E, Waite A, *et al.* 2012b, 'Frequency of the C9orf72 hexanucleotide repeat expansion in patients with amyotrophic lateral sclerosis and frontotemporal dementia: a cross-sectional study', *Lancet Neurology,* **11**(4): 323-330.

Malek A, Barchowsky A, Bowser R, Youk A & Talbot E 2012, 'Pesticide exposure as a risk factor for amyotrophic lateral sclerosis: A meta-analysis of epidemiological studies: Pesticide exposure as a risk factor for ALS', *Environmental Research*, **117**: 112-119.

Mani R 2004, 'The evaluation of disease modifying therapies in Alzheimer's disease: a regulatory viewpoint', *Statistics in Medicine,* **23**(2): 305-314.

Maruyama H, Morino H, Ito H, Izumi Y, Kato H, *et al.* 2010, 'Mutations of optineurin in amyotrophic lateral sclerosis', *Nature,* **465**(7295): 223-226.

Mascalchi M, Diciotti S, Giannelli M, Ginestroni A, Soricelli A, *et al.* 2014, 'Progression of brain atrophy in spinocerebellar ataxia type 2: a longitudinal tensor-based morphometry study', *PLoS One,* **9**(2): e89410.

Matusica D, Skeldal S, Sykes A, Palstra N, Sharma A, *et al.* 2013, 'An Intracellular Domain Fragment of the p75 Neurotrophin Receptor (p75NTR) Enhances Tropomyosin Receptor Kinase A (TrkA) Receptor Function', *Journal of Biological Chemistry*, **288**(16): 11144-11154.

McCombe P & Henderson R 2010, 'Effects of gender in amyotrophic lateral sclerosis', *Gender Medicine,* **7**(6): 557-570.

McGoldrick P, Joyce P, Fisher EM & Greensmith L 2013, 'Rodent models of amyotrophic lateral sclerosis', *Biochimica et Biophysica Acta* **1832**(9): 1421-1436.

Meininger V, Pradat PF, Corse A, Al-Sarraj S, Rix Brooks B, *et al.* 2014, 'Safety, pharmacokinetic, and functional effects of the nogo-a monoclonal antibody in amyotrophic lateral sclerosis: a randomized, first-in-human clinical trial', *PLoS One,* **9**(5): e97803.

Meyer H, Bug M & Bremer S 2012, 'Emerging functions of the VCP/p87 AAA-ATPase in the ubiquitin system', *Nature Cell Biology*, **14**(2): 117-123.

Miana-Mena FJ, Muñoz MJ, Yagüe G, Mendez M, Moreno M, *et al.* 2005, 'Optimal methods to characterize the G93A mouse model of ALS', *Amyotrophic Lateral Sclerosis and Other Motor Neuron Diseases*, **6**(1): 55-62.

Millecamps S, Robertson J, Lariviere R, Mallet J & Julien J 2006, 'Defective axonal transport of neurofilament proteins in neurons overexpressing peripherin', *Journal of Neurochemistry*, **98**(3): 926-938.

Millecamps S, Salachas F, Cazeneuve C, Gordon P, Bricka B, *et al.* 2010, 'SOD1, ANG, VAPB, TARDBP, and FUS mutations in familial amyotrophic lateral sclerosis: genotype-phenotype correlations', *Journal of Medical Genetics*, **47**(8): 554-560.

Miller R, Mitchell J & Moore D. 2012. Riluzole for amyotrophic lateral sclerosis (ALS)/motor neuron disease (MND). *Cochrane Database of Systematic Reviews* [Online], 10.1002/14651858.CD001447.pub3.

Miller RG, Jackson CE, Kasarskis EJ, England JD, Forshew D, *et al.* 2009, 'Practice parameter update: the care of the patient with amyotrophic lateral sclerosis: drug, nutritional, and respiratory therapies (an evidence-based review): report of the Quality Standards Subcommittee of the American Academy of Neurology', *Neurology*, **73**(15): 1218-1226.

Miller RG, Zhang R, Block G, Katz J, Barohn R, *et al.* 2014, 'NP001 regulation of macrophage activation markers in ALS: A phase I clinical and biomarker study', *Amyotrophic Lateral Sclerosis & Frontotemporal Degeneration*, 10.3109/21678421.2014.951940: 1-9.

Miller T, Pestronk A, David W, Rothstein J, Simpson E, *et al.* 2013, 'An antisense oligonucleotide against SOD1 delivered intrathecally for patients with SOD1 familial amyotrophic lateral sclerosis: a phase 1, randomised, first-in-man study', *Lancet Neurology*, **12**(5): 435-442.

Min J-H, Hong Y-H, Sung J-J, Kim S-M, Lee J, *et al.* 2012, 'Oral solubilized ursodeoxycholic acid therapy in amyotrophic lateral sclerosis: a randomized cross-over trial', *Journal of Korean medical science*, **27**(2): 200-206.

Mischak H, Kolch W, Aivaliotis M, Bouyssié D, Court M, *et al.* 2010, 'Comprehensive human urine standards for comparability and standardization in clinical proteome analysis', *Proteomics. Clinical Applications*, **4**(4): 464-478.

Mitchell J, Callagher P, Gardham J, Mitchell C, Dixon M, *et al.* 2010a, 'Timelines in the diagnostic evaluation of people with suspected amyotrophic lateral sclerosis (ALS)/motor neuron disease (MND) – a 20-year review: Can we do better?', *Amyotrophic Lateral Sclerosis*, **11**(6): 537-541.

Mitchell J, East B, Harris I & Pentland B 1991, 'Manganese, selenium and other trace elements in spinal cord, liver and bone in in motor neurone disease', *European Neurology* **31**(1): 7-11.

Mitchell J, McGoldrick P, Vance C, Hortobagyi T, Sreedharan J, *et al.* 2013, 'Overexpression of human wild-type FUS causes progressive motor neuron degeneration in an age- and dose-dependent fashion', *Acta Neuropathologica,* **125**(2): 273-288.

Mitchell J, Paul P, Chen HJ, Morris A, Payling M, *et al.* 2010b, 'Familial amyotrophic lateral sclerosis is associated with a mutation in D-amino acid oxidase', *Proceedings of the National Academy of Sciences, USA,* **107**(16): 7556-7561.

Mitchell JD 2000, 'Amyotrophic lateral sclerosis: toxins and environment', *Amyotrophic Lateral Sclerosis and Other Motor Neuron Diseases,* **1**(4): 235-250.

Mitchell R, Freeman W, Randazzo W, Stephens H, Beard J, *et al.* 2009, 'A CSF biomarker panel for identification of patients with amyotrophic lateral sclerosis', *Neurology,* **72**(1): 14-19.

Mitsumoto H, Santella RM, Liu X, Bogdanov M, Zipprich J, *et al.* 2008, 'Oxidative stress biomarkers in sporadic ALS', *Amyotrophic Lateral Sclerosis,* **9**(3): 177-183.

Mizutani T, Sakamaki S, Tsuchiya N, Kamei S, Kohzu H, *et al.* 1992, 'Amyotrophic lateral sclerosis with ophthalmoplegia and multisystem degeneration in patients on long-term use of respirators', *Acta Neuropathologica,* **84**(4): 372-377.

MND Australia. 2014. *What is MND? Facts and figures* [Online]. Available: www.mndaust.asn.au/Get-informed/What-is-MND/Facts-and-figures.aspx 2014].

Mobley WC, Woo JE, Edwards RH, Riopelle RJ, Longo FM, *et al.* 1989, 'Developmental regulation of nerve growth factor and its receptor in the rat caudate-putamen', *Neuron,* **3**(5): 655-664.

Morgan B, Coates J, Johnson G, Bujnak A & Katz M 2013, 'Characterization of intercostal muscle pathology in canine degenerative myelopathy: a disease model for amyotrophic lateral sclerosis', *Journal of Neuroscience Research,* **91**(12): 1639-1650.

Mori K, Weng S, Arzberger T, May S, Rentzsch K, *et al.* 2013, 'The C9orf72 GGGGCC Repeat Is Translated into Aggregating Dipeptide-Repeat Proteins in FTLD/ALS', *Science,* **339**(6125): 1335-1338.

Moser J, Bigini P & Schmitt-John T 2013, 'The wobbler mouse, an ALS animal model', *Molecular Genetics and Genomics,* **288**(5-6): 207-229.

Mufson EJ, Presley LN & Kordower JH 1991, 'Nerve growth factor receptor immunoreactivity within the nucleus basalis (Ch4) in Parkinson's disease: reduced cell numbers and co-localization with cholinergic neurons', *Brain Research,* **539**(1): 19-30.

Münch C & Betolotti A 2011, 'Self-propogation and transmission of misfolded mutant SOD1: prion or prion-like phenomenon?', *Cell Cycle,* **10**(11): 1711.

Münch C, Sedlmeier R, Meyer T, Homberg V, Sperfeld A, *et al.* 2004, 'Point mutations of the p150 subunit of dynactin (DCTN1) gene in ALS', *Neurology,* **63**(4): 724-726.

Nagaraj N & Mann M 2011, 'Quantitative Analysis of the Intra- and Inter-Individual Variability of the Normal Urinary Proteome', *Journal of Proteome Research,* **10**(2): 637-645.

Nardo G, Pozzi S, Pignataro M, Lauranzano E, Spano G, *et al.* 2011, 'Amyotrophic Lateral Sclerosis Multiprotein Biomarkers in Peripheral Blood Mononuclear Cells', *PLoS One,* **6**(10): e25545.

Nassenstein C, Braun A, Erpenbeck V, Lommatzsch M, Schmidt S, *et al.* 2003, 'The neurotrophins nerve growth factor, brain-derived neurotrophic factor, neurotrophin-3, and neurotrophin-4 are survival and activation factors for eosinophils in patients with allergic bronchial asthma', *Journal of Experimental Medicine,* **198**(3): 455-467.

Nelson L, Matkin C, Longstreth W & McGuire V 2000a, 'Population-based case-control study of amyotrophic lateral sclerosis in western washington state. II. diet', *American Journal of Epidemiology,* **151**(2): 164-173.

Nelson L, McGuire V, Longsreth W & Matkin C 2000b, 'Population-based case-control study of amyotrophic lateral sclerosis in western washington state. I. cigarette smoking and alcohol consumption', *American Journal of Epidemiology,* **151**(2): 156-163.

Neumann M, Rademakers R, Roeber S, Baker M, Kretzschmar H, *et al.* 2009, 'A new subtype of frontotemporal lobar degeneration with FUS pathology', *Brain,* **132**(Pt 11): 2922-2931.

Neumann M, Sampathu D, Kwong L, Truax A, Micsenyi M, *et al.* 2006, 'Ubiquitinated TDP-43 in frontotemporal lobar degeneration and amyotrophic lateral sclerosis.', *Science,* **314**(5796): 130-133.

Nishimura AL, Mitne-Neto M, Silva HC, Richieri-Costa A, Middleton S, *et al.* 2004, 'A mutation in the vesicle-trafficking protein VAPB causes late-onset spinal muscular atrophy and amyotrophic lateral sclerosis', *American Journal of Human Genetics,* **75**(5): 822-831.

Nolen B, Orlichenko L, Marrangoni A, Velikokhatnaya L, Prosser D, *et al.* 2013, 'An extensive targeted proteomic analysis of disease-related protein biomarkers in urine from healthy donors', *PLoS One,* **8**(5): e63368.

Norris FJ, Calanchini P, Fallat R, Panchari S & Jewett B 1974, 'The administration of guanidine in amyotrophic lateral sclerosis', *Neurology,* **24**(8): 721-728.

Noto Y, Misawa S, Kanai K, Shibuya K, Isose S, *et al.* 2012, 'Awaji ALS criteria increase the diagnostic sensitivity in patients with bulbar onset', *Clinical Neurophysiology,* **123**(2): 382-385.

Nuytemans K, Bademci G, Kohli M, Beecham G, Wang L, *et al.* 2013, 'C9ORF72 Intermediate Repeat Copies Are a Significant Risk Factor for Parkinson Disease', *Annals of Human Genetics,* **77**(5): 351-363.

Nykjaer A, Lee R, Teng K, Jansen P, Madsen P, *et al.* 2004, 'Sortilin is essential for proNGF-induced neuronal cell death', *Nature,* **427**(6977): 843-848.

Nzwalo H, de Abreu D, Swash M, Pinto S & de Carvalho M 2014, 'Delayed diagnosis in ALS: the problem continues', *Journal of the Neurological Sciences,* **343**(1-2): 173-175.

O'Reilly E, Wang H, Weisskopf M, Fitzgerald K, Falcone G, *et al.* 2013, 'Premorbid body mass index and risk of amyotrophic lateral sclerosis', *Amyotrophic Lateral Sclerosis & Frontotemporal Degeneration,* **14**(3): 205-211.

Oeda T, Shimohama S, Kitagawa N, Kohno R, Imura T, *et al.* 2001, 'Oxidative stress causes abnormal accumulation of familial amyotrophic lateral sclerosis-related mutant SOD1 in transgenic Caenorhabditis elegans', *Human Molecular Genetics,* **10**(19): 2013-2023.

Olazarán J, Gil-de-Gómez L, Rodriguez-Martín A, Valentí-Soler M, Frades-Payo B, *et al.* 2015. A Blood-Based, 7-Metabolite Signature for the Early Diagnosis of Alzheimer's Disease. *Journal of Alzheimers Disease* [Online], 10.3233/jad-142925.

Ono S, Imai T, Matsubara S, Takahashi K, Jinnai K, *et al.* 1999, 'Decreased urinary concentrations of type IV collagen in amyotrophic lateral sclerosis', *Acta Neurologica Scandinavica,* **100**(2): 111-116.

Ono S, Shimizu N, Imai T & Rodriguez GP 2001, 'Urinary collagen metabolite excretion in amyotrophic lateral sclerosis', *Muscle & Nerve,* **24**(6): 821-825.

Orlacchio A, Babalini C, Borreca A, Patrono C, Massa R, *et al.* 2010, 'SPATACSIN mutations cause autosomal recessive juvenile amyotrophic lateral sclerosis', *Brain,* **133**(Pt 2): 591-598.

Otomo A, Pan L & Hadano S. 2012. Dysregulation of the Autophagy-Endolysosomal System in Amyotrophic Lateral Sclerosis and Related Motor Neuron Diseases. *Neurology Research International* [Online], 10.1155/2012/498428.

Ott BR, Cohen RA, Gongvatana A, Okonkwo OC, Johanson CE, *et al.* 2010, 'Brain ventricular volume and cerebrospinal fluid biomarkers of Alzheimer's disease', *Journal of Alzheimers Disease,* **20**(2): 647-657.

Ottervald J, Franzen B, Nilsson K, Andersson LI, Khademi M, *et al.* 2010, 'Multiple sclerosis: Identification and clinical evaluation of novel CSF biomarkers', *Journal of Proteomics,* **73**(6): 1117-1132.

Otto M, Bowser R, Turner M, Berry J, Brettschneider J, *et al.* 2012. Roadmap and standard operating procedures for biobanking and discovery of neurochemical markers in ALS. *Amyotrophic Lateral Sclerosis* [Online], **13**(1).

Palecek J, Lips MB & Keller BU 1999, 'Calcium dynamics and buffering in motoneurones of the mouse spinal cord', *Journal of Physiology,* **520**(Pt 2): 485-502.

Pamphlett R 2012, 'Exposure to environmental toxins and the risk of sporadic motor neuron disease: an expanded Australian case-control study', *European Journal of Neurology,* **19**(10): 1343-1348.

Pamphlett R & Ward E 2012, 'Smoking is not a risk factor for sporadic amyotrophic lateral sclerosis in an Australian population', *Neuroepidemiology,* **38**(2): 106-113.

Pang JX, Ginanni N, Dongre AR, Hefta SA & Opiteck GJ 2002, 'Biomarker Discovery in Urine by Proteomics', *Proteome Research,* **1**(2): 161-169.

Parkhurst C, Zampieri N & Chao M 2010, 'Nuclear Localization of the p75 Neurotrophin Receptor Intracellular Domain', *Journal of Biological Chemistry,* **285**(8): 5361-5368.

Parkinson N, Ince PG, Smith MO, Highley R, Skibinski G, *et al.* 2006, 'ALS phenotypes with mutations in CHMP2B (charged multivesicular body protein 2B)', *Neurology,* **67**(6): 1074-1077.

Pasinetti GM, Ungar LH, Lange DJ, Yemul S, Deng H, *et al.* 2006, 'Identification of potential CSF biomarkers in ALS', *Neurology,* **66**(8): 1218-1222.

Pejcic M, Stojnev S & Stefanovic V 2010, 'Urinary proteomics - a tool for biomarker discovery', *Renal Failure,* **32**(2): 259-268.

Perlson E, Jeong G, Ross J, Dixit R, Wallace K, *et al.* 2009, 'A Switch in Retrograde Signaling from Survival to Stress in Rapid-Onset Neurodegeneration', *Journal of Neuroscience,* **29**(31): 9903-9917.

Perrin S 2014, 'Making mouse studies work', *Nature,* **507**(7493): 423-425.

Perry RH, Cooks RG & Noll RJ 2008, 'Orbitrap mass spectrometry: instrumentation, ion motion and applications', *Mass Spectrometry Reviews,* **27**(6): 661-699.

Peviani M, Caron I, Pizzasegola C, Gensano F, Tortarolo M, *et al.* 2010, 'Unraveling the complexity of amyotrophic lateral sclerosis: recent advances from the transgenic mutant SOD1 mice', *CNS & Neurological Disorders Drug Targets,* **9**(4): 491-503.

Philips T, Bento-Abreu A, Nonneman A, Haeck W, Staats K, *et al.* 2013, 'Oligodendrocyte dysfunction in the pathogenesis of amyotrophic lateral sclerosis', *Brain,* **136**(Pt 2): 471-482.

Piazza O, Sirén A & Ehrenreich H 2004, 'Soccer, neurotrauma and amyotrophic lateral sclerosis: is there a connection?', *Current Medical Research and Opinion,* **20**(4): 505-508.

Polotsky V & O'Donnell C 2007, 'Genomics of sleep-disordered breathing', *Proceedings of the American Thoracic Society,* **4**(1): 121-126.

Polymenidou M, Lagier-Tourenne C, Hutt KR, Huelga SC, Moran J, *et al.* 2011, 'Long pre-mRNA depletion and RNA missplicing contribute to neuronal vulnerability from loss of TDP-43', *Nature Neuroscience,* **14**(4): 459-468.

Poste G 2011, 'Bring on the biomarkers', *Nature,* **469**(7329): 156-157.

Pradat P, Bruneteau G, Gonzalez de Aguilar J, Dupuis L, Jokic L, *et al.* 2007, 'Muscle Nogo-A expression is a prognostic marker in lower motor neuron syndromes', *Annals of Neurology,* **62**(1): 15-20.

Pramatarova A, Laganière J, Roussel J, Brisebois K & Rouleau G 2001, 'Neuron-specific expression of mutant superoxide dismutase 1 in transgenic mice does not lead to motor impariment', *Journal of Neuroscience,* **21**(10): 3369-3374.

Pritchard C, Mayers A & Baldwin D 2013, 'Changing patterns of neurological mortality in the 10 major developed countries - 1979-2010', *Public Health,* **127**(4): 357-368.

Puls I, Jonnakuty C, LaMonte B, Holzbaur E, Tokito M, *et al.* 2003, 'Mutant dynactin in motor neuron disease', *Nature Genetics,* **33**(4): 455-456.

Pun S, Santos AF, Saxena S, Xu L & Caroni P 2006, 'Selective vulnerability and pruning of phasic motoneuron axons in motoneuron disease alleviated by CNTF', *Nature Neuroscience,* **9**(3): 408-419.

Pupillo E, Messina P, Giussani G, Logroscino G, Zoccolella S, *et al.* 2014, 'Physical activity and Amyotrophic Lateral Sclerosis: a European population-based, case-control study', *Annals of Neurology,* **75**(5): 708-716.

Rabizadeh S, Oh J, Zhong L, Yang J, Bitler C, *et al.* 1993, 'Induction of apoptotsis by the low-affinity NGF receptor', *Science,* **261**(5119): 345-348.

Raimondi A, Mangolini A, Rizzardini M, Tartari S, Massari S, *et al.* 2006, 'Cell culture models to investigate the selective vulnerability of motoneuronal mitochondria to familial ALS-linked G93ASOD1', *European Journal of Neuroscience,* **24**(2): 387-399.

Rakhit R, Cunningham P, Furtos-Matei A, Dahan S, Qi X, *et al.* 2002, 'Oxidation-induced misfolding and aggregation of superoxide dismutase and its implications for amyotrophic lateral sclerosis', *Journal of Biological Chemistry,* **277**(49): 47551-47556.

Ranganathan S, Nicholl G, Henry S, Lutka F, Sathanoori R, *et al.* 2007, 'Comparative proteomic profiling of cerebrospinal fluid between living and post mortem ALS and control subjects', *Amyotrophic Lateral Sclerosis,* **8**(6): 373-379.

Ranganathan S, Williams E, Ganchev P, Gopalakrishnan V, Lacomis D, *et al.* 2005, 'Proteomic profiling of cerebrospinal fluid identifies biomarkers for

amyotrophic lateral sclerosis', *Journal of Neurochemistry*, **95**(5): 1461-1471.

Rao S, Yin H & Weiss J 2003, 'Disruption of glial glutamate transport by reactive oxygen species produced in motor neurons', *Journal of Neuroscience*, **23**(7): 2627-2633.

Raoul C, Pettmann B & Henderson CE 2000, 'Active killing of neurons during development and following stress: a role for p75(NTR) and Fas?', *Current Opinion in Neurobiology*, **10**(1): 111-117.

Ravits JM & La Spada AR 2009, 'ALS motor phenotype heterogeneity, focality, and spread Deconstructing motor neuron degeneration', *Neurology*, **73**(10): 805-811.

Rayaprolu S, Fujioka S, Traynor S, Soto-Ortolaza A, Petrucelli L, *et al.* 2013, 'TARDBP mutations in Parkinson's disease', *Parkinsonism & Related Disorders*, **19**(3): 312-315.

Reddy L, Koirala S, Sugiura Y, Herrera A & Ko C 2003, 'Glial cells maintain synaptic structure and function and promote development of the neuromuscular junction in vivo', *Neuron*, **40**(3): 563-580.

Régal L, Vanopdenbosch L, Tilkin P, Van den Bosch L, Thijs V, *et al.* 2006, 'The G93C mutation in superoxide dismutase 1: clinicopathologic phenotype and prognosis', *Archives of Neurology*, **63**(2): 262-267.

Reich-Slotky R, Andrews J, Cheng B, Buchsbaum R, Levy D, *et al.* 2013, 'Body mass index (BMI) as a predictor of ALSFRS-R score decline in ALS patients', *Amyotrophic Lateral Sclerosis & Frontotemporal Degeneration*, **14**(3): 212-216.

Reid E, Kloos M, Ashley-Koch A, Hughes L, Bevan S, *et al.* 2002, 'A kinesin heavy chain (KIF5) mutation in hereditary spastic paraplegia (SPG10)', *American Journal of Human Genetics*, **71**(5): 1189-1194.

Renart J, Reiser J & Stark GR 1979, 'Transfer of proteins from gels to diazobenzyloxymethyl-paper and detection with antisera: a method for studying antibody specificity and antigen structure', *Proceedings of the National Academy of Sciences, USA*, **76**(7): 3116-3120.

Renton AE, Chiò A & Traynor B 2014, 'State of play in amyotrophic lateral sclerosis genetics', *Nature Neuroscience*, **17**(1): 17-23.

Renton Alan E, Majounie E, Waite A, Simón-Sánchez J, Rollinson S, *et al.* 2011, 'A Hexanucleotide Repeat Expansion in C9ORF72 Is the Cause of Chromosome 9p21-Linked ALS-FTD', *Neuron*, **72**(2): 257-268.

Rezania K & Roos RP 2013, 'Spinal Cord: motor neuron diseases', *Neurologic Clinics*, **31**(1): 219-239.

Richmond W, Colgan G, Simon S, Stuart-Hilgenfeld M, Wilson N, *et al.* 2005, 'Random urine calcium/osmolality in the assessment of calciuria in children with decreased muscle mass', *Clinical Nephrology*, **64**(4): 264-270.

Robberecht W & Philips T 2013, 'The changing scene of amyotrophic lateral sclerosis', *Nature Reviews Neuroscience*, **14**(4): 248-264.

Roberts K, Zeineddine R, Corcoran L, Li W, Campbell I, *et al.* 2013, 'Extracellular aggregated Cu/Zn superoxide dismutase activates microglia to give a cytotoxic phenotype', *Glia*, **61**(3): 409-419.

Roche J, Rojas-Garcia R, Scott K, Scotton W, Ellis C, *et al.* 2012, 'A proposed staging system for amyotrophic lateral sclerosis', *Brain*, **135**(Pt 3): 847-852.

Rodriguez-Tébar A, Dechant G & Barde Y 1990, 'Binding of brain-derived neurotrophic factor to the nerve growth factor receptor', *Neuron*, **4**(4): 487-492.

Rodriguez-Tébar A, Dechant G, Götz R & Barde Y 1992, 'Binding of neurotrophin-3 to its neuronal receptors and interactions with nerve growth factor and brain-derived neurotrophic factor', *The EMBO Journal*, **11**(3): 917-922.

Rogers M-L, Atmosukarto I, Berhanu D, Matusica D, Macardle P, *et al.* 2006, 'Functional monoclonal antibodies to p75 neurotrophin receptor raised in knockout mice', *Journal of Neuroscience Methods*, **158**(1): 109-120.

Rogers M-L, Bailey S, Matusica D, Nicholson I, Muyderman H, *et al.* 2010, 'ProNGF mediates death of Natural Killer cells through activation of the p75NTR–sortilin complex', *Journal of Neuroimmunology*, **226**(1-2): 93-103.

Rogers ML, Smith KS, Matusica D, Fenech M, Hoffman L, *et al.* 2014. Non-viral gene therapy that targets motor neurons in vivo. *Frontiers in Molecular Neuroscience* [Online], **7**.

Rosen D, Siddique T, Patterson D, Figlewicz D, Sapp P, *et al.* 1993, 'Mutations in Cu/Zn superoxide dismutase gene are associated with familial amyotrophic lateral sclerosis', *Nature*, **362**(6415): 59-62.

Ross AH, Grob P, Bothwell M, Elder DE, Ernst CS, *et al.* 1984, 'Characterization of nerve growth factor receptor in neural crest tumors using monoclonal antibodies', *Proceedings of the National Academy of Sciences, USA*, **81**(21): 6681-6685.

Rothstein J, Martin L & Kuncl R 1992, 'Decreased glutamate transport by the brain and spinal cord in Amyotrophic Lateral Sclerosis', *New England Journal of Medicine*, **326**(22): 1464-1468.

Rothstein J, Patel S, Regan M, Haenggeli C, Huang Y, *et al.* 2005, 'Beta-lactum antibiotics offer neuroprotection by increasing glutamate transporter expression', *Nature*, **433**(7021): 73-77.

Rothstein J, Tsai G, Kuncl R, Clawson L, Cornblath D, *et al.* 1990, 'Abnormal excitatory amino acid metabolism in amyotrophic lateral sclerosis', *Annals of Neurology*, **28**(1): 18-25.

Rothstein J, Van Kammen M, Levey A, Martin L & Kuncl R 1995, 'Selective loss of glial glutamate transporter GLT-1 in amyotrophic lateral sclerosis', *Annals of Neurology*, **38**(1): 73-84.

Roux P, Colicos M, Barker P & Kennedy T 1999, 'p75 neurotrophin receptors expression is induced in apoptotic neurons after seizure', *Journal of Neuroscience*, **19**(16): 6887-6896.

Rowland L & Shneider N 2001, 'Amyotrophic Lateral Sclerosis', *New England Journal of Medicine*, **344**(22): 1688-1700.

Rutherford NJ, Zhang YJ, Baker M, Gass JM, Finch NA, *et al.* 2008. Novel mutations in TARDBP (TDP-43) in patients with familial amyotrophic lateral sclerosis. *PLoS Genetics* [Online], **4**(9).

Rutkove SB, Caress JB, Cartwright MS, Burns TM, Warder J, *et al.* 2014, 'Electrical impedance myography correlates with standard measures of ALS severity', *Muscle & Nerve*, **49**(3): 441-443.

Rutkove SB, Caress JB, Cartwright MS, Burns TM, Warder J, *et al.* 2012, 'Electrical impedance myography as a biomarker to assess ALS progression', *Amyotrophic Lateral Sclerosis*, **13**(5): 439-445.

Ryu H, Smith K, Camelo S, Carreras I, Lee J, *et al.* 2005, 'Sodium phenylbutyrate prolongs survival and regulates expression of anti-apoptotic genes in transgenic amyotrophic lateral sclerosis mice ', *Journal of Neurochemistry*, **93**(5): 1087-1098.

Saika T, Senba E, Noguchi K, Sato M, Yoshida S, *et al.* 1991, 'Effects of nerve crush and transection on mRNA levels for nerve growth factor receptor in

the rat facial motoneurons', *Brain Research. Molecular Brain Research,* **9**(1-2): 157-160.

Sapp PC, Hosler B, McKenna-Yasek D, Chin W, Gann A, *et al.* 2003, 'Identification of Two Novel Loci for Dominantly Inherited Familial Amyotrophic Lateral Sclerosis', *American Journal of Human Genetics,* **73**(2): 397-403.

Sargsyan S, Blackburn D, Barber S, Grosskreutz J, De Vos K, *et al.* 2011. A comparison of in vitro properties of resting SOD1 transgenic microglia reveals evidence of reduced neuroprotective function. *BMC Neuroscience* [Online], **12**(91).

Sasaki S & Iwata M 1996, 'Ultrastructral study of synapses in the anterior horn neurons of patients with amyotrophic lateral sclerosis', *Neuroscience Letters,* **204**(1-2): 53-56.

Sasaki S, Nagai M, Aoki M, Komori T, Itoyama Y, *et al.* 2007, 'Motor neuron disease in transgenic mice with an H46R mutant SOD1 gene', *Journal of Neuropathology and Experimental Neurology,* **66**(6): 517-524.

Saxena S & Caroni P 2011, 'Selective Neuronal Vulnerability in Neurodegenerative Diseases: from Stressor Thresholds to Degeneration', *Neuron,* **71**(1): 35-48.

Schaub S, Wilkins J, Weiler T, Sangster K, Rush D, *et al.* 2004, 'Urine protein profiling with surface-enhanced laser-desorption/ionization time-of-flight mass spectrometry', *Kidney International,* **65**(1): 323-332.

Schepelmann K, Winter Y, Spottke A, Claus D, Grothe C, *et al.* 2010, 'Socioeconomic burden of amyotrophic lateral sclerosis, myasthenia gravis and facioscapulohumeral muscular dystrophy', *Neurology,* **257**(1): 15-23.

Schmalbruch H, Jensen H, Bjaerg M, Kamieniecka Z & Kurland L 1991, 'A new mouse mutant with progressive motor neuronopathy', *Journal of Neuropathology and Experimental Neurology,* **50**(3): 192-204.

Schor N 2005, 'The p75 neurotrophin receptor in human development and disease', *Progress in Neurobiology,* **77**(3): 201-214.

Scott S, Kranz JE, Cole J, Lincecum JM, Thompson K, *et al.* 2008, 'Design, power, and interpretation of studies in the standard murine model of ALS', *Amyotrophic Lateral Sclerosis,* **9**(1): 4-15.

Seeburger JL, Tarras S, Natter H & Springer JE 1993, 'Spinal cord motoneurons express p75NGFR and p145trkB mRNA in amyotrophic lateral sclerosis', *Brain Research,* **621**(1): 111-115.

Selvaraj BT, Frank N, Bender FL, Asan E & Sendtner M 2012, 'Local axonal function of STAT3 rescues axon degeneration in the pmn model of motoneuron disease', *Journal of Cell Biology,* **199**(3): 437-451.

Shan X, Chiang P, Price D & Wong P 2010, 'Altered distributions of Gemini of coiled bodies and mitochondria in motor neurons of TDP-43 transgenic mice', *Proceedings of the National Academy of Sciences, USA,* **107**(37): 16325-16330.

Shao C, Li M, Li X, Wei L, Zhu L, *et al.* 2011. A tool for biomarker discovery in the urinary proteome: a manually curated human and animal urine protein biomarker database. *Molecular and Cellular Proteomics* [Online], **10**(11).

Shaw I, Fitzmaurice P, Mitchell J & Lynch P 1995, 'Studies on cellular free radical protection mechanisms in the anterior horn from patients with amyotrophic lateral sclerosis', *Neurodegeneration* **4**(4): 391-396.

Shefner J, Watson M, Simionescu L, Caress J, Burns T, *et al.* 2011, 'Multipoint incremental motor unit number estimation as an outcome measure in ALS', *Neurology,* **77**(3): 235-241.

Shefner JM, Cudkowicz M & Brown RH, Jr. 2006, 'Motor unit number estimation predicts disease onset and survival in a transgenic mouse model of amyotrophic lateral sclerosis', *Muscle & Nerve,* **34**(5): 603-607.

Shefner JM, Wolff AA & Meng L 2013, 'The relationship between tirasemtiv serum concentration and functional outcomes in patients with ALS', *Amyotrophic Lateral Sclerosis & Frontotemporal Degeneration,* **14**(7-8): 582-585.

Shibata N, Nagai R, Uchida K, Horiuchi S, Yamada S, *et al.* 2001, 'Morphological evidence for lipid peroxidation and protein glycoxidation in spinal cords from sporadic amyotrophic lateral sclerosis patients', *Brain Research,* **917**(1): 97-104.

Silani V, Braga M, Botturi A, Cardin V, Bez A, *et al.* 2001, 'Human developing motor neurons as a tool to study ALS', *Amyotrophic Lateral Sclerosis and Other Motor Neuron Diseases,* **2**(Suppl 1): S69-S76.

Simone I, Ruggieri M, Tortelli R, Ceci E, D'Errico E, *et al.* 2011, 'Serum N-acetylaspartate level in amyotrophic lateral sclerosis', *Archives of Neurology,* **68**(10): 1308-1312.

Simpson E, Henry Y, Henkel J, Smith R & Appel S 2004, 'Increased lipid peroxidation in sera of ALS patients: a potential biomarker of disease burden', *Neurology,* **62**(10): 1758-1765.

Skeldal S, Matusica D, Nykjaer A & Coulson E 2011, 'Proteolytic processing of the p75 neurotrophin receptor: A prerequisite for signalling?', *BioEssays,* **33**(8): 614-625.

Skeldal S, Sykes A, Glerup S, Matusica D, Palstra N, *et al.* 2012, 'Mapping of the Interaction Site between Sortilin and the p75 Neurotrophin Receptor Reveals a Regulatory Role for the Sortilin Intracellular Domain in p75 Neurotrophin Receptor Shedding and Apoptosis', *Journal of Biological Chemistry,* **287**(52): 43798-43809.

Skvortsova V, Shadrina M, Slominsky P, Levitsky G, Kondratieva E, *et al.* 2004, 'Analysis of heavy neurofilament subunit gene polymorphism in Russian patients with sporadic motor neuron disease (MND)', *European Journal of Human Genetics,* **12**(3): 241-244.

Smith B, Newhouse S, Shatunov A, Vance C, Topp S, *et al.* 2013, 'The C9ORF72 expansion mutation is a common cause of ALS+/-FTD in Europe and has a single cofounder', *European Journal of Human Genetics,* **21**(1): 102-108.

Smith Bradley N, Ticozzi N, Fallini C, Gkazi Athina S, Topp S, *et al.* 2014, 'Exome-wide Rare Variant Analysis Identifies TUBA4A Mutations Associated with Familial ALS', *Neuron,* **84**(2): 324-331.

Smith R, Henry Y, Mattson M & Appel S 1998, 'Presence of 4-hydroxynonenal in cerebrospinal fluid of patients with sporadic amyotrophic lateral sclerosis', *Annals of Neurology,* **44**(4): 696-699.

Song W, Song Y, Kincaid B, Bossy B & Bossy-Wetzel E 2013, 'Mutant SOD1G93A triggers mitochondrial fragmentation in spinal cord motor neurons: Neuroprotection by SIRT3 and PGC-1α', *Neurobiology of Disease,* **51**: 72-81.

Southam KA, King AE, Blizzard CA, McCormack GH & Dickson TC 2013, 'Microfluidic primary culture model of the lower motor neuron-neuromuscular junction circuit', *Neuroscience Methods,* **218**(2): 164-169.

Spencer P, Nunn P, Hugon J, Ludolph A & DN R 1986, 'Motorneuron disease on Guam: possible role of a food neurotoxin', *Lancet,* **1**(8487): 965.

Spreux-Varoquaux O, Bensimon G, Lacomblez L, Salachas F, Pradat P, *et al.* 2002, 'Glutamate levels in cerebrospinal fluid in amyotrophic lateral sclerosis: a reappraisal using a new HPLC method with coulometric detection in a large cohort of patients', *Journal of Neurological Sciences,* **193**(2): 73-78.

Sreedharan J, Blair IP, Tripathi B, Hu X, Vance C, *et al.* 2008, 'TDP-43 Mutations in Familial and Sporadic Amyotrophic Lateral Sclerosis', *Science,* **319**(5870): 1668-1672.

Srinivasan B, Wang Z, Brun-Zinkernagel A, Collier R, Black R, *et al.* 2007, 'Photic injury promotes cleavage of p75NTR by TACE and nuclear trafficking of the p75 intracellular domain', *Molecular and Cellular Neurosciences,* **36**(4): 449-461.

Stallings N, Puttaparthi K, Luther C, Burns D & Elliott J 2010, 'Progressive motor weakness in transgenic mice expressing human TDP-43', *Neurobiology of Disease,* **40**(2): 404-414.

Stewart H, Rutherford NJ, Briemberg H, Krieger C, Cashman N, *et al.* 2012, 'Clinical and pathological features of amyotrophic lateral sclerosis caused by mutation in the C9ORF72 gene on chromosome 9p', *Acta Neuropathologica,* **123**(3): 409-417.

Stifani N. 2014. Motor neurons and the generation of spinal motor neuron diversity. *Frontiers in Cellular Neuroscience* [Online], **8**.

Strong M & Garruto R 1991, 'Chronic aluminium-induced motor neuron degeneration: clinical, neuropathological and molecular biological aspects', *Canadian Journal of Neurological Sciences,* **18**(Suppl 3): 428-431.

Subramaniam J, Lyons W, Liu J, Bartnikas T, Rothstein J, *et al.* 2002, 'Mutant SOD1 causes motor neuron disease independent of copper chaperone-mediated copper loading', *Nature Neuroscience,* **5**(4): 301-307.

Sun H, Kawahara Y, Ito K, Kanazawa I & Kwak S 2006, 'Slow and selective death of spinal motor neurons in vivo by intrathecal infusion of kainic acid: implications for AMPA receptor-mediated excitotoxicity in ALS', *Journal of Neurochemistry,* **98**(3): 782-791.

Süssmuth S, Sperfeld A, Hinz A, Brettschneider J, Endruhn S, *et al.* 2010, 'CSF glial markers correlate with survival in amyotrophic lateral sclerosis', *Neurology*, **74**(12): 982-987.

Swarup V, Phaneuf D, Bareil C, Robertson J, Rouleau G, *et al.* 2011, 'Pathological hallmarks of amyotrophic lateral sclerosis/frontotemporal lobar degeneration in transgenic mice produced with TDP-43 genomic fragments', *Brain,* **134**(Pt 9): 2610-2626.

Swash M & Desai J 2001, 'Motor neuron disease: Classification and nomenclature', *Amyotrophic Lateral Sclerosis and Other Motor Neuron Diseases,* **1**(2): 105-112.

Swiss Institute of Bioinformatics. 2014a. *PeptideCutter* [Online]. Available: web.expasy.org/peptide_cutter.

Swiss Institute of Bioinformatics. 2014b. *PeptideMass* [Online]. Available: web.expasy.org/peptide_mass.

Sykes A, Palstra N, Abankwa D, Hill J, Skeldal S, *et al.* 2012, 'The Effects of Transmembrane Sequence and Dimerization on Cleavage of the p75 Neurotrophin Receptor by γ-Secretase', *Journal of Biological Chemistry,* **287**(52): 43810-43824.

Syroid D, Maycox P, Soilu-Hänninen M, Petratos S, Bucci T, *et al.* 2000, 'Induction of postnatal schwann cell death by the low-affinity neurotrophin

receptor in vitro and after axotomy', *Journal of Neuroscience*, **20**(15): 5741-5747.

Takahashi Y, Fukuda Y, Yoshimura J, Toyoda A, Kurppa K, *et al.* 2013, 'ERBB4 mutations that disrupt the neuregulin-ErbB4 pathway cause amyotrophic lateral sclerosis type 19', *American Journal of Human Genetics*, **93**(5): 900-905.

Takata M, Tanaka H, Kimura M, Nagahara Y, Tanaka K, *et al.* 2013, 'Fasudil, a rho kinase inhibitor, limits motor neuron loss in experimental models of amyotrophic lateral sclerosis', *British Journal of Pharmacology*, **170**(2): 341-351.

Taniuchi M, Clark H & Johnson EJ 1986, 'Induction of nerve growth factor receptor in Schwann cells after axotomy', *Proceedings of the National Academy of Sciences, USA*, **83**(11): 4094-4098.

Tartaglia M, Rowe A, Findlater L, Orange J, Grace G, *et al.* 2007, 'Differentiation between primary lateral sclerosis and amyotrophic lateral sclerosis: examination of symptoms and signs at disease onset and during follow-up', *Archives of Neurology*, **64**(2): 232-236.

Teisner B, Davey M & Grudzinskas J 1983, 'Interaction between heparin and plasma proteins analysed by crossed immunoelectrophoresis and affinity chromatography', *Clinica Chimica Acta*, **127**(3): 413-417.

Theodorescu D, Wittke S, Ross M, Walden M, Conaway M, *et al.* 2006, 'Discovery and validation of new protein biomarkers for urothelial cancer: prospective analysis', *Lancet Oncology*, **7**(3): 230-240.

Thongboonkerd V, Chutipongtanate S & Kanlaya R 2006, 'Systematic Evaluation of Sample Preparation Methods for Gel-Based Human Urinary Proteomics: Quantity, Quality, and Variability', *Journal of Proteome Research*, **5**(1): 183-191.

Ticozzi N, Silani V, LeClerc A, Keagle P, Gellera C, *et al.* 2009, 'Analysis of FUS gene mutation in familial amyotrophic lateral sclerosis within an Italian cohort', *Neurology*, **73**(15): 1180-1185.

Ticozzi N, Tiloca C, Calini D, Gagliardi S, Altieri A, *et al.* 2014, 'C9ORF72 repeat expansions are restricted to the ALS-FTD spectrum', *Neurobiology of Aging*, **35**(4): 936.e13-936.e17.

Ticozzi N, Vance C, LeClerc A, Keagle P, Glass J, *et al.* 2011, 'Mutational analysis reveals the FUS homolog TAF15 as a candidate gene for familial amyotrophic lateral sclerosis', *American Journal of Medical Genetics Part B: Neuropsychiatric Genetics*, **156**(3): 285-290.

Tortelli R, Copetti M, Ruggieri M, Cortese R, Capozzo R, *et al.* 2014. Cerebrospinal fluid neurofilament light chain levels: marker of progression to generalized amyotrophic lateral sclerosis. *European Journal of Neurology* [Online], 10.1111/ene.12421.

Tortelli R, Ruggieri M, Cortese R, D'Errico E, Capozzo R, *et al.* 2012, 'Elevated cerebrospinal fluid neurofilament light levels in patients with amyotrophic lateral sclerosis: a possible marker of disease severity and progression', *European Journal of Neurology*, **19**(12): 1561-1567.

Tovar-y-Romo L, Santa-Cruz L & Tapia R. 2009. Experimental models for the study of neurodegeneration in amyotrophic lateral sclerosis. *Molecular Neurodegeneration* [Online], 10.1186/1750-1326-4-31.

Towbin H, Staehelin T & Gordon J 1979, 'Electrophoretic transfer of proteins from polyacrylamide gels to nitrocellulose sheets: a procedure and some

applications', *Proceedings of the National Academy of Sciences, USA*, **76**(9): 4350-4354.

Traynor B, Codd M, Corr B, Forde C, Frost E, *et al.* 2000, 'Clinical feautes of amyotrophic lateral sclerosis according to the El Escorical criteria and Airlie House diagnostic criteria', *Archives of Neurology,* **57**(8): 1171-1176.

Trieu V, Liu R, Liu X & Uckun F 2000, 'A specific inhibitor of janus kinase-3 increases survival in a transgenic mouse model of amyotrophic lateral sclerosis', *Biochemical and Biophysical Research Communications,* **267**(1): 22-25.

Tsermentseli S, Leigh P & Goldstein L 2012, 'The anatomy of cognitive impairment in amyotrophic lateral sclerosis: more than frontal lobe dysfunction', *Cortex,* **48**(2): 166-182.

Tsukamoto E, Hashimoto Y, Kanekura K, Niikrua T, Aiso S, *et al.* 2003, 'Characterization of the toxic mechanism triggered by Alzheimer's amyloid-beta peptides via p75 neurotrophin receptor in neuronal hybrid cells', *Journal of Neuroscience Research,* **73**(5): 627-636.

Tuffereau C, Bénéjean J, Blondel D, Kieffer B & Flamand A 1998, 'Low-affinity nerve-growth factor receptor (p75NTR) can serve as a receptor for rabies virus', *The EMBO Journal,* **17**(24): 7250-7259.

Turner B, Ackerley S, Davies K & Talbot K 2010, 'Dismutase-competent SOD1 mutant accumulation in myelinating Schwann cells is not detrimental to normal or transgenic ALS model mice', *Human Molecular Genetics,* **19**(5): 815-824.

Turner M, Cagnin A, Turkeimer F, Miller C, Shaw C, *et al.* 2004, 'Evidence of widespread cerebral microglial activation in amyotrophic lateral sclerosis: an [11C](R)-PK11195 positron emission tomography study', *Neurobiology of Disease,* **15**(3): 601-609.

Turner M & Kiernan M 2012, 'Does interneuronal dysfunction contribute to neurodegeneration in amyotrophic lateral sclerosis?', *Amyotrophic Lateral Sclerosis,* **13**(3): 245-250.

Turner MR & Benatar M. 2014. Ensuring continued progress in biomarkers for amyotrophic lateral sclerosis. *Muscle & Nerve* [Online], 10.1002/mus.24470.

Turner MR, Bowser R, Bruijn L, Dupuis L, Ludolph A, *et al.* 2013a, 'Mechanisms, models and biomarkers in amyotrophic lateral sclerosis', *Amyotrophic Lateral Sclerosis & Frontotemporal Degeneration,* **14**(Suppl 1): 19-32.

Turner MR, Hardiman O, Benatar M, Brooks BR, Chio A, *et al.* 2013b, 'Controversies and priorities in amyotrophic lateral sclerosis', *Lancet Neurology,* **12**(3): 310-322.

Turner MR, Kiernan MC, Leigh PN & Talbot K 2009, 'Biomarkers in amyotrophic lateral sclerosis', *The Lancet Neurology,* **8**(1): 94-109.

Turner MR, Rabiner EA, Hammers A, Al-Chalabi A, Grasby PM, *et al.* 2005, '[11C]-WAY100635 PET demonstrates marked 5-HT1A receptor changes in sporadic ALS', *Brain,* **128**(Pt 4): 896-905.

Turner MR & Talbot K 2013, 'Mimics and chameleons in motor neurone disease', *Practical Neurology,* **13**(3): 153-164.

Tyurina Y, Nylander K, Mirnics Z, Portugal C, Yan C, *et al.* 2005, 'The intracellular domain of p75NTR as a determinant of cellular reducing potential and response to oxidant stress', *Aging Cell,* **4**(4): 187-196.

Uchida A, Sasaguri H, Kimura N, Tajiri M, Ohkubo T, *et al.* 2012, 'Non-human primate model of amyotrophic lateral sclerosis with cytoplasmic mislocalization of TDP-43', *Brain,* **135**(Pt 3): 833-846.

UKMND-LiCALS Study Group, Morrison K, Dhariwal S, Hornabrook R, Savage L, *et al.* 2013, 'Lithium in patients with amyotrophic lateral sclerosis (LiCALS): a phase 3 multicentre, randomised, double-blind, placebo-controlled trial', *Lancet Neurology,* **12**(4): 339-345.

Underwood CK, Reid K, May L, Bartlett PF & Coulson E 2008, 'Palmitoylation of the C-terminal fragment of p75(NTR) regulates death signaling and is required for subsequent cleavage by gamma-secretase', *Molecular and Cellular Neurosciences,* **37**(2): 346-358.

UniProt consortium. 2014. *UniProtKB/Swiss-Prot* [Online]. Available: http://web.expasy.org/docs/swiss-prot_guideline.html.

Vaccaro A, Tauffenberger A, Aggad D, Rouleau G, Drapeau P, *et al.* 2012, 'Mutant TDP-43 and FUS cause age-dependent paralysis and neurodegeneration in C. elegans', *PLoS One,* **7**(2): e31321.

Valdez G, Tapia J, Lichtman J, Fox M & Sanes J 2012, 'Shared Resistance to Aging and ALS in Neuromuscular Junctions of Specific Muscles', *PLoS One,* **7**(4): e34640.

Valori C, Brambilla L, Martorana F & Rossi D 2013, 'The multifaceted role of glial cells in amyotrophic lateral sclerosis', *Cellular and Molecular Life Sciences,* **71**(2): 287-297.

Van Damme P, Bogaert E, Dewil M, Hersmus N, Kiraly D, *et al.* 2007, 'Astrocytes regulate GluR2 expression in motor neurons and their vulnerability to excitotoxicity', *Proceedings of the National Academy of Sciences, USA,* **104**(37): 14825-14830.

Van Den Bosch L, Tilkin P, Lemmens G & Robberecht W 2002, 'Minocycline delays disease onset and mortality in a transgenic model of ALS', *Neuroreport,* **13**(8): 1067-1070.

Van Den Bosch L, Vandenberghe W, Klaassen H, Van Houtte E & Robberecht W 2000, 'Ca(2+)-permeable AMPA receptors and selective vulnerability of motor neurons', *Journal of Neurological Sciences,* **180**(1-2): 29-34.

Van Langenhove T, van der Zee J, Sleegers K, Engelborghs S, Vandenberghe R, *et al.* 2010, 'Genetic contribution of FUS to frontotemporal lobar degeneration', *Neurology,* **74**(5): 366-371.

Van Weeman B & Schuurs A 1971, 'Immunoassay using antigen-enzyme conjugates', *FEBS Letters,* **15**(3): 232-236.

Vance C, Rogelj B, Hortobagyi T, De Vos KJ, Nishimura AL, *et al.* 2009, 'Mutations in FUS, an RNA processing protein, cause familial amyotrophic lateral sclerosis type 6', *Science,* **323**(5918): 1208-1211.

Vande Velde C, Dion P & Rouleau GA. 2011a. Amyotrophic lateral sclerosis: new genes, new models, and new mechanisms. *F1000 Biology Reports* [Online], 10.3410/B3-18.

Vande Velde C, McDonald K, Boukhedimi Y, McAlonis-Downes M, Lobsiger C, *et al.* 2011b, 'Misfolded SOD1 Associated with Motor Neuron Mitochondria Alters Mitochondrial Shape and Distribution Prior to Clinical Onset', *PLoS One,* **6**(7): e22031.

Vandenberghe W, Van Den Bosch L & Robberecht W 1998, 'Glial cells potentiate kainate-induced neuronal death in a motoneuron-enriched spinal coculture system', *Brain Research,* **807**(1-2): 1-10.

Veldink J, Kalmijn S, Groeneveld G, Wunderink W, Koster A, *et al.* 2007, 'Intake of polyunsaturated fatty acids and Vitamin E reduces the risk of developing amyotrophic lateral sclerosis', *Journal of Neurology, Neurosurgery, and Psychiatry*, **78**(4): 367-371.

Verbeek C, Deng Q, Dejesus-Hernandez M, Taylor G, Ceballos-Diaz C, *et al.* 2012, 'Expression of Fused in sarcoma mutations in mice recapitulates the neuropathology of FUS proteinopathies and provides insight into disease pathogenesis', *Molecular Neurodegeneration*, 10.1186/1750-1326-7-53.

Verstraete E, Veldink J, Hendrikse J, Schelhaas H, van den Heuvel M, *et al.* 2011, 'Structural MRI reveals cortical thinning in amyotrophic lateral sclerosis', *Journal of Neurology, Neurosurgery, and Psychiatry*, **83**(4): 383-388.

Vinceti M, Bonvicini F, Rothman K, Vescovi L & Wang F. 2010. The relation between amyotrophic lateral sclerosis and inorganic selenium in drinking water: a population-based case-control study. *Environmental Health* [Online], **9**(77).

Vinceti M, Bottecchi I, Fan A, Finkelstein Y & Mandrioli J 2012, 'Are environmental exposures to selenium, heavy metals, and pesticides risk factors for amyotrophic lateral sclerosis?', *Reviews on Environmental Health*, **27**(1): 19-41.

Vinceti M, Guidetti D, Bergomi M, Caselgrandi E, Vivoli R, *et al.* 1997, 'Lead, cadmium, and selenium in the blood of patients with sporadic amyotrophic lateral sclerosis', *Italian Journal of the Neurological Sciences* **18**(2): 87-92.

Vinceti M, Guidetti D, Pinotti M, Rovesti S, Merlin M, *et al.* 1996, 'Amyotrophic lateral sclerosis after long-term exposure to drinking water with high selenium content', *Epidemiology*, **7**(5): 529-532.

Vinceti M, Solovyev N, Mandrioli J, Crespi CM, Bonvicini F, *et al.* 2013, 'Cerebrospinal fluid of newly diagnosed amyotrophic lateral sclerosis patients exhibits abnormal levels of selenium species including elevated selenite', *Neurotoxicology*, **38**: 25-32.

Vinsant S, Mansfield C, Jimenez-Moreno R, Del Gazio Moore V, Yoshikawa M, *et al.* 2013, 'Characterization of early pathogenesis in the SOD1 mouse model of ALS: part II, results and discussion', *Brain and Behavior*, **3**(4): 431-457.

Volkening K, Levstra-Lantz C, Yang W, Jaffee H & Strong M 2009, 'Tar DNA binding protein of 43 kDa (TDP-43), 14-3-3 proteins and copper/zinc superoxide dismutase (SOD1) interact to modulate NFL mRNA stability. Implications for altered RNA processing in amyotrophic lateral sclerosis (ALS).', *Brain Research*, **1305**: 168-182.

Vucic S, Cheah BC, Yiannikas C & Kiernan M 2011, 'Cortical excitability distinguishes ALS from mimic disorders', *Clinical Neurophysiology*, **122**(9): 1860-1866.

Waibel S, Reuter A, Malessa S, Blaugrund E & Ludolph A 2004, 'Rasagiline alone and in combination with riluzole prolongs survival in an ALS mouse model', *Journal of Neurology*, **251**(9): 1050-1084.

Wang G, Zhou Y, Huang FJ, Tang HD, Xu XH, *et al.* 2014, 'Plasma metabolite profiles of Alzheimer's disease and mild cognitive impairment', *Journal of Proteome Research*, **13**(5): 2649-2458.

Wang L, Pytel P, Feltri ML, Wrabetz L & Roos RP 2012, 'Selective knockdown of mutant SOD1 in Schwann cells ameliorates disease in G85R mutant SOD1 transgenic mice', *Neurobiology of Disease*, **48**(1): 52-57.

Wang L, Sharma K, Grisotti G & Roos R 2009, 'The effect of mutant SOD1 dismutase activity on non-cell autonomous degeneration in familial amytrophic lateral sclerosis', *Neurobiology of Disease*, **35**(2): 234-240.

Wegorzewska I, Bell S, Cairns N, Miller T & Baloh R 2009, 'TDP-43 mutant transgenic mice develop features of ALS and frontotemporal lobar degeneration', *Proceedings of the National Academy of Sciences, USA*, **106**(44): 18809-18814.

Weisskopf M, McCullough M, Calle E, Thun M, Cudkowicz M, *et al.* 2004, 'Prospective Study of Cigarette Smoking and Amyotrophic Lateral Sclerosis', *American Journal of Epidemiology*, **160**(1): 26-33.

Weisskopf M, Morozova N, O'Reilly E, McCullough M, Calle E, *et al.* 2009, 'Prospective study of chemical exposures and amyotrophic lateral sclerosis', *Journal of Neurology, Neurosurgery, and Psychiatry*, **80**(5): 558-561.

Weisskopf MG, O'Reilly EJ, McCullough ML, Calle EE, Thun M, *et al.* 2005, 'Prospective study of military service and mortality from ALS', *Neurology*, **64**(1): 32-37.

Weskamp G, Schlöndorff J, Lum L, Becherer J, Kim T, *et al.* 2004, 'Evidence for a Critical Role of the Tumor Necrosis Factor Convertase (TACE) in Ectodomain Shedding of the p75 Neurotrophin Receptor (p75NTR)', *Journal of Biological Chemistry*, **279**(6): 4241-4249.

Weydt P, Hong SY, Kliot M & Möller T 2003, 'Assessing disease onset and progression in the SOD1 mouse model of ALS', *Neuroreport*, **14**(7): 1051-1054.

White M, Gao R, Xu W, Mandal S, Lim J, *et al.* 2010, 'Inactivation of hnRNP K by by expanded intronic AUUCU repeat induces apoptosis via translocation of PKCdelta to mitochondria in spinocerebellar ataxia 10', *PLoS Genetics*, **6**(6): e1000984.

Wijesekera L & Leigh PN. 2009. Amyotrophic lateral sclerosis. *Orphanet Journal of Rare Diseases* [Online], 10.1186/1750-1172-4-3.

Wills A, Hubbard J, Macklin E, Glass J, Tandan R, *et al.* 2014. Hypercaloric enteral nutrition in patients with amyotrophc lateral sclerosis: a randomised, double-blind, placebo-controlled phase 2 trial. *Lancet* [Online], 10.1016/S0140-6736(14)60222-1.

Wils H, Kleinberger G, Janssens J, Pereson S, Joris G, *et al.* 2010, 'TDP-43 transgenic mice develop spastic paralysis and neuronal inclusions characteristic of ALS and frontotemporal lobar degeneration', *Proceedings of the National Academy of Sciences, USA*, **107**(8): 3858-3863.

Wilson C, Zeile S, Chataway T, Nieuwenhuijs V, Padbury R, *et al.* 2011, 'Increased expression of peroxiredoxin 1 and identification of a novel lipid-metabolizing enzyme in the early phase of liver ischemia reperfusion injury', *Proteomics*, **11**(22): 4385-4396.

Wilson M, Boumaza I, Lacomis D & Bowser R 2010, 'Cystatin C: A Candidate Biomarker for Amyotrophic Lateral Sclerosis', *PLoS One*, **5**(12): e15133.

Wokke J 1996, 'Riluzole', *Lancet*, **348**(9030): 795-799.

Wolf D, McKinnon C, Daou M, Stephens R, Kaplan D, *et al.* 1995, 'Interaction with TrkA Immobilizes gp75 in the High Affinity Nerve Growth Factor Receptor Complex', *Journal of Biological Chemistry*, **270**(5): 2133-2138.

Wolf J, Safer A, Wöhrle JC, Palm F, Nix WA, *et al.* 2014. Factors predicting one-year mortality in amyotrophic lateral sclerosis patients – data from a population-based registry. *BMC Neurology* [Online], 10.1186/s12883-014-0197-9.

Wong PC, Pardo CA, Borchelt DR, Lee MK, Copeland NG, *et al.* 1995, 'An adverse property of a familial ALS-linked SOD1 mutation causes motor neuron disease characterized by vacuolar degeneration of mitochondria', *Neuron,* **14**(6): 1105-1116.

Wu CH, Fallini C, Ticozzi N, Keagle PJ, Sapp PC, *et al.* 2012, 'Mutations in the profilin 1 gene cause familial amyotrophic lateral sclerosis', *Nature,* **488**(7412): 499-503.

Xia C, Roberts E, Her L, Liu X, Williams D, *et al.* 2003, 'Abnormal neurofilament transport caused by targeted disruption of neuronal kinesin heavy chain KIF5A', *Journal of Cell Biology,* **161**(1): 55-66.

Xia R, Liu Y, Yang L, Gal J, Zhu H, *et al.* 2012. Motor neuron apoptosis and neuromuscular junction perturbation are prominent features in a Drosophila model of Fus-mediated ALS. *Molecular Neurodegeneration* [Online], 10.1186/1750-1326-7-10.

Xu Y, Gendron T, Zhang Y, Lin W, D'Alton S, *et al.* 2010, 'Wild-type human TDP-43 expression causes TDP-43 phosphorylation, mitochondrial aggregation, motor deficits, and early mortality in transgenic mice', *Journal of Neuroscience,* **30**(32): 10851-10859.

Xu Y, Zhang Y, Lin W, Cao X, Stetler C, *et al.* 2011, 'Expression of mutant TDP-43 induces neuronal dysfunction in transgenic mice', *Molecular Neurodegeneration,* 10.1186/1750-1326-6-73.

Yamamoto T 2010, 'The 4th Human Kidney and Urine Proteome Project (HKUPP) Workshop 26 September 2009, Toronto, Canada', *Proteomics,* **10**(11): 2069-2070.

Yamanaka K, Boillee S, Roberts E, Garcia M, McAlonis-Downes M, *et al.* 2008a, 'Mutant SOD1 in cell types other than motor neurons and oligodendrocytes accelerates onset of disease in ALS mice', *Proceedings of the National Academy of Sciences, USA,* **105**(21): 7594-7599.

Yamanaka K, Chun SJ, Boillee S, Fujimori-Tonou N, Yamashita H, *et al.* 2008b, 'Astrocytes as determinants of disease progression in inherited amyotrophic lateral sclerosis', *Nature Neuroscience,* **11**(3): 251-253.

Yan H & Chao MV 1991, 'Disruption of cysteine-rich repeats of the p75 nerve growth factor receptor leads to loss of ligand binding', *J Biol Chem,* **266**(18): 12099-104.

Yang G, Wang S, Zhou R & Sun S 1983, 'Endemic selenium intoxication of humans in China', *American Journal of Clinical Nutrition,* **37**(5): 872-881.

Yang Y, Hentati A, Deng H, Dabbagh O, Sasaki T, *et al.* 2001, 'The gene encoding alsin, a protein with three guanine-nucleotide exchange factor domains, is mutated in a form of recessive amyotrophic lateral sclerosis', *Nature Genetics,* **29**(2): 160-165.

Ye B, Skates S, Mok SC, Horick NK, Rosenberg HF, *et al.* 2006, 'Proteomic-based discovery and characterization of glycosylated eosinophil-derived neurotoxin and COOH-terminal osteopontin fragments for ovarian cancer in urine', *Clinical Cancer Research,* **12**(2): 432-441.

Zetterberg H, Jacobsson J, Rosengren L, Blennow K & Andersen P 2007, 'Cerebrospinal fluid neurofilament light levels in amyotrophic lateral sclerosis: impact of SOD1 genotype', *European Journal of Neurology,* **14**(12): 1329-1333.

Zhang S, Zettler C, Cupler EJ, Hurtado P, Wong K, *et al.* 2000, 'Neurotrophin 4/5 immunoassay: identification of sources of errors for the quantification of neurotrophins', *Neuroscience Methods,* **99**(1-2): 119-127.

Zhang SH, Zhou XF, Deng YS & Rush RA 1999, 'Measurement of neurotrophin 4/5 in rat tissues by a sensitive immunoassay', *Neuroscience Methods,* **89**(1): 69-74.

Zhang SH, Zhou XF & Rush RA 2001, 'Extraction and quantification of the neurotrophins', *Methods in Molecular Biology,* **169**: 31-41.

Zhao Y, Cudkowicz ME, Shefner JM, Krivickas L, David WS, *et al.* 2014, 'Systemic pharmacokinetics and cerebrospinal fluid uptake of intravenous ceftriaxone in patients with amyotrophic lateral sclerosis', *Journal of Clinical Pharmacology,* **54**(10): 1180-1187.

Zhou H, Huang C, Chen H, Wang D, Landel C, *et al.* 2010, 'Transgenic rat model of neurodegeneration caused by mutation in the TDP gene', *PLoS Genetics,* **6**(3): e1000887.

Zinman L & Cudkowicz M 2011, 'Emerging targets and treatments in amyotrophic lateral sclerosis', *Lancet Neurology,* **10**(5): 481-490.

Zubarev R & Makarov A 2013, 'Orbitrap Mass Spectrometry', *Analytical Chemistry,* **85**(11): 5288-5296.

Zupan AA & Johnson EM 1991, 'Evidence for endocytosis-dependent proteolysis in the generation of soluble truncated nerve growth factor receptors by A875 human melanoma cells', *Journal of Biological Chemistry,* **266**: 15384-15390.

Zupan AA, Osborne PA, Smith CE, Siegel NR, Leimgruber R, *et al.* 1989, 'Identification, purification, and characterization of truncated forms of the human nerve growth factor receptor', *Journal of Biological Chemistry,* **264**(20): 11714-11720.